Identification of host cellular factors that interact with Influenza A NS1 protein for viral replication

By

Md Niaz Rahim

A Thesis
Submitted to the Faculty of Graduate Studies of
The University of Manitoba
In Partial Fulfillment of the Requirements of the Degree of

Doctor of Philosophy

Department of Medical Microbiology and Infectious Diseases,
University of Manitoba
Winnipeg, Manitoba
Canada

ABSTRACT

Influenza A virus (IAV) is considered one of the main threats that causes contagious respiratory disease in humans. Each year it threatens the human population with epidemics and pandemics. Limited anti-Influenza drugs are available that target viral proteins. The Influenza virus can mutate rapidly and can quickly develop resistance against available drugs. Therefore, developing novel host-targeted therapeutics effective against different IAVs may be very beneficial.

Influenza virus is an intracellular parasite that uses host cell system to favour its replication process and evade host cell defense system. The Influenza A viral non-structural protein 1(NS1) is a multifunctional protein that is expressed to high levels in infected cells; thus, interacting proteins may be ideal targets for drug development. In this study nine broadly cross-reactive anti-NS1 monoclonal antibodies (mAbs) were generated, characterized and used to co-immunoprecipitate IAV NS1 and its interacting host proteins. 183 proteins were consistently identified in this NS1 interactome study. Importantly, most proteins clustered into different cellular pathways, biological processes and molecular functions, such as mRNA splicing, gene expression, processing of capped intron-containing pre-mRNA and nucleoside, nucleotide and nucleic acid metabolism. Among these, 124 proteins detected in my study represent novel NS1-interacting targets not previously identified. RNAi screening then identified 11 NS1-interacting host factors as vital for IAV replication. From RNAi screening two NS1-interacting candidates, NUMA1 and PRPF19 were chosen for further analysis. IAV production was dramatically reduced in NUMA1 knockdown (KD) cells. Although viral transcription and translation were not inhibited, transport of viral structural proteins to the cytoplasmic membrane was

obstructed during maturation steps in NUMA1 KD cells. IAV maturation was also inhibited and new virion production was significantly reduced in PRPF19 KD cells.

Overall, a list of novel NS1-interacting host factors were identified utilizing some broadly cross reactive anti-NS1 mAbs in my study, and 11 of them were required for IAV replication. Further research on these new proteins may discover new targets for anti-Influenza drug development.

ACKNOWLEDGEMENT

I would like to express my deepest gratitude to my supervisor Dr. Kevin Coombs for his invaluable guidance, expertise, motivation and enthusiastic support over the years. He has been a motivation for me to become an independent researcher. I am lucky to have him as my supervisor and I will try my best to pass on the research principles and passions that he has inculcated in me.

My sincere thanks go to my thesis advisory committee members Dr. Sabine Mai and Dr. Xiaojian Yao for their guidance and insightful discussions for my project focus and experimentations during committee meetings. I would like to thank Dr. Keith Fowke for joining my committee to evaluate my candidacy examination. I would also like to thank Dr. John Wilkins for his advice during my studies.

I would like to give my heartfelt thanks to the past and present members of the Coombs' lab for their valuable support over the years. In no particular order, they are: Kola Opanubi, Dr. Anh Tran, Dr. Andrea Kroeker, Dr. Alicia Berard, Dr. Shahiduzzaman, Mark Lebar, Abdullah Awadh, Neil Salter, Sidrah Khawaja, Katherine Kresta, and Jonah Lin. I would like to thank the members of the Manitoba Centre for Proteomics and System biology, namely Patricia Sauder, Peyman Ezzati and Dr. Namita Kanwar.

I would like to thank our collaborator Dr. Earl Brown at University of Ottawa for providing us with recombinant NS1 protein. I also acknowledge Dr. Ludger Klewes at Genomic Centre for Cancer Research and Diagnosis for helping me with super resolution microscopy and Dana Henderson at Department of Human Anatomy for helping me with Electron Microscopy. My special thanks to all the amazing office supports of Department

of Medical Microbiology, especially Angela Nelson, Sharon Tardi and Natasha Hollett to help me about departmental paper works and procedures. I would also like to acknowledge Manitoba Health Research Council, Manitoba institute of Child Health Research, CIHR International Infectious Disease and Global Health training program, Department of Medical Microbiology and University of Manitoba for the financial supports.

Last, but not the least, I would like to express my immense gratefulness to my parents and to my wife, Sharmeen Atahar for their inspiration, support and strength all these years.

DEDICATION

In loving memory of my Mother,

Late Farida Rahim

List of copyright materials for which permissions were obtained

1. **Rahim MN**, Selman M, Sauder PJ, Forbes NE, Stecho W, Xu W, Lebar M, Brown EG, Coombs KM. Generation and characterization of a new panel of broadly-reactive monoclonal anti-NS1 antibodies for detection of Influenza A virus. *Journal of General Virology*. 2013. 94(3): 592-604.

   Reprinted with permission from editorial board and *Journal of General Virology* via Copyright Clearance Center. Order License Id: 3840301421171

   Figure 9: Phylogenetic comparisons of various influenza virus proteins.

   Figure 10: Anti-NS1 mAbs detected denatured form of IAV NS1.

   Figure 11: Anti-NS1 mAb detects native IAV NS1 proteins.

   Figure 12: Several anti-NS1 mAbs detect native NS1 proteins of various IAVs.

   Figure 13B: Kinetics of Influenza A NS1 expression.

   Figure 14: Amino acid sequence alignment of six IAV NS1 proteins.

   Figure 15: Epitope mapping of anti-NS1 mAbs.

   Figure 16A, C and D: Characterization of NS1 mAb epitopes.

   Table 5: Lists and typing of the anti-NS1 mAbs.

   Table 6: Characteristics of anti-NS1 monoclonal antibodies.

2. **Figure 6:** Structure of NS1 and Schematic diagram of the multiple functions of NS1 within infected cells. (*J Gen Virol*, 2008. 89(Pt 10): p. 2359-76).

   Reprinted with permission from *Journal of General Virology* via Copyright Clearance Center. Order License Ids: 4044431270085 and 3847170025710.

3. **Figure 7:** Proposed roles of host factors in the Influenza Virus Life Cycle. (*Cell Host Microbe*, 2014. 16(6): p. 795-805).

   Reprinted with permission from *Cell Host Microbe* via Copyright Clearance Center. Order License Id 3904270182569.

FIGURES

TABLES

ABBREVIATIONS

A/PR/8/34 (PR8)	8^{th} isolate of influenza A strain from Puerto Rico in 1934
BSA	Bovine serum albumin
co-IP	Co-immunoprecipitation
cRNA	Complementary RNA
DAVID	Database for Annotation, Visualization and Integrated Discovery
DC	Dendritic cells
DMEM	Dulbecco's modified eagle medium
ECL	Enhanced chemiluminescence
EM	Electron microscopy
FBS	Fetal bovine serum
FRET	Fluorescence resonance energy transfer
GO	Gene ontology
HA	Hemagglutinin
hpi	Hours post infection
IAV	Influenza A Virus
IFN	Interferon
IL	Interleukin
KD	Knockdown
KEGG	Kyoto Encyclopedia of Genes and Genomes
MDCK	Madin Darby canine kidney epithelial cell line
MOI	Multiplicity of Infection
mRNA	Messenger RNA
N/T	Non-targeting control of siRNA
NA	Neuraminidase
NEP	Nuclear export protein
NES	Nuclear export signal
NK	Natural killer
NLS	Nuclear localization signal
NP	Nucleoprotein
NS1	Non-structural protein 1
NSi	Non-silencing control of siRNA
PA	Polymerase acid protein
PB1	Polymerase basic 1 protein
PB2	Polymerase basic protein 2
PBS	Phosphate buffered saline
PFU	Plaque-forming unit
PKR	Protein kinase R
RdRp	RNA-dependent RNA polymerase
RIG-I	Retinoic acid-inducible gene-I

RNAi	RNA interference
RTF	Reverse Transfection Format
RT-PCR	Real time PCR
SDS-PAGE	Sodium dodecyl polyacrylamide sulphate gel electrophoresis
SIM	Structured illumination microscopy,
siRNA	Small interfering RNA
SOIV	Swine-origin influenza virus
STRING	Search Tool for the Retrieval of Interacting Genes/Proteins
TLR	Toll-like receptor
TNF	Tumour necrosis factor
vRNA	Viral RNA
vRNP	Viral Ribonucleoprotein
WT	Wild type

CONTENTS

Part 1.Introduction

1.1 Background of Influenza virus

In 1901, a severe epidemic occurred among chickens with a high mortality rate described as the "fowl plague". This was found to be caused by a virus, which was identified in 1955 as an avian influenza virus [1, 2]. In humans, Influenza A virus (IAV) was first isolated from a patient in 1933 and the isolated virus could be propagated in ferrets [3]. IAV is a negative-sense, single stranded RNA virus that has a segmented genome. It belongs to the family *Orthomyxoviridae* that contains viruses of six different genera such as Influenza A, Influenza B, Influenza C, Thogotovirus, Isavirus and Quaranfilvirus (Figure 1). Influenza A causes disease in humans frequently and Influenza B also occasionally causes disease in humans. IAVs are classified into different subtypes based on the antigenic properties of surface glycoproteins Hemagglutinin (HA) and Neuraminidase (NA) [4]. 18 HA subtypes and 11 NA subtypes have been identified [5, 6]. So far, six HA types (H1, H2, H3, H5, H7 and H9) and two NA subtypes (N1 and N2) were found to infect human. Influenza B viruses have two antigenically distinct lineages called the Yamagata and Victoria lineages [7].

The major natural hosts of Influenza viruses are wild waterfowl and shorebirds [8]. These viruses are well adapted and able to infect a wide range of hosts including humans, ducks, birds, chicken, turkeys, pigs, horses, and dogs [1, 9]. The symptoms associated with influenza virus infection widely depend on genomic material of virus and type of host infected. Influenza infection by most of the strains in avian species are usually asymptomatic; however, a few strains cause symptomatic infections and death [9]. Although the natural host of any Influenza strain such as aquatic birds may not show

any symptoms, other animals may be affected with mild to severe disease symptoms. The uniquely human adapted IAVs from other hosts have caused pandemics several times in the past 100 years. The significance of influenza virus research has increased in the last two decades due to emerging concerns of future pandemic threats.

1.2 History of Influenza Outbreaks

IAVs are able to cause both epidemics and pandemics. Although effective vaccines are available and updated each year, about 200,000 people are infected and hospitalized annually in the United States of America and Canada. Moreover, the mortality can reach millions if serious flu pandemics occur [10, 11]. It is assumed that outbreaks of Influenza virus are usually associated with frequent human contact with certain groups of animals, where specific viruses may develop the ability to cross the species barrier and infect human. It is believed that Influenza viruses acquire these abilities due to the mutations of certain genes that allow the viruses to recognize host cell surface proteins of different species [12].

1.2.1 The "Spanish Flu" Pandemic virus of 1918-1919

A pandemic occurred during the First World War in 1918 known as the "Spanish Flu". This was one of the most fatal events in human history, killing an estimated 50 million or more people worldwide [13]. The results of this high mortality rate were largely associated with secondary bacterial infection that caused pneumonia; however, co-pathogenic mechanisms of such fatal diseases were not known [8, 14]. Viral genomes from tissue samples of several victims were analyzed and confirmed that the causative agent was avian-descended H1N1 influenza virus [8, 15].

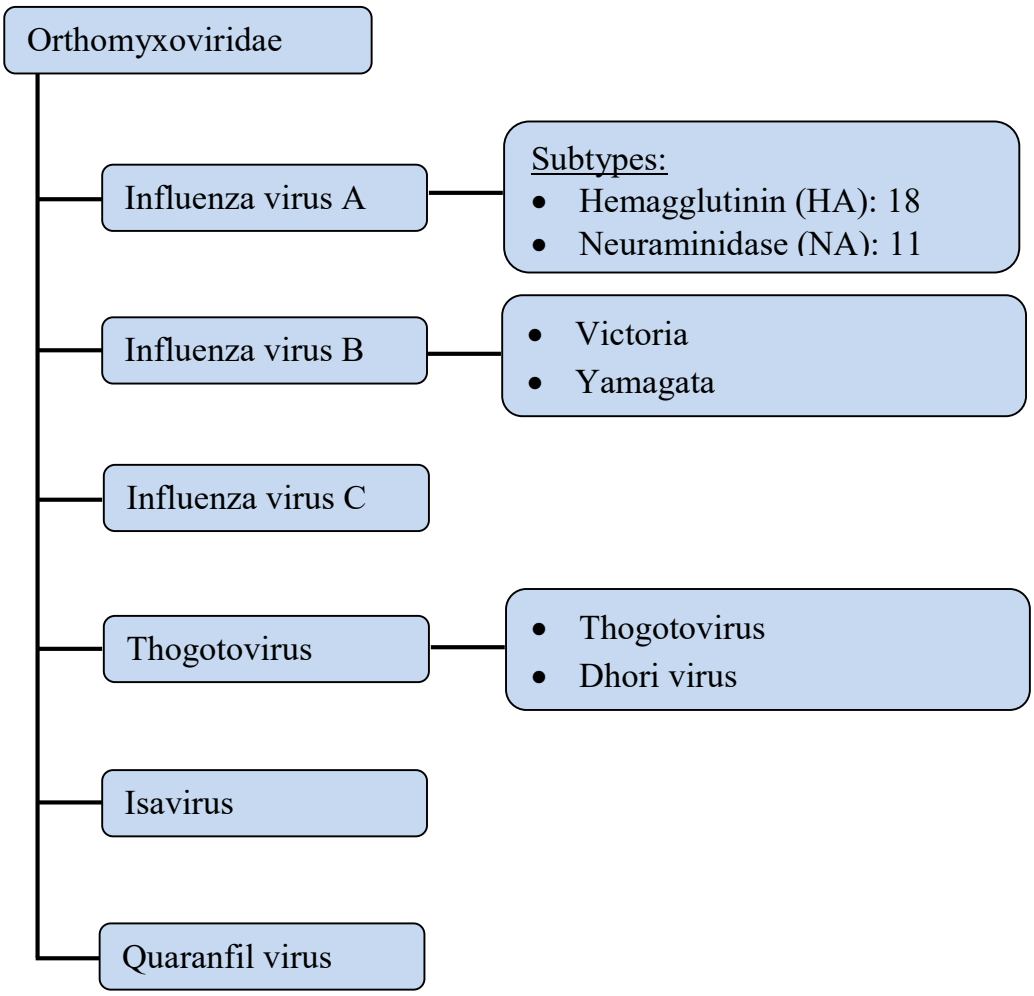

Figure 1: Classification of the members of Orthomyxoviridae family

1.2.2 The “Asian Flu” Pandemic of 1957-58

The Asian pandemic flu first emerged in 1957. It was caused by H2N2 type influenza virus that was first identified in China. It then reached Singapore, Hong Kong and the USA. This virus was not restricted by age groups; it infected children and adults, causing lethal diseases without bacterial co-infection [16]. This H2N2 type influenza virus was a descendant of the 1918 Spanish pandemic virus. The gene segments that encode HA, NA and polymerase basic protein 1 (PB1) of this virus originated from avian influenza and the other five remaining segments were the same as the 1918 pandemic influenza strain [17, 18].

1.2.3 The “Hong Kong” Pandemic of 1968

In 1968, the Hong Kong pandemic was caused by Influenza A H3N2 subtype. This virus was a reassortant of an avian Influenza and the circulating H2N2 type influenza viruses. In this reassortant, the virus acquired avian like novel HA (H3 subtype) and PB1 gene segments from avian species [17, 18]. The NA segment was retained from previous circulating H2N2 Asian Pandemic Influenza virus. Since the NA type of this pandemic strain was similar to the previous pandemic, it was suggested that antibodies to NA reduced the severity of the disease in comparison to previous pandemics [8].

1.2.4 The Swine Origin Influenza virus (SOIV) Pandemic of 2009

In 2009, the pandemic was caused by a novel H1N1, which was first detected in a widespread outbreak in Mexico. Genomic studies of this pandemic strain indicated that it was derived from two different influenza viruses of North American and Eurasian swine

lineages that had been circulating for several years before transmitting to humans [19, 20]. The North American swine influenza viruses were originated from the reassortment of avian, swine and human influenza viruses. In the Mexican outbreak, the flu infections were associated with severe pneumonia [21] and most of the cases in the US and other countries were self-limited [19]. In Mexico a total of 854 cases of pneumonia occurred, which resulted in the deaths of 59 people [19, 22].

1.3 Influenza A virus (IAV) Structure and proteins

IAVs are filamentous and spherical particles which are 100-120 nm in diameter. The viruses acquire host derived lipid membranes, which form the envelope of the virus particle (Figure 2). The IAV surface glycoproteins HA and NA are embedded within this lipid bilayer membrane at about a four to one ratio, respectively [23]. A small number of M2 proteins are also embedded in this membrane and the matrix protein (M1) lies underneath the envelope. The nuclear export protein (NEP/NS2) is also part of the IAV structure [24]. The envelope membrane including HA, NA, M2 and M1 surrounds the viral core. The inner part of the virion contains ribonucleoproteins (RNPs) that consist of viral RNA segments coated with nucleoproteins (NP) and polymerase proteins [25].

1.3.1 Hemagglutinin (HA)

HA is the major surface antigenic protein of IAV. It is recognized by the adaptive immune system of the host. After IAV infection and replication, the immune system generates neutralizing antibodies [26]. HA is an important virulence factor and responsible for host specific IAV infection [27, 28]. The carboxy terminus of HA is inserted into the viral envelope and the hydrophilic end projects from the virus surface.

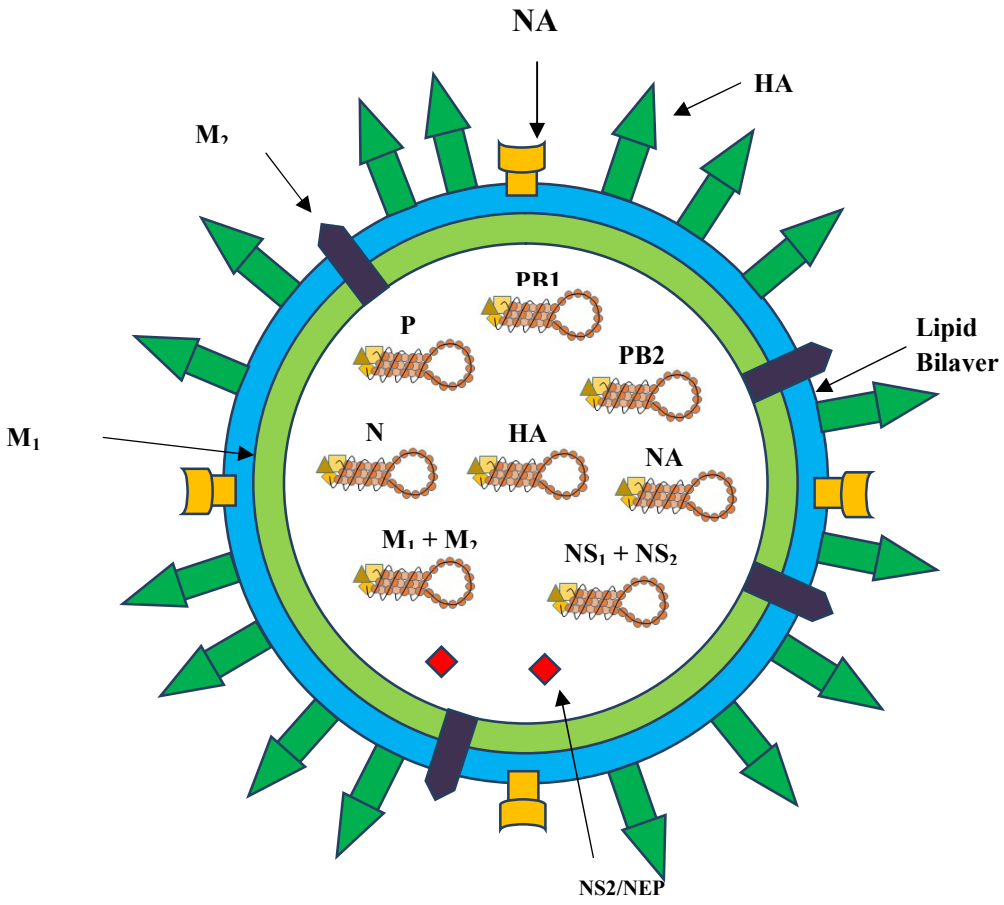

Figure 2: Influenza virion structure.

Schematic diagram of a cross-sectional image of IAV structural components. Hemagglutinin (HA), neuraminidase (NA) and proton ion channel protein M2 are embedded in the lipid membrane. Matrix (M1) protein forms a shell beneath the lipid membrane. The interior part of the virus contains 8 pieces of viral ribonucleoproteins (RNPs). Each RNP contains negative sense RNA that codes one or two viral protein. Detail structure of RNP is described in Figure 3. Non-structural protein 1(NS1) is not packaged with the progeny viral particles; however it is indicated in the background. NEP, PA, PB1 and PB2 refer to nuclear export protein, acidic polymerase protein, basic polymerase protein 1 and basic polymerase protein 2, respectively.

HA is responsible for binding host cell receptors. The avian IAV HA and the human IAV HA usually recognizes 2,3-linked sialic acid and 2,6-linked sialic acid receptors, respectively [29]. Proteolytic cleavage of HA to HA1 and HA2 subunits is required for the full HA activity [12].

HA plays a vital role in facilitating the fusion between virion and host endosomal membrane. The acidic pH of endosome triggers the conformational change in HA that induces the fusion peptide HA2 to form fusion pores. The viral RNPs get into the cytoplasm through these pores [12, 29]. Currently 18 HA subtypes have been identified in nature [5, 6].

1.3.2 Neuraminidase (NA)

NA is the second major IAV integral membrane glycoprotein and surface antigen. NA plays an important role in releasing the virus from host cells. During budding of new virions, the new progeny viral HA has a tendency to bind with host cell sialic acid receptors; however, the viral NA cleaves sialic acid residues on the cell surface and promotes viral release to spread from one cell to another [12]. Currently 11 NA subtypes have been identified in nature [5, 6].

1.3.3 M1 Protein

M1 matrix is the most abundant IAV protein. M1 protein makes a layer just beneath the lipid envelope and surrounds the nucleocapsids of the virion. It forms a bridge between the inner core proteins and the surface glycoproteins of the virus [30]. It is proposed that M1 plays an important role in the assembly of progeny viruses. M1 is

found both in the cytoplasm and nucleus of the infected cell [9] and it is involved in nuclear export of viral RNPs [31].

1.3.4 M2 protein

M2 is another integral membrane protein. M2 can serve as a proton ion channel in infected host cells. It is responsible for acidification of the IAV core, and thus, it facilitates the entry of viral RNPs into the cytoplasm [32]. Membrane bound domain of M2 protein interacts with M1 and plays crucial roles in assembling IAV proteins and vRNPs, which helps the budding process [33].

1.3.5 PA, PB1 and PB2

IAV RNA dependent RNA polymerase complex is a major virulence factor and it consists of acidic polymerase protein (PA), basic polymerase protein 1 (PB1) and basic polymerase protein 2 (PB2) (Figure 3). The RNA polymerase complex plays an important role in the pathogenicity of the 1918 H1N1 Spanish flu [34] .

Cap snatching is an important part of influenza virus transcription where small host RNA segments are used for the initiation of viral transcription. PB2 protein recognizes and binds to the $5^{/}$ cap of the host's mRNA [35]. Viral PA protein contains endonuclease activity, which is important in generating mRNA cap from host for viral transcription [36, 37]. PB1 is an essential protein for structural integrity and catalytic activity of Influenza RNA polymerase [38]. After cap snatching, PB1 plays roles in elongating viral mRNA by catalyzing sequential addition of nucleotides. PB1 is also involved in binding to the vRNA and complementary RNA (cRNA) to initiate

transcription and replication [39, 40]. PB1 mRNA encodes two truncated forms of PB1 proteins such as PB1-F2 and PB1-N40 through alternate open reading frame (ORF) [41, 42]. PB1-F2 is a virulence factor and was found to induce apoptosis in infected cells [43]. The high virulence of both the H5N1 and 1918 H1N1 viruses was due to a single amino acid change (N66S) of PB1-F2 protein [44].

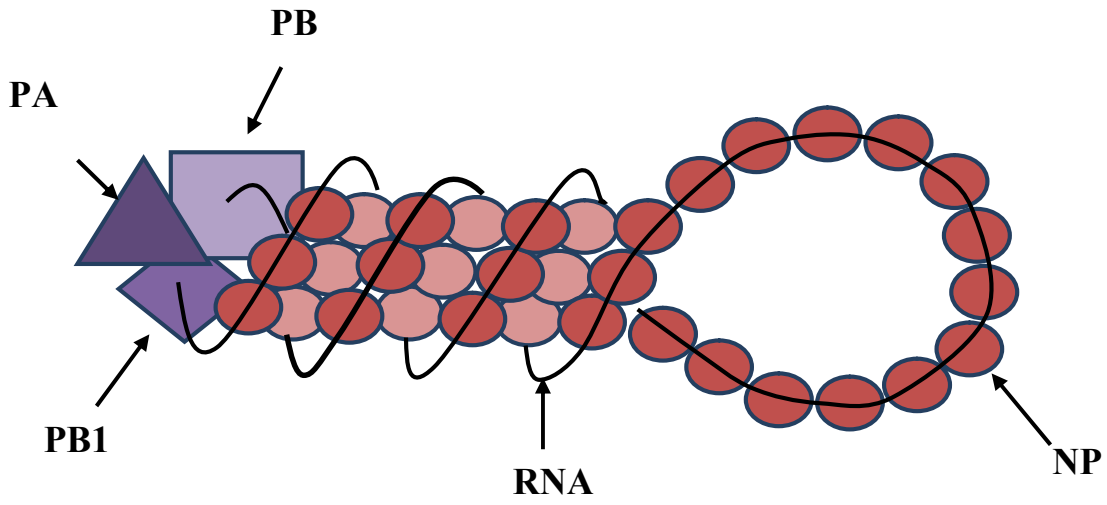

Figure 3: Schematic illustration of IAV RNP structure.

The viral genome consists of ribonucleoprotein complexes (RNPs). RNP consists of single-stranded, negative-sense RNA coated with NP protein in a pinloop structure. Viral polymerases proteins (PA, PB1 and PB2) are attached at one end.

1.3.6 Nucleoprotein (NP)

NP is the second most abundant protein in the Influenza virion and is expressed in high amounts in infected cells. It serves as the structural component of viral RNP by coating almost the entire vRNA (Figure 3). After viral entry and uncoating in the host cell, RNPs need to be transported to the nucleus for transcription. NP contains a nuclear localization signal (NLS) that plays an important role in the trafficking of vRNPs into the nucleus with the help of the cellular cargo protein karyopherin α [45].

1.3.7 NEP/NS2

After transcription and formation of vRNPs inside the nucleus, they need to migrate to the cytoplasm for the assembly of new virions. Influenza virus nuclear export protein (NEP), which was previously known as NS2, works as an adaptor protein in chromosomal region maintenance 1 (Crm1) mediated export of viral RNPs from the nucleus of the host cell [46, 47]. A methionine/leucine-rich nuclear export signal (NES) in the N-terminus of NEP/NS2 showed a vital role for RNP export [47].

1.3.8 NS1

Influenza virus NS1 is a non-structural protein and expressed at high abundance through the viral life cycle in infected cells. It is a 215-237 amino acid long dimeric protein and has two binding domains. The RNA binding domain resides in the N terminus of NS1. This domain is a homodimer where each monomer consists of three α-helics. These six symmetric α-helics of the RNA binding domain bind with several RNA

species [48-50]. Amino acid R at position 38 is vital for RNA binding, however other adjacent amino acids also play a role in RNA binding activity [50]. The effector domain

resides in the C-terminus of NS1, which mediates interactions with host proteins and stabilizes the RNA binding domain [48, 51]. This RNA binding domain contains NES that helps NS1 localization both in host cell nucleus and cytoplasm [52]. Influenza NS1 is considered an auxiliary virulence factor [53]. Several studies showed that partially deleted NS1 proteins attenuated the viruses and did not cause diseases, but it led to the development of the immune responses in birds and different animal species [54-56].

Influenza NS1 is a multi-functional protein. It regulates viral RNA synthesis, mRNA splicing, viral protein synthesis, and suppresses host immune responses (reviewed in [48]) (Figure 6). According to phylogenetic analysis, Influenza A NS1 can be divided into two major groups: allele A and B. Allele A contains NS1 proteins of swine, human, and equine IAVs; and allele B contains only avian IAVs [57, 58]. The Influenza viral antigenic changes mainly occurred by selective pressure on HA and NA surface, however NS1 protein sequences of different virus strains are highly conserved. During viral infection, NS1 modulates host immune responses and interact with host factors. I will be discussing more about the NS1, its roles and interaction in sections 1.8 and 1.9.

1.3.9 Influenza NS3

Frobes et al. (2012) identified and characterized a panel of adaptive mutations in A/Hong Kong/ 1/1968 (H3N2) NS1 proteins [59]. Selman et al. (2012) showed that influenza virus adaptation to a new host occurred by the selection of a mutation, NS1 D125G (GAT→GGT), which introduced a new splice site into the NS gene and produced

the novel NS3 protein by alternative splicing [60]. The 125G (GGT) codon was mostly found in viruses, which had switched recently to new host species such as in mice.

1.4 Influenza A virus genome

The IAV genome consists of eight segmented, negative sense, single stranded RNAs. These RNA segments exist in the form of ribonucleoproteins (RNP). The RNP consists of viral RNAs, which are coated with NP and three polymerase proteins (PB1, PB2 and PA) (Figure 3) [40]. The ends of all vRNAs form a helical hairpin that is bound with polymerase complexes. Each viral RNA segment contains non-coding regions; however, sequences are highly conserved at the $5^{/}$ and $3^{/}$ends of each RNA segments [25]. Segments 1, 3, 4 and 5 encode the PB2, PA, HA and NP proteins, respectively [25]. In IAVs, segment 2 encodes polymerase complex subunit PB1 protein. In some of the IAVs, segment 2 also codes for accessory protein PB1-F2 that has pro-apoptotic activity [25, 42]. Segment 6 encodes NA in IAVs. Segment 7 encodes M1 protein and alternative splicing variant (mRNA) of this segment also produces the M2 protein [61]. Segment 8 encodes non-structural NS1protein and alternative splicing variant of segment 8 synthesizes NEP/NS2 protein [62, 63].

RNA viral RNA polymerases lack exonuclease proofreading ability and increase mutation rate during genomic replication [64]. Amino acid mutation rate of avian influenza viruses in aquatic birds is relatively low, because these are well adapted in birds. However, the amino acid mutation and evolutionary rate of mammalian Influenza viruses are much higher [9]. After viral infection, at first surface glycoproteins HA and NA are recognized by the host's innate immune system. Mutations occur in the antigenic

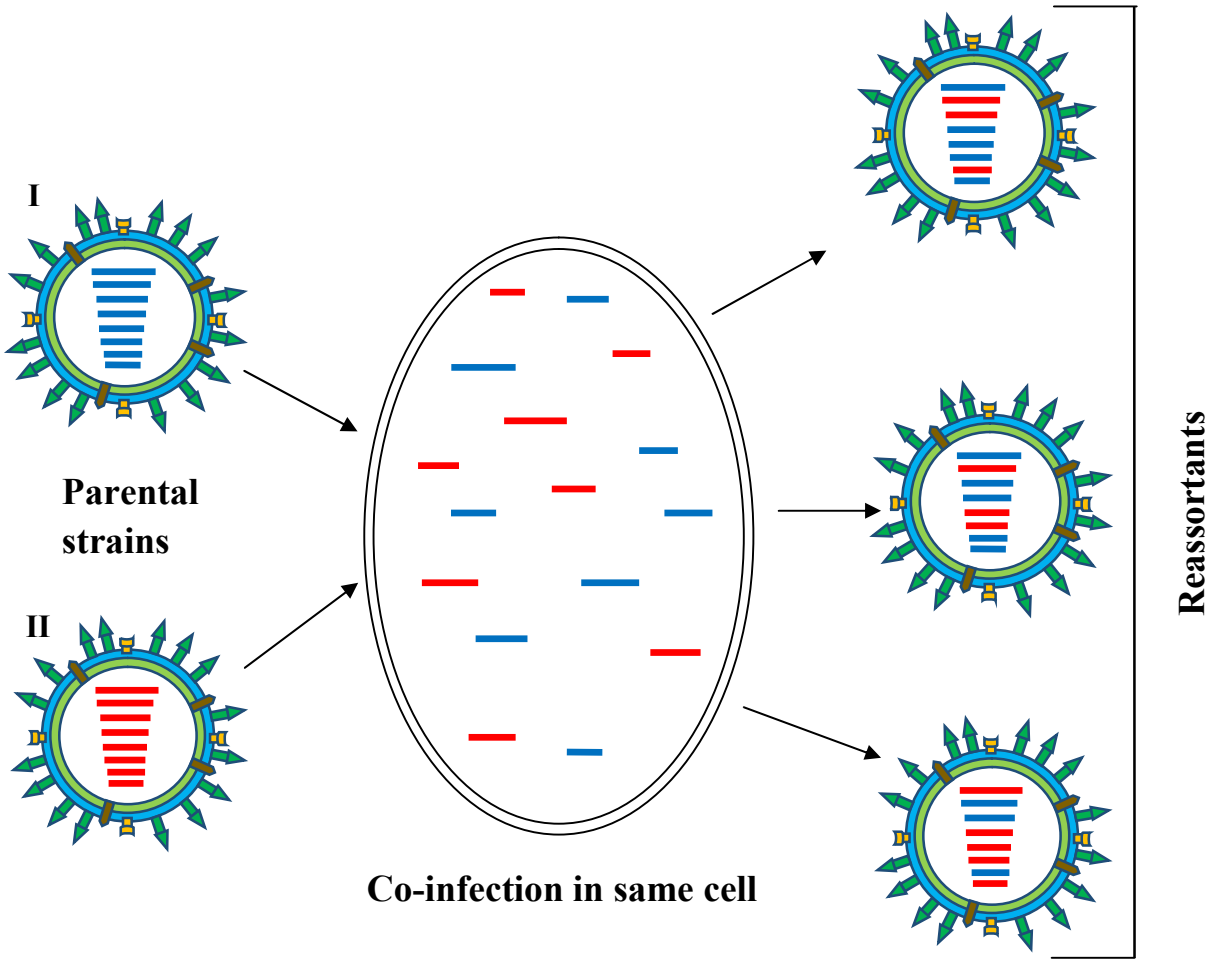

Figure 4: Generation of reassortants.

Schematic diagram illustrates the co-infection of two different parental IAVs I and II in the same cell. Blue and Red solid lines indicate the RNA segments of parental strains I and II, respectively. Co-infection of parental strains I and II results the production of progeny virions (reassortants) by exchanging genetic material from both parents.

domains HA and NA since these are under selective pressure of host immunity [65]. After mutations, the mutated HA and/or NA of new variants are able to escape from the host's neutralizing antibodies and innate immune system. This event of mutation and change in the antigenicity of the influenza viral surface glycoproteins is called antigenic drift [66] .

The segmented nature of the genome allows Influenza virus to acquire a significant feature called "Antigenic shift". When two or more human and animal viruses (or different Influenza virus types or strains) co-infect the same host, there is a possibility that an exchange of genetic materials between viruses can occur during the viral replication process and generate a new type of virus (Figure 4). New progeny viruses may express entirely new antigenic proteins against which human populations may not have pre-existing immunity. Due to antigenic shifts, pandemics arise. Influenza A H1N1 and SOIV-H1N1, which are the causative agents for "Spanish flu" and "2009 pandemic flu" respectively, were generated by antigenic shifts [67, 68]. It is now accepted that the spread of the pandemics was mostly due to the acquisition of novel surface antigenic proteins, to which most of the world's population was immunologically naïve [25, 69].

1.5 Influenza A virus life cycle

1.5.1 Virus attachment

Influenza virus HA recognizes N-acetylneuraminic acid (sialic acid receptor) on host cell surface to initiate infection (Figure 5). HA has two subunits, HA1 and HA2, which are linked by disulfide bonds. HA1 contains the receptor binding domain. Human Influenza viruses bind to the sialic acid receptor attached to galactose sugar with α2,6

linkage (SAα2,6Gal) and avian influenza viruses mainly bind to sialic acid receptor with α2,3 linkage [29]. Most parts of human tracheal epithelial cells contain sialic acid receptor with α2,6 linkage (SAα2,6Gal) whereas the gut epithelium of ducks mostly contain sialic acid receptor with α2,3 linkage [29]. α2,3 linked sialic acid receptors are also found in the epithelium of human respiratory tract at low abundance that may allow binding to avian Influenza viruses [70]. Influenza viruses originated from swine can recognize both receptors. Therefore, it is believed that swine plays an important role in assorting the segmented genomes of human and avian influenza viruses, to generate deadly pathogenic viruses [71, 72].

1.5.2 Viral entry, fusion, and uncoating

Following attachment of Influenza virus to sialic acid receptors, the virus enters the host cell through receptor mediated endocytosis and forms viral endosome (Figure 5). The low pH of the endosome triggers the conformational change of HA. This change in HA protein maintains the HA1 binding domain but exposes HA2, the fusion peptide that fuses the viral envelope with the endosomal membrane and forms fusion pore through which vRNPs are released into host cell cytoplasm (reviewed in [29, 73]). M2 ion channel protein plays a role in uncoating step. M2 allows H^+ ion influx from the endosome into the viral particle, which helps vRNPs to detach from M1 protein matrix and thereby the vRNPs are released [32].

1.5.3 Entry of viral ribonucleoproteins (vRNPs) into the nucleus

For transcription and replication of viral RNA, influenza vRNPs must enter the nucleus. NP, PB1, PB2 and PA of vRNP contain nuclear localization signals (NLSs) that

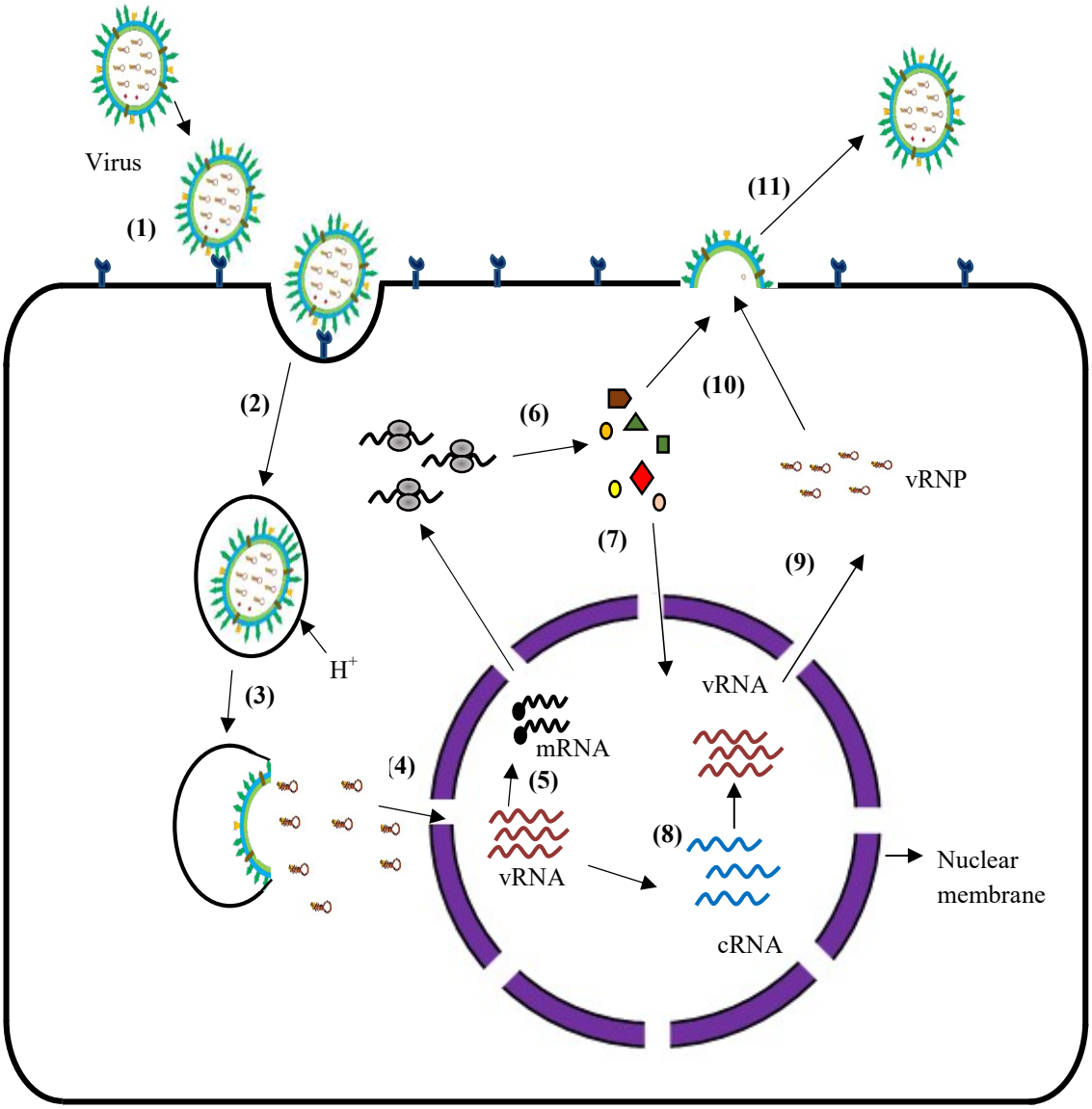
Virus
(1)
(2)
(3)
(4)
(5)
(6)
(7)
(8)
(9)
(10)
(11)
H+
mRNA
vRNA
vRNA
cRNA
vRNP
Nuclear membrane

Figure 5: Influenza virus lifecycle

(1) Virus attaches to the sialic acid receptor of host cell membrane. (2) Viral entry via receptor-mediate endocytosis. (3) Acidification of endosomal membranes causes the fusion between viral and endosomal membranes. (4) Viral ribonucleoproteins (RNPs) are released and transported to the nucleus. Viral RNPs consist of viral RNA (vRNA), polymerase complex and nucleoproteins (NP). (5) Viral mRNAs are transcribed from viral RNAs in the nucleus. (6) Viral proteins are translated in cytoplasm. (7) Specific viral proteins are transported back to the nucleus. (8) Viral genomic RNA synthesis occurs inside the nucleus. In addition to transcription, vRNAs are also synthesized in the host nucleus for new progeny viruses. First viral polymerase complex uses negative sense RNA as template and synthesize complementary positive sense RNA (cRNA). Thereafter, viral polymerase synthesizes more negative sense genomic vRNA using cRNA as template. Newly produced vRNAs are coated with NP and associated with polymerase complexes and vRNPs are formed. (9) Progeny vRNPs are exported to the cytoplasm. (10) Viral assembly occurs at cell membrane and (11) progeny viruses are released from the cell by neuraminidase activity.

utilize cellular import machinery to enter the nucleus [47]. Nuclear import occurs through Crm-mediated pathway where various karyopherins including importin α and β play roles [71].

1.5.4 Transcription and viral genome replication

Once viral RNAs arrive in the nucleus, viral RNA transcription and replication begin. IAV mRNA transcription occurs in a primer-dependent manner using vRNA as template. Mature cellular messenger RNA (mRNA) contains a $5^{/}$ methylated cap and a poly (A) tail in the $3^{/}$ end. Influenza vRNP has a poly(A) tail but no $5^{/}$ cap. Viral mRNA capping occurs in a unique manner during viral transcription where the virus steals host pre mRNA transcripts to initiate its own transcription; known as cap-snatching [74]. PB2 binds to the $5^{/}$ cap of the host's pre mRNA [35]. PA has endonuclease activity and it is believed that PA cleaves mRNA cap for viral transcription [36, 37]. PB1 elongates viral mRNA by catalyzing sequential addition of nucleotides using vRNA as template. Addition of poly (A) tail in influenza virus transcription is not similar to cellular polyadenylation. IAV RNA encodes a stretch of 5-7 uracil residues, which is transcribed into positive sense adenosines and form poly (A) tail [25]. After polyadenylation, viral mRNAs are transported to the cytoplasm and translated like host mRNA. Influenza viral RNA segments 7 and 8 encode two proteins each, which occur via the alternative splicing mechanism. Influenza viruses use host's splicing machinery to produce those proteins by alternative splicing [74, 75].

In addition to transcription, vRNAs are also synthesized in the host nucleus for new progeny viruses. vRNA replication is a two-step process. First, viral RNA-dependent

RNA polymerase (RdRp) complex uses negative sense RNA as template and synthesizes full length complementary positive sense RNA (cRNA). Initiation of cRNA synthesis occurs without a capped primer. It is proposed that NP is required for the synthesis of full-length cRNA [74]. Then, viral RdRp synthesizes more negative sense genomic vRNA using cRNA as template and newly synthesized vRNAs are coated with NP [74].

1.5.5 Export of vRNP from nucleus to cytoplasm

It is proposed that vRNPs are exported from the nucleus to the cytoplasm through nuclear pores via Crm1-mediated pathway [47, 71]. Influenza M1, NEP/NS2 and RNPs form a complex in the nucleus, which is involved in vRNP export. First, M1 binds to the vRNP and NEP/NS2, then NEP/NS2 protein interacts with the export receptor Crm1 and several nucleoporins, which all facilitate the transport of vRNPs into the cytoplasm [47, 71].

1.5.6 Virus assembly and budding from host cells

To produce infectious viruses, all 8 RNA segments need to be incorporated into the new progeny virions. There are two models of viral RNA packaging that have been proposed. The first model proposes that the vRNA segments are packaged randomly in the progeny virions [76, 77]. The second model proposes that vRNA segments contain specific signals and these dictate which vRNAs will be packed into new virions. Packaging signals have been identified in the $5^{/}$ and $3^{/}$ coding and non-coding regions of some vRNAs [71, 78-81].

Formation of complete virion particles requires all structural proteins and vRNPs to be transported to the cellular plasma membrane. Glycoproteins HA, NA and M2 use exocytic pathway and are transported to the cytoplasmic membrane through the trans-Golgi network (reviewed in [82]). HA and NA are transported to the plasma membrane containing lipid rafts, but M2 protein does not need to be attached to plasma membrane lipid raft. There are two possible mechanisms by which M1 carries vRNP to the assembly site. M1 interacts with vRNP and is transported to the plasma membrane either through the cytoskeleton or by piggy-backing on NA and HA cytoplasmic tails (reviewed in [82]). Virion budding requires the formation of plasma membrane curvature where M1 plays a major role. NA and HA cause deformation of plasma membrane and initiate budding. M1, which is bound to the NA and HA cytoplasmic tails in plasma membrane, starts polymerization, and forms inner structure of new virion [83]. M1 may have a role for recruiting M2 in virion budding site. M2 alters membrane curve at the neck of the buds, which causes membrane scission and the detachment of enveloped virions [83]. After separating enveloped virions from plasma membrane, the HA of the new progeny virions becomes attached to sialic acid receptors of the host cells [29]. NA has sialidase activity that removes the sialic acid, and thereby facilities viral release from the host cell [12].

1.6 Antiviral drugs against Influenza viruses

Currently two classes of clinically approved anti-influenza drugs are available: M2 inhibitors and NA inhibitors. M2 inhibitors Amantadine and Rimantidine target IAV M2 ion channel protein, which is required for effective uncoating of vRNPs during virus entry [84]. Unfortunately, both of these M2 inhibitors lack antiviral activities against

Influenza B viruses [85]. Amantadine- and Rimantidine-resistant Influenza viruses have been increasing, which limits the effectiveness of the M2 inhibitors from preventing the spread of Influenza viruses among the human population [86, 87]. In addition, H5N1 isolated from birds and humans also showed resistance to M2 inhibitors [88]. Influenza NA is an essential protein for viral infectivity. Zanamivir and oseltamivir are NA inhibitors, which were found to inhibit different strains of influenza A and B viruses. NA inhibitors inhibit the release of new progeny viruses from infected cells; therefore, they reduce the spread of Influenza viruses to other cells. NA inhibitors have been effective in controlling some recent outbreaks including the 2009 H1N1 pandemic [89]; however, resistance to NA inhibitors has also been emerging [90, 91].

1.7 Host's Immune responses to Influenza virus infection

Influenza viruses initiate infection in the human respiratory tract. Viruses enter the host through nasal and oral cavities, pass through the mucous membrane of respiratory epithelium, and invade the respiratory epithelial cells. Afterwards, these can spread to both immune and non-immune cells in the respiratory tracts [92, 93]. The innate immune system acts as the first line of defense to control Influenza virus replication. The host's innate immune system can detect viral RNA, which is an Influenza viral pathogen associated marker pattern (PAMP), via pathogen recognition receptors (PRRs). There are three classes of PRRs that can recognize Influenza virus infection that include Toll-like receptors (TLR), retinoic acid-inducible gene I (RIG-I) and NOD-like receptor family LLR-pyrin domain containing 3 (NLRP3) (reviewed in [92, 94]).

1.7.1 Recognition of influenza virus by TLR

TLR3 recognizes double-stranded RNA (dsRNA) in the endosome [95]. Although Influenza virus contains ssRNA, it is proposed that TLR3 can recognize unknown RNA structures, which are found in phagocytosed virus infected cells [96]. TLR3 induces the production of pro-inflammatory cytokines and restricts influenza virus replication. TLR7 recognizes influenza virals sRNA in the endosomes of plasmacytoid dendritic cells (DC) and activates either interferon regulatory factor 7 (IRF7) or nuclear factor-κB (NF-κB). Both IRF7 and NF-κB are transcription factors that stimulate type I interferon (IFN) and pro-inflammatory cytokine expressions, respectively, to block viral replication and produce antibody responses (reviewed in [92]).

1.7.2 Recognition of viral RNA by RIG-I

RIG-I like helicase receptors are present in the cytoplasm of macrophages, epithelial cells, and dendritic cells. These are vital for viral detection and type I IFN production. After infection, Influenza viral ssRNA replicates and is released into the cytoplasm from the nucleus. RIG-I recognizes $5^{/}$ triphosphate of viral ssRNA in the cytoplasm [92, 97, 98]. After recognizing viral ssRNA, RIG I binds to ATP and induces conformational changes. This facilitates the RIG I caspase recruitment domains to bind with the signalling adaptor mitochondrial antiviral signalling protein (MAVS) [99, 100]. MAVS signalling results in production of pro-inflammatory cytokines that leads to NF-κB activation, and the production of type I IFNs via IRF3 activation (reviewed in [92]).

1.7.3 Role of NLRP3 inflammasome in infected cells

The NLRPs form the inflammasome complex, which catalytically activates pro-caspase 1 into its activated form. Therefore, the active complex cleaves pro-IL-18 and pro IL-1β into the active forms IL-18 and IL1β, respectively [92]. Inflammasome activation mediated by NLRP3 has been found to be an important immune response during influenza virus infection [101]. Formation of NLRP3 inflammasome is activated when host cells are stressed and cell membranes are damaged [102]. Triggering of inflammasome mediated cytokine production requires two signals. Signal 1 activates NFκB to induce the transcription and translation of pro-IL18, pro-IL-1β and NLRP3 genes, which is mediated by TLR, Tumor Necrosis Factor Receptor (TNFR) and IL-1 receptor [92, 102]. Signal 2 is induced by host cell damage; thereby it activates caspase 1 and induces the IL-18 and IL-1β secretions. Influenza virus ssRNA, PB1-F2 fibrils in the phagosomes and proton flux through virus encoded M2 ion channel protein in the trans-Golgi networks have been reported to provide signal 2 [101, 103, 104].

1.7.4 Roles of macrophages, natural killer cells and dendritic cells

Macrophages play important roles in innate immunity. Alveolar macrophages play essential role in controlling H1N1 influenza viruses in pigs [105]. After infection of the alveoli, alveolar macrophages are activated and phagocytose influenza virus infected cells. Activated macrophages also produce nitric oxide synthase 2 (NOS2) and tumor necrosis factor alpha (TNF-α), which contribute to influenza virus mediated pathology [94, 106, 107]. In addition, activated macrophages can also modulate adaptive immune responses by developing antigen-specific T cells during influenza virus infection [108].

Natural killer (NK) cells can destroy influenza virus-infected cells by antibody-dependent cell cytotoxicity (ADCC) process, where NK cells can recognize specific antibodies bound to the virus-infected cells [94]. NK cell cytotoxic receptors NKp44 and NKp46 can recognize influenza virus HA protein during viral attachment, which triggers NK cells to lyse infected cells [109, 110].

Dendritic cells (DCs) are antigen presenting cells (APCs) and these are the essential members of innate immune responses. These cells present viral antigens to T lymphocytes and act as a link between innate and adaptive immunity. During infection, dendritic cells acquire and present antigens with major histocompatibility complex (MHC) in two different mechanisms. During influenza virus infection in the DC, the viral proteins are processed in the cytosol by proteasomes and loaded onto MHC class I (MHC-I) molecules in endoplasmic reticulum. Then viral peptide-MHC-I complexes are transported to the cell membrane via Golgi network and presented to virus specific CD8+ cytotoxic T cells (CTLs) (reviewed in [94]). In the second mechanism, DCs get viral antigens by phagocytosing viral particles and infected apoptotic cells. Viral proteins are degraded in the endosomes and antigenic peptides are loaded on MHC-II molecules. The viral peptide-MHC-II complexes are then transported to the cell membrane and presented to CD4+ helper T cells (reviewed in [94]).

1.7.5 Role of IFN-stimulated genes (ISGs) against Influenza virus

Type I IFN can induce expression of different other genes called IFN-stimulated genes (ISGs) in neighbour cells, which develop the antiviral state. MX proteins are the products of ISGs and were identified to limit influenza virus replication [111]. MXA and

MXB are human myxovirus-resistant proteins, which are induced by IFN stimulations. MXA is a cytosolic protein and it restricts influenza A virus replication [112]. IFN-inducible transmembrane (IFITM) proteins play roles in restricting different viral replication including Influenza virus. These proteins inhibit viral attachment and endocytosis by blocking membrane fusion step [92, 113, 114]. The 2′-5′-oligoadenylate synthase (OAS) proteins can degrade viral RNA in host cell cytoplasm with the help of ribonuclease L (RNase L) and inhibit viral replication (reviewed in [92]). Protein kinase R (PKR) is another product of ISGs. It is a serine/threonine kinase that helps to initiate eukaryotic translation. During viral infections, PKR also inhibits the viral protein translation process by binding dsRNA and restricts virus replication [92]. Activation of PKR in infected cells can also induce apoptosis and autophagy, which limit the spread of the progeny viruses from the host [115]. Genetically PKR deficient mice were found to be more susceptible to influenza virus infection compared to the control mice [116]. Although influenza virus contains ssRNA, panhandle secondary structures are formed between viral RNA termini that stimulated PKR during infection [92, 117].

1.8 Escaping host defence by influenza virus and role of NS1

Host's immune pressure (selective pressure) on IAVs forces them to develop strategies (natural selection) for escaping the host immune system. The host's immune pressure, segmented nature of influenza viral RNA, and high mutation rates enable influenza virus to generate new types or strains via antigenic shift or drift that are partially, or not, recognized by the host's existing adaptive immune system. In addition, Influenza virus proteins bind to different machineries of the immune system to escape the host's innate immune system (reviewed in [94, 118]).

IAV NS1 is a multifunctional protein, and the main role of this protein is to antagonise the host innate immune system (Figure 6) (reviewed in [48, 94, 119]). Influenza virus with truncated NS1 induced strong IFN secretion and reduced the morbidity in several animal models including swine, mice, and macaques [55, 120, 121].

NS1 protein inhibits host's RIG-I signalling cascade by different mechanisms. In the first mechanism, NS1 protein blocks the activation of transcriptional factors NFκB and IRF3, which are required for the activation of IFN transcription [50, 122, 123]. RIG-I usually binds to the viral RNA and changes its conformation, exposing the N-terminal CARD domain. This CARD domain is activated by ubiquitination catalyzed by E3 ligase TRIM25, enabling IFN transcription to occur [124]. In the second mechanism, it is proposed that NS1 binds to TRIM25 and suppresses IFN production (reviewed in [50]). NS1 of laboratory adapted strain Influenza A/PR/8/34 (H1N1) interacts directly with RIG-I [125, 126]. However, it is not clear whether this interaction blocked IRF3 activation or not. In another mechanism, NS1 can bind with 30 kDa subunit of the cellular cleavage and polyadenylation specificity factor (CPSF30), which is required for the processing of host pre-mRNAs into mature mRNAs [50, 127]. These mRNAs include antiviral and IFN mRNAs.

Influenza NS1 can inhibit antiviral activity of IFN-induced protein PKR, which is expressed in mammalian cells and activated by either dsRNA or cellular PACT (Protein Activator of the interferon-induced protein kinase). It is assumed that NS1-ED (effector domain) binds to PKR and inhibits its conformational changes (reviewed in [50]). $P58^{IPK}$ is a cellular inhibitor that makes a complex with heat shock protein 40 (HSP 40) and regulates the activity of PKR. IAV infections can upregulate $P58^{IPK}$ expression

A

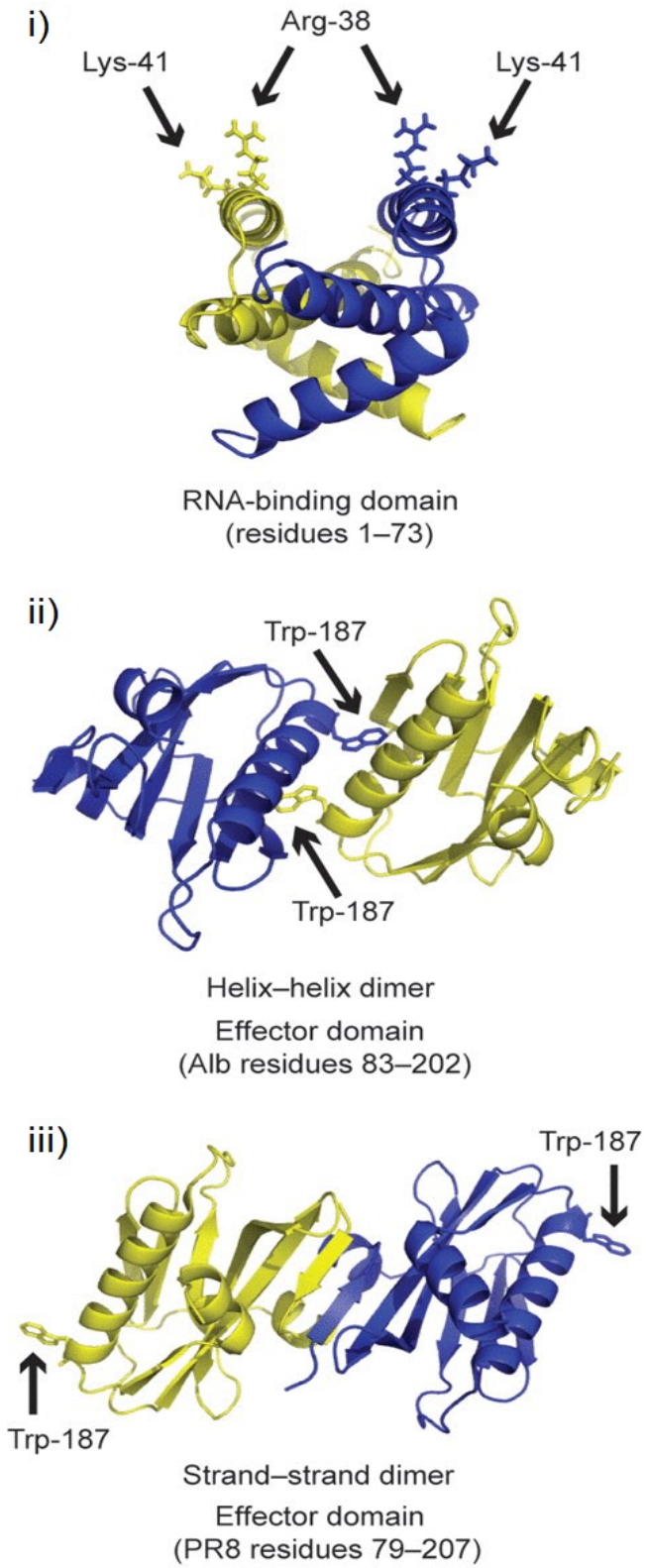
i)
Arg-38
Lys-41
Lys-41
RNA-binding domain
(residues 1–73)
ii)
Trp-187
Trp-187
Helix–helix dimer
Effector domain
(Alb residues 83–202)
iii)
Trp-187
Trp-187
Strand–strand dimer
Effector domain
(PR8 residues 79–207)

B.

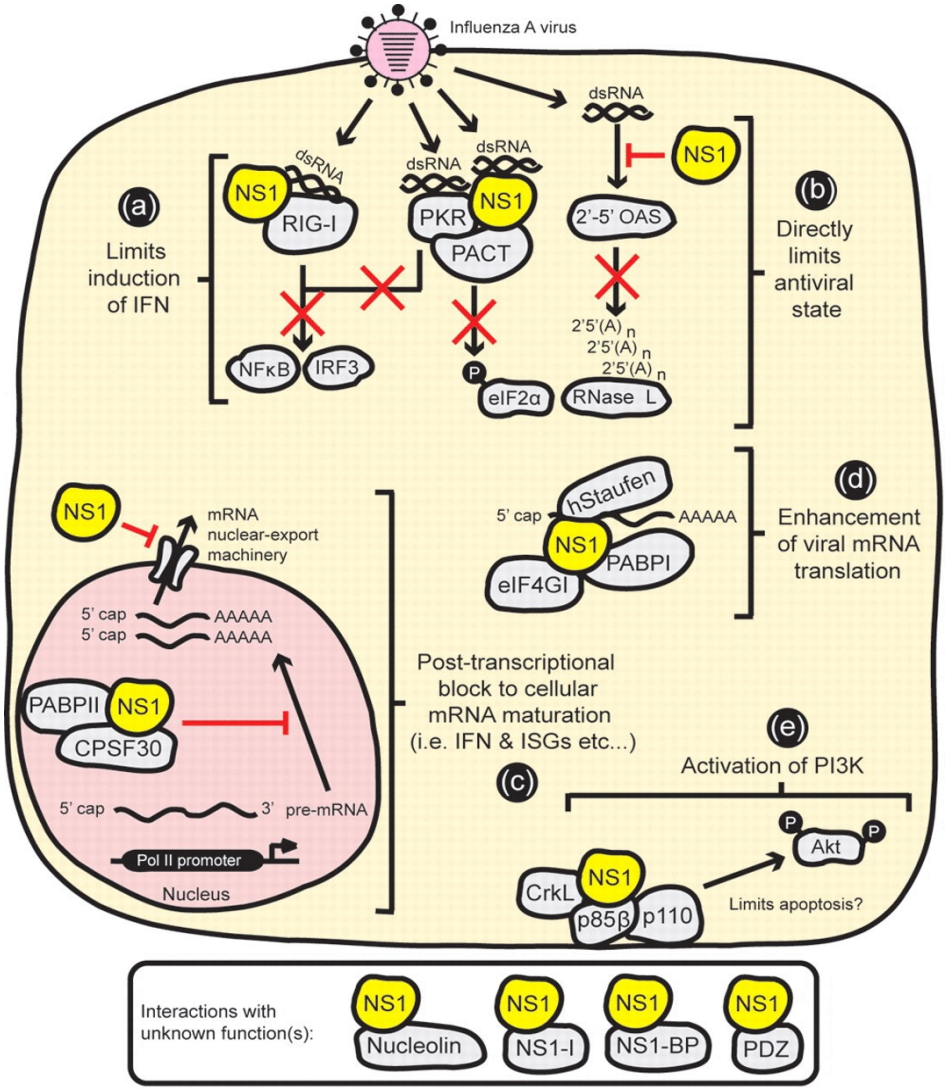

(Hale, B.G., et al., *J Gen Virol*, 2008. 89(Pt 10): p. 2359-76.)[48]

Figure 6: Structure of NS1 and Schematic diagram of the multiple functions of NS1 within infected cells.

A. Structure of the influenza A virus NS1 protein. (i) Cartoon ribbon representation of the dimeric RNA-binding domain (A/Udorn/72 [H3N2]; residues 1–73). Arg-38 and Lys-41, which are critical for RNA-binding, are highlighted. (ii) and (iii) Cartoon ribbon representations of the two proposed effector domain dimerization conformations. (ii) A/Duck/Albany/76 [H12N5] residues 83–202 (helix–helix dimer). (iii) A/Puerto Rico/8/34 [H1N1] residues 79–207 (strand–strand dimer). Trp-187, which has been shown experimentally to be essential for dimerization of the avian NS1 protein effector domain, is highlighted in both structures. For all structures (i–iii), monomers are coloured blue and yellow. Images were prepared using MacPyMol (PDB files: 1NS1, 2GX9, 3D6R). B. Multifunctional roles of NS1. (a) Pre-transcriptional limitation of IFN-β induction. (b) Inhibition of the antiviral properties of PKR and OAS/RNase L. (c) Post-transcriptional block to processing and nuclear export of all cellular mRNAs. (d) Enhancement of viral mRNA translation. (e) Activation of PI3K. Interactions with unknown consequences and/or localizations are detailed in the lower box. [48].

(Permission was obtained from *Journal of General Virology* for republishing in my thesis)

[128]. Although the mechanism of upregulation is not known, it is suggested that IAV infection causes the detachment of $P58^{IPK}$ from HSP40 (reviewed in [119]). On the other hand influenza M2 protein can associate with $P58^{IPK}$-HSP40 complex and can inhibit $P58^{IPK}$ release. Therefore, the M2 inhibits protein synthesis, induces apoptosis and enhances viral particle release [129]. OAS ($2^{/}$-$5^{/}$ oligo A synthetase), an IFN-induced protein, is activated by dsRNA to produce poly (A) chain that activates RNase L expression. RNase L can cleave viral ssRNA and thereby inhibit viral replication [130]. NS1 RBD (RNA binding domain) binds dsRNA and inhibits the activation of OAS/RNase L pathway [50, 131]. Influenza PB1 protein also inhibits cellular antiviral activities. PB1-F2 binds to MAVS, which inhibits type I IFN production [132]. Influenza PB2 protein can also inhibit IFN-β production by binding and inhibiting IFN promoter stimulator 1 (IPS-1) [133].

1.9 Influenza A viruses –host interaction

Influenza viruses are obligate intracellular parasites. Successful viral infection requires the co-operation of host cells. Viruses extensively utilize host cell machineries for productive replication. Influenza viruses also influence cell signalling pathways to evade the host's immune system. During Influenza virus infection, host proteins have been found to be expressed differentially compared to non-infected cells, which are probably required to support viral life cycle or maintain host cell stress response. These differentially regulated proteins are involved in different cellular pathways and functions such as host cell immunity, cell adhesion, signal transduction and transcription [134-137]. Several studies have detected host factors that are involved in IAV replication by

genome-wide RNAi screenings [114, 138, 139]. From the beginning to the end of influenza virus replication, different host proteins play important roles. Watanabe et al. identified, reviewed, and mapped the influenza virus –host interactions in the individual steps of the viral life cycle (Figure 7) [140]. During Influenza virus replication, it is assumed that different viral proteins interact with various host factors to achieve successful replication. A complete understanding of virus-host interactions can provide us detailed mechanisms of influenza virus replication from which some strategies can be identified to prevent viral infections. In the last two decades, many host proteins were found to interact with Influenza NP and RNA-dependent RNA polymerase complex (PA, PB1 and PB2) where some of these regulated the viral replication process [141-146].

During infection, Influenza A NS1 protein is expressed at a very high level, and it has multiple accessory functions by interacting with different host factors (reviewed in [48, 94, 119]). Although the NS1 proteins are not incorporated within new progeny viruses, high expression level indicates that NS1 may play crucial roles during viral replication. According to the VirHostNet 2.0 (http://virhostnet.prabi.fr/) [147] as of May 2016, 202 cellular proteins were previously detected and/or reported to interact with Influenza A NS1. Many of the NS1-interacting host factors play important roles during viral infection that include: p85 subunit of Phosphoinositide 3-kinase (PI3K), CPSF30, poly A binding protein (PABII), TRIM25, hnRNA-F, HSP 90, RNA-Associated Protein 55 (RAP55), hnRNP A2/B1, RNA Helicase A, β-Tubulin, Staufen1, DDX21 RNA helicase, PACT, and PRP19. Most of the interactome studies were done by using tag sequences such as TAP/Strep/Flag/V5/FS tags within NS1 sequences, and where co-immunoprecipitations (co-IPs) were done targeting the tags and NS1 interacting host

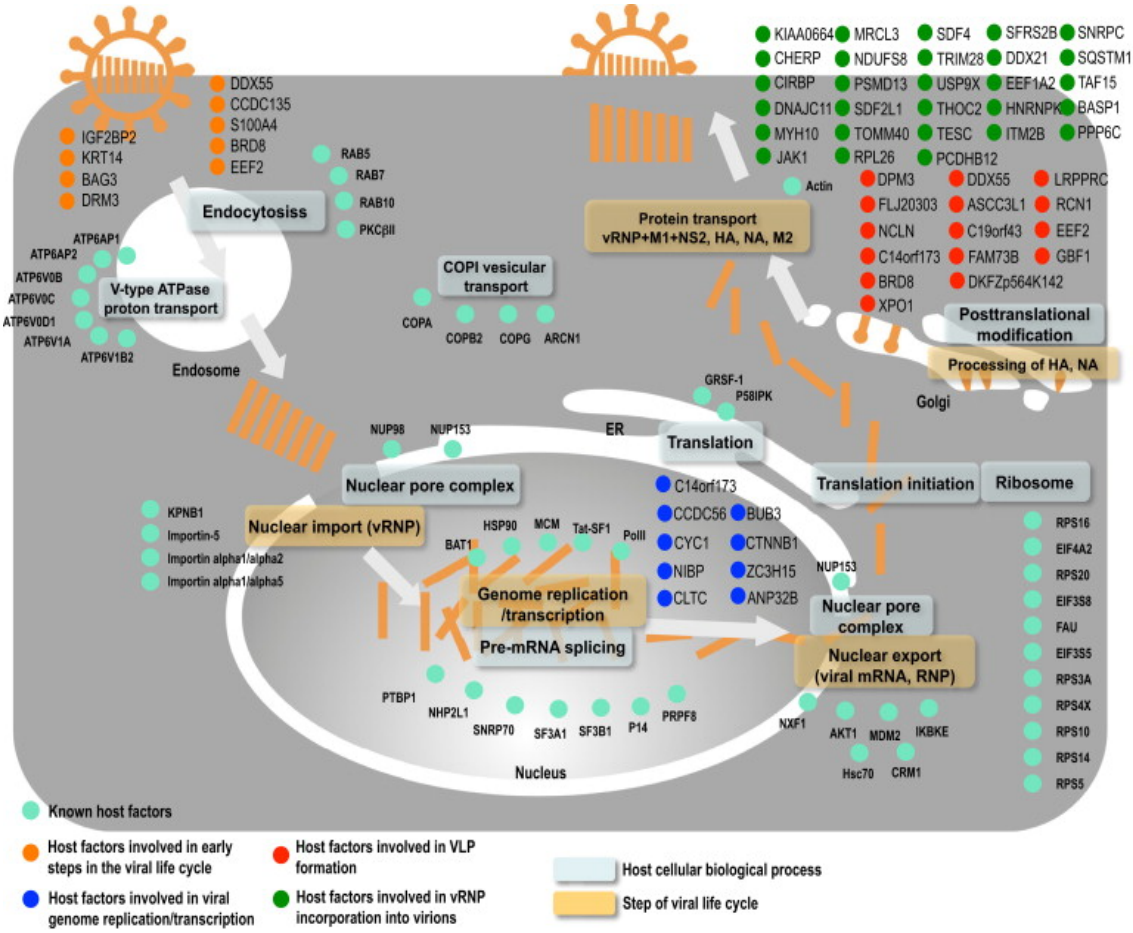

(Watanabe, T., et al. *Cell Host Microbe*, 2014. 16(6): p. 795-805) [140]

Figure 7: Proposed roles of host factors in the Influenza Virus Life Cycle.

The light orange boxes refer individual steps of viral life cycle; the gray boxes refer host cellular processes that are probably involved. Host factors identified in Watanabe et al's study are grouped according to the viral life cycle steps they affected; light green circles refer host factors identified in other studies. [140].

(Permission was obtained from the journal *Cell Host Microbes* for republishing in my thesis)

proteins were identified by mass spectrometry [148-154]. Few other interactome studies were conducted by yeast 2 hybrid systems [155, 156].

In my studies, I identified many NS1-interating host proteins, described later in this thesis, which were not previously identified at the time of my experiments. Among these, NUMA1 and PRPF19 are the two NS1-interacting proteins, knocking down of their expressions in human bronchial cells significantly reduced IAV production in my studies. Therefore, I targeted NUMA1 and PRPF19 and studied them in more detailed.

1.10 Nuclear mitotic apparatus protein (NuMA)

NuMA, which is also known as NUMA1, was the first protein discovered in 1980 that shuttles from the nucleus to the spindle poles during mitosis [157]. NuMA is considered an important structural component of both the nucleus and spindle poles, and it plays essential roles during the assembly and maintenance of the mitotic spindle in the cell cycle (reviewed in[158]). It is a 236 kDa coiled protein, resistant to high salt and detergent, and it forms nuclear matrix in interphase cells [159-161]. NuMA is mainly an insoluble nuclear protein that binds to chromatin during interphase. Phosphorylation and dephosphorylation of NuMA (at the start and end of mitosis, respectively) regulates its differential localization in the cytoplasm and nucleus [161]. When the nuclear membrane starts disassembling, NuMA is phosphorylated by $p34^{cdc2}$, scattered into the cytoplasm, trans-located at the spindle poles via dynein-mediated mechanism, and remains in spindle poles until anaphase [162-164].

Cellular genomes are segregated through microtubule spindles in each cell cycle. The microtubule spindles are assembled at the beginning and disassembled after the end

of mitosis. Spindle assembly event initiates when nuclear membrane breaks, where mitotic microtubules are nucleated at the centrosomes and the minus-end of microtubules are anchored to the spindle poles [158]. NuMA plays a vital role by tethering the microtubule to the spindle poles [158]. Although previous studies showed that NuMA needed to be associated with dynein and dynactin for binding with microtubules [164, 165], the C-terminal tail of NuMA was also found to bind directly with tubulin [166]. NuMA is dephosphorylated, and released from the spindle poles after the onset of anaphase. Therefore, reformation of daughter nuclei starts following the disassembly of spindle poles (reviewed in [162]).

Taimen et al. (2004) first noticed that NuMA was cleaved and excluded from condensed chromatin in Human rhinovirus 1B (HRV 1B) and measles virus (MV) infected HeLa cells [167]. It was thought that these viral infections activated some proteases that cleaved NuMA. In addition, caspase inhibitor prevented the cleavage of NuMA and nuclear breakdown that indicated NuMA as a target in virus-infected programmed cell death [167]. NuMA protein is solubilized and modified extensively, including phosphorylation at unknown sites during Herpes Simplex Virus (HSV) infection [168]. Knocking down NuMA expression in Hep-2 cells also decreased HSV growth.

1.11 Pre-mRNA-processing factor 19 (PRP19)

Pre-mRNA-processing factor 19 (PRP19), which is also known as PSO4 or PRPF19, is a 55 kDa protein that is considered a splicing factor in human and different yeast species [169, 170]. Human PRP19 protein contains N- terminal U box domain, a

central coiled domain, C-terminal WD40 region and other domains (reviewed in [170]). The U-box domain has ubiquitin ligase activity and other domains bind with host factors [171-173].

Splicing is an important post transcriptional modification step in eukaryotic cell, which removes intron sequences. Splicing takes place in spliceosome. The spliceosome is assembled by sequential interactions of snRNPs U1, U2, U4, U5, U6 and additional host factors. PRP19 plays vital roles in assembling and activating spliceosome. U1 and U4 are dissociated from U4/U6-U5 complex immediately after arrival of the PRP19-associated complex, also known as nineteen complex (NTC) in yeast, and consequently the spliceosome becomes activated [170, 174, 175]. In addition, NTC plays essential role to maintain the stable interactions of U5 and U6 after the dissociation of U4 and activation of spliceosome [176].

Different environmental chemicals can cause DNA damage by breaking its double strands and intra-strand cross-links. PRP19 plays vital roles in cellular response to DNA damage that includes DNA damage repair, which decreases apoptosis and enhances cell survival [170, 177-179]. PRP19 can randomly bind to the double strand break sites of DNA and recruit deoxynucleotidyl transferase, metnase, and other host factors for repairing the damage [179, 180]. Depletion of PRP19 induces apoptosis in HeLa cells [181]. In another study, apoptosis was reduced in HeLa cells where PRP19 was over expressed and exposed to DNA damage [182]. This survival strategy is perhaps due to the important role of PRP19 during DNA damage.

1.12 Rational and Goal

Influenza A virus (IAV) is considered one of the major threats that causes contagious respiratory disease in humans. Every year Influenza virus threatens the human population with epidemics and pandemics. In recent years, human infections with avian influenza viruses such as H5N1 and H7N9 subtypes have pointed towards the potential of this virus to cause pandemics in the future. Although two classes of anti-influenza drugs (M2 and NA inhibitors) are available, emergence of drug-resistant Influenza viruses is becoming a serious concern. In the future, influenza virus may lose sensitivity to all available drugs due to the segmented nature of genomes and high mutation rate. Therefore, development of new concepts and drugs are needed to overcome the problem of antiviral resistance.

The roles of Influenza multi-functional NS1 protein have already been described in previous sections. This NS1 is assumed to interact with various host proteins to serve its multi-functional role during viral replication. Identification of novel and essential NS1-interacting host factors can divulge detailed mechanism of virus replication and serve as alternative non-viral targets to develop new antiviral therapies.

Although many host factors have been identified to interact with Influenza NS1, most of the studies were conducted by either yeast 2 hybrid systems or introducing peptide-tag sequences within NS1 sequences where tagged-NS1 proteins were expressed, co-immunoprecipitated (IPs) targeting the tags and NS1-interactors were identified by mass spectrometry . I believe that adding or inserting or substituting any tag sequences within the NS1sequence may impede its native structure where epitope masking can

occur. Therefore, the natural affinities of host factors to native NS1 protein may be interfered with when the recombinant NS1 proteins are expressed in host cells. Although many cellular factors have been reported to interact with NS1, I strongly believe that more host candidates with significant roles in viral life cycle can be identified during IAV infections, particularly if native NS1 protein is expressed.

The overall goal of my project is to develop and characterize broadly cross reactive monoclonal antibodies that can detect native Influenza A NS1, to identify host factors that interact with native IAV NS1, and to determine how some of these factors affect Influenza A virus growth.

1.13 Hypothesis and Objectives

I hypothesize that different cellular proteins interact with Influenza A virus NS1 and that some of these are required and critical for virus replication.

The objectives for my study are the following:

Objective 1: To generate and characterize broadly cross-reactive anti-NS1 monoclonal antibodies (mAbs).

Objective 2: To identify interactions between IAV-NS1 and host's cellular proteins using tools from Objective 1.

Objective 3: To determine the effects of these cellular factors on IAV replication and target a few NS1-interacting proteins for analyzing their roles in viral replication.

Part 2. Materials and Methods

2.1 Media and solutions

All media and solutions were made in double distilled water (ddH_2O).

2.1.1 Medium for culturing Madin-Darby canine kidney (MDCK) cells

1x Complete Dulbecco's Modified Eagle Medium (DMEM; Gibco, cat# 12100-061), supplemented with 5% fetal bovine serum (FBS; Gibco, cat# 12483), 2 mM l-glutamine (Gibco, cat# 25030-081), 2 mM sodium pyruvate (100 mM; Gibco, cat# 11360-070) and 1x MEM non-essential amino acids (Gibco, cat# 11140-050).

2.1.2 Medium for culturing human alveolar basal epithelial (A549) cells

1x Complete DMEM, supplemented with 10% FBS, 2 mM l-glutamine, 2 mM sodium pyruvate and 1x MEM non-essential amino acids.

2.1.3 Medium for Influenza A virus infection overlay

1x DMEM, supplemented with 2 mM l-glutamine, 2 mM sodium pyruvate and 1x MEM non-essential amino acids.

2.1.4 Medium for Influenza A virus plaque assay overlay

1x DMEM, supplemented with 0.6% type I agarose (Sigma Aldrich, cat# A6013), 2mM l-glutamine, 2mM sodium pyruvate and 1x MEM non-essential amino acids.

2.1.5 RIPA buffer

RIPA buffer contained 150 mM NaCl, 1.0% NP-40 (IGEPAL® CA-630), 0.5% sodium deoxycholate (DOC), 0.1% sodium dodecyl sulphate (SDS) and 50 mM Tris (pH 8).

2.2 Cells and Viruses

MDCK and A549 cells were cultured in complete Dulbecco's modified Eagle's medium (DMEM) supplemented with 5% or 10% fetal bovine serum (FBS) as specified in section 2.1. IAV strains (Table 1) PR8 (H1N1), B59 (H1N1), NCal (H1N1), NY55 (H3N2), HK1 (H3N2) and B10 (H3N2) were grown in 10-day-old embryonated chicken eggs. Some virus strains were grown in MDCK cells by infecting at a multiplicity of infection (MOI) of 0.01 for 48 hrs and concentrated at 64,000 ×g for 2 hrs at 4^0C.

Table 1: Influenza virus strains used in this study

Influenza A virus	Subtype	Abbreviation	Characteristics
A/Puerto Rico/8/1934	H1N1	PR8	Lab adapted, attenuated
A/Brisbane/59/2007	H1N1	B59	Seasonal strain
A/New Caledonia/20/1999	H1N1	NCal	Seasonal strain
A/Brisbane/10/2006	H3N2	B10	Seasonal strain
A/Hong Kong/1/1968	H3N2	HK1	Pandemic prototype strain
A/New York/55/2004	H3N2	NY55	Seasonal strain

2.3 Virus titration

Viral stocks and experimental samples were titrated by plaque assay in MDCK cells. Briefly, the virus samples were diluted into serum-free 1x DMEM media in 1:10 serial dilutions. MDCK cell monolayers were washed twice with 1x phosphate buffered saline (PBS; 137 mM NaCl, 0.3 mM KCl, 0.8 mM Na_2HPO_4, 0.1 mM KH_2PO_4) and infected with different dilutions of the virus samples. The monolayers were overlaid with 1x DMEM plaque assay overlay media as specified in section 2.1, supplemented with 2.5 µg/mL trypsin, 1x gentamicin and 1x amphotericin B. Infected cells were incubated at 35^0C in 5% CO_2 humidified environment for 65-72 hrs. After incubation, cell monolayers were fixed with 2% formaldehyde for 2 hrs, agarose plaques were removed from the top of the cell monolayers, washed twice with distilled water and stained with crystal violet stain for 1 hr. After staining, cell monolayers were washed and viral plaques were counted. Viral titre was determined as plaque forming unit (pfu) per mL.

$$\text{Pfu/mL} = \frac{\text{Number of plaques}}{\text{Dilution factor X volume (mL) of diluted virus added in monolayer}}$$

2.4 Mice immunization and antibody production

An overview of the experimental design is shown in Figure 8. His 6-tagged HK1 NS1 (H3N2 subtype) was kindly provided by Dr. Earl Brown, which was used to immunize 6-8 week old BALB/c female mice. Mice were immunized with 40µg His 6-tagged NS1 in 100 µL PBS and 100 µL of Titre-Max Gold adjuvant (Cedarlane Laboratories). A month after first immunization, the mice were boosted with 40-50 µg more His 6-tagged NS1. The spleen cells were collected from immunized mice and fused

with myeloma SP2/0 cells. The immunization and cell fusion process were performed by our lab technician according to the Canadian Council on Animal Care's guidelines. The hybridomas were grown in RPMI 1640 (Gibco, Invitrogen) supplemented with 20% mouse spleen-conditioned medium and 15% FBS. After 10-13 days, the supernatants were collected and screened using GST-tagged PR8 NS1 (H1N1) as antigen in enzyme-linked immunosorbent assays (ELISA). The positive clones were validated by Western blot analysis and sub cloned by limiting dilution method [183].

After sub-cloning, isotyping was performed with a mouse antibody isotyping kit (Amersham). The hybridomas were grown in serum-free RPMI (Gibco) for 2 weeks, and the supernatants were collected and passed through protein G columns (GE Healthcare, Canada). The columns were washed five to six times and antibodies were eluted with glycine elution buffer (100 mM Glycine-HCl, p^H 2.7). The glycine was removed by dialysis in PBS overnight at 4^0 C and the concentrations of the antibodies in PBS were measured by bicinchoninic acid assay (BCA) (Pierce).

2.5 Western Blot analysis

MDCK, A549, and Mouse M1 (kindly provided by Dr. Earl Brown) were infected with different strains of IAVs (Table 1) at an MOI of 1, 3 or 5. Cell lysates were obtained at different times (0 to 24 hour post infection) by lysing the cells in 0.5% NP-40 or RIPA buffer with complete protease inhibitors (Roche). Cells lysates were tested for protein concentration by a Pierce™ BCA Protein Assay Kit (Thermo Scientific). Samples were mixed with SDS electrophoresis sample buffer with 90 mM DDT, boiled and subjected to

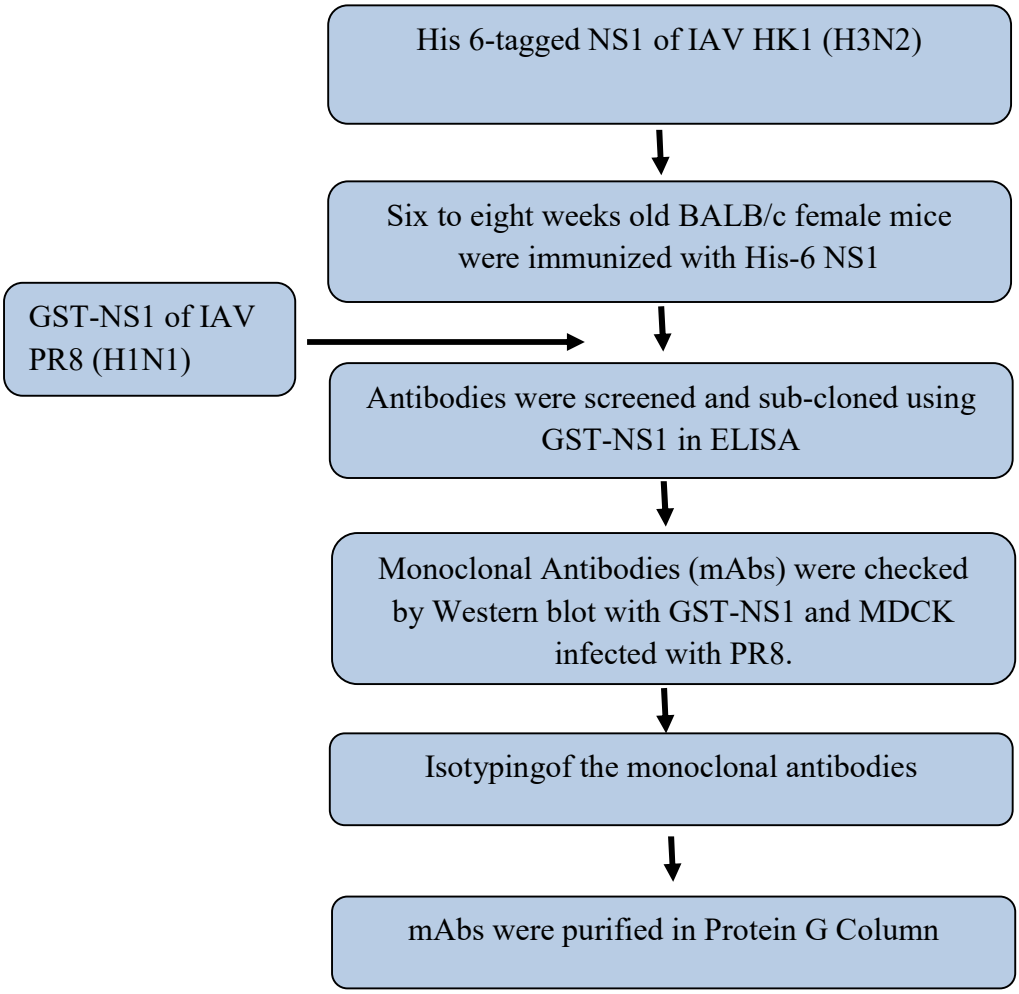

Figure 8: Flow diagram showing the different steps to produce anti-NS1 mAbs.

electrophoresis in 4–12% gradient Novex NuPAGE SDS-PAGE Gels (Invitrogen). Proteins from the gels were transferred to Immobilon-P PVDF membranes (Millipore). Slot blot analysis was done where equivalent amounts of cell lysates were boiled and immobilized on activated Immobilon-P PVDF membranes (Millipore), in a slot blot unit (Hoefer PR 648). All membranes were blocked in 5% skim milk treated with primary and secondary antibodies conjugated with HRP (list of antibodies are in Table 2). Signals were detected using enhanced chemiluminescence (ECL) reagent (prepared in house) and images were taken in an Alpha Innotech Fluor Chem® Q Imaging System and processed by Adobe® Photoshop® software.

2.6 Immunofluorescence Microscopy

MDCK cells were seeded in autoclaved 12-spot (6 mm diameter) slides (15,000 cells per spot) and grown 24h at 37^0 C. The spots were washed 2 times with PBS, cells were counted and different strains of IAV (Table1) were added to spots. Viral adsorption was done at 4^0C for 1 hour at MOI 1 or 5, then spots were overlaid with serum-free IAV infection overlay media specified in section 2.1, supplemented with 2.5 µg/mL trypsin, 1x gentamicin and 1x amphotericin B. After infection, the spots were fixed at different times (0-24 hr post infection) with 4% paraformaldehyde for 15-20 mins. After fixing, the cells were permeabilized with 0.1% (v/v) Triton X100 for 5 mins, blocked with 1% BSA (bovine serum albumin) in PBS for 1.5 hrs and probed with primary antibodies (Table 2) diluted in 1%BSA/PBS (1:500 dilution) overnight at 4^0 C. Afterwards, cells were washed 4 times with PBS, treated with Alexa Fluor 546- conjugated goat anti-mouse secondary antibodies diluted in 1% BSA/PBS (1:250), DAPI (diluted 1:5000) and phalloidin Alexa

Fluor 488 (diluted 1:200) for 1 hr at room temperature. Slides were washed 4 times with PBS, images were taken after adding ProLong Gold mounting (Invitrogen) with a Zeiss LSM710 laser-scanning microscope (Carl Zeiss Micro Imaging).

2.7 Epitope mapping of mAbs and Competitive ELISA

Purified mAbs were sent to Pepscan Therapeutics (The Netherlands) for linear overlapping peptide epitope mapping [184]. 216 copies of 15 mer (amino acid) peptides were synthesized with 1 amino acid overlap by Pepscan, which were targeted to the PR8 NS1. All peptides were bound to a Pepscan array and each array was treated with each antibody and bound antibody was detected by ELISA.

Competitions between different epitopes were determined according to the procedure described in Harlow et al. 1988 [183]. Briefly, 96-well plates were coated overnight with 25 ng GST–PR8-NS at 4^0 C. Wells were washed 3 times with washing buffer (0.05% Tween 20 in PBS), blocked with 1% BSA in PBS, and treated with the different tested blocking antibodies (50 µg) overnight at 4^0C. The plates were washed five times with washing buffer and incubated with biotinylated mAbs (5 µg) for 2 hr. Wells were washed and treated with Extra Avidin (Sigma E2636) for 1 hr. After washing five times with washing buffer, wells were developed with alkaline phosphatase/p-nitrophenyl phosphate. Absorbance was measured at 405 nm on a BioTek Synergy 4 plate reader.

Table 2: List of primary and secondary antibodies used in this study

Antibody	Host	Clone	Catalogue	Assay	Source
Primary Antibodies:					
Polyclonal α-PRP19	Rabbit		A300-101A	WB, IP, IF	Bethyl Laboratory
Polyclonal α-RPF1	Rabbit		Ab121833	WB, IP	Abcam
Polyclonal α-RBM28	Rabbit		PA5-22103	WB, IP	Thermo Fisher
Polyclonal α-UTP6	Rabbit		PA5-21716	WB, IP	Thermo Fisher
Polyclonal α-NUMA	Rabbit		A301-510A	WB, IP, IF	Bethyl Laboratory
Monoclonal α-NP	Mouse	F26-9		WB, IF	Gift fromDr. Mingyi Li
Monoclonal α-beta-actin	Mouse	8H10D10	3700S	WB	Cell Signalling
Monoclonal α-M1	Mouse	GA2B	MA1-80736	WB, IF	Thermo Fisher
Polyclonal α-M2	Rabbit		PA5-32233	WB, IF	Thermo Fisher
Monoclonal α-β1 Integrin	Mouse	JB1A		ELISA	Gift from Dr. Wilkins, MCPSB*
Monoclonal α-Emprin (IgG2a)	Mouse			IP (Isotype control)	Gift from Dr. Wilkins, MCPSB*
Monoclonal α-HSA (IgG1)	Mouse	6G11		IP (Isotype control)	Gift from Dr. Wilkins, MCPSB*
Monoclonal α-SYN (IgG2b)	Mouse	6S1-3B		IP (Isotype control)	Gift from Dr. Wilkins, MCPSB*
Monoclonal α-NS1	Mouse	3F5		WB, IF, IP ELISA	Generated in this study
Monoclonal α-NS1	Mouse	5F4		WB, IF, ELISA	Generated in this study
Monoclonal α-NS1	Mouse	7D11		WB, IF, IP ELISA	Generated in this study
Monoclonal α-NS1	Mouse	4E10		WB, IF, IP ELISA	Generated in this study
Monoclonal α-NS1	Mouse	8C7		WB, IF, ELISA	Generated in this study

Antibody	Host	Clone	Catalogue	Assay	Source
Monoclonal α-NS1	Mouse	10C7		WB, IF, ELISA	Generated in this study
Monoclonal α-NS1	Mouse	13D8		WB, IF, ELISA	Generated in this study
Monoclonal α-NS1	Mouse	5D6		WB, IF, ELISA	Generated in this study
Monoclonal α-NS1	Mouse	5B10		WB, IF, ELISA	Generated in this study
Secondary Antibodies:					
Polyclonal α-mouse HRP	Horse		7076S	WB	Cell Signalling
Polyclonal α-rabbit HRP	Goat		7074S	WB	Cell Signalling
Monoclonal HRP VeriBlot			Ab131366	IP, WB	Abcam
Alexa Fluor® 546 α-mouse	Goat		A11003	IF	Life Technologies
Alexa Fluor® 488 α-rabbit	Goat		A11034	IF	Life Technologies
Alexa Fluor® 488 phalloidin**			A12379	IF	Life Technologies
DAPI**			D1306	IF	Life Technologies

WB: Western Blot, IF: Immunofluorescence, IP: Immunoprecipitation
*MCPSB: Manitoba centre for proteomics and systems biology. **Stain

2.8 Nuclear and cytoplasmic fractionation

A549 cells were grown in P150 (150cm^2) plates and infected with PR8 (MOI 5). At 6 and 24 hr post infection (hpi) (both PR8 infected and mock infected), cells were harvested by scraper, washed 3 times with ice-cold PBS by resuspending and pelleting (350×g for 5 mins). The cell pellet was resuspended in cytolysis buffer (0.4% NP40, 1x

protease inhibitor from Roche) on ice for 10 mins, centrifuged (500 ×g for 5 mins) and the supernatants (Cytosol) were collected in a fresh set of tubes. The pellets were resuspended in cytolysis buffer supplemented with 8% sucrose, centrifuged and supernatants were collected and added to the previous set of tubes; this was considered as the cytoplasmic fractions. The remaining pellets were washed 4 times with PBS supplemented with 8% sucrose and 0.25x protease inhibitor by resuspension and pelleting (350 × g for 5 mins). The pellets were resuspended in RIPA buffer, and sonicated 10 seconds placing the tubes in ice. Thereafter, the supernatant was collected by centrifuging at 10,000 × g for 10 min, which was considered as the nuclear fraction. Both the cytoplasmic and nuclear extracts were tested for protein concentration by a Pierce™ BCA Protein Assay Kit (Thermo scientific).

2.9 Co-Immunoprecipitation (Co-IP)

The nuclear and cytoplasmic lysates were pre-cleared in protein G agarose beads before starting Co-IP. In the pre-clearing step, the lysates were incubated with protein G agarose for 90 mins at 4^0C in a rotator then centrifuged at 10,000 × g and supernatants were collected. Co-IPs were done using Dynabeads protein G (Invitrogen) and magnet. Beads were washed 3 times with TBST (Tris-Buffered Saline supplemented with 0.05% Tween 20) and resuspended in TBST. Anti-NS1 mAb mixtures and relevant isotype controls were added into the beads and incubated for 90 min in a rotator to allow the Abs to bind to beads at room temperature. Beads were washed 4 times with TBST and treated with pre-cleared cytoplasmic and nuclear fractions in a rotator overnight at 4^0 C. The unbound fractions were discarded and beads were washed 4 times and resuspended in

TBST. This resuspended bead-Ab-antigen complex is considered as the immunoprecipitated (IP) product. Co-IPs were also done using anti-NUMA1, anti-PRPF19, anti-UTP6 and anti-RPF1antibodies.

2.10 Processing of IP product for Western blot analysis and Mass Spectrometry

The TBST was discarded from IP product and beads were washed 2 times with RIPA buffer. The beads were washed once with Ammonium Bicarbonate buffer supplemented with NP40 (0.1% NP40 in 100 mM Ammonium Bicarbonate buffer) and resuspended with Ammonium Bicarbonate buffer only. 10% of the resuspended beads (Immunoprecipitated beads) were separated with magnet, mixed with SDS electrophoresis sample buffer and 90 mM DDT, boiled and subjected to electrophoresis in 4–12% gradient Novex NuPAGE SDS-PAGE Gels (Invitrogen). 90% of the resuspended beads were saved for Mass Spectrometry analysis. Beads were separated by using magnet. The Immunoprecipitated beads were resuspended in 1µg of trypsin in 100mM ammonium bicarbonate solution in a tube and rotated overnight at 37^0 C for digestion. After tryptic digestion, equal volumes of Trifluoroaceticacid (TFA)/ Acetonitrile (ACN) [100% ACN & 1% TFA] were added into the tubes and the tubes were vortexed for 10-15 min. The supernatants containing digested peptides were collected into new tubes and the tubes were centrifuged at 17,000 × g for 5 mins. Dried peptides were collected by drying the supernatants in a vacuum dryer and resuspended in 50 µl of 0.5% TFA. Desalting of the peptides was done using C18 Millipore® Ziptips. C18 tips were activated by pipetting with 20 µl of 100% ACN 3-4 times and washing 20 µl of 0.05% TFA 5-10 times. Then the activated ziptips were used for mixing the resuspended peptide samples in 0.5% TFA 10-15 times; that allowed the peptides to bind

to the zip-tip beads. The tips were washed with 0.1% TFA 5-10 times and the peptides were eluted from the C18 zip-tips by adding 33-35% ACN in 0.05% TFA. The eluted peptides were analyzed in a high speed Triple TOF 5600 mass spectrometer (AB SCIEX, Concord, Canada). Raw MS data were analyzed using the Protein Pilot^{TM} 3.0 (ABSciex) program. The proteins were identified based on cumulative peptide number and scores.

2.11 Transfection of cells by siRNA

Reverse transfection format (RTF) SMART pool siRNA library, targeting 107 genes were designed in 96 well culture plate formats and purchased from Dharmacon. The library was supplied as eight replicates containing 6.25 pmol of siRNA per well. The Gene symbol and siRNA sequences are included in Appendix A1. Reverse transfection of this siRNA array was carried out according to manufacturer's (Dharmacon) protocol. Briefly, siRNAs were rehydrated with DharmaFECT-1 cell culture media and transfection reagent (Dharmacon) in each well of 96 well plates and incubated for 60 min allowing the transfection reagent to form complex with siRNA at room temperature. After incubation, 4×10^3 A549 cells were added to each well, incubated at 37^0 C with 5% CO_2 for 48 hrs and infected with virus.

A549 cells were also treated with 25 nM of two ON-Target plus siRNAs (Dharmacon) targeting individual host genes according to the manufacturer's protocol (Table 3). ON-Target plus non-targeting siRNA control was also included. The stock siRNAs and transfection reagent DharmaFECT® 1 (Dharmacon) were diluted separately with Opti-MEM® I reduced serum medium (Life Technology). These two diluents were gently mixed, incubated for 20 mins at room temperature and added to the A549 cells for

transfection. Each set of A549 cells were re-treated with the same siRNA after 24 hrs of first transfection for another 24 hrs. At 48 hrs post-transfection (from the beginning of the transfection), cells were infected with virus with MOIs 0.05 and 3. Knock down efficiencies of individual genes were checked by Western blot and IP analysis using specific antibodies to relevant proteins.

2.12 Cell viability assay

Cell viability assays were done using Cell Proliferation Reagent WST-1 (Roche) as per manufacturer's protocol. Briefly, A549 cells were grown in 96 well plates, treated with siRNAs according to the procedure specified in section 2.11. 9 μL WST-1 reagents were added into every well, incubated 2 hrs and 96 well plates were read absorbances at 440 nm and 610 nm in ELISA plate readers. Both positive (cells treated with 0.5% SDS) and negative (cells with no treatment) controls were included. The 610 nm readings were subtracted from 440 nm for each well and cell viabilities of knock down cells were calculated comparing with non-silencing siRNA controls.

Table 3: Sequences of ON-Target plus siRNA for genes

Gene	Oligo ID	siRNA
NUMA1	J-005272-05	GGUGGCAACUGAUGCUUUA
	J-005272-06	GAACCAGCCUCACCUAUCU
	J-005272-07	GCAAACGGGUCUCCCUAGA
	J-005272-08	GGAGUUCGCUACCCUGCAA
PRPF19	J-004668-05	GAUAACAACUUUGAGGUAA
	J-004668-06	GCACGGAUGUCCAGAUCUA
	J-004668-07	GUACUAAUGUGGCCAACUU
	J-004668-08	GAUCUGCGCAAGCUUAAGA

2.13 Structured illumination microscopy (SIM)

A549 cells were grown overnight on 18 × 18 mm² high performance cover glasses with restricted thickness-related tolerance, D=0.17 mm +/- 0.005 mm (Zeiss, cat#474030-9000-000). On the next day, the cells were treated with individual siRNA according to the procedure described in section 2.11. At 48 hrs post-transfection, A549 cells were infected with PR8 (Table 1) at MOI 3. Opti-MEM®-I reduced serum medium was used as overlay media. At 20 hpi the infected A549 cells were fixed with 3.7% formaldehyde for 20 mins, washed 4x with PBS, permeabilized with 0.2% triton-X 100 for 10 mins, washed again 4x with PBS, blocked with 3% BSA/ PBS for 1 hour and probed with primary antibodies diluted in 3% BSA/PBS for 6 hrs at 4^0C. After that, cover glasses

were washed 4 × with PBT (PBS, 3% BSA and 0.05% Tween20), treated with Alexa Fluor 488 or 546-conjugated secondary antibodies (Table 2) diluted in 1% BSA/PBS (1:250) for 1 hr, washed 4x with PBT, treated with DAPI for 5 mins and mounted with Vectashield or Prolong gold (Life Technology) mounting medium. The cover glasses were sealed with nail polish. Images were taken with a Zeiss Elyra PS1 SIM equipped with a Plan-Apochromat 63 × /1.40 Oil immersion objective at Genomic Centre for Cancer Research and Diagnosis (GCCRD). The 2D and 3D images were processed according to the procedure described in Righolt et al. 2014 [185].

2.14 Electron microscopy (EM)

A549 cells were grown in P100 cell culture plates overnight. On the next day, cells were treated with individual siRNAs. At 48 hrs post-transfection, A549 cells were infected with PR8 at a MOI 3. At 20 hpi, cells were harvested by scraper, gently washed 3x with ice-cold PBS by resuspending and pelleting (350xg for 5 mins). Then the cell pellets were resuspended in EM Grade Karnovsky fixative (2.5% glutaraldehyde and 4% paraformaldehyde in 0.1M phosphate buffer, pH 7.2) and sent to the Histology lab, Department of Human Anatomy for further processing. Images were obtained on a Philips CM10 Electron Microscope.

2.15 RNA extraction and real-time PCR

IAV infected A549 cells were harvested, washed 3x with cold PBS and total cellular mRNA was extracted with RNeasy Mini Kit (QIAGEN). 250 ng of purified mRNA was used to synthesize cDNA with Go Script TM Reverse Transcription System kit (Promega). Real time PCR was performed using Luminaries Color HiGreen High

ROX qPCR kit (Thermo Fisher). According to the manufacture's protocol PCR master mix (10µl) consisted of: 5 µl Luminaries Color HiGreen High ROX qPCR master mix (2X), 4.4 µl (100 ng) template cDNA and 0.3 µl each of 10 µM forward and reverse primers (Table 4). PCRs were run in triplicates on an Applied Biosystems 7300 Real-Time PCR System. The program of cycle condition was 50^0 C for 2 min, 95^0 C for 2 min, and 50 cycles of (95^0 C for 15 sec. and 60^0 C for 30 sec.).The Ct values were normalized to 18S rRNA control and compared to non-targeting siRNA control.

Table 4: Primers for quantitative real time PCR.

Target gene	Sequence: 5/ to 3/
NS1 of PR8	Fwd: CTTCGCCGAGATCAGAAATC
	Rev: TGGACCATTCCCTTGACATT
NP of PR8	Fwd: AGAGGGTCGGTTGCTCACAA
	Rev: TGGCTACGGCAGGTCCATA

2.16 Bioinformatics and statistical analyses

Lists of IAV-NS1 interacting host proteins were generated from Protein Pilot analysis. The gene symbol and Uniprot IDs of all proteins were uploaded into DAVID (https://david.ncifcrf.gov/) for functional tool analysis. NS1-interacting proteins were also uploaded into Consensus Path Database (CPDB) (http://consensuspathdb.org/) for pathway and enrichment analysis. Groups of proteins identified in individual pathways in

DAVID were uploaded in to STRING (http://string-db.org/) to monitor the protein-protein interactions. Interaction among viral proteins and host factors were also analyzed by using VirHostNet 2.0 (http://virhostnet.prabi.fr/) database.

Statistical analyses were calculated in Microsoft-Excel and SigmaPlot® softwares. P-values were determined using Student's t-test.

Part 3. Results

3.1 Anti-NS1 monoclonal antibody (mAb) production and typing

During viral replication different Influenza strains or types may interact with different host proteins and my target was to look for the proteins that are common to most of the circulating strain types including H1N1 and H3N2. Amino acid (aa) sequences of our six laboratory IAV strains PR8, NY55, B10, B59, NCal and HK1 (Table 1) were analyzed. 94–99% sequence identities between any two PA proteins were observed among these six Influenza A H1N1 and H3N2 strains (Figure 9). 38–97% sequence identities were found between any two Influenza A HA proteins of those six H1N1 and H3N2 strains (Figure 9). Similar comparisons were done with NS1 proteins, where 83-92% sequence identities were observed between any two strains of these six H1N1 and H3N2 IAV strains (Figure 9). Amino acid sequences of PR8-NS1and HK1-NS1 proteins were the most divergent among these six strains. The first objective was to generate broadly cross reactive mAbs that could detect NS1 of different IAV types. For that reason the immunizations were done with NS1 derived from Influenza A HK1 (H3N2) and hybridomas were screened using NS1 derived from Influenza A PR8 (H1N1).

Monoclonal antibodies (mAbs) against IAV-NS1 can allow detection of host interacting proteins by specific immunoprecipitation (IP) experiment. In order to find these common host-virus interacting proteins, broadly cross reactive anti-NS1 mAbs were generated that could be used for the co-immunoprecipitation of IAV-NS1 and host interacting proteins. To generate broadly cross reactive mAbs, mice were immunized with HK1 His_6-tagged NS1. Therefore, mouse spleens were fused with myeloma cells to

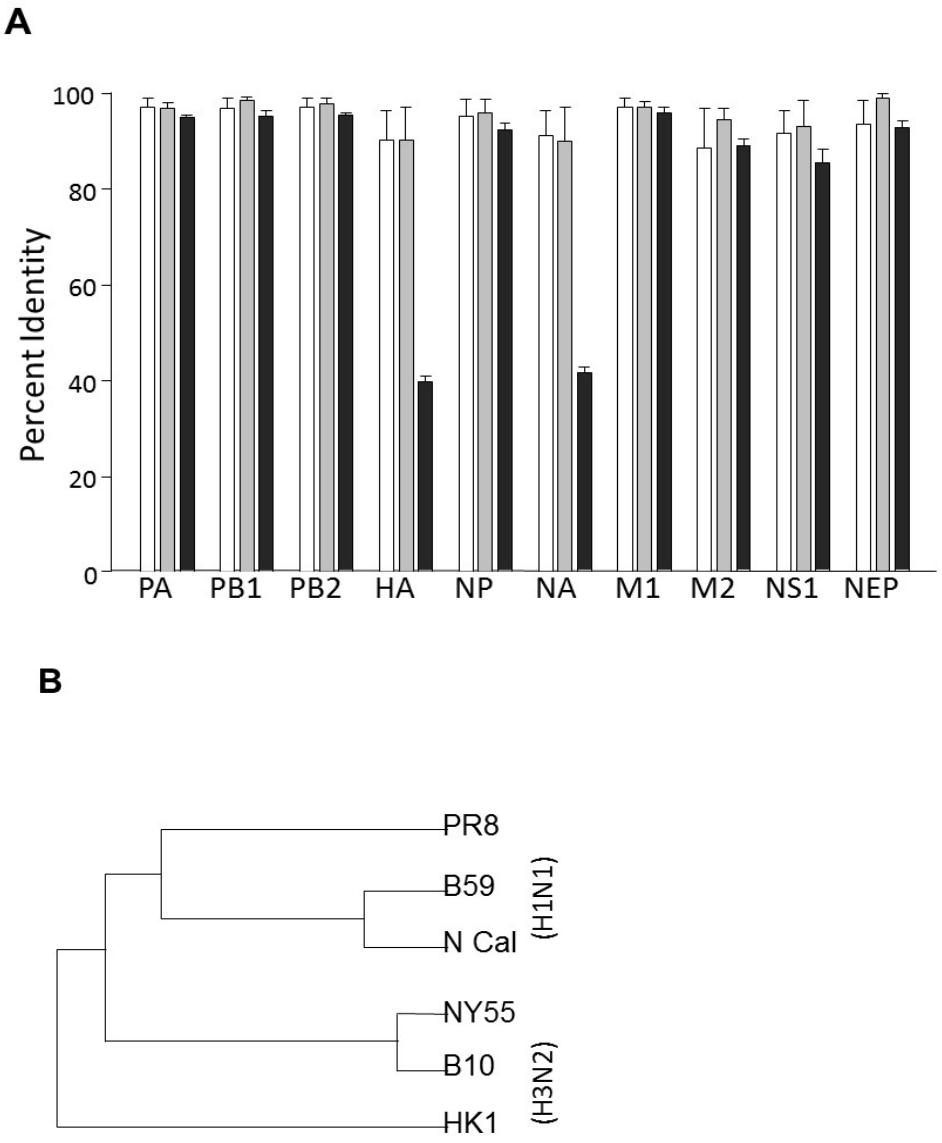

Part A is published in *Journal of General Virology* (Rahim et al. 2013) [186]

Figure 9: Phylogenetic comparisons of various influenza virus proteins.

(A) Percentage of identities between selected H1N1 types: PR8, B59 and NCal (open bars), selected H3N2 types: B10, HK1 and NY55 (shaded bars) and H1N1 and H3N2 clones (filled bars) of each of the influenza virus proteins. (B) Dendrogram of selected influenza virus NS1 proteins.

produce hybridomas (hybrid cells) that can both produce antibodies and multiply indefinitely. Several hundreds of monoclonal hybridomas were produced and screened for NS1 sensitivity by using PR8 GST-tagged NS1 in ELISA. The 13 strongest NS1 reacting mAb clones were identified among these hybridomas. Isotyping of these 13 mAbs was done, where only one clone was IgM and the rest of the clones were IgG types. Subtyping of these IgGs indicated that two were IgG1, four were IgG2a, five were IgG2b and one was IgG3 types (Table 5). I was able to grow and purify 9 of these mAbs by protein G affinity chromatography. Therefore, I targeted these 9 mAbs for subsequent characterizations. All 9 mAbs were grown into large scale and purified on protein G columns.

3.2 Anti-NS1 mAbs are specific for multiple Influenza A viral NS1

Sensitivity and specificity of these mAbs were checked initially against PR8, NY55, B10, B59 and NCal (Table 1) infection in MDCK cells.

3.2.1 mAbs detect denatured form of NS1 of multiple strains

MDCK cells were infected separately with different IAVs specified in section 3.2, and whole cell lysates were collected at 24 hours post infection (hpi), and run in SDS-PAGE. After electrophoresis the proteins were transferred to PVDF membranes and immunoprobed with mAb 3F5. This 3F5 mAb clearly detected NS1 from 5 different IAV strains with a single band at a visible molecular weight of ~26 kDa that corresponds to the molecular weight of NS1, and there was no band in mock- infected cell lysates (Figure 10A). Similar results were found when cell lysates were tested with mAb 7D11 (Figure 10B). Consequently, PR8-infected MDCK cell lysate was subjected to

Table 5: Lists and typing of the anti-NS1 mAbs:

Clone	Ig type	Isotype	Light chain
2C3	IgG	IgG3	Kappa
3F5	IgG	IgG2b	Kappa
4E10	IgG	IgG1	Kappa
5F4	IgG	IgG2b	Kappa
5D6	IgG	IgG2a	Lambda
5B10	IgG	IgG2b	Kappa
7D11	IgG	IgG2a	Kappa
8C7	IgG	IgG2b	Kappa
9D9	IgG	IgG2a	lambda
10C7	IgG	IgG2a	lambda
10G7	IgG	IgG1	lambda
13D8	IgG	IgG2b	Kappa
15C10	IgM	IgM	Kappa

Published in *Journal of General Virology* (Rahim et al. 2013) [186].

immunoprecipitation using 3F5, and a 26 kDa band was observed in SDS-PAGE. To confirm the identity of the 26 kDa band, it was cut and purified from the gel, analyzed by mass spectrometry, and identified as PR8-NS1.

Analysis of 3F5 and 7D11 mAbs indicated that these mAbs bound to IAV-NS1 almost without any background. Therefore, I used slot bolt equipment to screen all of the 9 purified mAbs including 3F5, 4E10, 5B10, 5F4, 5D6, 7D11, 8C7, 10C7 and 13D8 against 5 different IAV infections, as well mock infection. 25 μg of MDCK cell lysates infected with each IAV strain were bound to PVDF membranes, fixed with isopropanol and probed with 1 μg of each purified mAb. 3F5, 4E10, 5D6, 5F4, 7D11, 8C7, 10C7 and 13D8 detected the denatured form of NS1 of five strains (Figure 10C). The mAbs showed different affinities (Table 6). 5B10 detected NS1 of only PR8, NY55 and NCal. 5D6 detected the NS1 of all strains with almost similar affinities. 10C7 showed strong and equal reactivity to all tested IAV NS1 except NCal NS1. Some mAbs also showed strain specific reactivity. For example 8C7 showed strong reactivity to NS1 proteins derived from PR8, NY55 and NCal and weaker reactivity to other tested strains.

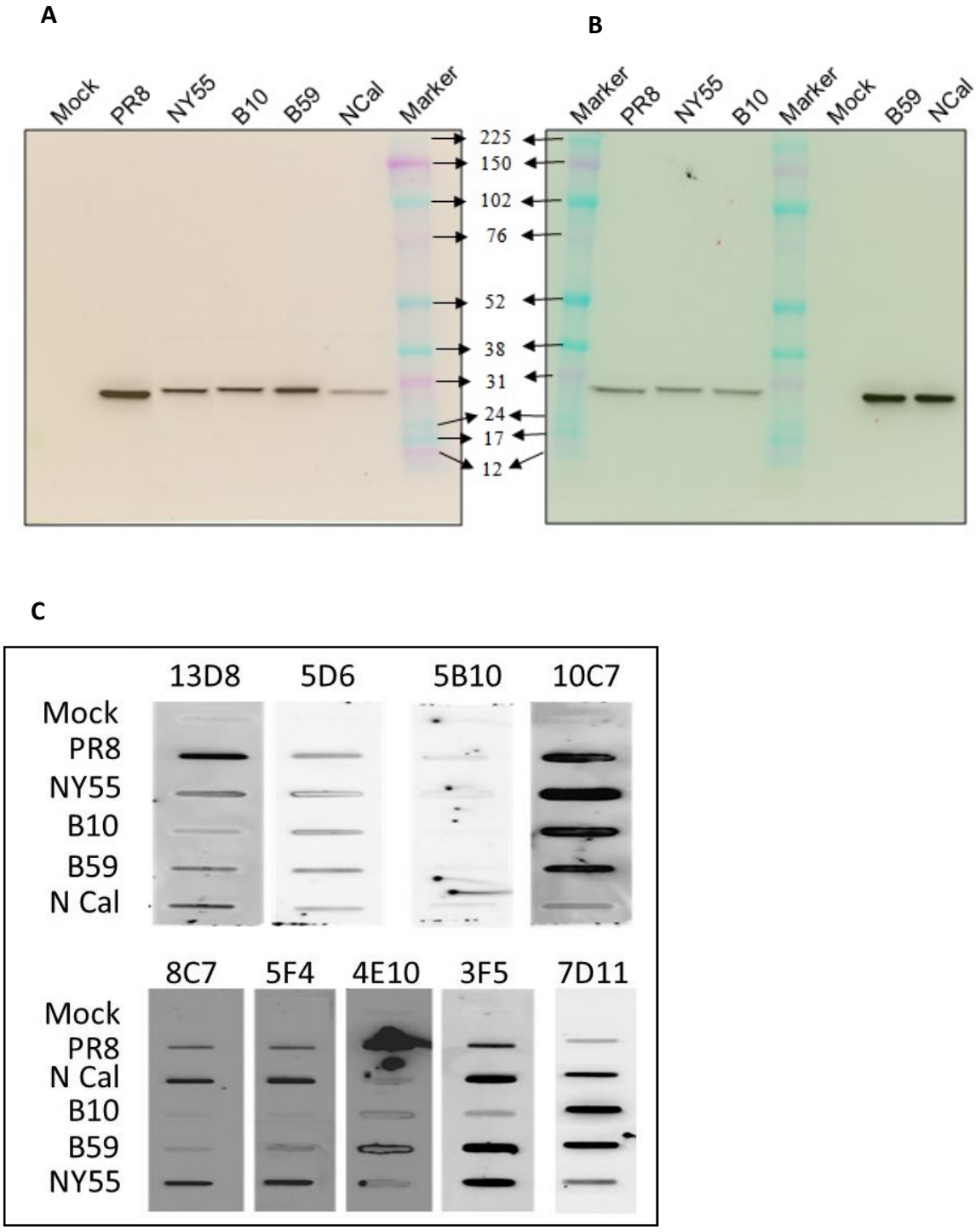

Published in *Journal of General Virology* (Rahim et al. 2013) [186].

Figure 10: Anti-NS1 mAbs detected denatured form of IAV NS1.

(A) Western blot with mAb 3F5. MDCK cells were infected with five different IAV strains (mock infection was included), lysed with 0.5% NP40. Cell lysates were resolved in SDS-PAGE, transferred to PVDF membrane, and treated with 3F5 mAb. (B) Western blot with mAb 7D11 for different IAV strains. (C) Slot blot analysis of anti-NS1 mAbs against indicated IAV strains. MDCK cells were infected with different IAV strains separately. Infected cells were harvested and cytosolic fractions were prepared with 0.5% NP40. Equal concentrations (25µg) of all cell lysates were bound to PVDF membranes and identical concentrations (1µg) of all mAbs were treated. Primary mAbs were detected by treating with secondary HRP-anti mouse Ab [186].

3.2.2 mAbs detect native form of NS1 of multiple strains

To evaluate the ability of these mAbs to detect native IAV NS1 protein, I performed immunofluorescence microscopy. MDCK cells were infected at MOI 1 separately with five IAVs specified in section 3.2, fixed at 24 hpi and initially tested with anti-NS1 mAb 3F5. This mAb detected all tested IAVs (Figure 11). 3F5 showed strong reactions with B59 and NCal-infected MDCK cells and weak reaction with B10-infected MDCK cells. In later experiments all mAbs were tested in MDCK cells infected with those five different IAVs. mAbs showed variability in their capability to detect NS1 proteins derived from different IAVs (Figure 12, Table 6). For example, mAbs 13D8 and 5F4 reacted with all IAV strains. 8C7 and 10C7 reacted with PR8, B59 and NCal strains. 5D6 reacted moderately with PR8 and B59, whereas it reacted very weakly with B10. All five tested mAbs detected PR8 and B59. Thus many of the mAbs recognized different IAV native NS1 proteins.

3.3 NS1 is detected as early as 5-7 hour post infection

Time course experiments were conducted with MDCK and A549 cells that were infected with PR8, NY55 and B59 at MOI 5. Infected cells were harvested at 3, 4, 5, 6, 7, 8, 9 and 10 hpi, and subjected to Western blot analysis. In MDCK cells, NS1 proteins of all three viruses expressed earlier compared to in infected A549 cells. 5 hpi and 6 hpi are the earliest time points when viral NS1 could be detected in MDCK andA549 cells, respectively (Figure 13A).

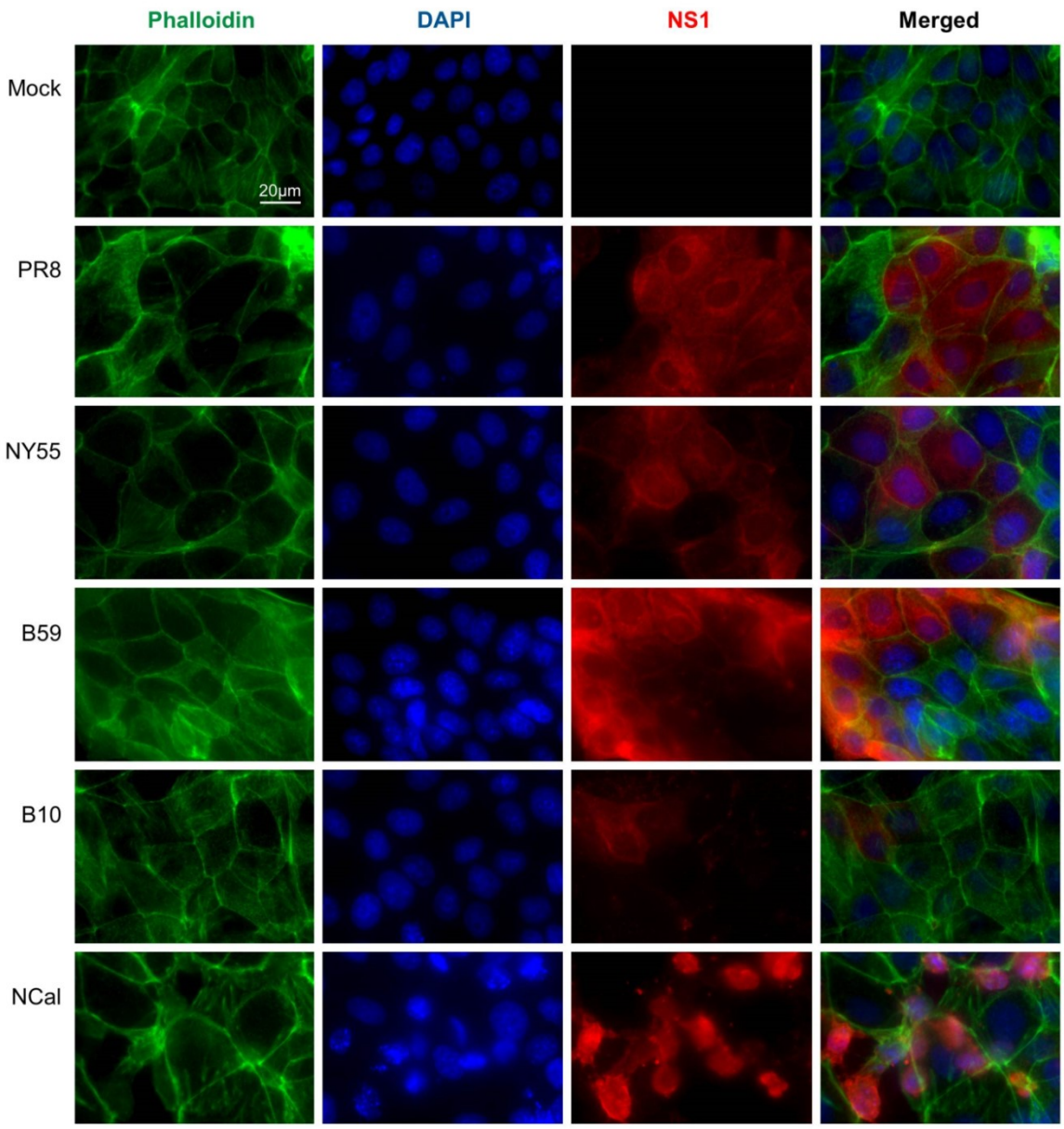

Published in *Journal of General Virology* (Rahim et al. 2013) [186].

Figure 11: Anti-NS1 mAb detects native IAV NS1 proteins.

MDCK cells were infected with PR8, NY55, B59, B10 and NCal at MOI 1. Mock infected cells were also included. Cells were fixed at 24 hpi, treated with 3F5 anti-NS1 mAb, secondary Alexa Fluor 546 conjugated goat anti-mouse Ab (red), Alexa Fluor 488 Phalloidin for actin (Green) and DAPI for Nuclei staining (blue). Bar, 20µm. Merged images of all channels are included.

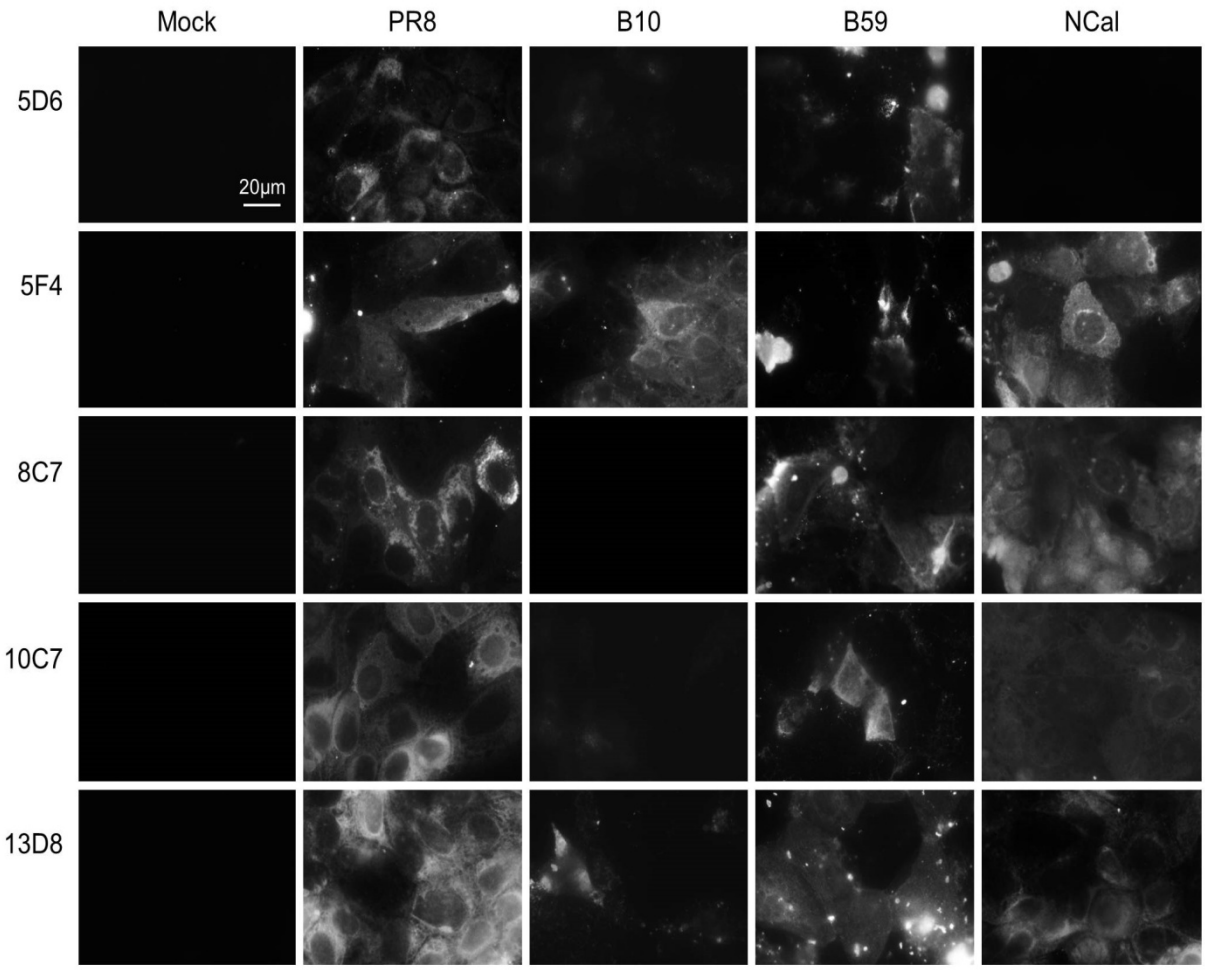

Published in *Journal of General Virology* (Rahim et al. 2013) [186].

Figure 12: Several anti-NS1 mAbs detect native NS1 proteins of various IAVs.

MDCK cells were infected with PR8, NY55, B59, B10 and NCal at MOI 1. Mock infected cells were also included. Cells were fixed at 24 hpi, treated with anti-NS1 mAbs 5D6, 5F4, 8C7, 10C7, and 13D8. Bar, 20µm.

NS1 expression and subcellular distribution were monitored by immunofluorescence microscopy. MDCK cells were infected with PR8 at MOI 5, fixed and stained at different time points to detect NS1 protein. Detection of NS1 in immunofluorescence microscopy was less sensitive compared to Western blot analysis and NS1 was not detectable before 8 hpi in immunofluorescence (Figure 13B). Subcellular distribution of NS1 changed at different times after infection. Initially NS1 was detected inside the nucleus where it remained for a few hours. It was found in the cytoplasm at 12 hpi and it diffused more into the cytoplasm with longer incubation times (Figure 13B).

3.4 Epitope mapping of the NS1 mAbs

3.4.1 Reactivity of the mAbs against NS3 protein

Previous studies have described mutations in IAVs genes that lead to adaptations in mice [59]. For example, IAV HK1 possessed several mutations in the NS1 protein that included a (GAT→GGT) D125G aa substitution. This D125G mutation initiated an alternative spliced transcript that produced NS1 protein with a deletion of an internal motif, aa 125-167, and this novel protein is called NS3 [60]. The aa sequences of all IAV strains are aligned together, where the deleted region in HK1 D125G mutant is denoted by a solid line above the aa sequences (Figure 14). Dr. Earl Brown kindly provided us M1 cells infected with wild-type HK1 and D125G-mutated HK1 viruses. I tested the anti-NS1 mAbs to check their reactivity to HK1 NS1 and D125G-mutated NS1 variant, NS3 proteins in Western blot analysis to determine if any of our anti-NS1 mAbs were able to

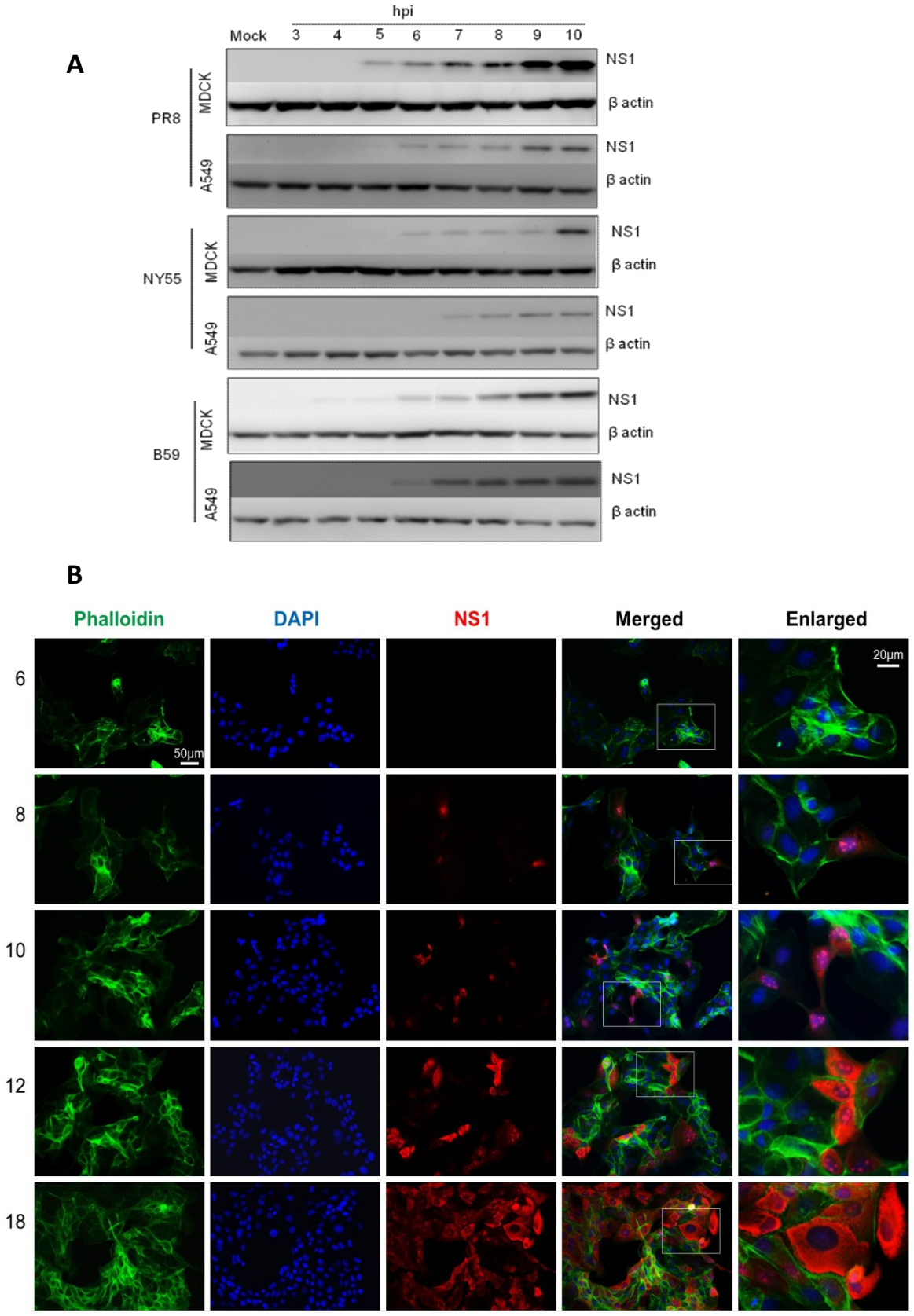

Published in *Journal of General Virology* (Rahim et al. 2013) [186].

Figure 13: Kinetics of Influenza A NS1 expression.

(A) mAb detected IAV NS1 at 5 hpi. MDCK and A549 cells were infected with PR8, NY55 and B59 at MOI 5. Cell lysates were collected at indicated time points, resolved in SDS-PAGE and transferred to PVDF membranes. The membranes were treated with 3F5 anti-NS1 mAb. Membranes were also treated with mouse anti-β-actin Ab for loading control. Primary Abs were detected by treating the membranes with HRP-anti mouse secondary antibodies. (B) NS1 was detected at 8 hpi. MDCK cells were infected with PR8 at a MOI 5, fixed at 6, 8, 10, 12 and 18 hpi. Cells were treated with anti-NS1 mAb 8C7, secondary Alexa Fluor 546 conjugated goat anti-mouse Ab (red), Alexa Fluor 488 Phalloidin for actin (green) and DAPI for Nuclei staining (blue). The far right column shows enlarged images of the indicated box region of the merged image. Bar, 20 μm for the images of right column; and 50 μm for other images.

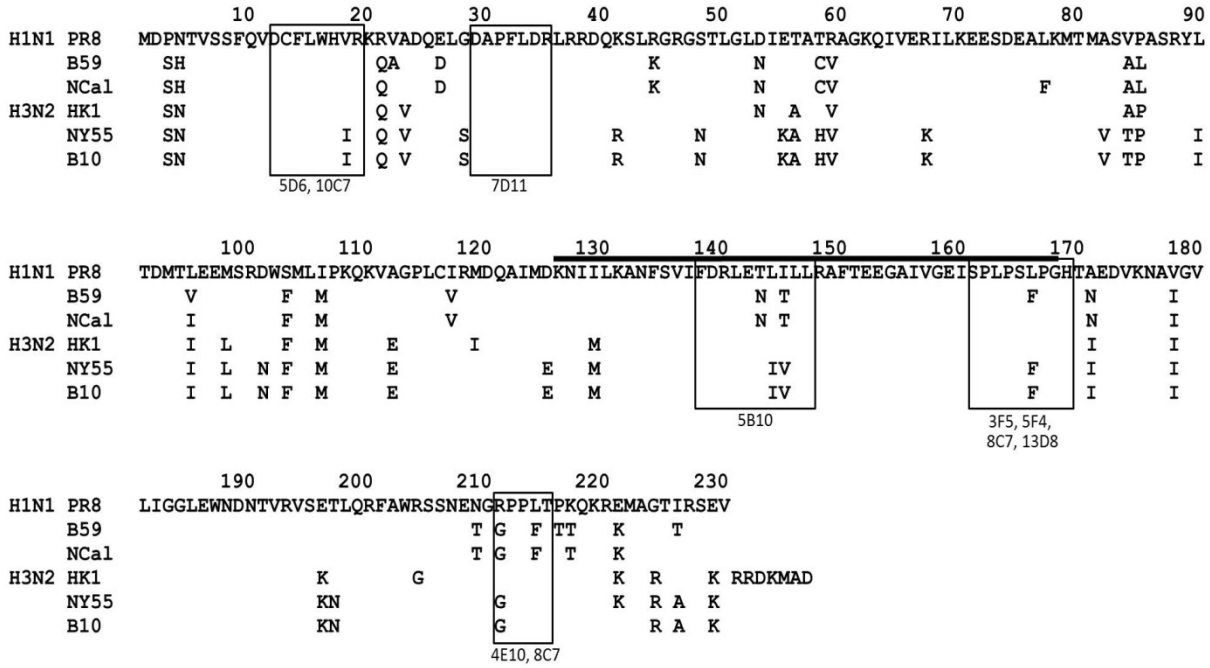

Published in *Journal of General Virology* (Rahim et al. 2013) [186].

Figure 14: Amino acid sequence alignment of six IAV NS1 proteins.

Amino acid 125-167 region is denoted by a back line over the sequences and is missing in a mouse adapted HK1 mutant, which was recognized as NS3 protein [60]. The strains are identified in Table 1. The five boxes within the aa sequences indicate epitopes which were subsequently mapped for individual mAbs (mAb IDs are indicated below the boxes).

detect an epitope within the deleted region (aa 125-167). Most of the anti-NS1 mAbs detected both HK1 NS1 and NS3 (Figure 15A). 3F5, 5F4 and 13D8 reacted with only NS1 but not NS3, which indicates that these three mAbs recognize an epitope residing between 125-167 aa of NS1 protein (Figures 15A and 14). In addition, mAb 5B10 reacted with NS3 at very low level. Reactivities of 3F5, 13D8 and 5D6 were also tested in wild-type HK1 and D125G-mutated HK1 infected A549 cell lysates, which showed similar sensitivities to that observed in M1 cells (Appendix B1).

3.4.2 Reactivity of mAbs by overlapping peptide library analysis

These 9 mAbs were sent to Pepscan Therapeutics (The Netherlands) for overlapping peptide library analysis to determine more exact epitopes of NS1 recognized by each mAb. Each mAb reacted with a distinct set of peptides from which epitope mapping of all mAbs were done (Figure 15B). Five different epitopes were identified that are recognized by 9 anti-NS1 mAbs. Most mAbs such as 3F5, 5F4, 5B10, 13D8, 4E10, 7D11 reacted with a limited number of linear small peptides and generated single and specific peaks (Figure 15B). The 3F5 mAb showed strong reactions with peptides between NS1 aa 161 and 169, which indicated the sequence ^{161}SPLPSLPGH^{169} as the epitope of 3F5 mAb. mAbs 5F4 and 13D8 also showed similar reactivity and recognized NS1 ^{161}SPLPSLPGH^{169} epitope (Table 6). 5B10 mAb reacted strongly with the peptides between NS1 aa 138 and 147. Therefore, the sequence ^{138}FDRLETLILL^{147} within NS1 was assigned as 5B10 epitope, which overlapped with a previously identified nuclear export signal sequence [187, 188] (Table 6). NS1 epitope ^{29}DAPFLDR^{35} was recognized by mAb 7D11 and resides in the NS1 N-terminal RNA-binding domain.

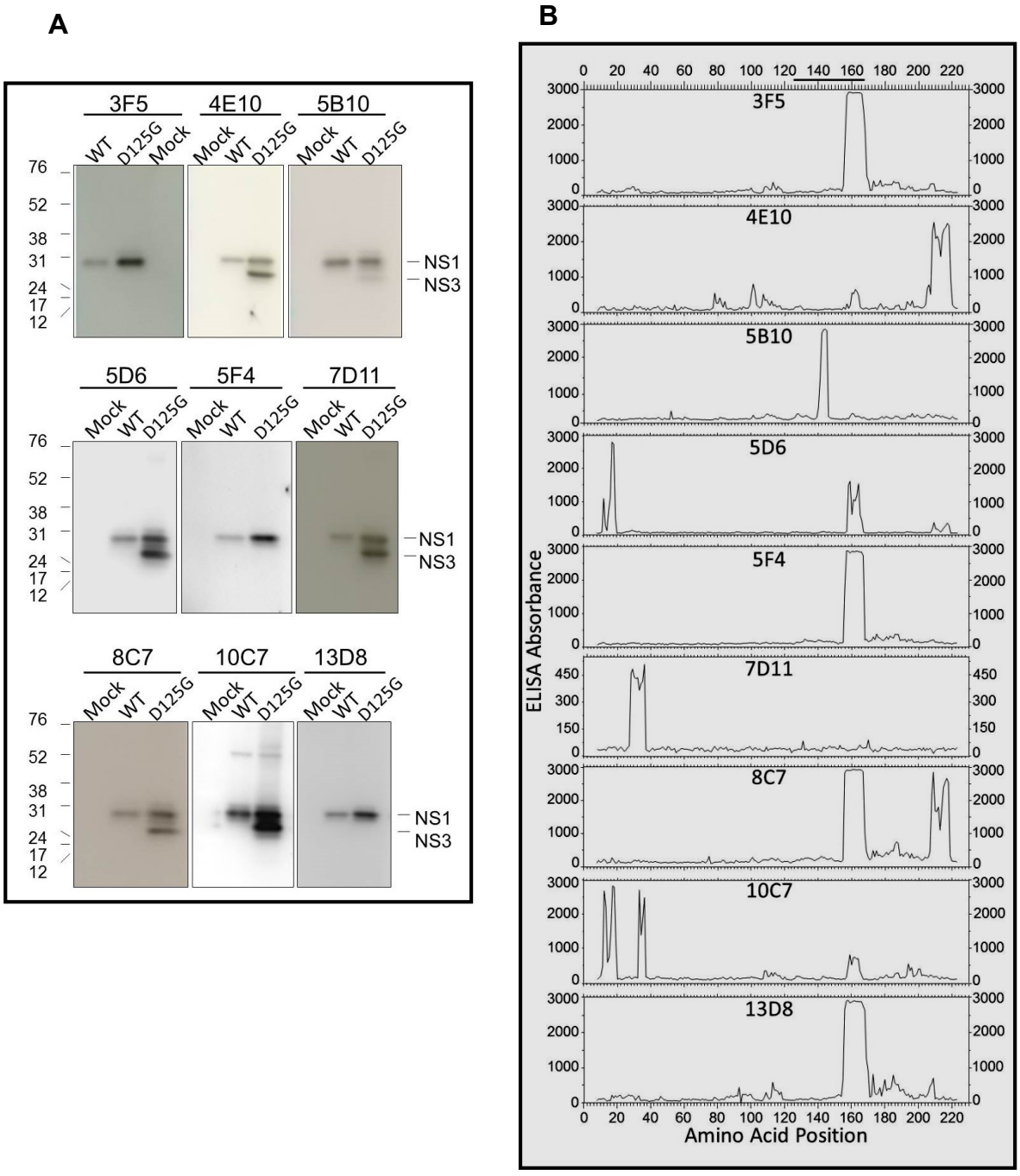

Published in *Journal of General Virology* (Rahim et al. 2013) [186].

Figure 15: Epitope mapping of anti-NS1 mAbs.

(A) M1 cells were infected with both wild-type HK1 and D125G mutant HK1. Cell lysates were resolved in SDS-PAGE and transferred to PVDF membranes. The membranes were probed with different anti-NS1 mAbs to detect NS1 and NS3. The molecular weight markers are indicated on the left side of the membranes (B) Epitope mapping of anti NS1 mAbs with overlapped 15 aa long peptides generated from PR8-NS1 sequences. Reactivity of mAbs to each peptide was determined by secondary anti-mouse antibody in ELISA and is shown on the y-axis. Amino acid 125-167 region is denoted by a black line over the sequences which is missing in D125G mutated NS3.

Table 6: Characteristics of anti-NS1 monoclonal antibodies

Ab Clone	NS1 Reactivity by [a]		NS3 Western	Epitope[b]
	Immunoblotting	Immunofluorescence		
3F5	+++	+++	-	^{161}SPLPSLPGH^{169}
4E10	+	-	+++	^{211}RPPLT^{215}
5B10	+/–	+	+/–	^{138}FDRLETLILL^{147}
5D6	+++	+/–	+++	^{12}DCFLWHVR^{19}
5F4	+	+++	-	^{161}SPLPSLPGH^{169}
7D11	+++	+	+++	^{29}DAPFLDR^{35}
8C7	+	+++	+++	^{161}SPLPSLPGH^{169} ^{211}RPPLT^{215}
10C7	+++	+++	+++	^{12}DCFLWHVR^{19}
13D8	+++	+++	-	^{161}SPLPSLPGH^{169}

[a] Reactivity indicated as: +++, strong; +, medium; +/–, weak; and –, none. Values represent composite scores, based upon reactivity against multiple test viruses, as exemplified in Figures 10-12 and 15A.

[b] Epitopes were determined by Pepscan Therapeutics using linear overlapping peptide analysis. Values correspond to aa positions within NS1.

Published in *Journal of General Virology* (Rahim et al. 2013) [186].

^{29}DAPFLDR^{35} sequences are highly conserved among all tested IAV stains in this study (Figure 14), and mAb 7D11 detected NS1 of all six IAVs (Figures 10C and 15A). 4E10 and 10C7 recognized NS1 epitopes ^{211}RPPLT^{215} and ^{12}DCFLWHVR^{19}, respectively (Table 6).

A few anti-NS1 mAbs reacted with multiple linear peptides located in different regions. 8C7 reacted with multiple peptides near aa 210 and 160 (Figure 15B). These multiple reactions were probably caused due to the cross reactivity to these similar epitope regions containing PPLTPKPQK (near aa 210) and SPLPSLPGH (near aa 160) sequences (Figure 14). To determine the contributions of these individual regions, competitive ELISAs were performed. ELISA plates were coated with GST-PR8-NS1, treated with an excess of different mAbs to block relevant epitopes, and biotinylated mAb 8C7 was added to test the capability of 8C7 to react. Biotinylated mAb 8C7 showed strong reactions to PR8-NS1 treated with no Ab, an irrelevant Ab JB1A (mouse anti-human β_1 integrin) and mAb 7D11, which detects a distant epitope (Figure 16A). On the other hand, reactions of biotinylated mAb 8C7 with PR8-NS1 treated with mAb 3F5 (recognizes NS1 epitope near aa160) and mAb 4E10 (recognizes NS1 epitope near aa 210) reduced the signal (OD in ELISA) to 20% and ~80%, respectively (Figure 16A). 8C7 reactivity to NS3 (Figure 15A) and competitive ELISA results (Figure 16A) suggested that mAb 8C7 recognizes both epitopes. Similarly, mAb 5D6 reacted with several peptides near aa 20 and 160. Competitive ELISAs were performed for precise epitope mapping. GST-PR8-NS1 coated ELISA plates were treated with no Ab, an irrelevant Ab JB1A, 10C7 that recognizes an epitope near NS1 aa 20, and 5F4 that recognizes an epitope near NS1 aa 160. Biotinylated mAb 5D6 bound efficiently

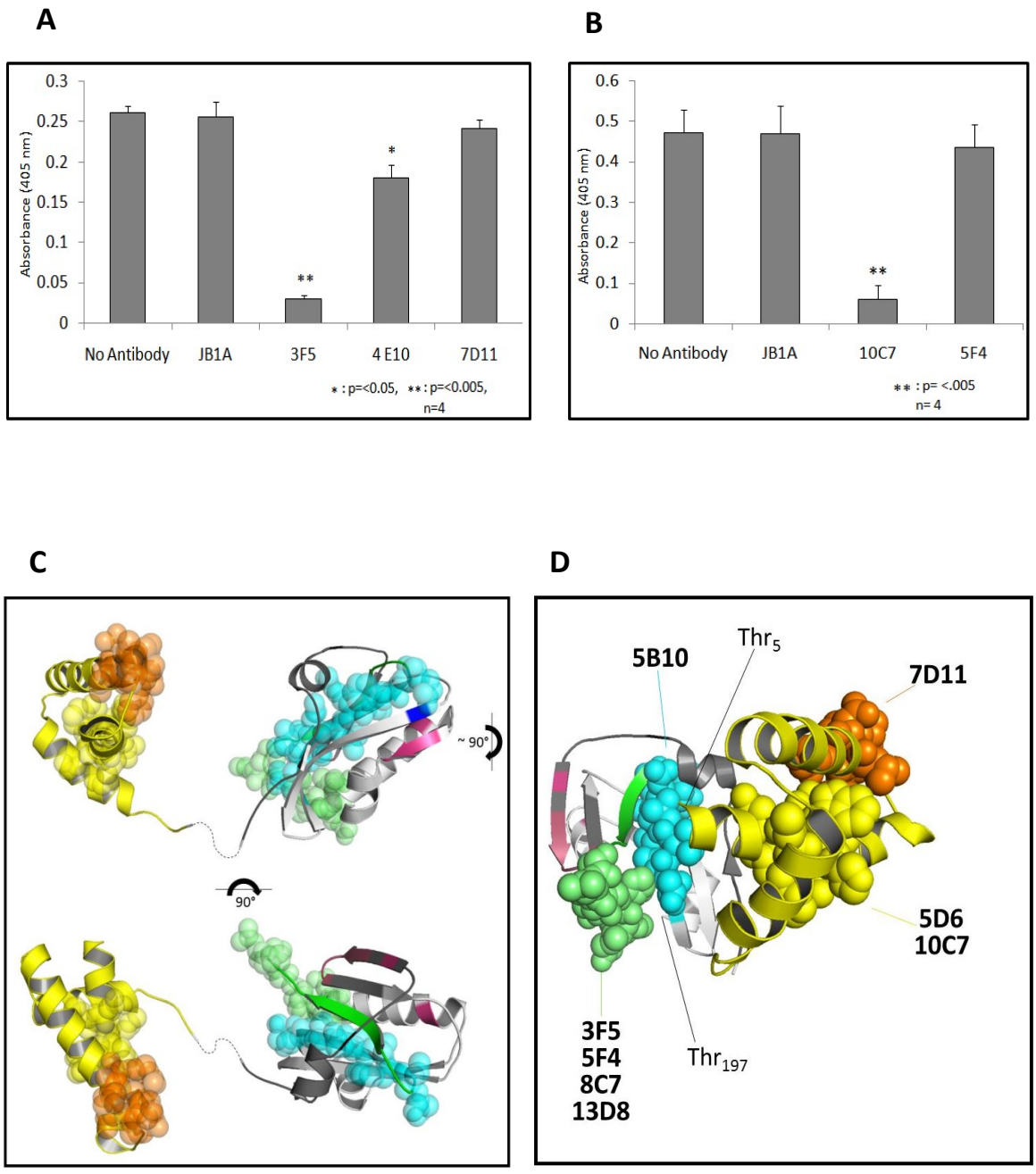

Figure A, C and D are published in *Journal of General Virology* (Rahim et al. 2013) [186].

Figure 16: Characterization of NS1 mAb epitopes.

(A) Competitive ELISA for 8C7 reactivity. ELISA plates were coated over night with 25 ng GST-PR8-NS1 per well at 4^0 C. Wells were treated with PBS, 50 µg of irrelevant Ab JB1A that recognizes human β1 integrin and the indicated mAbs. Thereafter, the wells were treated with biotinylated mAb 8C7 for 2 hour and probed with 1: 2000 dilution of Extra Avidin. Alkaline phosphatase/p-nitrophenyl phosphate was added and the absorbances were measures on a BioTek Synergy 4 reader. The self-competing 8C7 readings were subtracted from all readings (n=4). (B) Competitive ELISA for 5D6 reactivity. Similar competitive ELISAs were performed where the indicated Abs were treated and biotinylated mAb 5D6 was used to compete with the indicated Abs. (D and E) Placement of epitopes within the H5N1 NS1 atomic structure (protein data bank 3F5T [189]. Some properties of NS1 sequences were found in [187], which are indicated in different colors. Red portion contains critical nuclear localization signal 1 (NLS-1; aa 35, 38 and 41); yellow part is the RNA-binding domain surrounding aa 1–73, black portion consists of aa 96 and 97 that interact with TRIM25; gray part (aa81-113) interacts with eIF4GI; bright pink (aa 103, 105–110, 117, 119–126, 151, 153, 155–157, 180, 181, 183, 184 and 187–189) is the CPSF30-binding site; blue (aa 123, 124, 126, 127) is the protein kinase R-binding site; cyan (aa 137-147) contains nuclear export signal; and green part masks the nuclear export signal (aa 148–161). In figures C and D, coloured epitopes are shown as semi-transparent spheres with 90^0 rotations and as solid spheres, respectively. Different colors represent various NS1 regions recognized by the indicated mAbs. Images of Figure 16Ccorrespond to similar orientation described in [189]. The dashed lines indicate the disordered aa 75–79. [186].

to PR8-NS1, which were treated with no Ab and JB1A (Figure 16B). Biotinylated mAb 5D6 binding was reduced to ~13% by 10C7; however, no significant reduction was observed by 5F4, where biotinylated 5D6 binding was ~92% (Figure 16B). Linear peptide epitope map analysis (Figure 15B), competitive ELISA results and positive reactivity of 5D6 to NS3 protein (Figure 15A) suggested that ^{12}DCFLWHVR^{19} (near NS1 aa 20) is the mAb 5D6 epitope. Positive reaction with the 160 aa region might be caused due to the cross reactivity to the similar aa sequences of aa 160 and aa 20 regions.

Sequences of all nine mAb epitopes were mapped on IAV NS1 amino acid sequences (Table 6). Eight of those sequences were placed within three-dimensional H5N1 NS1 atomic structure by PyMOL software (Figure 16C & 16D). mAbs 4E10 and 8C7 recognized NS1 ^{211}RPPLT^{215} region, which resides near a disordered carboxyl terminus of NS1 and lacks distinct structure.

3.4.3 The novel mAbs recognize highly conserved IAV-NS1 epitopes

More than 1800 non-redundant human influenza A viral NS1 protein sequences were available in the NCBI Influenza virus Resource database [190] at the time when the anti-NS1 mAbs were characterized. Three of the five epitopes that were identified in this study were highly conserved among all (>1800) IAV NS1 sequences. Anti NS1 mAbs 3F5, 5F4 and 13D8 recognized the NS1 peptide sequences SPLPSLPGH and SPLPSFPGH, which were found in all of the tested IAV (Figure 14) and >97% of the available IAV NS1 sequences at the time of the characterizations. Anti-NS1 mAbs 5D6 and 10C7 recognized the peptide sequences DCFLWHVR and DCFLWHIR, which are found in all of the six tested IAV NS1 sequences (Figure 14) and > 95% of all IAV NS1

sequences. Similarly, epitope (DAPFLDR sequence) of anti-NS1 mAb 7D11 was found in all of the six tested IAV strains and > 95% of the IAV NS1 sequences, which were available at the time of the mAb characterizations.

3.5 Anti-NS1 mAbs immunoprecipitated PR8 NS1 from infected cells

Madin-Darby Canine Kidney (MDCK) and human lung adenocarcinoma epithelial (A549) cells are widely used as models of efficient IAV replication. Since human A549 cells are physiologically relevant, I used this cell line in all of my interactome studies. My target was to identify IAV NS1 protein from virus-infected cell lysates by immunoprecipitation (IP) with our anti-NS1 mAbs, so that the NS1 interacting host partners could also be pulled down with NS1. Viruses are intracellular parasites and utilize host cell system during their entire replication cycle. To target a wide range of host factors during IAV replication cycle, I selected two different time points for NS1 IP including an early and a later time post infection. In my initial experiments, our anti-NS1 mAbs detected IAV NS1 at 6 hpi at the earliest in PR8 infected A549 cells (Figure 13A). Therefore, I selected 6 hpi (early time post infection) and 24 hpi (later time post infection) for my IP experiments. I used a mixture of three anti-NS1 mAbs: 3F5, 4E10 and 7D11, which exhibited strong reactivity to IAV NS1 (Figure 10C) and recognized different NS1 epitopes (Table 6), so that the highest number of the NS1 interacting partners could be detected.

A549 cells were infected with PR8 at MOI 5, and mock-infected A549 cells were also included in each experiment. Infected A549 cells were harvested at 6 hpi and 24 hpi,

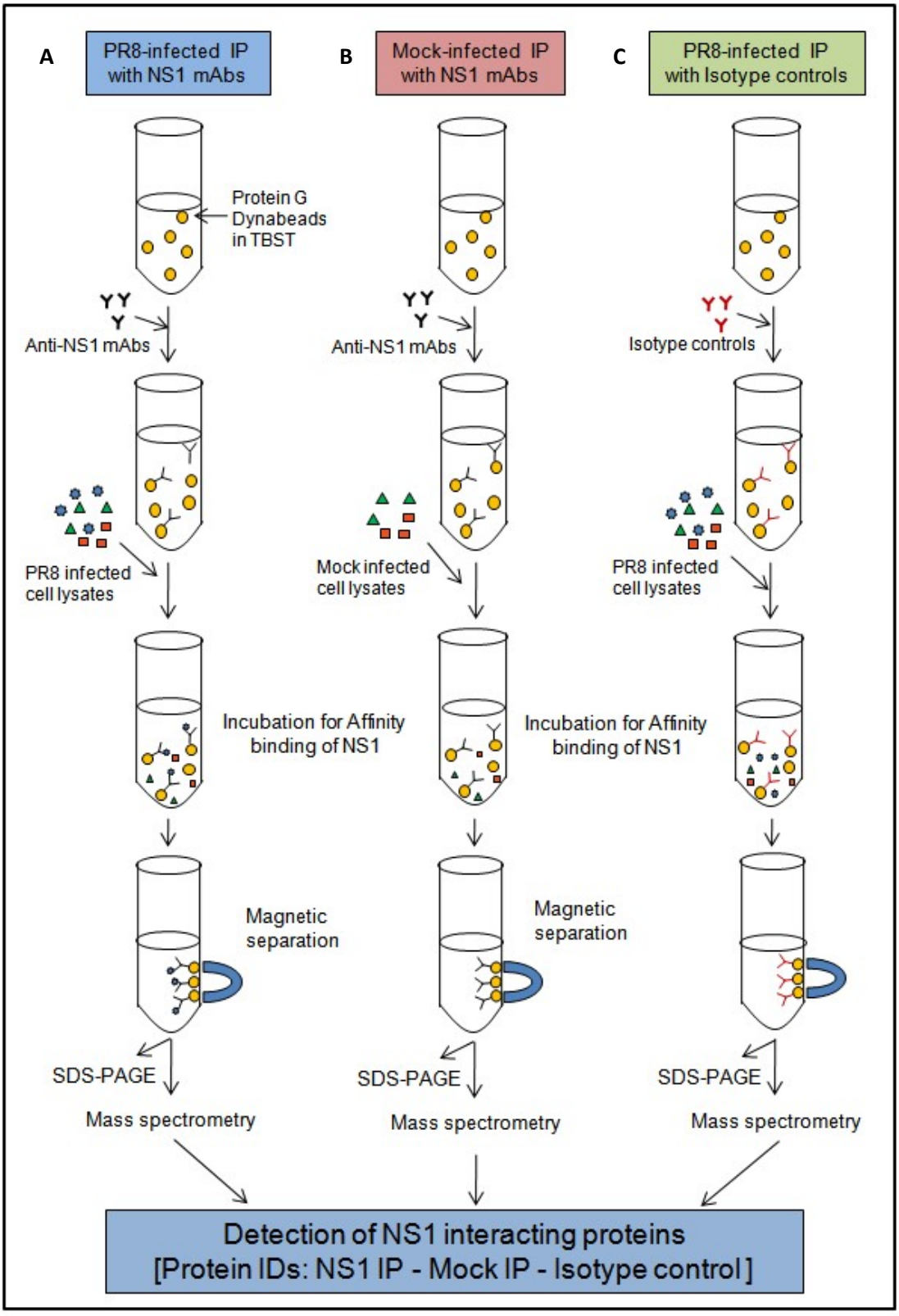
A
PR8-infected IP with NS1 mAbs
B
Mock-infected IP with NS1 mAbs
C
PR8-infected IP with Isotype controls
Protein G Dynabeads in TBST
Anti-NS1 mAbs
Anti-NS1 mAbs
Isotype controls
PR8 infected cell lysates
Mock infected cell lysates
PR8 infected cell lysates
Incubation for Affinity binding of NS1
Incubation for Affinity binding of NS1
Magnetic separation
Magnetic separation
SDS-PAGE
SDS-PAGE
SDS-PAGE
Mass spectrometry
Mass spectrometry
Mass spectrometry
Detection of NS1 interacting proteins
[Protein IDs: NS1 IP - Mock IP - Isotype control]

Figure 17: Experimental overview of IP.

Three sets of IPs were performed in each experiment using protein G Dynabeads. A) Protein G Dynabeads were treated with anti-NS1 mAb mixture (3F5, 4E10 and 7D11 mAbs), washed with TBST, incubated with PR8-infected cell lysates for affinity binding of NS1. Thereafter, immunoprecipitated products (Dynabeads, Abs and antigens) were separated using a magnet. 10% of the IP products were resolved in SDS PAGE and detected by Western blot and rest of the 90% products were run in mass spectrometry. B) IPs were done using anti-NS1 mAb mixture treated with mock-infected cell lysates. C) IPs were done using mixture of isotype controls including α-Emprin, α-HSA and α-SYN Abs (different Abs exhibiting similar isotypes to anti-NS1 mAbs).

lysed with different reagents (section 2.8) to extract both cytoplasmic and nuclear fractions. Both nuclear and cytoplasmic fractions of 6 and 24 hpi were co-immunoprecipitated with an anti-NS1 mAb mixture (3F5, 4E10 and 7D11 mAbs) using Dynabeads protein G (Invitrogen) and a magnet. In addition, IP experiments using the anti-NS1 mAb mixture with mock-infected cell lysates and a mixture of isotypic controls (different Abs, but contain isotypes similar to anti-NS1 mAbs) with PR-infected cell lysates were also included. α-Emprin, α-HSA and α-SYN Abs were used as a mixture of isotype controls (Table 2). The outlines of the three different IP experiments are shown in Figure 17. 10% of the IP products and their inputs (only cell lysates without IP) were resolved in 4-12% gradient SDS-PAGE, analyzed by Western blot using anti-NS1 mAb mixture as primary antibody and HRP-conjugated secondary anti-mouse Ab (Figure 18). The remaining 90% of the samples were preserved in -80^{0}C for MS analysis.

In 6 hpi experiments, NS1 proteins (~26 kDa) were detected in both cytosol and nuclear inputs (Figure 18A). In nuclear inputs, NS1 band intensity was higher than that of cytosol, which indicated the higher NS1 abundance in nucleus at early period of infection and correlated with my previous finding of NS1 subcellular distribution (Figure 13B). Bands of Immunoglobulin heavy and light chains were observed around 52 and 24 kDa regions, respectively in each IP (Figure 18A). NS1 bands were also found slightly above the 24 kDa regions in both PR8 infected cytosolic and nuclear IPs with anti-NS1 mAb mixture, which was not seen in mock-inflected cytosolic and nuclear IPs with anti-NS1 mAb mixture and PR8-infected IPs with isotype controls (Figure 18A). Molecular weights of NS1 and light chains are very similar that are around 23 to 26 kDa. To confirm the absence of non-specific NS1 binding in PR8-infected IP with isotype controls

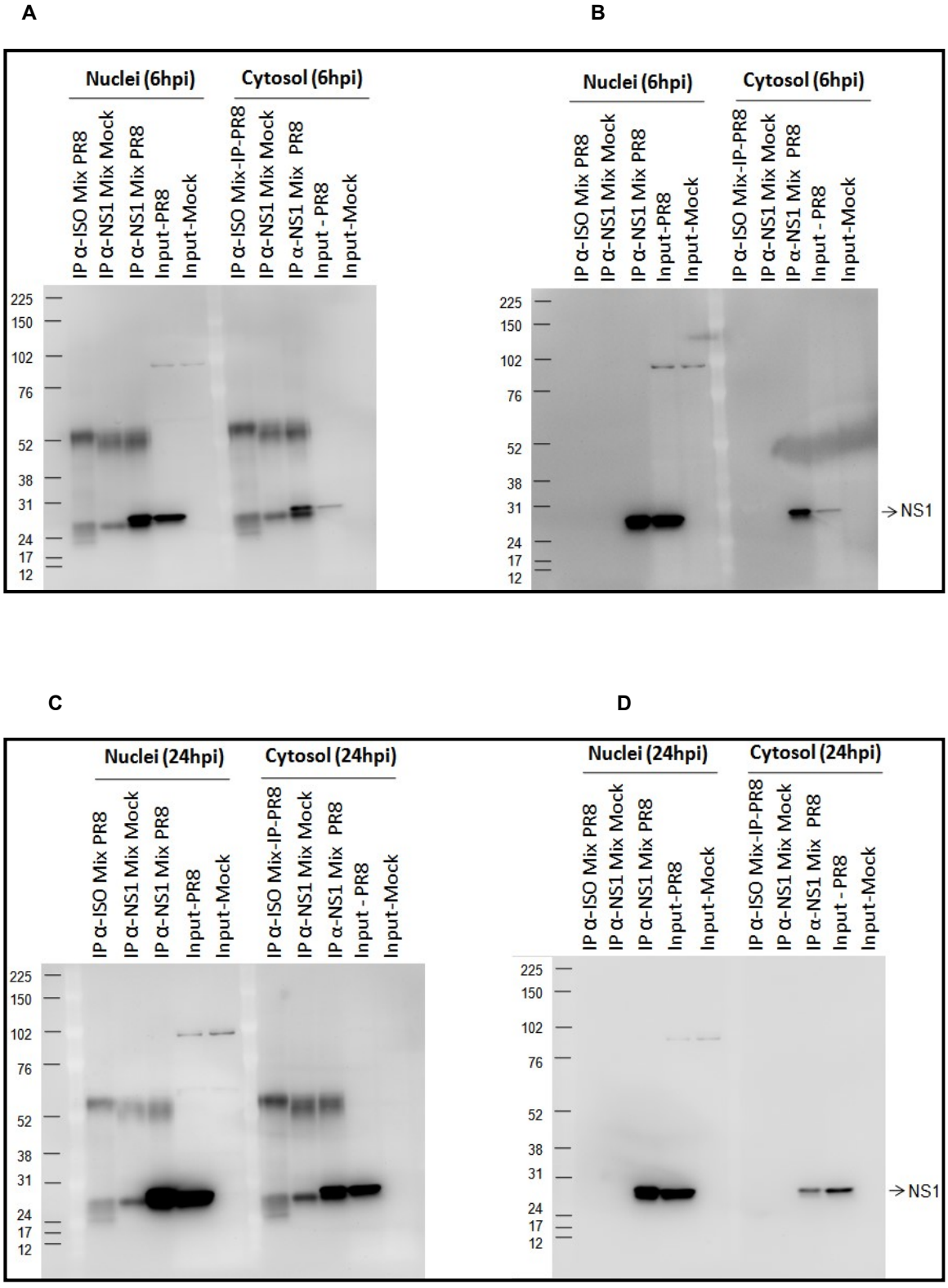
A
B
Nuclei (6hpi)
Cytosol (6hpi)
IP α-ISO Mix PR8
IP α-NS1 Mix Mock
IP α-NS1 Mix PR8
Input-PR8
Input-Mock
IP α-ISO Mix-IP-PR8
IP α-NS1 Mix PR8
Input - PR8
225
150
102
76
52
38
31
24
17
12
→NS1
C
D
Nuclei (24hpi)
Cytosol (24hpi)

Figure 18: Western blot analysis of IAV NS1 Immunoprecipitation.

A) A549 cells were infected with IAV PR8 at MOI 5 and harvested at 6 hpi. Mock infection was also included. Cytosolic and nuclear fractions were extracted and immunoprecipitated with α (anti)-NS1 mAb mixture (mAbs: 3F5, 4E10 and 7D11) and a mixture of isotope controls (Abs: SYN, Emprin and HSA). Inputs (cytosolic and nuclear fractions) and 10% of the IP products were resolved in 4-12% SDS-PAGE, transferred to PVDF membrane and treated with primary anti-NS1 mAb mixture. Primary mAbs, heavy and light chains of immunoglobulins, which were used in IPs were detected by secondary HRP-anti mouse Ab. B) Inputs and IPs of 6 hpi were analyzed by Western blot using primary anti-NS1 mAb mixture. Secondary HRP-VeriBlot Ab detected complete primary anti NS1 Abs. C) PR8 and mock infected A549 cells were harvested at 24 hpi. Cytosolic and nuclear extracts were immunoprecipitated with anti-NS1 mAb mixture and Isotype controls. Inputs and IP products were analyzed by Western blot analysis treating with anti-NS1 mAb mixture. Secondary HRP-anti mouse Ab detected primary mAbs, heavy and light chains. D) Inputs and IPs of 24 hpi were analyzed by Western blot using primary anti-NS1 mAb mixture. Secondary HRP-VeriBlot Ab detected complete primary anti NS1 Abs.

and mock infected IP with anti-NS1 mAb mixture, an additional 4-12% gradient gel was run in each IP experiment with the same samples. Thereafter, the proteins were transferred to PVDF membranes, probed with primary anti-NS1 mAb mixture and secondary HRP-link VeriBlot Ab (Table 2). This VeriBlot Ab can only detect complete immunoglobulin (not individual Heavy or Light chains), and it detected NS1 only in PR8-infected inputs (cytosolic and nuclear) and in PR8 infected cytosolic and nuclear IPs with anti-NS1 mAb mixture (Figure 18B).

In 24 hpi experiments, similar results were found in Western blot analysis. Immunoprecipitation with the anti-NS1 mAb mixture successfully pulled down NS1 protein in both PR8-infected cytosol and nuclei (Figure 18C). No non-specific NS1 binding was seen in PR8-infected IPs (cytosol and nuclei) with isotype controls and mock-infected IPs with anti-NS1 mAbs (Figure 18C). In cytosolic and nuclear inputs, a faint non-specific band near 102 kDa region was found in many cases, which was presumably caused by cross reactivity with other non-specific peptides (Figure 18). However, no such non-specific band was detected in NS1 IP in PR8 infected cell lysates with anti NS1 mAb mixture (Figure 18B and D).

Reactivity of isotype controls including α-Emprin, α-HSA and α-SYN Abs to IAV-NS1 was also checked in independent experiments. PR8 infected cell lysates were subjected to immunoprecipitation with α-Emprin, α-HSA and α-SYN Abs separately. Additional IP was also included by using these isotype controls as a mixture. No non-specific NS1 binding was found in the IPs with individual and mixture of isotype controls (Figure 19).

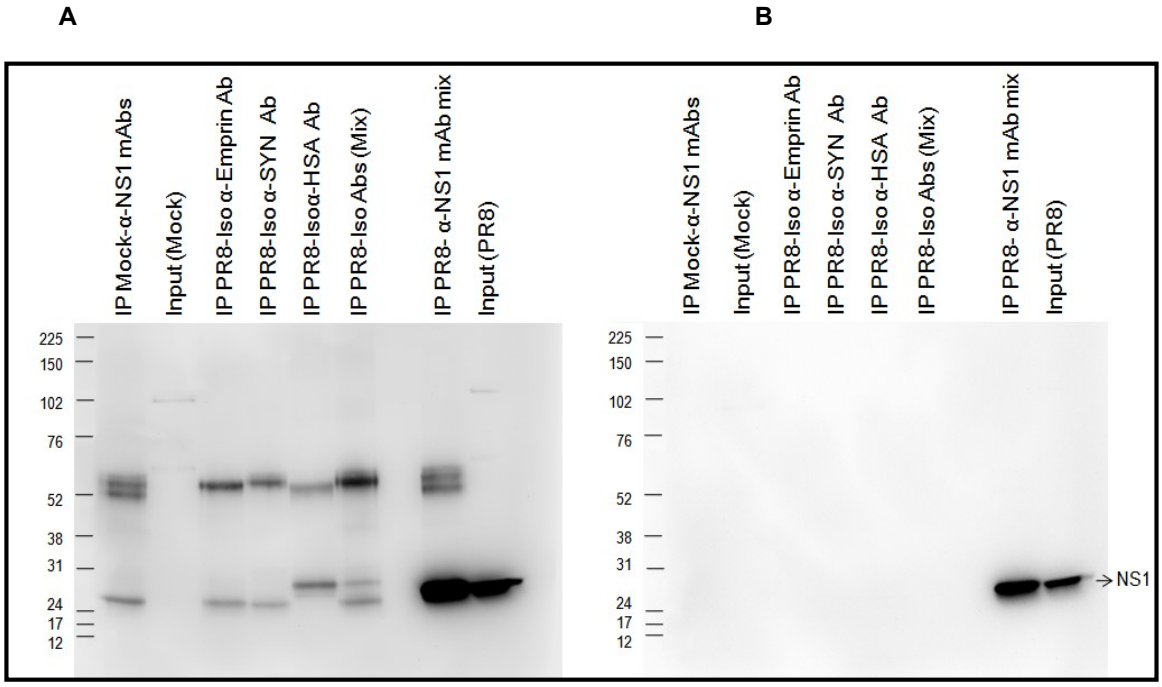

Figure 19: Western blot analysis of NS1 immuniprecipitaion with isotype controls.

A) A549 cells were infected with IAV PR8, harvested at 24 hpi. Nuclear fractions were extracted and immunoprecipitated with individual isotype controls such as α-Emprin, α-SYN and α-HSA. IPs were also conducted with anti-NS1 mAb mixture and a mixture of isotype controls. Inputs and IPs were resolved in 4-12% SDS-PAGE and analyzed by Western blot treating with primary anti-NS1 mAb mixture. Primary mAbs, heavy and light chains of immunoglobulins were detected by secondary HRP-anti mouse Ab. B) Inputs and IPs were analyzed by Western blot using primary anti-NS1 mAb mixture. Secondary HRP-VeriBlot Ab detected complete primary anti NS1 Abs only in PR8-infected input and PR8-infected-IP with anti-NS1 mAb mixture. NS1 was not detected in any IPs of isotype controls.

3.6 Identifying NS1- interacting host proteins by Mass Spectrometry (MS)

Three sets of IPs were performed in each experiment including PR8-infected IP with anti-NS1 mAb mixture, PR8-infected IP with isotype controls and mock-infected IP with anti-NS1 mAb mixture (Figure 17). After confirming the presence of NS1 in PR8-infected IP with anti-NS1 mAb mixture and absence in PR8-infected IP with isotype controls and mock-infected IP with anti-NS1 mAb mixture (Figure 18), 90% of the IP products were processed and analyzed with MS for protein identifications. Four different biological and technical experiments were done to detect NS1-interacting host factors by MS. In MS analysis, positive identification was only considered when at least 2 peptides of representative protein were detected with an unused score ≥ 2. The unused score represents the $-\log_{10}$ probability of a false positive; for example unused scores of 2 and 3 correspond to p=0.01 and 0.001, respectively.

All protein IDs in PR8-infected IP with isotype controls and mock-infected IP with anti-NS1 mAb mixture were considered as background (non-specific binding). The protein IDs, which were detected only in PR8-infected IP with anti-NS1 mAb mixture after removing the backgrounds, are considered as NS1 interacting factors (Figure 17). From the cytosol and nuclei of 6hpi and 24hpi, 233 and 138 NS1 interacting host factors were identified in biological replicates 1 and 2, respectively (Appendices A2 and A3). Two technical replications were carried out during biological experiment 3. 324 NS1-interacting proteins were identified in each technical replicate of biological experiment 3 that included all protein IDs from cytosol and nuclei of 6 hpi and 24hpi (Appendices A4 and A5). Among these four biological and technical replicates, 183 unique NS1 interacting host factors were identified in at least two different biological replicates

Table 7: **NS1-interacting host proteins identified in at least 2 biological experiments.**

Uniprot	Gene Symbol	Protein	Peptides (95%)				Unused score *			
			Bio 1	Bio 2	Bio3 Tech1	Bio3 Tech2	Bio1	Bio2	Bio3 Tech 1	Bio3 Tech2
P55265	ADAR	Double-stranded RNA-specific adenosine deaminase	4	4	20	20	2.86	7.54	37.77	35.31
Q14692	BMS1	Ribosome biogenesis protein BMS1 homolog	3	9	7	5	4.29	17.6	16.75	10.34
Q14137	BOP1	Ribosome biogenesis protein BOP1	4	9	7	9	8	17.8	14.19	15.1
Q8TDN6	BRIX1	Ribosome biogenesis protein BRX1 homolog	2	5	8	10	3.54	11.06	15.72	16.79
Q9Y224	C14orf166#	UPF0568 protein C14orf166	3	-	8	9	6	-	13.56	14.89
Q1ED39	C16orf88	Protein C16orf88	-	4	6	8	-	8	13.53	16.01
Q9Y3I0	C22orf28	UPF0027 protein C22orf28	6	-	12	10	9.47	-	20.52	21.07
Q7Z7K6	CENPV	Centromere protein V	4	2	3	3	7.76	2.96	5.84	5.67
Q969X6	CIRH1A	Cirhin OS	-	10	6	11	-	18.31	13.36	19.31
Q13206	DDX10	Probable ATP-dependent RNA helicase DDX10	-	2	4	3	-	2.29	8.05	5.44
Q92841	DDX17#	Probable ATP-dependent RNA helicase DDX17	5	2	18	16	7.4	4.03	29.5	28.76
Q9NVP1	DDX18	ATP-dependent RNA helicase DDX18	9	14	12	13	17.53	20.77	22.19	20.23
Q9NR30	DDX21#	Nucleolar RNA helicase 2	14	5	14	16	27.57	10.05	25.03	30.43
Q9GZR7	DDX24	ATP-dependent RNA helicase DDX24	4	4	11	8	8.15	7.07	20.93	15.19
Q96GQ7	DDX27	Probable ATP-dependent RNA helicase DDX27	-	4	5	5	-	9.11	10.71	10.45
O00571	DDX3X#	ATP-dependent RNA helicase DDX3X	4	-	9	12	8	-	14.93	18.22
P17844	DDX5	Probable ATP-dependent RNA helicase DDX5	3	-	-	7	5.88	-	-	11.15
Q8TDD1	DDX54	ATP-dependent RNA helicase DDX54	2	6	2	2	4	11.81	3.78	3
Q9NY93	DDX56#	Probable ATP-dependent RNA helicase DDX56	-	4	-	2	-	7.22	-	4.45
O43143	DHX15#	Putative pre-mRNA-splicing factor ATP-dependent RNA helicase DHX15	5	-	28	22	8.66	-	46.27	40.65
Q7L2E3	DHX30#	Putative ATP-dependent RNA helicase DHX30	2	9	53	59	3.05	17.57	87.85	100.67
O60832	DKC1	H/ACA ribonucleoprotein complex subunit 4	3	3	5	3	4.52	6.14	10.8	6.18
Q5QJE6	DNTTIP2	Deoxynucleotidyltransferase terminal-interacting protein 2	-	8	5	4	-	14.42	10.49	8.82
Q99848	EBNA1BP2	Probable rRNA-processing protein EBP2	2	7	7	7	3.5	11.2	12.59	13.09
P19525	EIF2AK2	Interferon-induced, double-stranded RNA-activated protein kinase	-	3	6	6	-	6.6	12.89	12.21
P56537	EIF6	Eukaryotic translation initiation factor 6	2	6	4	5	2.6	9.54	4.01	5.14
Q15717	ELAVL1#	ELAV-like protein 1	5	9	15	16	7.14	19.31	24.84	23.5
Q8IY81	FTSJ3	Putative rRNA methyltransferase 3	5	16	10	8	9.87	30.25	21.22	15.88
Q96I24	FUBP3	Far upstream element-binding protein 3	3	3	11	11	4.21	6.85	21.46	20.94
P35637	FUS#	RNA-binding protein FUS	4	-	3	3	7.38	-	4	5.4
P51114	FXR1#	Fragile X mental retardation syndrome-related protein 1	2	-	3	2	4.01	-	2.9	2.68
Q13823	GNL2	Nucleolar GTP-binding protein 2	-	3	2	2	-	4.88	2.57	3.41
Q9BVP2	GNL3	Guanine nucleotide-binding protein-like 3	-	4	4	4	-	9.03	8.98	8.39
Q9BZE4	GTPBP4	Nucleolar GTP-binding protein 1	5	9	14	14	9.64	18.5	26.81	25.87
P07305	H1F0#	Histone H1.0	-	3	5	3	-	4.23	6.25	4.09
Q92522	H1FX	Histone H1x	-	2	2	2	-	4.36	3.34	2.82

Table 7

Uniprot	Gene Symbol	Protein	Peptide (95%)				Unused Score*			
			Bio 1	Bio 2	Bio3 Tech1	Bio3 Tech2	Bio1	Bio2	Bio3 Tech1	Bio3 Tech2
Q9BTM1	H2AFJ	Histone H2A.J	-	2	2	-	-	2.8	4.4	-
Q71UI9	H2AFV	Histone H2A.V	-	2	5	4	-	3.35	6.96	6.22
O75367	H2AFY	Core histone macro-H2A.1	2	3	5	8	5.1	4.84	9.07	14
Q9H583	HEATR1	HEAT repeat-containing protein 1	7	14	14	9	12.41	27.31	26.58	18.09
P16401	HIST1H1B#	Histone H1.5	4	6	10	8	6.05	9.63	17.07	14
Q93077	HIST1H2AC	Histone H2A type 1-C	-	4	2	-	-	6.87	4.27	-
Q8IUE6	HIST2H2AB	Histone H2A type 2-B	-	4	11	11	-	8.13	10.21	12.76
Q13151	HNRNPA0	Heterogeneous nuclear ribonucleoprotein A	4	3	5	5	5.07	4.36	9.15	8.94
P22626	HNRNPA2B1	Heterogeneous nuclear ribonucleoproteins A2/B1	3	3	11	15	6.66	5.21	18.47	23.97
P51991	HNRNPA3#	Heterogeneous nuclear ribonucleoprotein A3	4	-	8	37	8.06	-	17.75	58.02
Q99729	HNRNPAB#	Heterogeneous nuclear ribonucleoprotein A/B	3	-	3	3	3.2	-	3.05	2.57
Q14103	HNRNPD	Heterogeneous nuclear ribonucleoprotein D0	-	2	3	4	-	4	5.38	7.08
P52597	HNRNPF#	Heterogeneous nuclear ribonucleoprotein F	3	-	16	14	5.21	-	18.27	19.02
P31943	HNRNPH1	Heterogeneous nuclear ribonucleoprotein H	6	4	-	-	7.82	6.59	-	-
P55795	HNRNPH2#	Heterogeneous nuclear ribonucleoprotein H2	2	-	10	-	4	-	12.4	-
P31942	HNRNPH3	Heterogeneous nuclear ribonucleoprotein H3	2	-	3	2	2.6	-	5.07	4.08
P14866	HNRNPL#	Heterogeneous nuclear ribonucleoprotein L	-	30	33	36	-	32.72	28.44	32.15
P52272	HNRNPM#	Heterogeneous nuclear ribonucleoprotein M	12	6	26	26	16.03	11.55	37.44	32.3
O43390	HNRNPR#	Heterogeneous nuclear ribonucleoprotein R	13	12	27	27	19.81	21.8	43.09	37.93
Q9BUJ2	HNRNPUL1#	Heterogeneous nuclear ribonucleoprotein U-like protein 1	7	5	10	9	13.72	10.45	13.58	17.97
Q1KMD3	HNRNPUL2#	Heterogeneous nuclear ribonucleoprotein U-like protein 2	5	7	19	20	8.38	12.28	26.64	24.43
Q5SSJ5	HP1BP3#	Heterochromatin protein 1-binding protein 3	2	6	13	15	3.12	10.71	25.87	27.64
Q58FF8	HSP90AB2P	Putative heat shock protein HSP 90-beta 2	6	-	-	2	8.86	-	-	3.89
P08107	HSPA1A#	Heat shock 70 kDa protein 1A/1B	3	-	5	5	6.23	-	10.38	9.08
P54652	HSPA2#	Heat shock-related 70 kDa protein 2	3	-	7	9	5.8	-	13.36	17.7
P04792	HSPB1#	Heat shock protein beta-1	2	2	2	2	4.25	2.77	4	4
Q9NZI8	IGF2BP1	Insulin-like growth factor 2 mRNA-binding protein 1	4	5	12	15	57	7.42	20.61	15.59
O00425	IGF2BP3	Insulin-like growth factor 2 mRNA-binding protein 3	3	3	9	8	6.03	5.03	17.24	15.92
Q12905	ILF2#	Interleukin enhancer-binding factor 2	9	-	18	27	18.29	-	26.79	40.47
Q12906	ILF3#	Interleukin enhancer-binding factor 3	23	19	48	53	42.2	35.75	60.93	74.73
Q96G21	IMP4	U3 small nucleolar ribonucleoprotein protein IMP4	-	3	2	4	-	6.11	2.35	7.13
Q07666	KHDRBS1	KH domain-containing, RNA-binding, signal transduction-associated protein 1	3	-	5	4	4.51	-	7.85	6.39
P48668	KRT6C	Keratin, type II cytoskeletal 6C	-	6	-	5	-	10.19	-	8.84
P83111	LACTB	Serine beta-lactamase-like protein LACTB, mitochondrial	2	3	2	-	3.56	4.77	2.4	-
P02545	LMNA	Lamin-A/C	3	-	-	5	4.97	-	-	9.82
Q9BXY0	MAK16	Protein MAK16 homolog	-	4	5	4	-	6.29	9.39	8.01
P43243	MATR3#	Matrin-3	4	15	22	25	7.12	29.4	36.94	40.98

Table 7

Uniprot	Gene Symbol	Protein	Peptide (95%)				Unused Score*			
			Bio 1	Bio 2	Bio3 Tech1	Bio3 Tech2	Bio1	Bio2	Bio3 Tech1	Bio3 Tech2
Q9BYG3	MKI67IP	MKI67 FHA domain-interacting nucleolar phosphoprotein	7	5	6	5	12.02	7.21	11.84	7.51
O00566	MPHOSPH10	U3 small nucleolar ribonucleoprotein protein MPP10	-	6	4	5	-	11.27	3.88	10.01
Q9BQG0	MYBBP1A#	Myb-binding protein 1A	5	11	5	14	10.67	20.55	11.75	27.46
O00159	MYO1C#	Myosin-Ic	-	2	3	4	-	4.43	5.67	7.7
Q9H0A0	NAT10#	N-acetyltransferase 10	4	3	4	7	8.49	6.54	7.26	13.43
P19338	NCL	Nucleolin	5	-	7	9	8.15	-	12.97	18.66
Q9Y221	NIP7	60S ribosome subunit biogenesis protein NIP7 homolog	-	2	4	-	-	3.74	5.8	-
O15226	NKRF#	NF-kappa-B-repressing factor	-	8	11	12	-	12.94	22.84	22.1
Q9H8H0	NOL11	Nucleolar protein 11	-	9	7	6	-	15.16	12.65	12.92
Q9H6R4	NOL6	Nucleolar protein 6	2	5	7	8	2.27	7.92	13.17	13.42
Q9UMY1	NOL7	Nucleolar protein 7	-	5	3	3	-	8.47	6	5.82
Q9Y3C1	NOP16	Nucleolar protein 16	2	3	3	4	4	6.58	3.74	8.07
P46087	NOP2	Putative ribosomal RNA methyltransferase NOP2	11	12	22	23	19.36	25.03	37.05	40.73
O00567	NOP56#	Nucleolar protein 56	13	15	24	27	23.87	22.4	43.65	44.13
Q9Y2X3	NOP58#	Nucleolar protein 58	9	-	17	19	12.35	-	29.8	31.99
Q14980	NUMA1	Nuclear mitotic apparatus protein 1	6	4	9	12	11.12	8.69	17.94	23.27
Q13310	PABPC4#	Polyadenylate-binding protein 4	4	6	7	10	7.81	6.46	14.6	15.16
Q9NWT1	PAK1IP1	p21-activated protein kinase-interacting protein 1	3	2	2	3	6	3.47	2.92	5.89
Q15365	PCBP1#	Poly(rC)-binding protein 1	2	-	2	-	3.8	-	4.01	-
Q14690	PDCD11	Protein RRP5 homolog	13	19	27	28	24.61	37.82	56.56	54.56
O00541	PES1	Pescadillo homolog	3	4	7	5	6.72	9.09	12.5	9.42
Q96HS1	PGAM5	Serine/threonine-protein phosphatase PGAM5, mitochondrial	3	-	4	5	4.34	-	7.22	8.01
P78527	PRKDC	DNA-dependent protein kinase catalytic subunit	2	-	3	-	3.27	-	3.73	-
Q9UMS4	PRPF19#	Pre-mRNA-processing factor 19	-	4	10	10	-	8.67	16.95	18.41
Q13523	PRPF4B	Serine/threonine-protein kinase PRP4 homolog	2	-	8	5	3.42	-	15.43	10.27
P26599	PTBP1#	Polypyrimidine tract-binding protein 1	10	9	14	15	14.9	18.56	24.28	23.42
Q15269	PWP2	Periodic tryptophan protein 2 homolog	2	6	6	6	2.73	11.3	11.52	11.13
Q9P0K7	RAI14	Ankycorbin	7	-	-	2	11.95	-	-	4
Q9UKM9	RALY#	RNA-binding protein Raly	3	11	20	23	6.36	17.52	26.01	28.69
Q96PK6	RBM14	RNA-binding protein 14	-	5	7	9	-	8.46	13.26	17.49
Q96T37	RBM15	Putative RNA-binding protein 15	3	-	6	8	3.57	-	12.18	15.66
P49756	RBM25	RNA-binding protein 25	2	-	-	5	3.6	-	-	9.28
Q9NW13	RBM28	RNA-binding protein 28	2	6	10	8	4.01	12.02	18.29	14.38
P42696	RBM34	RNA-binding protein 34	-	4	2	3	-	8	4.45	6.33
Q9BWF3	RBM4	RNA-binding protein 4	-	2	4	3	-	4.22	7.82	4.92
P38159	RBMX#	Heterogeneous nuclear ribonucleoprotein G		5	15	12	-	7.4	25.26	21.86
O95758	ROD1	Regulator of differentiation 1	-	2	5	4	-	4.42	8.43	6.59
Q9H9Y2	RPF1	Ribosome production factor 1	-	4	2	3	-	7.3	3.59	6
Q9H7B2	RPF2	Ribosome production factor 2 homolog	3	7	8	8	6.15	12.33	13.61	14
P62913	RPL11#	60S ribosomal protein L11	2	-	2	4	3.16	-	4	7.32
P30050	RPL12	60S ribosomal protein L12	2	-	2	2	4	-	4	2.79
P26373	RPL13#	60S ribosomal protein L13	2	-	-	4	3.46	-	-	8.4
P50914	RPL14#	60S ribosomal protein L14	2	-	2	3	3.59	-	4.01	3.06
P61313	RPL15#	60S ribosomal protein L15	2	-	3	3	4.03	-	4.97	6.04
P62829	RPL23#	60S ribosomal protein L23	3	-	5	3	2	-	8.8	4.02
P62750	RPL23A#	60S ribosomal protein L23a	2	-	2	-	3.57	-	4.39	-

Table 7

Uniprot	Gene Symbol	Protein	Peptide (95%)				Unused Score*			
			Bio 1	Bio 2	Bio3 Tech1	Bio3 Tech2	Bio1	Bio2	Bio3 Tech1	Bio3 Tech2
P61353	RPL27	60S ribosomal protein L27	2	-	6	5	4	-	10.64	8.68
P39023	RPL3#	60S ribosomal protein L3	6	-	9	8	9.09	-	18.72	15.38
Q9Y3U8	RPL36#	60S ribosomal protein L36	2	-	2	3	3.54	-	4.38	4.94
P46777	RPL5	60S ribosomal protein L5	-	4	3	-	-	6.66	5.48	-
Q02878	RPL6#	60S ribosomal protein L6	3	7	11	13	6.41	14.44	17.38	21.66
P18124	RPL7#	60S ribosomal protein L7	4	-	3	6	-	5.31	6.6	11.46
P62424	RPL7A#	60S ribosomal protein L7a	4	-	8	11	7.11	-	15.34	18.93
Q6DKI1	RPL7L1	60S ribosomal protein L7-like 1	-	3	3	4	-	6.44	5.02	8.34
P62263	RPS14#	40S ribosomal protein S14	3	-	-	2	6	-	-	2.26
P23396	RPS3#	40S ribosomal protein S3	3	-	2	4	4.51	-	2.55	7.39
P62241	RPS8#	40S ribosomal protein S8	2	-	3	4	4	-	4.82	8
Q9P2E9	RRBP1	Ribosome-binding protein 1	7	-	18	19	15.03	-	36.88	38.71
P56182	RRP1	Ribosomal RNA processing protein 1 homolog A	2	3	6	4	4.19	6.66	9.28	8.38
Q5JTH9	RRP12	RRP12-like protein	2	3	4	2	2.49	6.02	5.4	3.86
Q14684	RRP1B	Ribosomal RNA processing protein 1 homolog B	4	4	11	12	7.29	7.06	18.98	20.86
Q9Y3A4	RRP7A	Ribosomal RNA-processing protein 7 homolog A	-	2	-	3	-	4.13	-	4.17
O43159	RRP8	Ribosomal RNA-processing protein 8	-	2	4	3	-	3.32	8.02	6
O43818	RRP9	U3 small nucleolar RNA-interacting protein 2	3	4	5	4	6	7.01	11.04	8.16
Q15050	RRS1	Ribosome biogenesis regulatory protein homolog	4	11	7	9	7.01	18.42	9.17	17.81
O76021	RSL1D1	Ribosomal L1 domain-containing protein 1	9	-	20	17	17.26	-	37.44	34.24
P60903	S100A10	Protein S100-A10	3	-	-	2	6	-	-	2.49
Q14151	SAFB2#	Scaffold attachment factor B2	6	2	10	12	12.26	2.64	20.4	22.78
Q9H7N4	SCAF1	Splicing factor, arginine/serine-rich 19	-	2	3	-	-	4	5.92	-
Q13435	SF3B2	Splicing factor 3B subunit 2	-	3	9	8	-	3.83	17.43	15.05
Q15393	SF3B3	Splicing factor 3B subunit 3	3	-	7	7	5.85	-	13.05	9.58
Q08170	SFRS4	Splicing factor, arginine/serine-rich 4	3	-	-	2	4	-	-	3.59
Q13247	SFRS6	Splicing factor, arginine/serine-rich 6	3	-	3	3	4	-	5.48	3.59
Q16629	SFRS7	Splicing factor, arginine/serine-rich 7	2	-	3	-	3.28	-	5.57	-
Q9NWH9	SLTM	SAFB-like transcription modulator	3	3	11	10	5.82	3.09	20.01	18.56
O60264	SMARCA5	SWI/SNF-related matrix-associated actin-dependent regulator of chromatin subfamily A member 5	2	-	3	3	3.35	-	6.1	5.79
O75643	SNRNP200	U5 small nuclear ribonucleoprotein 200 kDa helicase	-	10	23	20	-	19.16	48.66	37.55
P08621	SNRNP70	U1 small nuclear ribonucleoprotein 70 kDa	2	-	6	7	3.25	-	11.58	13.86
P18583-5	SON#	Isoform D of Protein SON	-	5	4	3	-	9.39	8.16	6.11
Q13501	SQSTM1	Sequestosome-1	2	-	2	6	3.89	-	4.37	10
Q8IYB3	SRRM1	Serine/arginine repetitive matrix protein 1	-	2	2	4	-	2.67	4.12	7.68
O95793	STAU1#	Double-stranded RNA-binding protein Staufen homolog 1	-	2	5	8	-	3.7	9.86	16.03
O75683	SURF6	Surfeit locus protein 6	2	-	-	3	3.1	-	-	6.24
O60506	SYNCRIP#	Heterogeneous nuclear ribonucleoprotein Q	8	-	11	10	14.4	-	17.7	19.41
Q92804	TAF15	TATA-binding protein-associated factor 2N	2	-	-	3	3.06	-	-	4
Q13148	TARDBP	TAR DNA-binding protein 43	2	-	3	2	4	-	5.96	3.26
Q12788	TBL3	Transducin beta-like protein 3	3	8	5	9	6.01	16.72	10.19	18.46
Q13428	TCOF1	Treacle protein	3	-	6	7	6	-	12.4	13.24
Q9NXF1	TEX10	Testis-expressed sequence 10 protein	-	4	3	3	-	6.75	4.79	6

Table 7

Uniprot	Gene Symbol	Protein	Peptide (95%)				Unused Score*			
			Bio 1	Bio 2	Bio3 Tech1	Bio3 Tech2	Bio1	Bio2	Bio3 Tech1	Bio3 Tech2
P42166	TMPO	Lamina-associated polypeptide 2, isoform alpha	2	-	-	6	4	-	-	12.22
Q13595	TRA2A	Transformer-2 protein homolog alpha	2	-	5	6	2.04	-	8.55	9.86
Q14258	TRIM25#	E3 ubiquitin/ISG15 ligase TRIM25	2	-	2	2	2.66	-	2.62	4
Q14669	TRIP12	Probable E3 ubiquitin-protein ligase TRIP12	-	2	10	7	-	4.39	21.08	12.7
Q9BVJ6	UTP14A	U3 small nucleolar RNA-associated protein 14 homolog A	-	3	6	5	-	6.01	11.86	8.75
Q8TED0	UTP15	U3 small nucleolar RNA-associated protein 15 homolog	3	8	6	9	4.65	13.57	6.6	17.59
Q9Y5J1	UTP18	U3 small nucleolar RNA-associated protein 18 homolog	4	12	10	5	8.99	17.71	15.09	10.54
Q9NYH9	UTP6	U3 small nucleolar RNA-associated protein 6 homolog	3	3	7	7	6	6.4	13.09	12.81
P21796	VDAC1	Voltage-dependent anion-selective channel protein 1	2	-	-	2	2.46	-	-	4.01
Q9Y277	VDAC3	Voltage-dependent anion-selective channel protein 3	2	-	3	2	3.02	-	6.01	4.12
Q9GZL7	WDR12	Ribosome biogenesis protein WDR12	2	7	3	2	3.38	14.26	4.27	4.26
Q9UNX4	WDR3	WD repeat-containing protein 3	3	10	9	8	6	20.94	18.64	15.57
Q8NI36	WDR36	WD repeat-containing protein 36	-	8	12	17	-	19.87	25.61	33.36
Q15061	WDR43	WD repeat-containing protein 43	-	4	6	7	-	6.52	8.33	12
O15213	WDR46	WD repeat-containing protein 46	3	6	9	9	6	10.03	16.71	17.11
Q6RFH5	WDR74	WD repeat-containing protein 74	2	6	-	-	4.14	10.11	-	-
Q8IWA0	WDR75	WD repeat-containing protein 75	4	10	5	13	6.17	17.11	12.14	21.8
Q9H0D6	XRN2	5'-3' exoribonuclease 2	2	6	14	12	2.71	12.14	28.48	23.17
Q7Z2W4	ZC3HAV1	Zinc finger CCCH-type antiviral protein 1	5	6	8	6	9.06	9.94	16.91	11.3
Q96KR1	ZFR	Zinc finger RNA-binding protein	10	20	34	33	15.16	35.58	42.02	48.56
Q5BKZ1	ZNF326	Zinc finger protein 326	3	-	5	7	6	-	8.37	10.49

* Represents the -$\log_{10}$ probability of a false positive (for example, Unused score of 2.0 corresponds to p= 0.01; Unused score of 3 corresponds to p = 0.001)

Protein IDs found to interact with Influenza virus NS1 in VirHostNet 2.0 database (As of May 2016)

The Table is ordered alphabetically by gene symbol.

(Table 7 and Figure 20A). These 183 proteins were screened for Influenza virus-host interaction in the VirHostNet 2.0 (http://virhostnet.prabi.fr/) database; and as of May 2016, 59 (32%) of these 183 host factors were previously reported in different databases and literature to interact with Influenza virus NS1 protein (Gene symbols are marked with # in Table 7). These 59 candidates served as positive controls of my experiments. In addition to the host factors, PR8 Matrix protein 1 (M1) and Nucleoprotein (NP) were detected in NS1 IP with high peptide and unused scores, which were also previously found to interact with IAV NS1 in the VirHostNet 2.0 database.

Two technical replicates were conducted in biological experiment 3, which were run in MS on different days. 324 proteins were identified in each run where 259 proteins (~80%) overlapped between the two replicates, which indicated the consistent performance of our mass spectrometer throughout all runs (Figure 20B).

3.7 Bioinformatics analysis of NS1 interacting proteins

The multifunctional IAV-NS1protein is expected to interact with various host factors to serve its multiple functions. So, categorizing the NS1-interacting host factors identified in my MS analysis can divulge potential pathways and functions where NS1 plays important roles during viral replication. I analyzed the protein candidates with an online-based tool, the Database for Annotation, Visualization and Integrated Discovery (DAVID; https://david.ncifcrf.gov/) [191]. In addition, protein candidates were also uploaded into STRING 10.0 (http://string-db.org/) to globally visualize all protein-protein interactions.

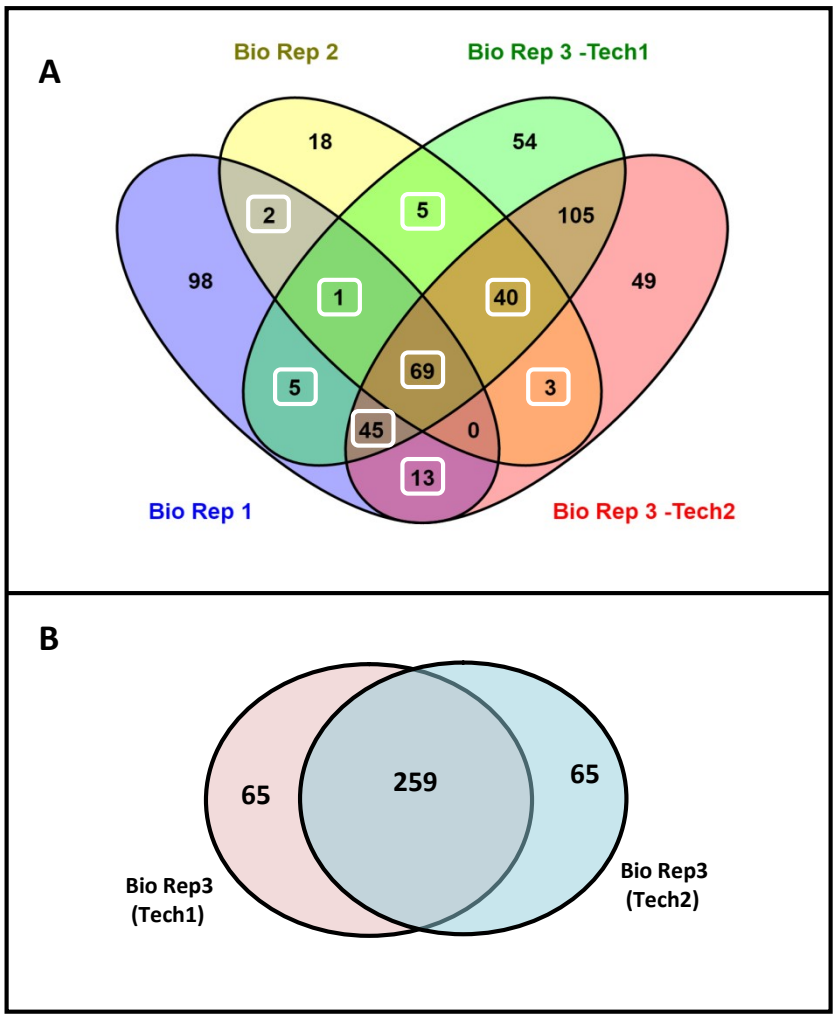

Figure 20: Venn diagram of different numbers of overlapped proteins in MS analysis.

A) 134 to 324 NS1-interacting host proteins were found in the cytosol and nuclei at 6 and 24 hpi in four different biological and technical replicates. The protein IDs of each replicate were placed in Venny 2.1 program to generate this Venn diagram. 183 NS1-interacting host proteins (marked with white box) were detected in at least two different biological replicates. B) 324 proteins were identified in each technical replicate of biological experiment 3. Venn diagram shows the number of protein overlapped in 2 technical replicates.

3.7.1 Pathway and functional analysis by DAVID

183 NS1-interacting protein IDs were uploaded into DAVID to generate functional categories such as pathways, biological processes and molecular functions. The pathway categorizations were based on KEGG (Kyoto Encyclopedia of Genes and Genomes) and Reactome terms. The molecular and functional categorizations were based on Gene Ontology (GO) and Panther terms. DAVID highlights enriched known pathways, molecular functions and biological processes that include the most proteins from the tested protein list. Protein IDs with $p = < 0.05$ were considered as positive hits in DAVID analysis. The NS1-interacting host factors were involved in eight different pathways when these were analyzed in DAVID with Panther term, such as gene expressions, 3' -UTR-mediated translational regulation, processing of capped intron-containing pre-mRNA, spliceosome, Influenza infection and metabolism of proteins (Figure 21A). David (Panther) analysis of 183 genes showed various biological and molecular classes (Figure 21B and C). The top biological processes enriched were nucleoside, nucleotide and nucleic acid metabolism, mRNA splicing, pre-mRNA processing and protein biosynthesis. Similar molecular functions such as nucleic acid binding, mRNA splicing factor, mRNA processing factor and ribosomal protein were also enriched. Appendices A6-A8 list the individual NS1 interacting proteins that were associated with each pathway, biological process and molecular function.

Influenza virus is an intracellular parasite and it widely utilizes the host cell system for its gene expression. It has been described that selective translation of IAV mRNAs occurred over cellular mRNAs, which was probably mediated by the $5^{/}$ UTR of viral mRNAs [48, 192, 193]. It is reported that NS1 plays important role to initiate

A. Pathways in DAVID Analysis

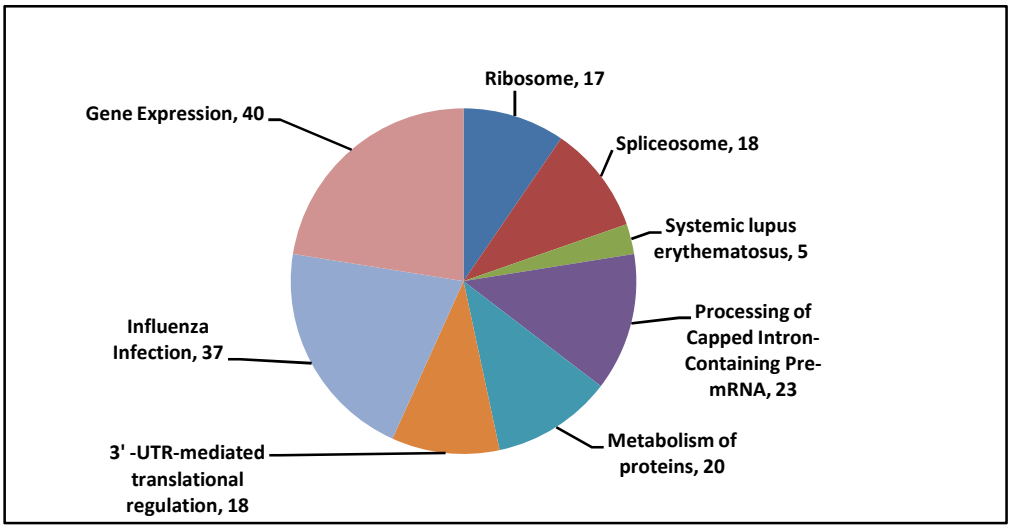

B. DAVID: Biological Process (Panther)

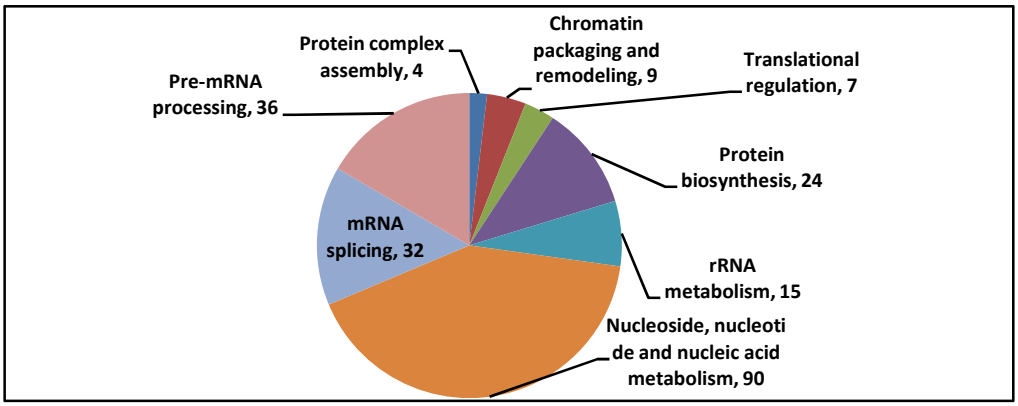

C. DAVID: Molecular Function (Panther)

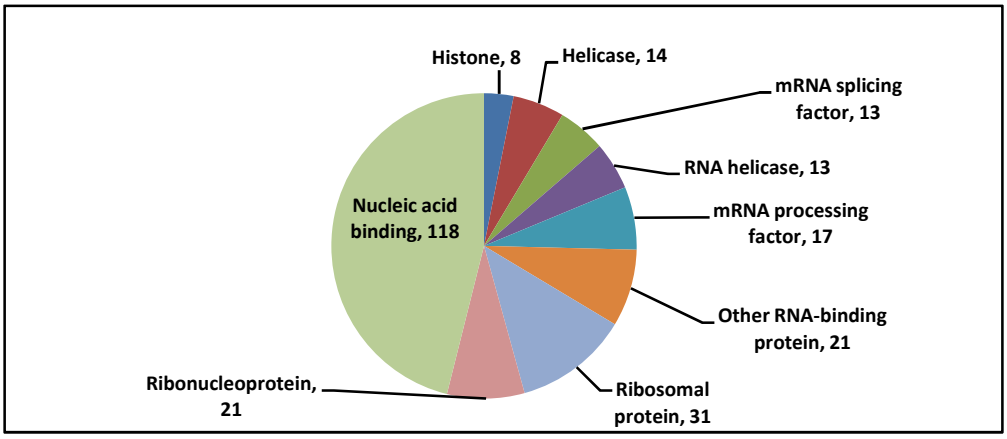

Figure 21: Functional analysis of NS1-interacting host factors by DAVID.

Pathways, biological processes and molecular functions of 183 NS1 interacting proteins were analyzed in DAVID. A) In pathway analysis, 57 candidates were recognized by KEGG and Reactome terms. Different colors indicate different pathways and number of proteins involved in the respective pathways. B) 116 protein candidates were detected and mapped with Panther term to categorize into biological processes C) The 119 protein candidates were recognized and mapped with Panther ontology to classify different molecular functions.

translation of viral mRNAs without affecting host- mRNAs [194]. NS1 interacts with the 5′ UTR of viral mRNAs, translation initiation factor eIF4GI and PABP1; thereby enhancing viral mRNA translation [48, 192, 195, 196]. In addition NS1 interacts with viral RNP and regulates IAV replication [196, 197]. In my NS1 interactome studies, numerous host factors were identified in DAVID that are involved in gene expression, translational regulation, protein metabolism, nucleic acid binding and mRNA processing (Figure 21 and Appendices A6-A8). These host factors may be utilized by IAV NS1 protein to favour viral replication.

After viral entry, IAV RNPs get into the nucleus for transcription and viral RNA replication. Influenza RNA-dependent RNA polymerase (RdRp) performs cap-snatching from host pre-mRNA to initiate transcription by viral mRNA-capping and it is suggested that NS1 play roles as it interacts with various host factors [48, 198]. Influenza viral RNA segments 7 and 8 encode two proteins each, which occur via the alternative splicing mechanism. Influenza viruses utilize the host's splicing machinery for alternative splicing [74, 75, 198]. NS1 interacts with spliceosome subunits U2 and U6, inhibits spliceosome recruitment and blocks cellular gene expressions [199, 200]. NS1 binds with the CPSF30, which is an essential factor of cellular 3′ end polyadenylation, therefore, inhibits host pre-mRNA maturation [127]. NS1 also interacts with the factors involved in mRNA export, such as NXF1/Tap, and blocks host mRNA export [201]. In my NS1-interactome studies numerous host factors were identified in DAVID analysis, which have important roles in different pathways, biological processes and molecular functions, such as splicing,

A. DAVID: Biological Process (GO)

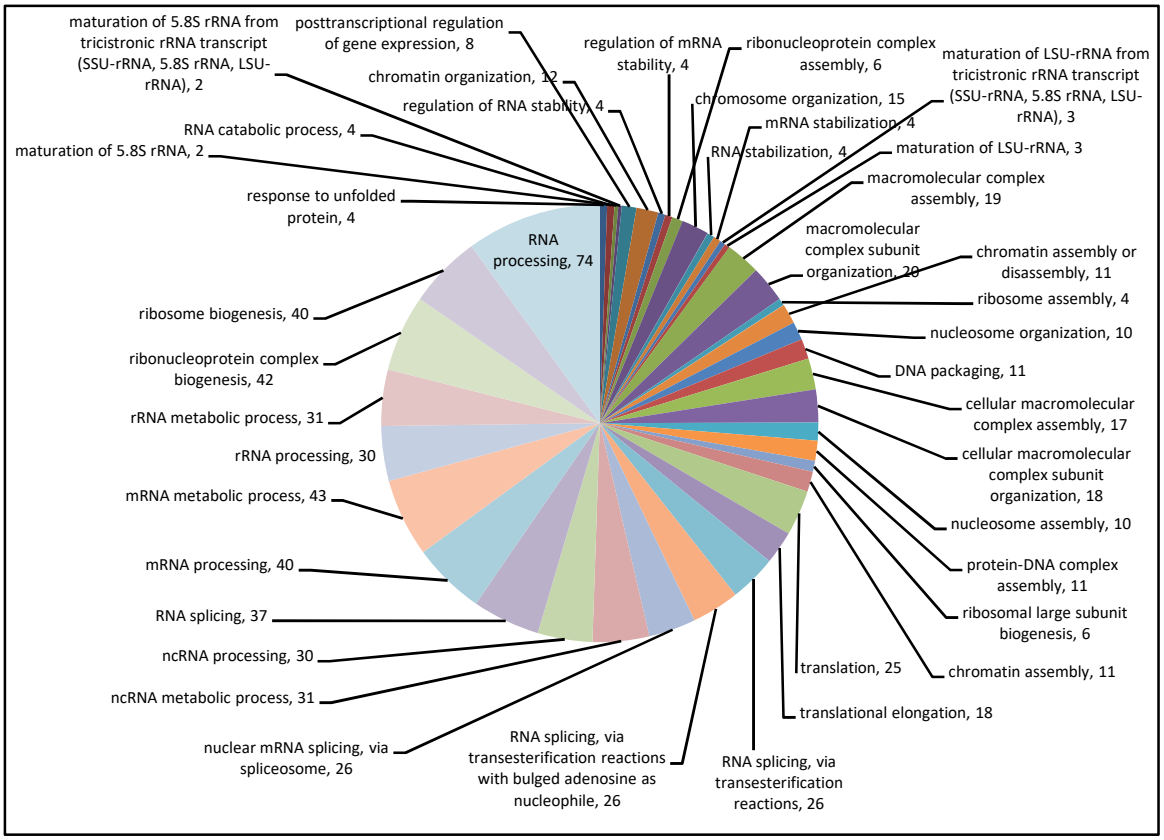

B. DAVID: Molecular Function (GO)

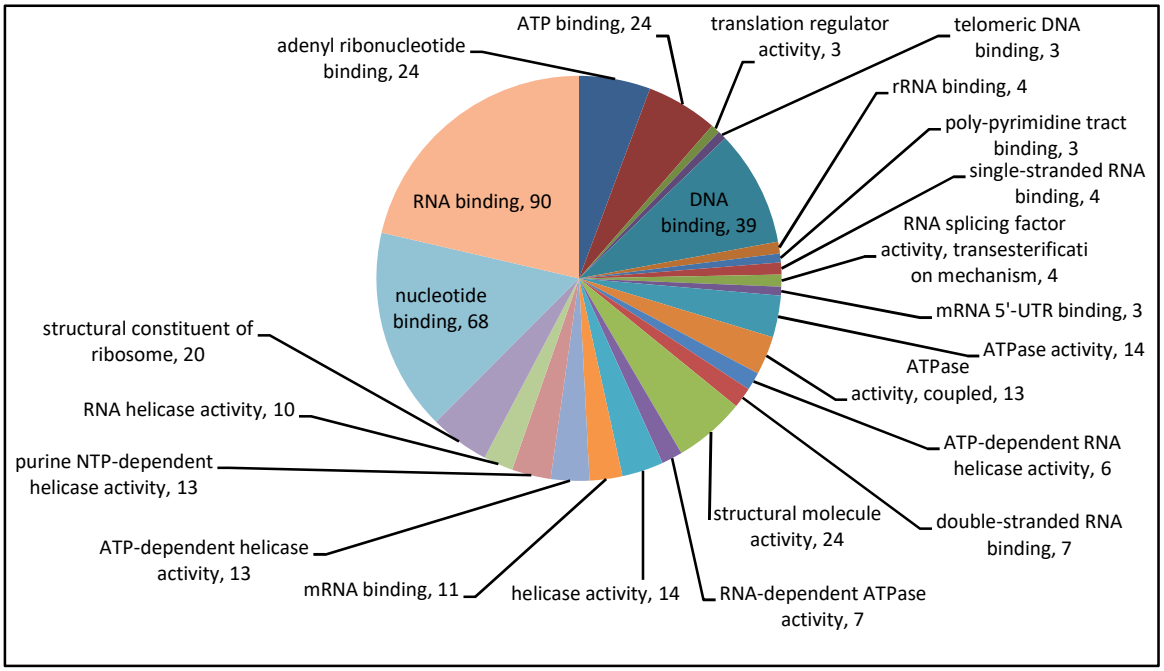

Figure 22: Biological processes and molecular functions of 183 proteins in DAVID with GO terms.

A) 117 candidates of NS1 interactome studies were identified in DAVID and mapped into biological processes. Names of different biological processes are marked with different colors, which also indicate the number of protein in respective biological processes. B) 132 candidates were identified and mapped into different molecular functions.

3' -UTR-mediated translational regulation and pre-mRNA processing (Figure 21, Appendices A6-A8). These NS1 interacting factors may indicate their involvements in Influenza virus replication, which can be utilized by Influenza viruses during replication.

183 NS1 interacting host factors were also mapped in DAVID on GO term for functional classifications. Gene Ontology analysis showed diverse biological processes and molecular functions (Figure 22). The top biological processes enriched were RNA processing, mRNA metabolic process, RNA splicing and translation. Some top molecular functions enriched were RNA binding, nucleotide binding, DNA binding and structural molecule activity. Lists of all candidates involved in different biological processes and molecular functions are included in Appendices A9 and A10.

3.7.2 Network analysis by STRING

STRING is an online-based database that provides protein-protein interactions with known and predicted protein candidates. These protein networks include both direct (physical) and indirect (functional) interactions. I uploaded protein IDs identified in each pathway of DAVID to observe protein-protein interactions in STRING database. Different protein-protein interactions were seen among the NS1-interacting host factors of individual pathways (Figure 23 A-G). Tight interactions among the proteins of different pathways, such as ribosome, 3' -UTR-mediated translational regulation and metabolism indicate the strong associations of these pathways with NS1 during Influenza virus replication. All 183 protein IDs were also analyzed collectively in STRING to check their interaction network (Figure 23H). Many of these 183 NS1-interacting proteins also interacted with one another.

A

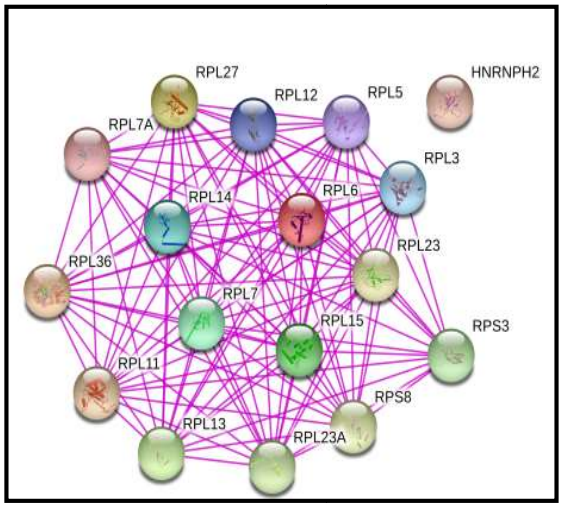
RPL27
RPL12
RPL5
HNRNPH2
RPL7A
RPL3
RPL14
RPL6
RPL23
RPL36
RPL7
RPL15
RPS3
RPL11
RPS8
RPL13
RPL23A

B

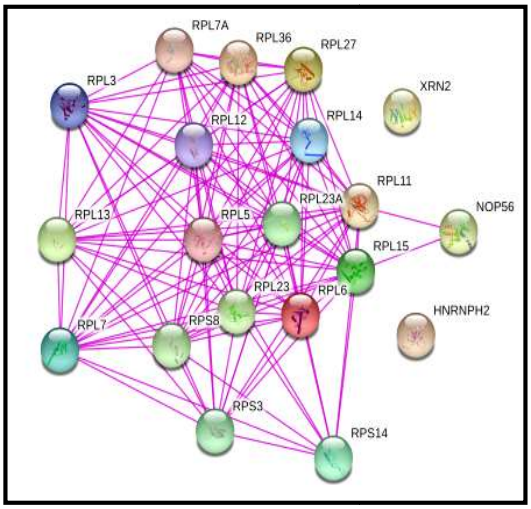
RPL7A
RPL36
RPL27
RPL3
XRN2
RPL12
RPL14
RPL11
RPL23A
NOP56
RPL13
RPL5
RPL15
RPL23
RPL6
HNRNPH2
RPL7
RPS8
RPS3
RPS14

C

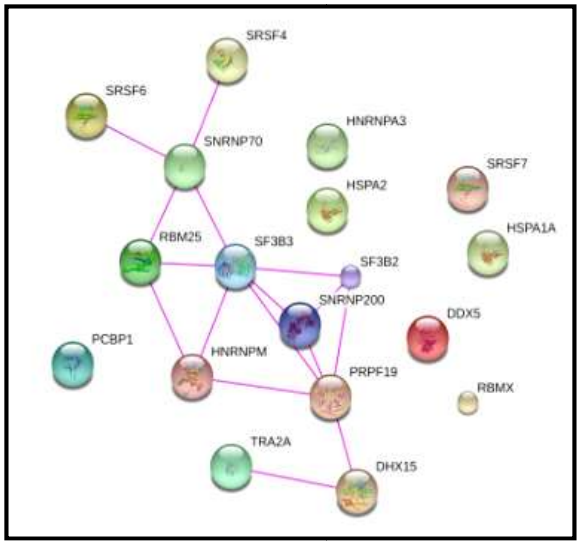
SRSF4
SRSF6
HNRNPA3
SNRNP70
SRSF7
HSPA2
HSPA1A
RBM25
SF3B3
SF3B2
SNRNP200
DDX5
PCBP1
HNRNPM
PRPF19
RBMX
TRA2A
DHX15

D

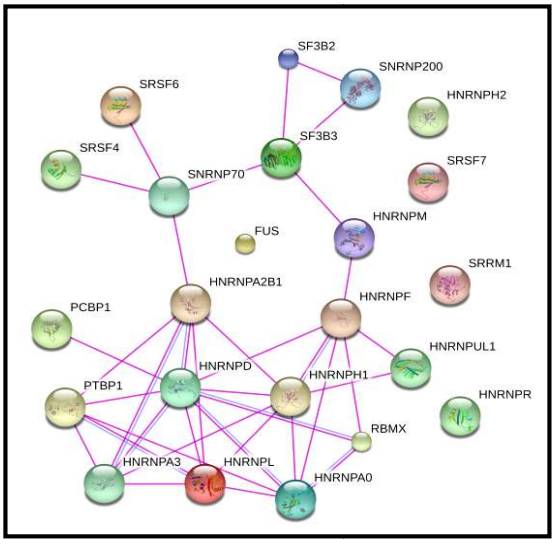
SF3B2
SNRNP200
SRSF6
HNRNPH2
SF3B3
SRSF4
SRSF7
SNRNP70
HNRNPM
FUS
SRRM1
HNRNPA2B1
HNRNPF
PCBP1
HNRNPUL1
HNRNPD
HNRNPH1
PTBP1
HNRNPR
RBMX
HNRNPA3
HNRNPL
HNRNPA0

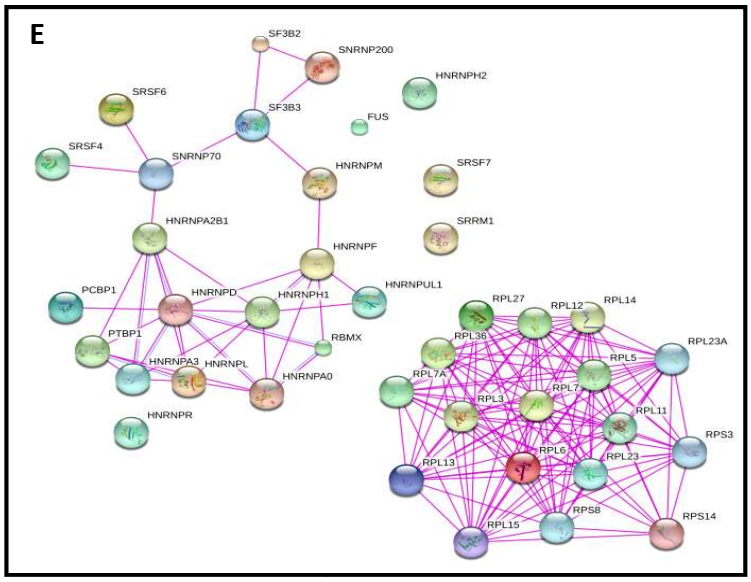
E
SF3B2
SNRNP200
HNRNPH2
SRSF6
SF3B3
FUS
SRSF4
SNRNP70
HNRNPM
SRSF7
HNRNPA2B1
SRRM1
HNRNPF
HNRNPUL1
PCBP1
HNRNPD
HNRNPH1
RPL27
RPL12
RPL14
RPL36
RPL23A
PTBP1
RBMX
RPL5
HNRNPA3
HNRNPL
RPL7A
HNRNPA0
RPL7
RPL3
RPL11
HNRNPR
RPS3
RPL6
RPL23
RPL13
RPS8
RPS14
RPL15

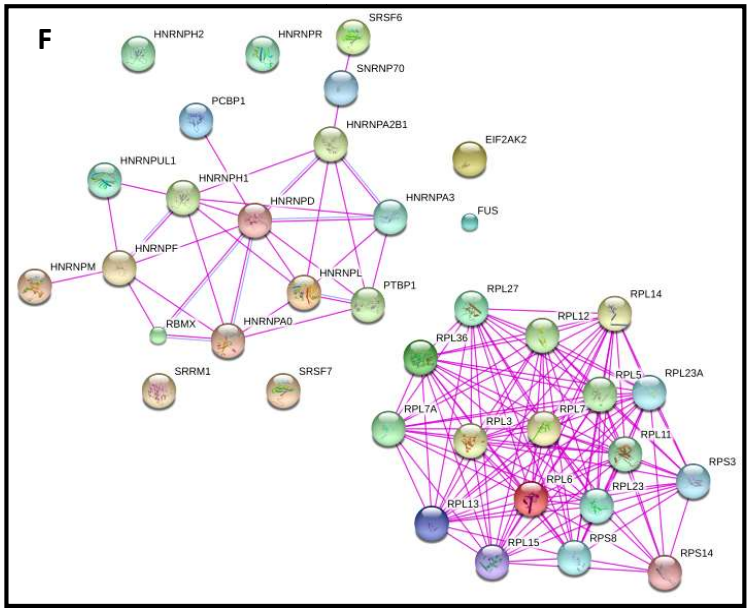
F
HNRNPH2
HNRNPR
SRSF6
SNRNP70
PCBP1
HNRNPA2B1
EIF2AK2
HNRNPUL1
HNRNPH1
HNRNPD
HNRNPA3
FUS
HNRNPF
HNRNPM
HNRNPL
PTBP1
RPL27
RPL14
RPL12
RBMX
HNRNPA0
RPL36
SRRM1
SRSF7
RPL5
RPL23A
RPL7A
RPL7
RPL3
RPL11
RPS3
RPL6
RPL23
RPL13
RPS8
RPL15
RPS14

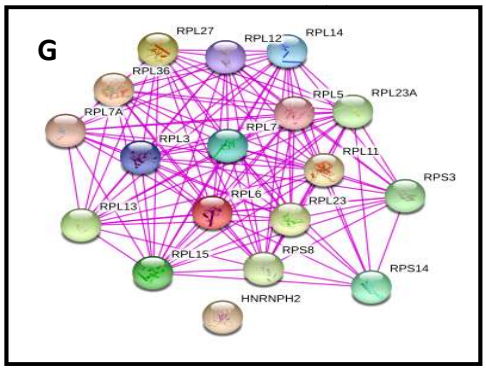
G
RPL27
RPL12
RPL14
RPL36
RPL5
RPL23A
RPL7A
RPL7
RPL3
RPL11
RPS3
RPL6
RPL23
RPL13
RPS8
RPL15
RPS14
HNRNPH2

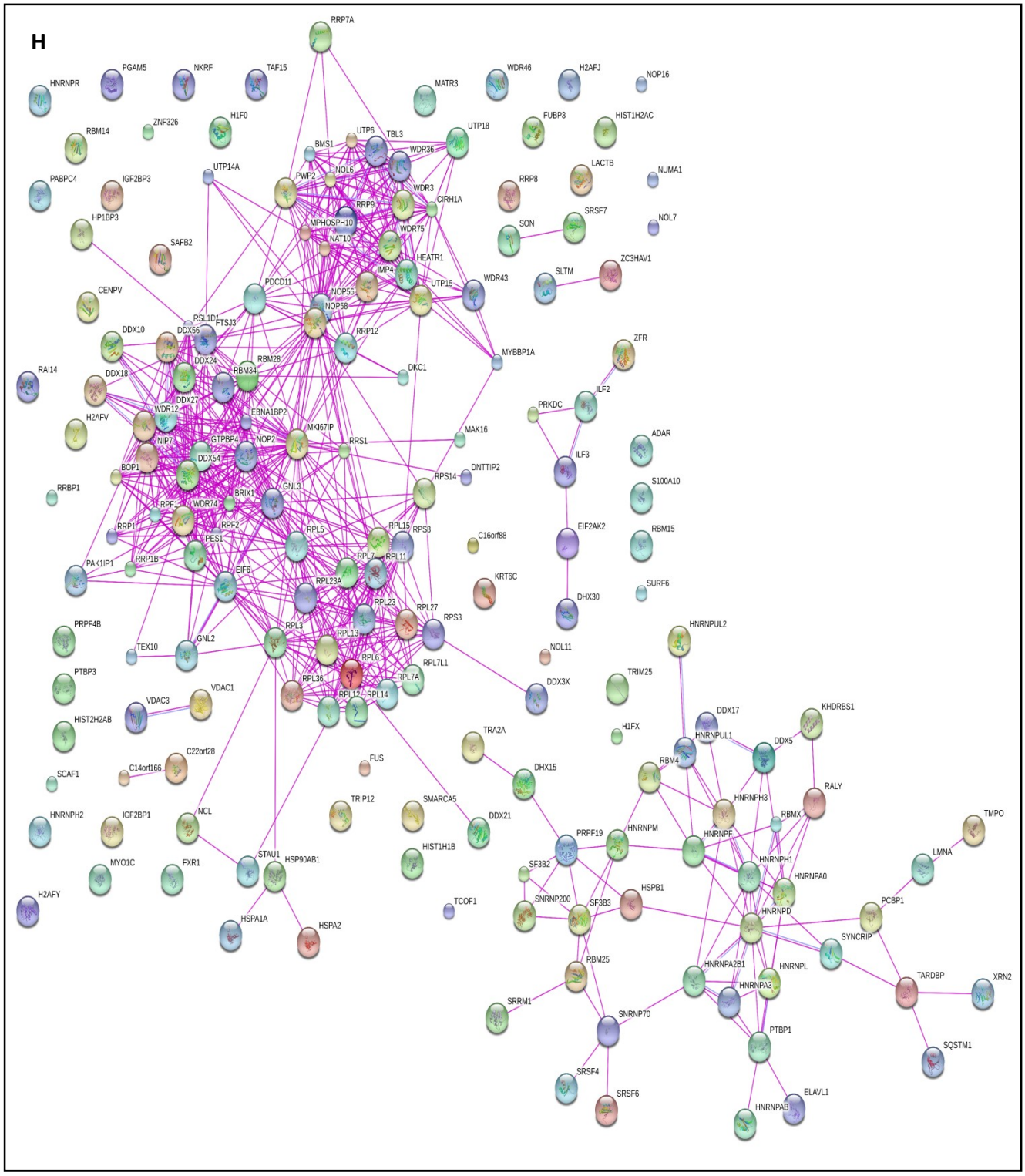
H
RRP7A
PGAM5
NKRF
TAF15
HNRNPR
MATR3
WDR46
H2AFJ
NOP16
ZNF326
H1F0
FUBP3
HIST1H2AC
RBM14
UTP6
TBL3
UTP18
BMS1
WDR36
UTP14A
LACTB
NUMA1
PABPC4
IGF2BP3
PWP2
NOL6
RRP8
WDR3
CIRH1A
RRP9
SRSF7
NOL7
HP1BP3
MPHOSPH10
SON
WDR75
SAFB2
NAT10
HEATR1
ZC3HAV1
IMP4
SLTM
PDCD11
UTP15
WDR43
CENPV
NOP56
NOP58
RSL1D1
FTSJ3
RRP12
DDX10
DDX56
ZFR
MYBBP1A
DDX24
RBM28
RAI14
DDX18
RBM34
DKC1
ILF2
DDX27
PRKDC
WDR12
EBNA1BP2
H2AFV
MKI67IP
MAK16
ADAR
NIP7
GTPBP4
NOP2
RRS1
ILF3
DDX54
BOP1
DNTTIP2
RPS14
S100A10
RRBP1
BRIX1
GNL3
RPF1
WDR74
EIF2AK2
RBM15
RRP1
RPF2
RPL5
RPL15
RPS8
C16orf88
PES1
RPL7
RPL11
PAK1IP1
RRP1B
EIF6
KRT6C
SURF6
RPL23A
RPL23
RPL27
DHX30
PRPF4B
RPL3
RPS3
HNRNPUL2
TEX10
GNL2
RPL13
NOL11
RPL6
RPL7L1
PTBP3
RPL36
DDX3X
TRIM25
VDAC3
VDAC1
RPL12
RPL14
RPL7A
DDX17
KHDRBS1
HIST2H2AB
TRA2A
H1FX
HNRNPUL1
DDX5
C22orf28
C14orf166
FUS
RBM4
SCAF1
DHX15
RALY
TRIP12
SMARCA5
HNRNPH3
RBMX
TMPO
HNRNPH2
IGF2BP1
NCL
DDX21
PRPF19
HNRNPM
HNRNPF
HIST1H1B
LMNA
MYO1C
FXR1
STAU1
HSP90AB1
SF3B2
HNRNPH1
HNRNPA0
H2AFY
HSPB1
SNRNP200
SF3B3
PCBP1
TCOF1
HNRNPD
HSPA1A
HSPA2
SYNCRIP
RBM25
HNRNPA2B1
HNRNPL
TARDBP
XRN2
SRRM1
HNRNPA3
SNRNP70
PTBP1
SQSTM1
SRSF4
SRSF6
ELAVL1
HNRNPAB

Figure 23: Interaction networks of proteins identified in NS1-inteactome studies.

Protein IDs of different pathways were uploaded in STRING to analyze protein-protein interaction. These pathways include A) Ribosome B) Metabolism of proteins C) Spliceosome D) Processing of Capped Intron-Containing Pre-mRNA, E) Gene expression, F) Influenza Infection and G) 3' -UTR-mediated translational regulation. H) Interaction network of all 183 proteins were also analyzed collectively in STRING. Each node represents the proteins produced by a single gene. Small and large nodes represent proteins of unknown and known/predicted 3D structure, respectively. The pink lines represent the protein-protein interactions that are experimentally determined.

3.8 Assessing the necessity of NS1- interacting proteins by siRNA array

183 host factors were identified in at least two different biological replicates in NS1 interactome studies. In order to test the roles of these host factors in IAV replication, a high-throughput, custom siRNA array was used. The array was designed in a 96-well plate format. Each well contained a specific siRNA SMART pool, which was responsible for knocking down that specific gene and protein expression. 107 proteins were selected to design two 96 well plates for the knockdown study. The plate maps with gene symbols of these proteins are included in Figure 24. Most of these 107 proteins belonged to different pathways, molecular functions and biological processes identified in DAVID analysis. A few proteins were included based on the fact that they were identified in MS with very high score (peptide numbers and unused scores) and some were previously detected to interact with NS1 in VirHostNet 2.0 database.

After rehydrating the siRNAs, A549 cells were added to the 96 well plates and incubated for 48 hrs to knockdown (KD) individual genes in different wells (Figure 24). To check whether the siRNAs were toxic for the A549 cells or not, cell viability assays were conducted after 48 hrs of knockdown by WST-1 assays. Cell viability of each KD cell was compared with a non-targeting control siRNA pool (A549 cells transfected with scrambled siRNA). After transfection, cells were more than 80% viable compared to non-targeting control (N/T) in almost all siRNA treatments (Figure 25A). The lowest viability was seen in SNRNP200 siRNA treatment, which was 62.8%. After 48 hour post-transfection (Knockdown), A549 cells were infected with IAV-PR8 at MOI 0.05.

A

	1	2	3	4	5	6	7	8	9	10	11	12
A		IGF2BP3	PES1	MPHOSPH10	NOP56	DDX3X	DHX15	RRP8	SMARCA5	SYNCRIP	DKC1	
B	H2AFY	SNRNP200	SURF6	RSL1D1	ROD1	HSPB1	H1F0	HSPA1A	HIST1H1B	DDX5	VDAC1	RBM34
C	MATR3	NOP2	RBM25	FXR1	HSPA2	ADAR	EIF6	PRKDC	KHDRBS1	SFRS4	TBL3	ILF2
D	TARDBP	DDX10	PABPC4	TCOF1	SF3B2	PRPF4B	TRA2A	GNL2	BOP1	SAFB2	PDCD11	BMS1
E	RRS1	WDR43	PWP2	SF3B3	ELAVL1	HNRNPUL2	RPL7L1		DHX30	ZC3HAV1	HIST2H2AB	BMS1
F	FTSJ3	WDR36	DDX54	BRIX1	UTP15	H1FX	TAF15	DDX17	HIST1H2AC		CIRH1A	IMP4
G	DDX27	N/T	FUBP3	ZFR	RBM14	RBM15	HNRNPAB	EBNA1BP2	MYBBP1A	H2AFJ	N/T	UTP14A
H		N/T	GNL3	RBM4	MAK16	MKI67IP	GTPBP4	DDX24	NAT10	XRN2	N/T	

B

	1	2	3	4	5	6	7	8	9	10	11	12
A									HEATR1	NOL6	RPF2	
B									SCAF1	RPF1	DDX18	
C									RBM28	SLTM	UTP6	
D									RAI14	PRPF19	WDR3	
E									NOP58	RRP7A	UTP18	
F									DNTTIP2	HP1BP3		
G									NUMA1	TRIP12	N/T	
H									NOL11	NOP16	N/T	

Figure 24: Plate maps of siRNA array.

107 siRNAs were mapped in 96 well plate 1 (A) and plate 2 (B). The gene symbols are written in each well. Blue color wells contained non-targeting siRNA controls (N/T) and the yellow color indicated empty wells. All siRNAs were lyophilized in the wells of 96 well plates. siRNAs were rehydrated with siRNA buffer, A549 cells were added in each well and transfected with siRNA for 48 hrs. Thereafter, KD A549 cells of each well were infected with IAV-PR8. Supernatants from each well were harvested at 43 hpi for viral plaque assays.

Supernatants were harvested at 43 hpi to detect viral titres in order to determine how efficiently the virus replicated. Thereafter, the remaining cells were treated with WST-1 reagent to determine cell viability after viral infection. 73 KD-infected cells were more than 70% viable compared to N/T. In 34 KD cases, PR8 infection reduced the cell viability to 69.6% - 26.9% (Figure 25B). The minimum cell viability (26.9%) was found in PR8 infected NOL6 KD cells. Cell viabilities of KD-infected cells were most likely reduced through a cytopathic effect during virus production. In some KD cases, cell viabilities were increased significantly after viral infection, suggesting that the KD may protect the cell from a cytopathic effect (Figure 25B).

IAV titres produced in each of the 107 KD wells were determined by plaque assay. Knocking down 11 genes significantly reduced the virus titre from 30% to 2.6% of the N/T in three different biological experiments (Figure 25C, Table 8). The lowest IAV titres were generated in NUMA1 KD A549 cells, which was 2.6% of N/T. Among these 11 KD gene candidates, HNRNPUL2, ILF2 and PRPF19 were detected as NS1-interacting factors in VirHostNet 2.0 database and NUMA1, RBM28, RBM34, RPF1, SYNCRIP, SF3B3, UTP6 and SNRNP200 were novel discoveries (the analysis was done in May 2016). In addition, knocking down PRPF19 reduced Influenza virus titre in previous study [153]. Although knocking down some genes, such as DHX30, H2AFJ, FXR1, DDX54, ELAVL1, RRS1 and NOP56 increased viral titres (Figure 25C), I focused my studies on the 11gene candidates that significantly reduced virus titre after KD. These 11 gene candidates play roles in various biological processes, molecular functions and pathways (Table 8).

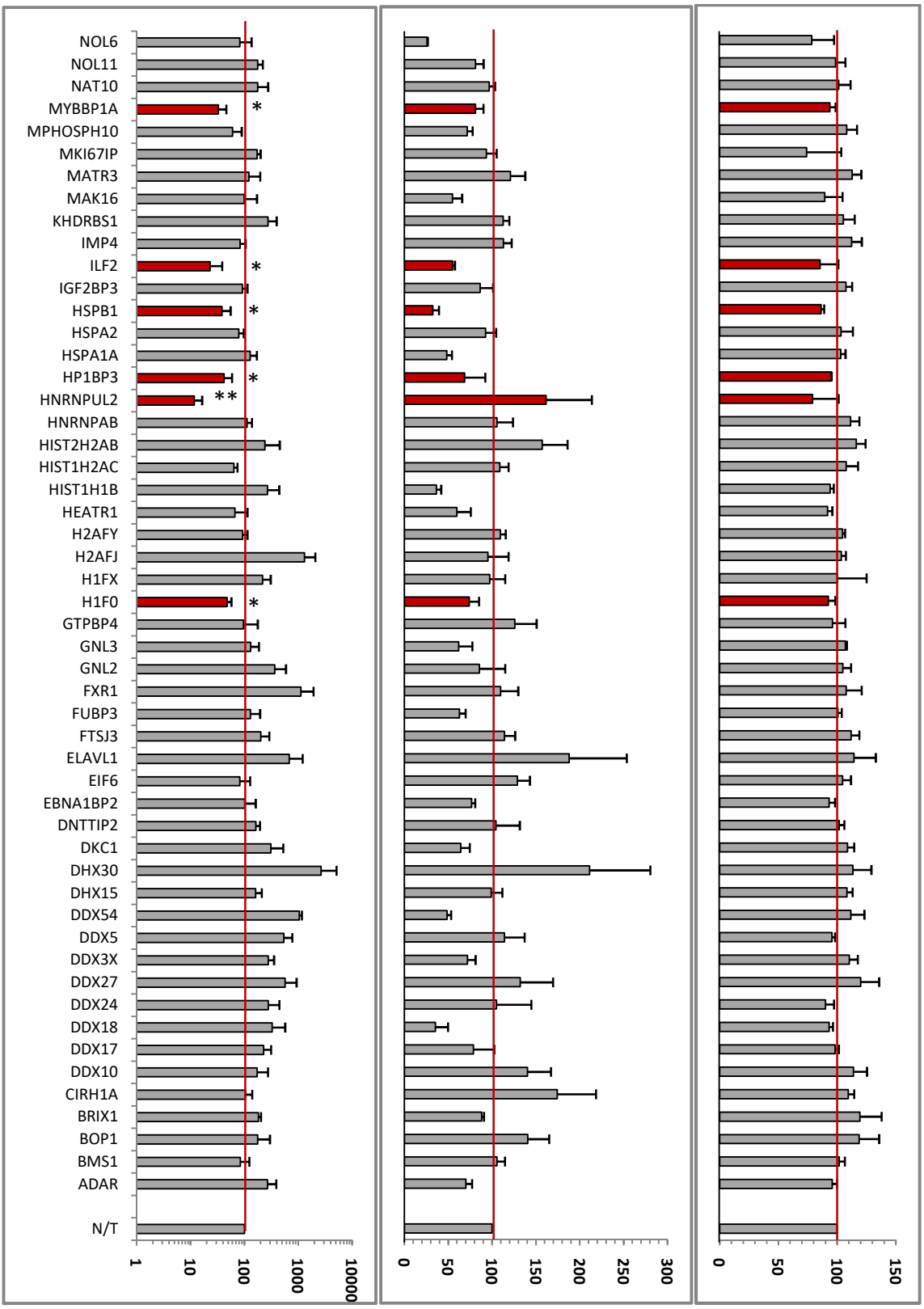

Virus titre (% of Non-targeting control)

Viable KD-infected cells (% of Non-targeting control)

Viable KD cells (% of Non-targeting control)

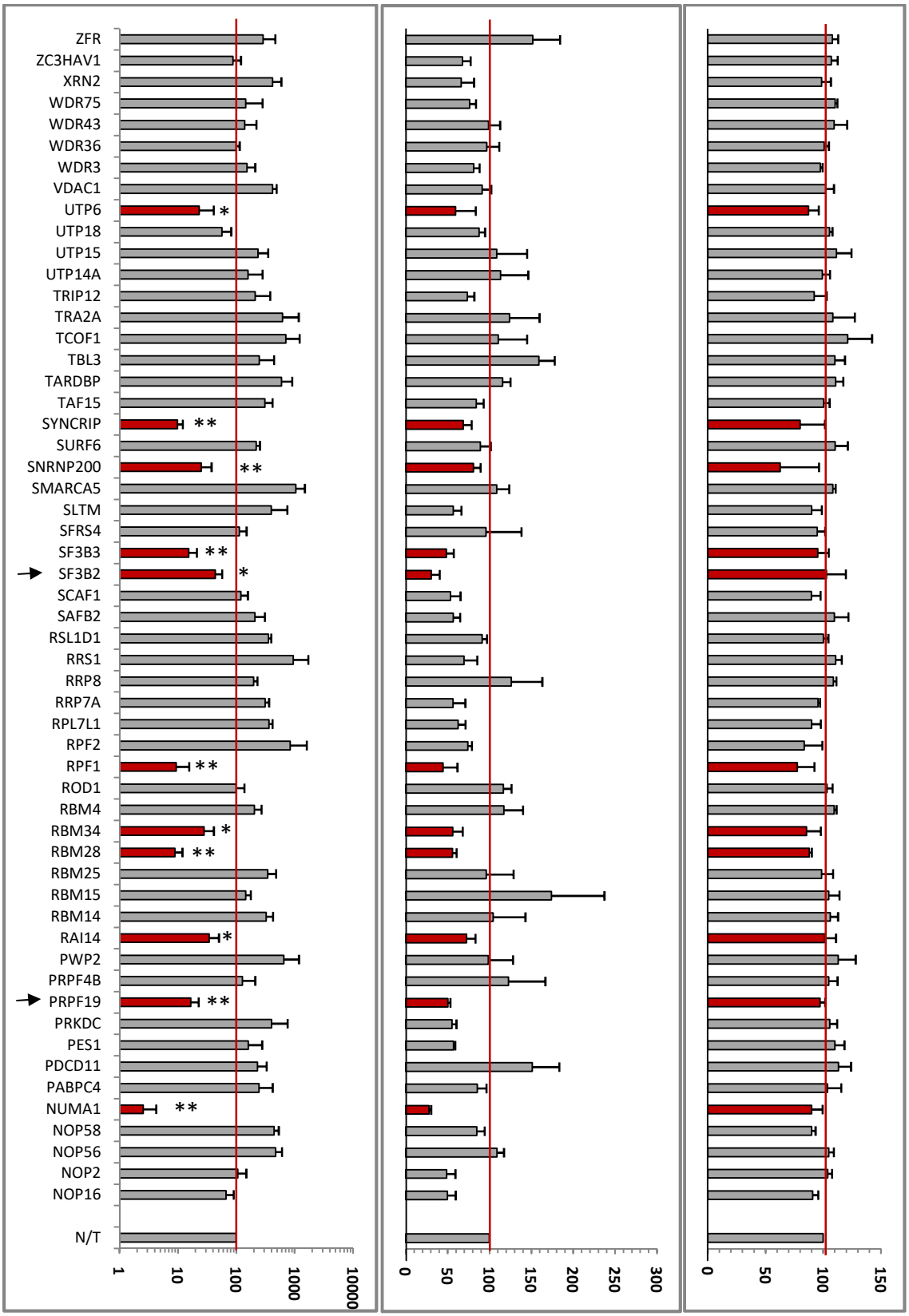
ZFR
ZC3HAV1
XRN2
WDR75
WDR43
WDR36
WDR3
VDAC1
UTP6
UTP18
UTP15
UTP14A
TRIP12
TRA2A
TCOF1
TBL3
TARDBP
TAF15
SYNCRIP
SURF6
SNRNP200
SMARCA5
SLTM
SFRS4
SF3B3
SF3B2
SCAF1
SAFB2
RSL1D1
RRS1
RRP8
RRP7A
RPL7L1
RPF2
RPF1
ROD1
RBM4
RBM34
RBM28
RBM25
RBM15
RBM14
RAI14
PWP2
PRPF4B
PRPF19
PRKDC
PES1
PDCD11
PABPC4
NUMA1
NOP58
NOP56
NOP2
NOP16
N/T
1
10
100
1000
10000
Virus titre (% of Non-targeting control)
C
0
50
100
150
200
250
300
Viable KD-infected cells (% of Non-targeting control)
B
0
50
100
150
Viable KD cells (% of Non-targeting control)
A

Figure 25: Testing the effects of 107 genes knock down in A549 cells by siRNA array.

(A) siRNA array was designed in 96 well plate format, cell viability (%) of siRNA transfected A549 cells was determined by WST-1 assays. Cell viability of non-targeting control (N/T) was considered as 100% (B) Transfected cells were infected with PR8 at MOI 0.05. Cell viability was measured at 43 hpi by WST-1 assay. (C) Virus replication was determined a 43 hpi by titering the supernatants from infected KD cells by plaque assay in MDCK cells. Maroon bars indicate the gene candidates knocking down of which significantly reduced viral titre compare to N/T. * indicates $p<0.05$, ** indicates $p<0.005$. Number of independent experiments, n=3. Knocking down of PRPF19 and SF3B2 (indicated by arrows) reduced influenza virus production in previous studies [140, 153].

Table 8: **Functional properties of the following genes, knocking down of which significantly reduced Influenza A virus production.**

Gene	Biological process[#]	Molecular function[#]	Pathway*
HNRNPUL2	• Chromatin assembly and organization • Chromosome organization • Cellular macromolecular complex assembly and subunit organization • Nucleosome assembly and organization • DNA packaging • Protein-DNA complex assembly	• Nucleic acid binding • RNA-binding protein	
ILF2	• Chromatin organization • Cellular macromolecular complex assembly and subunit organization • Chromatin assembly or disassembly • Nucleosome organization and assembly • Protein-DNA complex assembly	• Adenyl ribonucleotide binding • ATP binding • DNA binding • Double-stranded RNA binding • Nucleotide binding	
NUMA1		• Structural molecule activity	
PRPF19	• mRNA processing • RNA processing • Nucleoside, nucleotide and nucleic acid metabolism • mRNA splicing • Pre-mRNA processing	• mRNA splicing factor • Other RNA-binding protein • Nucleic acid binding • mRNA processing factor	• Gene Expression • Spliceosome • Processing of Capped Intron-Containing Pre-mRNA
RBM28	• mRNA splicing and processing • mRNA metabolic process • Nucleoside, nucleotide and nucleic acid metabolism	• RNA-binding protein • Nucleic acid binding	• Ribosome biogenesis
RBM34		• Nucleotide binding • RNA binding	
RPF1	• RNA metabolic process • Ribonucleoprotein complex biogenesis • rRNA processing • Ribosome biogenesis • Nucleoside, nucleotide and nucleic acid metabolism	• rRNA binding • Nucleic acid binding • Ribonucleoprotein	

Table 8

Gene	Biological process#	Molecular function#	Pathway*
SF3B3	• Nucleoside, nucleotide and nucleic acid metabolism • mRNA splicing • Pre-mRNA processing	• Nucleic acid binding • mRNA processing factor • mRNA splicing factor	• Processing of Capped Intron-Containing Pre-mRNA • Spliceosome • Gene Expression
SNRNP200	• Nucleoside, nucleotide and nucleic acid metabolism • mRNA splicing • Pre-mRNA processing	• Nucleotide binding • ATP binding • ATP-dependent helicase activity • Purine NTP-dependent helicase activity • mRNA splicing factor • mRNA processing factor	• Gene Expression • mRNA Splicing • Processing of Capped Intron-Containing Pre-mRNA
SYNCRIP	• Nucleoside, nucleotide and nucleic acid metabolism • mRNA splicing • Pre-mRNA processing	• Nucleotide binding • ATP binding • ATPase activity • ATP-dependent helicase activity • Purine NTP-dependent helicase activity	• Spliceosome • Processing of Capped Intron-Containing Pre-mRNA • Gene Expression • Spliceosome
UTP6	• Nucleoside, nucleotide and nucleic acid metabolism	• Nucleic acid binding	• Ribosome biogenesis

Biological processes and molecular functions were determined by DAVID analysis.

* Pathways were detected by DAVID and Consensus Path Data base (CPDB http://consensuspathdb.org/).

Some important biological processes and molecular functions include chromatin assembly, packaging and remodelling; cellular macromolecular complex assembly and subunit organization; nucleoside, nucleotide and nucleic acid metabolism; nucleic acid binding; mRNA splicing; mRNA processing; structural molecule activity; and ribonucleoprotein complex biogenesis. Some important pathways include gene expression, spliceosome and processing of capped intron-containing pre-mRNA.

The cell viabilities of these 11 infected-KD cells were compared with the viral titre at 43 hpi. Therefore, ratios of viral titre and cell viability for all 11 KD A549 cells were calculated. The viral titre and cell viability ratios of all gene candidates were reduced significantly compared to the N/T except ILF2 (Figure 26).

3.9 Reciprocal IP of host factors

To validate interactions between NS1 and host factors, a few host candidates were selected for reciprocal IP based on their ability to reduce viral replication (Figure 25), functional properties and availability of antibodies from different companies. NUMA1, PRPF19, UTP6 and RPF1 were selected for reciprocal IPs. A549 cells were grown overnight, infected with IAV-PR8 at MOI 5 and harvested at 24 hpi. Cellular proteins were extracted from harvested cells. Protein G Dynabeads were treated with anti-NUMA1 antibody (Table 2) and a relevant isotype control in separate tubes. Abs and beads were incubated to allow bindings between those. Thereafter, beads were washed and equal amount of infected cell lysates were added into both tubes of anti-NUMA1 and isotype control and treated overnight at 4^0C. The Dynabeads-Ab-antigen complexes were

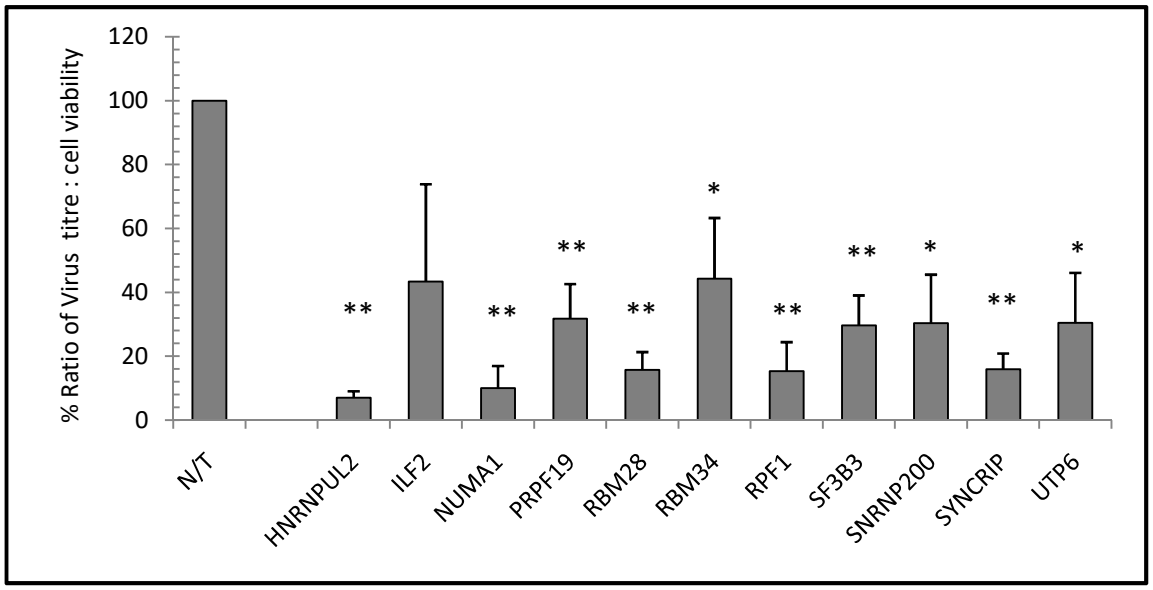

Figure 26: Ratio of viral titre and cell viability in knock down A549 cells.

The virus titre and cell viability ratio of non-targeting control was considered as 100%. Significant reduction of the virus titre and cell viability ratios are indicated by * $p<0.05$ and ** $p<0.005$. Number of independent experiments, n=3.

A

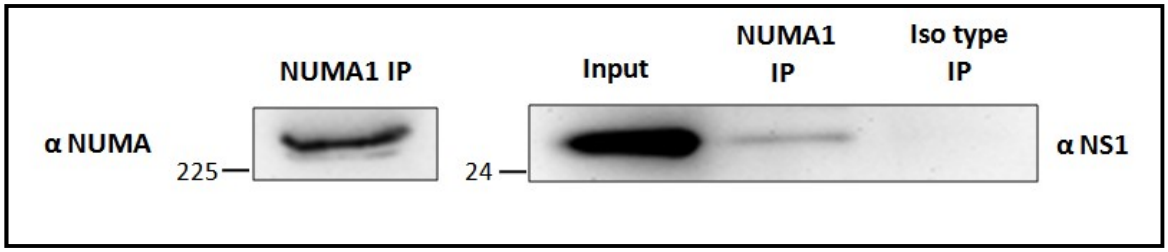
NUMA1 IP
Input
NUMA1 IP
Iso type IP
α NUMA
225
24
α NS1

B

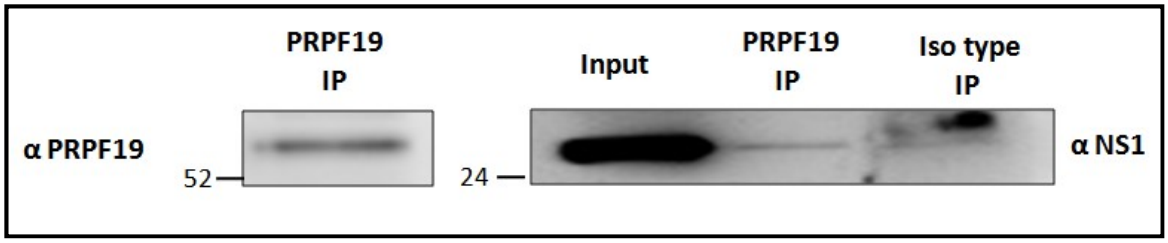
PRPF19 IP
Input
PRPF19 IP
Iso type IP
α PRPF19
52
24
α NS1

C

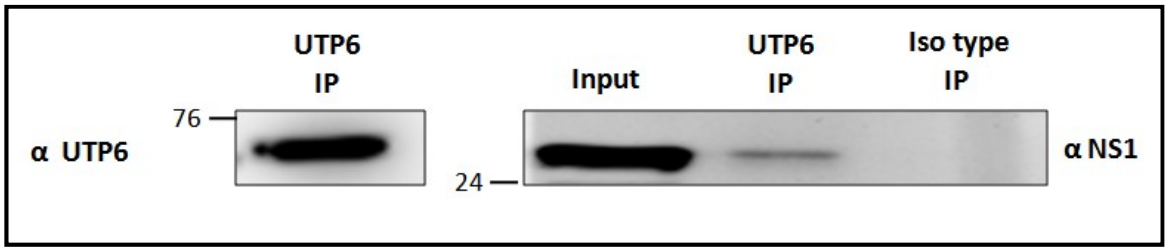
UTP6 IP
Input
UTP6 IP
Iso type IP
α UTP6
76
24
α NS1

D

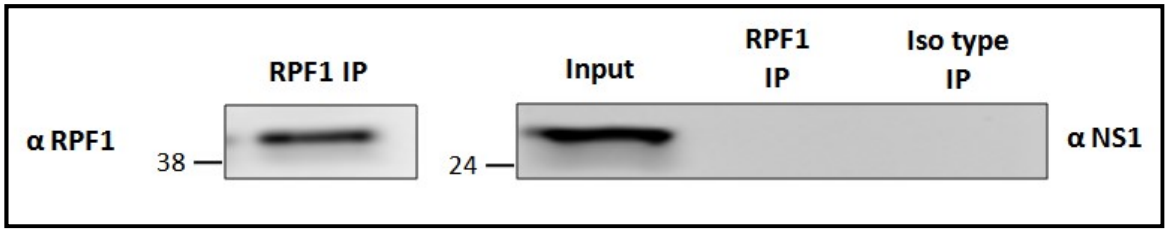
RPF1 IP
Input
RPF1 IP
Iso type IP
α RPF1
38
24
α NS1

Figure 27: Reciprocal IPs of host factors identified in NS1 interactome studies.

A) PR8 infected A549 cell lysates were immunoprecipitated with anti-NUMA Abs and isotype control. Infected cell lysates and IP products were resolved in 4-12% SDS-PAGE, transferred to PVDF membrane and probed with ani-NUMA1 Ab and anti-NS1 mAb mixture. B) IP of PRPF19 with PR8-infected cell lysates. Input and IP product were analyzed by Western blot probing with anti-PRPF anti-NS1 mAbs. C) UTP6 IP was done with infected cell lysates and analyzed with anti-UTP6 Ab and NS1 mAb mixture. D) RPF1 IP was done with infected cell lysates and analyzed by Western blot analysis probing with anti-RPF1 Ab and anti-NS1 mAb mixture.

separated by a magnet, washed and analyzed by Western blot analysis using both anti-NUMA1 and anti-NS1 Abs. A strong NUMA1 signal was seen near the 225 kDa region in infected input (infected cell lysate only) and NUMA1 IP (Figure 27 A). NUMA1 IP was also probed with an anti-NS1 mAb mixture and the NS1 band was seen in NUMA1 immunoprecipitated products without any background in isotype control, which indicated the NS1-NUMA1 interaction (Figure 27A).

Co-IPs were also performed with PR8-infected cell lysates using anti-PRPF19, anti-UTP6 and anti-RPF1 Abs (Table 2) in separate experiments. Isotype controls were also included in each experiment. PRPF19 was detected in PRPF19 IP, which also co-immunoprecipitated IAV-NS1 (Figure 27B). Similarly UTP6 was detected in UTP6 IP, which also co-immunoprecipitated IAV-NS1 protein (Figure 27C). RPF1 was detected in RPF1 IP; however, no NS1 band was seen when the RPF1 IP product was probed with anti-NS1 mAb (Figure 27D).

3.10 Role of NUMA1 in Influenza virus replication

Nuclear mitotic apparatus protein 1 (NUMA1) was detected in all four biological and technical replicates of NS1 interactome studies with significant peptide numbers and unused scores (Table 7). In addition, reciprocal IPs validated the interaction between NS1 and NUMA1 (Figure 27A). In initial siRNA screening, IAV production was significantly reduced to 2.6% of the N/T in three different independent studies (Figure 25C), which indicated an important role of NUMA1 in IAV replication.

3.10.1 NUMA1 knockdown cells inhibited IAV production

To validate the siRNA array results, NUMA1 KD was carried out with a Smart Pool of NUMA1 siRNA (Dharmacon). At the beginning of this KD experiment, A549 cells were treated with different concentrations of siRNA to find optimal and non-toxic siRNA concentrations for A549 cells. A549 cells were transfected with 25 nM and 50 nM NUMA1 siRNA every 24 hrs for 48hrs, and 100 nM siRNA for 48 hrs. A549 cells were treated with similar concentrations of Non-targeting control siRNA (NSi). After 48 hour post-transfection cell viability was measured by WST-1 assay. The cell viability was significantly reduced when A549 cells were treated with 100 nM and 50 nM in both NUMA1 siRNA and NSi treatments; however, cells treated with 25 nM siRNA (both NUMA1 siRNA and NSi) were almost 100% viable compared to the wild type untreated A549 cells (Figure 28A). After 48 hrs post-transfections, cellular proteins were extracted to check KD efficiency by immune blot analysis. I tried to measure the KD efficiency of NUMA1 siRNA by Western blot analysis; however, I could not detect NUMA1 protein using anti-NUMA1 Ab (Table 2). So, I carried out IP experiments to check KD efficiency of NUMA siRNA. NUMA1 was immunoprecipitated from an equal amount of NUMA1 KD and NSi KD cell lysates. In the IPs identical concentrations of Protein G beads and anti-NUMA Ab were used. IP products were resolved in 4-12% SDS-PAGE analyzed in immunoblot analysis with anti NUMA1 Abs (Table 2). Double treatment of 25 nM siRNA significantly reduced NUMA1 protein expression to ~15% of the NSi treated cells (Figure 28B, C). 1/40 part of the cell lysates that was used for IP was also resolved and analyzed by Western blot using anti-β-actin Ab (Table 2). The β-actin band intensities of both NSi and NUMA KD lysates were similar, which worked as the cell lysate loading

A

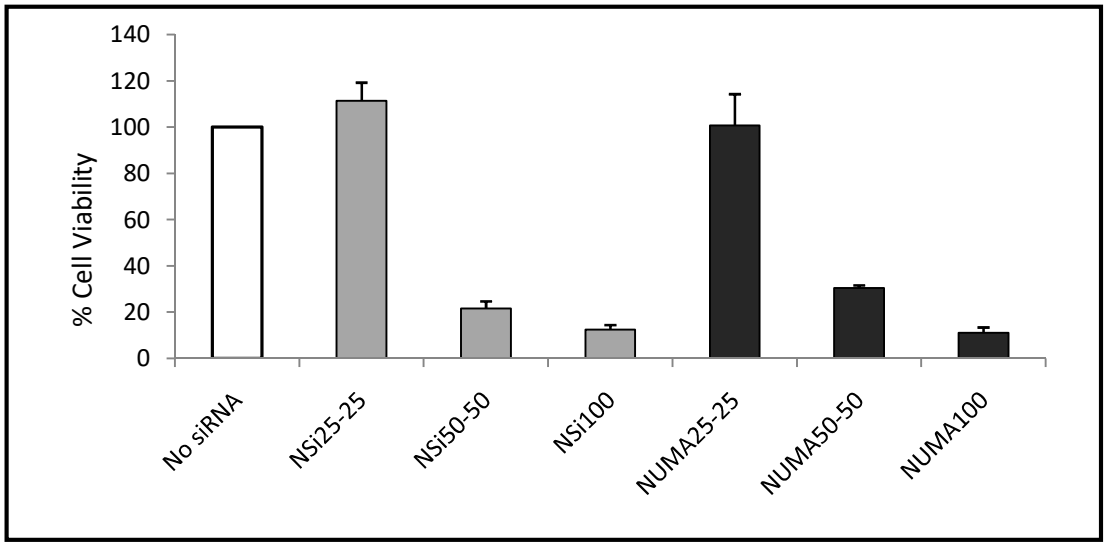
140
120
100
80
60
40
20
0
% Cell Viability
No siRNA
NSi25-25
NSi50-50
NSi100
NUMA25-25
NUMA50-50
NUMA100

B

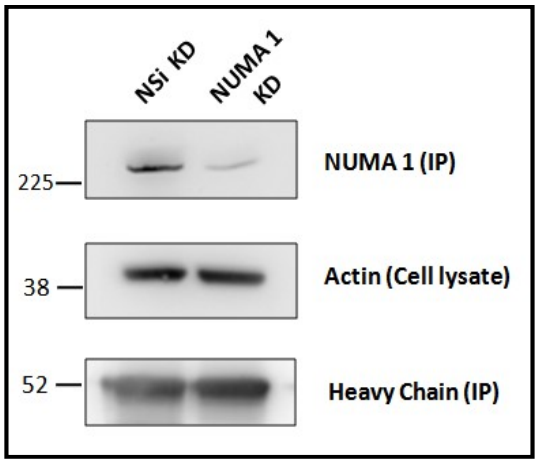
NSi KD
NUMA 1 KD
225
NUMA 1 (IP)
38
Actin (Cell lysate)
52
Heavy Chain (IP)

C

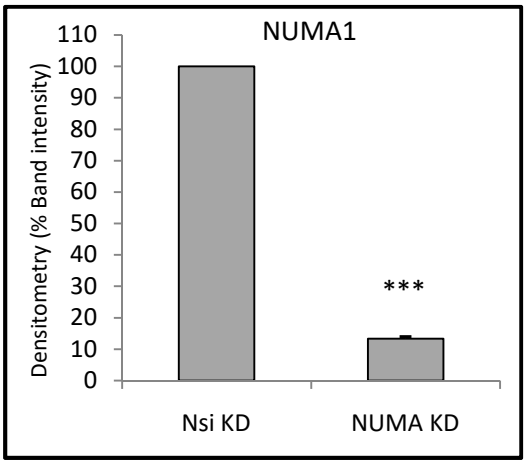
NUMA1
110
100
90
80
70
60
50
40
30
20
10
0
Densitometry (% Band intensity)
***
Nsi KD
NUMA KD

D

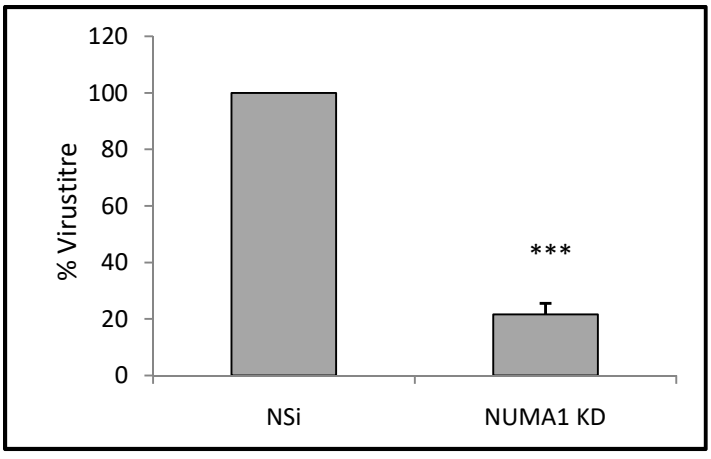
120
100
80
60
40
20
0
% Virustitre
***
NSi
NUMA1 KD

Figure 28: Characterization of NUMA1 Knockdown and IAV production.

A) Optimization of NUMA1 siRNA and NSi (Non- targeting siRNA) in A549 cells. A549 cells were treated with smart pool of NUMA1 siRNA and NSi at three different concentrations (25, 50 and 100 nM) in different combinations, such as 25 nM every 24 hrs for 48 hrs; 50 nM every 24 hrs for 48 hrs; and 100nM for 48 hrs. The corresponding cell viabilities of the transfected cells were measured and compared with untreated A549 cells, n=4. B) NUMA1 KD efficiency in A549 cells. A549 cells were treated with 25 nM siRNA every 24 hrs for 48 hrs. Identical concentration of NUMA1 KD and NSi KD cell lysates were immunoprecipitated with equal amount of anti NUMA1 Ab. IP products were analyzed in NUMA1 Western blot to check KD efficiency. Detection of anti-NUMA1 Ab heavy chain served as Ab loading control in IP. 1/40 part of cell lysates were analyzed by β-actin Western blot for monitoring loading control of cell lysates used in IP. C) Densitometry was done from immunoblots of NUMA1 IP products to check KD efficiency of NUMA1 siRNA (25nM), n=2, *** $P<0.0005$. D) NUMA1 KD and NSi cells were infected with PR8 at MOI 0.05 for 43 hours and virus titres were measured by plaque assay as plaque forming unit (pfu)/ml in MDCK cells. Percentages of infectious virus production in NUMA1 KD cells are shown where virus productions in NSi treated are considered as 100%. n=4, *** $P<0.0005$. NSi is non-targeting siRNA.

control in IP (Figure 28B). Band intensities of anti-NUMA Ab's heavy chains in both IPs were very similar, which worked as anti-NUMA Ab loading control used in IPs (Figure 28B). Therefore, 25 nM siRNA treatment every 24 hrs for 48 hrs (25-25 nM) was considered as optimal siRNA treatment at which cells remained healthy with efficient NUMA1 knockdown.

Both NUMA1 KD and NSi A549 cells were infected with IAV-PR8 at MOI 0.05. Supernatants were harvested at 43 hpi and infectious viral titres were determined as plaque forming unit (pfu)/ml by plaque assays in MDCK cells. Knocking down of NUMA1 significantly reduced PR8 production to ~21% compared to the NSi in four different independent experiments (Figure 28D), which validated the NUMA1 KD results in the siRNA array.

3.10.2 Effects of NUMA1 in Influenza A virus transcription and translation

Since the virus production was consistently reduced in NUMA1 KD cells, I intended to identify the specific virus replication step that was inhibited in NUMA1 KD cells. NUMA1 is mainly a nuclear protein, but it is also found in the cytoplasm [161]. After infection, viral ribonucleoproteins (vRNPs) need to get into the nucleus to start transcription. At first I wanted to determine if the import of incoming vRNPs or transcription process was inhibited in NUMA 1 KD cells by analyzing viral mRNA. NUMA1 KD and NSi KD A549 cells were infected with IAV-PR8 at MOI 3. Infected cells were harvested at 18 hpi and total RNA was extracted. Real time PCR was conducted targeting viral NS1 and NP mRNAs. Synthesis of viral mRNAs NP and NS1 was not reduced in NUMA1 KD cells; however, expression of these transcripts was

A

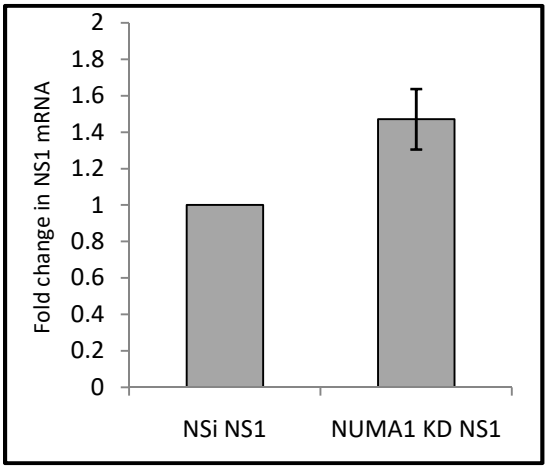
Fold change in NS1 mRNA
2
1.8
1.6
1.4
1.2
1
0.8
0.6
0.4
0.2
0
NSi NS1
NUMA1 KD NS1

B

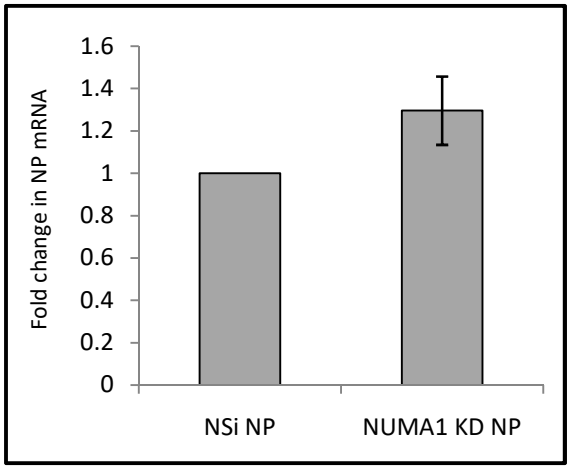
Fold change in NP mRNA
1.6
1.4
1.2
1
0.8
0.6
0.4
0.2
0
NSi NP
NUMA1 KD NP

C

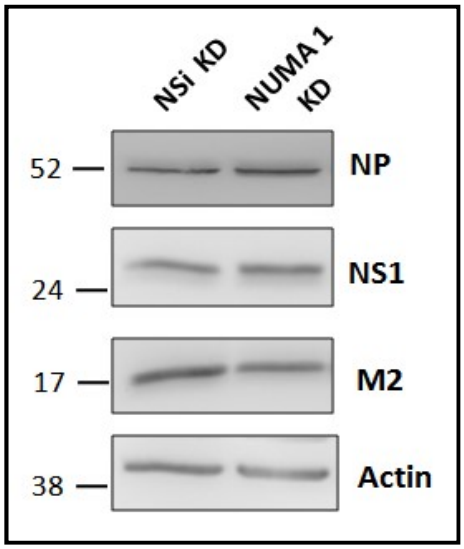
NSi KD
NUMA 1 KD
52
NP
24
NS1
17
M2
38
Actin

D

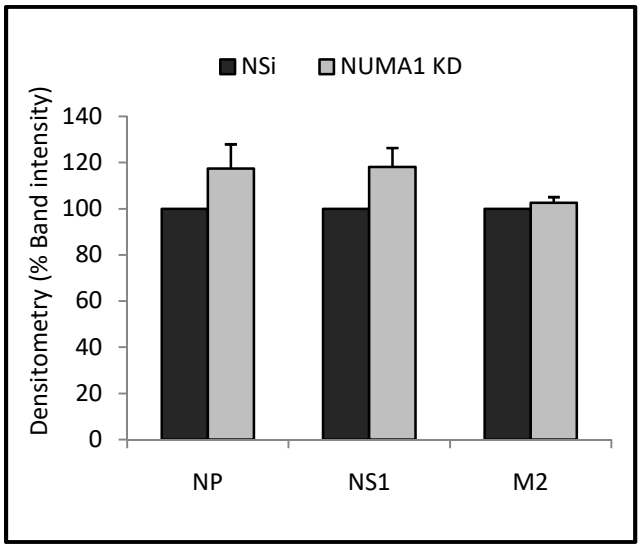
NSi
NUMA1 KD
Densitometry (% Band intensity)
140
120
100
80
60
40
20
0
NP
NS1
M2

Figure 29: IAV transcription and translation were not inhibited in NUMA1 KD A549 cells.

A) NS1 mRNA levels in PR8-infected NUMA1 KD and NSi cell lysates were quantified by real-time PCR, n=4. B) Quantification of NP mRNA levels in PR8 infected KD cell lysates. C) Western blots were carried out to determine different viral protein production in PR8 infected NUMA1 KD and NSi cells. Whole cell lysates of 18 hrs infected A549 cells were electrophoresed on 4-12% SDS-PAGE, transferred to PVDF blots. Thereafter, the blots were probed for detecting NP, NS1, M2 and β-actin. D) Densitometry was done to measure infected bands from the Western blots of NP, NS1 and M2 at 18 hpi. Bands of different viral proteins were normalized to β-actin. Protein bands of NSi were considered as 100%. n=2. NSi is non-targeting siRNA.

higher in NUMA1 KD cells (Figure 29A). Silencing of NUMA1 expression did not affect early vRNP entry into nucleus and transcription of NS1 and NP.

After transcription viral mRNAs are transported to the cytoplasm and translated utilizing host cell's machinery and resources. I planned to check whether export of viral mRNAs to the cytoplasm and/or translation step was inhibited in NUMA1 KD cells by analyzing viral structural and non-structural proteins. Whole cell lysates were extracted from PR8-infected (MOI 3) both NUMA1 KD and NSi cells at 18hpi. Cell lysates were analyzed by Western blot probing for IAV proteins that are expressed at early (NS1 and NP) and at late (M2) time points. All viral proteins were produced at similar or higher levels in infected NUMA1 KD A549 cells than NSi cells (Figure 29B). Therefore, this high protein expression in NUMA1 KD cells indicates that the deficiency in NUMA1 did not inhibit the transport of viral mRNAs to the cytoplasm and the translation process.

Although the viral proteins synthesized efficiently, infectious virus production was significantly reduced (Figure 28D). To become infectious, all 8 viral RNAs need to be incorporated into the new progeny virion. vRNA segments contain specific signals that indicate vRNAs to be packaged into new virion [71, 78-81]. However, random packaging can also occur in progeny viral assembly [76, 77] that may lack the presence of all vRNAs. I suspected that NUMA1 depletion might affect infectious virus production. To investigate this issue, NUMA1 KD and NSi cells were infected with PR8 at MOI 0.05, supernatants were harvested at 43 hpi, and thereafter, viruses were pelleted by ultracentrifugation and resuspended in an equal volume of PBS for both NSi and NUMA1 KD. Viral titres of both regular and concentrated supernatants were determined

A

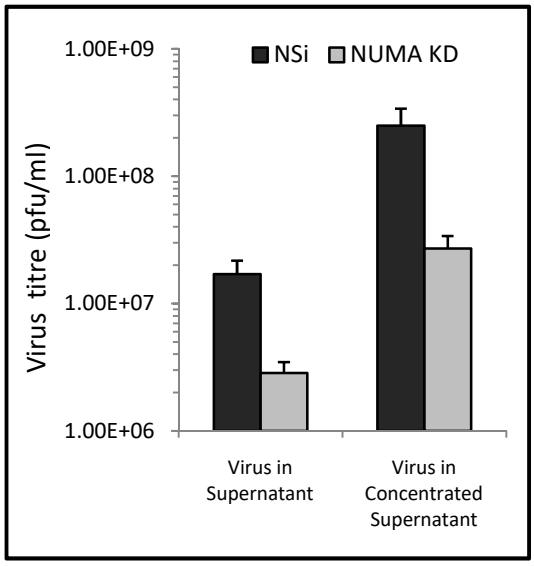
1.00E+09
1.00E+08
1.00E+07
1.00E+06
Virus titre (pfu/ml)
NSi
NUMA KD
Virus in Supernatant
Virus in Concentrated Supernatant

B

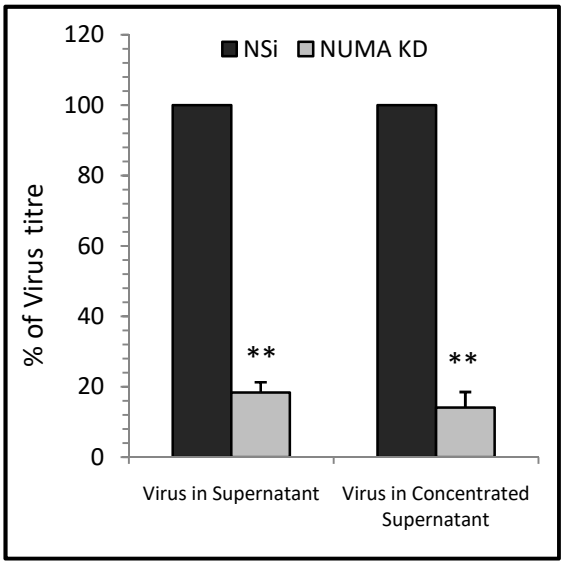
120
100
80
60
40
20
0
% of Virus titre
NSi
NUMA KD
**
**
Virus in Supernatant
Virus in Concentrated Supernatant

C

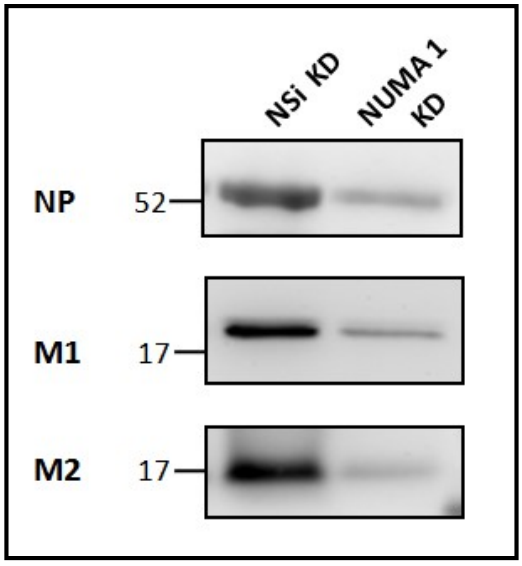
NSi KD
NUMA 1 KD
NP
52
M1
17
M2
17

D

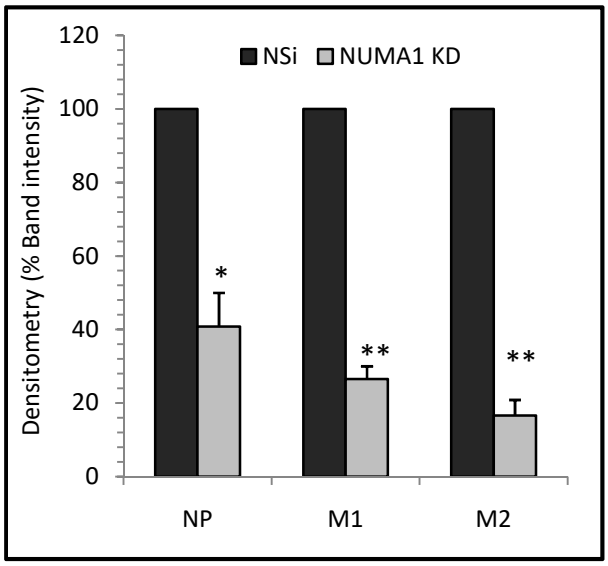
120
100
80
60
40
20
0
Densitometry (% Band intensity)
NSi
NUMA1 KD
*
**
**
NP
M1
M2

Figure 30: Purifying viruses and detecting virion proteins obtained from infected supernatants.

A) NUMA1 KD and NSi cells were infected with PR8 at MOI 0.05. Supernatants were harvested at 43 hpi, concentrated (purified) by ultracentrifugation. Viruses of regular and concentrated supernatants were titred by plaque assay and plotted into bar diagram as pfu/ml. B) Percentages of viral titres were plotted considering NSi titre as 100%, n=2, ** $p<0.005$. C) Equal volumes of purified viruses were loaded for Western blot analysis. Blots were probed with antibodies against NP, M1 and M2. D) Densitometry was done to measure the intensities (%) of NP, NS1 and M2 bands from purified viruses generated both from NUMA1 KD and NSi cells by Western blot analysis. Band intensities of NSi were considered as 100%. n=2. * $p<0.05$, ** $p<0.005$. NSi is non-targeting siRNA.

by plaque assay (Figure 30A and B). I determined viral titres of both supernatant and concentrated purified viruses (Figure 30B). To measure proteins in viral particles released from the cells, identical volumes of purified viruses generated from NSi and NUMA1 KD cells were analyzed by Western blot for detecting virion structural proteins NP, M1 and M2 (Figure 30C). NP, M1 and M2 of virion particles in NUMA KD cell supernatant were significantly reduced to 40%, 26% and 16%, respectively compared to the NSi (Figure 30C and D), and the infectious virus production (pfu/ml) was also reduced to ~20% in NUMA1 KD cells (Figure 28D). The average of NP, M1 and M2 proteins in particle expression was 27% of NSi. Therefore, I found that the average structural protein reduction was similar to the infectivity reduction in plaque assays in the supernatant of infected-NUMA KD cells (Figure 30 B and D).

3.10.3 NUMA1 KD affects localization of viral M1 and M2 proteins

Although NUMA1 depletion significantly reduced infectious IAV production (Section 3.10.1), viral transcription and translation processes were not affected/inhibited (Section 3.10.2). In addition, NS1 and NP protein levels were also increased in infected-NUMA1 KD cells compared to those in infected- NSi cells (Figure 29D). I wanted to check if virion maturation steps such as normal distribution of viral proteins and viral protein transportation to the assembly or budding sites are affected in NUMA1 KD cells. IAV M1 protein plays important roles in assembly of progeny viruses, such as it helps in transporting vRNPs from the nucleus to the budding sites [33, 82]. Therefore, I wanted to determine whether the virus production was reduced due to the relocation of viral M1 in infected NUMA1 KD cells. To investigate this, I infected NUMA1 KD and NSi KD cells with PR8 at MOI 3 on cover glasses, fixed at 20 hpi, and treated with anti-M1 Ab (Table

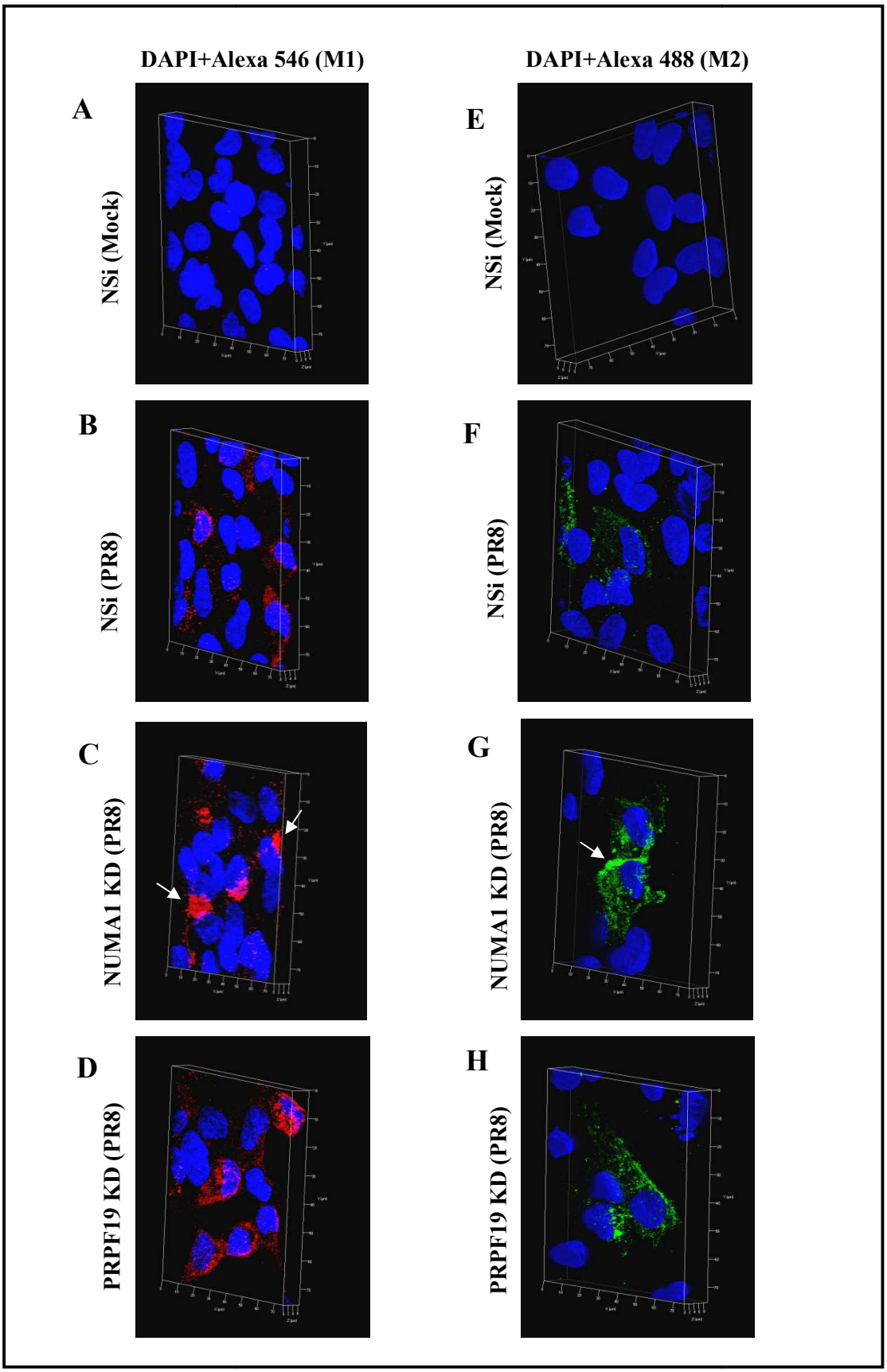
DAPI+Alexa 546 (M1)
DAPI+Alexa 488 (M2)
A
NSi (Mock)
E
NSi (Mock)
B
NSi (PR8)
F
NSi (PR8)
C
NUMA1 KD (PR8)
G
NUMA1 KD (PR8)
D
PRPF19 KD (PR8)
H
PRPF19 KD (PR8)

Figure 31: Localization of M1 and M2 in KD cells by SIM.

Mock infected NSi (A), PR8-infected NSi (B), PR8-infected NUMA1 KD (C) and PR8-infected PRPF19 KD (D) A549 cells were fixed at 20 hpi, stained for IAV M1 protein and analyzed by super resolution SIM. M1 proteins were detected with Alexa Fluor 546 anti-M1 (Red). The white arrows indicate the cluster of M1 in NUMA KD cells (C). Mock infected NSi (E), PR8-infected NSi (F), PR8-infected NUMA1 KD (G) and PR8-PRPF19 KD (H) A549 cells were fixed, stained for IAV M2 protein. M2 proteins were detected with Alexa Fluor 488 anti-M2 (Green). The white arrows indicate the accumulation of M2 near cytoplasmic membrane of NUMA KD cells (G). Scale bars of X, Y and Z axes of all 3D images are 10 μm, 10μm and 2μm, respectively.

2). Cover glasses with mock infections were also included. Thereafter, the samples were analyzed by superresolution Structured Illumination Microscopy (SIM) in the Genomic Centre for Cancer Research and Diagnosis (GCCRD), Manitoba. Mounting of the cover slides was initially carried out with Vectashield mounting medium, but the Alexa 546 fluorescent signal started bleaching very fast. Therefore, I used Prolong gold antifade reagent as mounting media. 3D images of SIM were generated where M1 proteins were accumulated and formed clusters in cytoplasmic region, adjacent to the nucleus of infected-NUMA1 KD A549 cells (Figure 31C, white arrow indicates the M1). However, similar M1 clustering was not observed in infected-NSi cells, where M1 was distributed almost evenly in cytoplasm (Figure 31B). Thus, the SIM results indicated that M1 protein trafficking was interrupted in NUMA1 KD cells and NUMA1 may be involved in M1 trafficking.

M2 protein plays important roles in viral assembly and budding steps near the cytoplasmic membrane [33, 83]. Therefore, I extended my analysis to monitor IAV M2 protein localization in infected-NUMA KD A549 cells. I conducted SIM in PR8-infected NUMA1 KD and NSi A549 cells at 20 hpi. Mounting of the M1 cover slides was carried out with Vectashield mounting medium. In NUMA1 depleted A549 cells, mostly the M2 proteins accumulated near the plasma membrane (Figure 31G, white arrow indicates the M2 accumulation at cytoplasmic membrane). However, similar accumulation of M2 proteins near cytoplasmic membrane was not seen in infected-NSi cells. In NSi cells M2 proteins were evenly distributed in cytoplasm (Figure 31F).

3.10.4 Monitoring viral production by Electron Microscopy (EM)

Electron microscopy was carried out to observe viral production. NUMA1 KD and NSi KD A549 cells were infected with PR8 at MOI 3 for 20 hours. Infected cells were harvested and processed for EM. Samples were analysed by EM in Histology lab, Department of Human Anatomy. In infected-NSi cells, numerous IAVs were imaged to bud out of the infected cells. Small spherical structures that are consistent with the ~100 nm size IAVs are indicated with black arrows (Figure 32A). On the other hand, viral production was significantly less in infected NUMA1 KD cells (Figure 32B), which was consistent with previous results of virion production in NUMA1 KD cells (Figure 28D). In higher magnification, tiny dense spherical particles of ~ 20 nm size were seen to form clusters (indicated with black arrows) in the cytoplasmic region (Figure 32D). IAV neuraminidase is usually 60-100 Å (6-10 nm) long [202, 203] and IAV RNP is ~30-50 nm in diameter [204], which all raise the possibility of those dense particles as viral proteins. However, immunoelectron microscopy could confirm the clustering of viral proteins. Similar clustering of M1 proteins was also seen in Super resolution SIM of infected-NUMA1 KD cell cytoplasm (Figure 31C). Similar clustering was not seen in infected-NSi KD cells.

3.11 Role of PRPF19 in Influenza virus replication

Pre-mRNA-processing factor 19 (PRPF19), which is also known as PSO4 or PRP19 plays important roles in splicing of human and different yeast species [169].

A

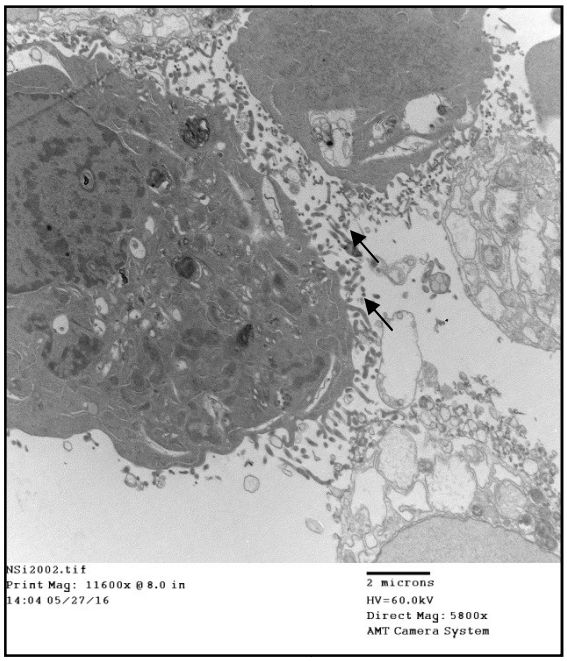
NSi2002.tif
Print Mag: 11600x @ 8.0 in
14:04 05/27/16
2 microns
HV=60.0kV
Direct Mag: 5800x
AMT Camera System

B

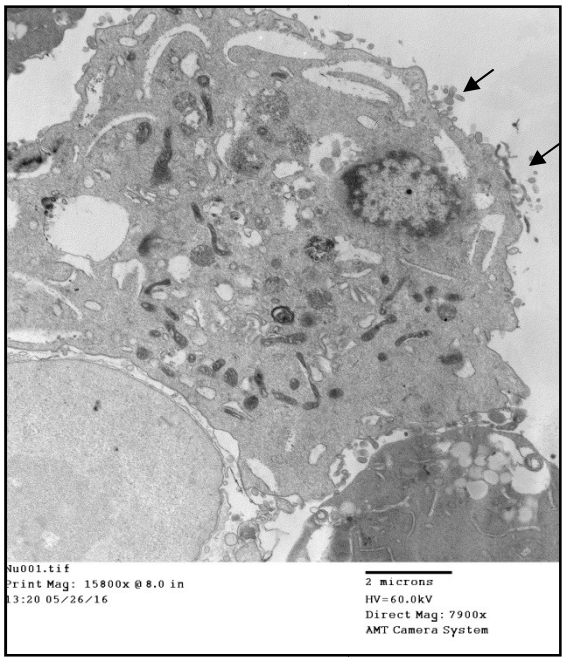
Nu001.tif
Print Mag: 15800x @ 8.0 in
13:20 05/26/16
2 microns
HV=60.0kV
Direct Mag: 7900x
AMT Camera System

C

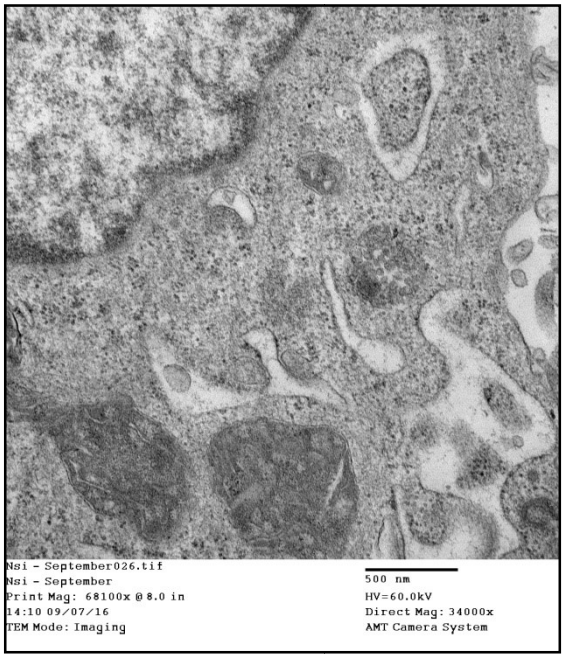
Nsi - September026.tif
Nsi - September
Print Mag: 68100x @ 8.0 in
14:10 09/07/16
TEM Mode: Imaging
500 nm
HV=60.0kV
Direct Mag: 34000x
AMT Camera System

D

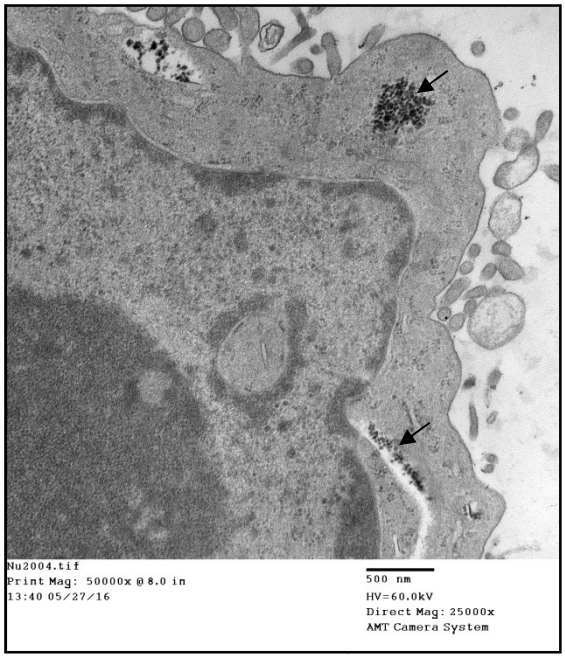
Nu2004.tif
Print Mag: 50000x @ 8.0 in
13:40 05/27/16
500 nm
HV=60.0kV
Direct Mag: 25000x
AMT Camera System

Figure 32: Monitoring IAV production by Electron Microscopy (EM).

A) NSi KD A549 cells were infected with PR8 at MOI 3 for 20 hrs. Infected cells were harvested, washed, processed with EM Grade Karnovsky fixative and stained with uranyl acetate. All processed samples were analyzed by EM in Histology lab, Department of Human Anatomy. Numerous virions (~100 nm) were budded out of infected NSi KD cells, which are indicated with black arrows. Magnification was 11600X and scale bar 2 μm. B) Viral production was significantly reduced in PR8-infected NUMA KD A549 cells at 20 hpi. Magnification was 11600X and scale bar 2 μm. C) Clustering of viral proteins was not seen in PR8-infected NSi KD cells. D) Viral proteins were seen to form cluster within cytoplasmic region in PR8-infected NUMA1 KD cells, the protein clusters were indicated with black arrows. Bar 500 nm.

PRPF19 was detected in three different biological and technical experiments of my NS1-interactome studies with significant peptide numbers and unused scores (Table 7). In addition, reciprocal IPs confirmed that PRPF19 and NS1 were true interacting partners (Figure 27B).

3.11.1 Replication of IAV in PRPF19 depleted cells

In my siRNA array results, PRPF19 KD significantly reduced IAV production to 16.67% (Figure 25C). To validate this, PRPF19 KD experiment was carried out in A549 cells with a Smart Pool of PRPF19 siRNA. At the beginning non-toxic concentrations of siRNAs were optimized. A549 cells were treated with 25 nM and 50 nM siRNA every 24 hrs for 48 hrs, and 100 nM siRNA for 48 hrs. These included both PRPF19 and NSi siRNAs. A549 cells treated with 25 nM of PRPF19 and NSi siRNAs were almost 100% viable compared to the untreated A549 cells (Figure 33A). After 48 hrs post-transfection with different concentration of siRNAs, cellular proteins were extracted to check KD efficiency by immune blot analysis. Both PRPF19 KD and NSi KD cell lysates were resolved in 4-12% SDS-PAGE, transferred to PVDF membranes and analyzed in immunoblot analysis with anti-PRPF19 Ab (Table 2). Double treatment of 25 nM, 50 nM and single treatment of 100 nM PRPF19 siRNAs significantly reduced PRPF19 protein expression to 16.1, 8.7 and 6.9%, respectively of the NSi treated cells (Figure 33B and C). The membrane was also probed for β-actin as loading control. Since double treatment of 25 nM siRNA was nontoxic for the cells and significantly reduced PRPF19 expression, it was considered as the optimal siRNA concentration for PRPF19 knockdown.

A

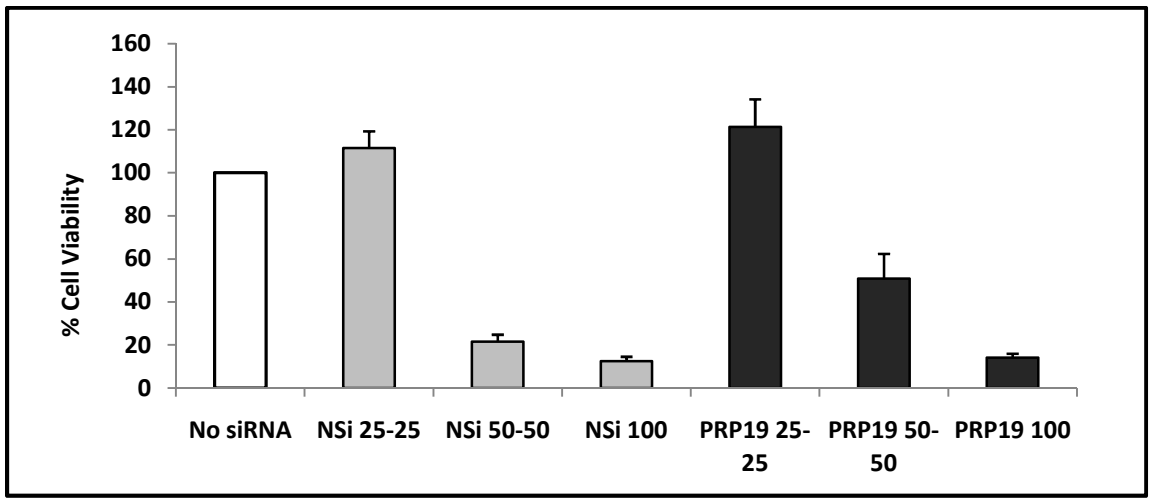
% Cell Viability
160
140
120
100
80
60
40
20
0
No siRNA
NSi 25-25
NSi 50-50
NSi 100
PRP19 25-25
PRP19 50-50
PRP19 100

B

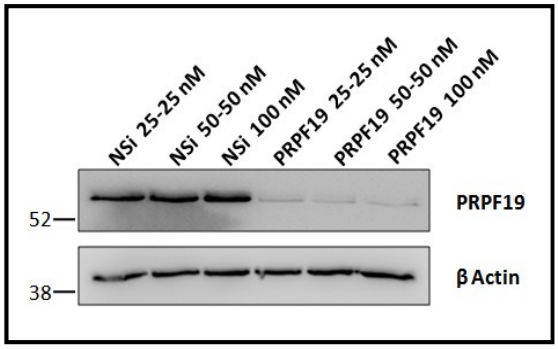
NSi 25-25 nM
NSi 50-50 nM
NSi 100 nM
PRPF19 25-25 nM
PRPF19 50-50 nM
PRPF19 100 nM
52
38
PRPF19
β Actin

C

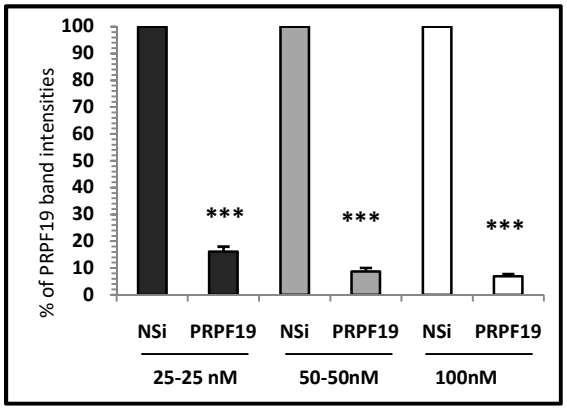
% of PRPF19 band intensities
100
90
80
70
60
50
40
30
20
10
0
***
***
***
NSi
PRPF19
NSi
PRPF19
NSi
PRPF19
25-25 nM
50-50nM
100nM

D

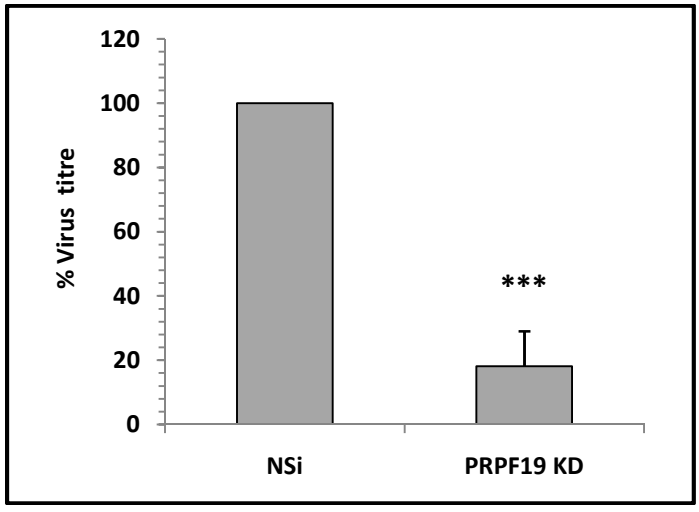
% Virus titre
120
100
80
60
40
20
0
***
NSi
PRPF19 KD

Figure 33: Characterization of PRPF19 Knockdown and IAV production.

A) Optimization of PRPF19 siRNA and NSi in A549 cells. A549 cells were treated with NUMA1 and NSi siRNAs at three different concentrations (25, 50 and 100 nM) in different combinations, such as 25 nM every 24 hrs for 48 hrs; 50 nM every 24 hrs for 48 hrs; and 100 nM for 48 hrs. The corresponding cell viabilities of the transfected cells were calculated by comparing with untreated A549 cells, n=4. B) KD efficiency of PRPF19 siRNA was determined by Western blot. A549 cells were treated with different combinations of siRNAs. 15 μg of PRPF19 KD and NSi cell lysates were resolved in 4-12% SDS-PAGE, transferred to PVDF membranes, probed with antibodies against PRPF19 and β-actin proteins. C) Densitometry of PRPF19 protein was determined for the Western blots. n=2, *** $P<0.0005$. D) PRPF19 KD and NSi cells were infected with PR8 at MOI 0.05 for 43 hours and infectious virus titres were measured as plaque forming unit (pfu)/ml. Percentages of infectious virus production in PRPF19 KD cells are shown where virus productions in NSi were considered as 100%. n=4, *** $P<0.0005$. NSi is non-targeting siRNA.

Both PRPF19 KD and NSi KD A549 cells were infected with PR8 at MOI 0.05. Infectious virus productions were determined as plaque forming unit (pfu)/ml at 43 hpi by plaque assays. Knocking down of PRPF19 significantly reduced PR8 production to 18.1% compared to the NSi in four different independent experiments (Figure 33D). During my study with PRPF19, a research article came online in May 2016 also showing PRP19 (PRPF19) interacts with Influenza NS1 protein [153]. Consistent with my findings, they also reported that IAV production was reduced when PRP19 expression was inhibited [153]. However, the specific step/mechanism of viral replication that is inhibited was not further described. Therefore, I intended to determine the specific step of IAV replication that is inhibited in PRPF19 KD A549 cells in my studies.

3.11.2 Detection of Influenza viral transcripts and proteins in PRPF19 depleted cells

PRPF19 (PRP19) plays crucial roles in assembling and activating of the spliceosome during alternative splicing event [170, 174]. Alternative splicing is an important step between eukaryotic transcription and translation. Influenza RNA segments 7 and 8 each encode two proteins. Segment 8 encodes NS1 and NEP/NS2, and segment 7 encodes M1 and M2 proteins, which occur via the alternative splicing. IAVs utilize the host's splicing machinery to produce these proteins by alternative splicing [74, 75]. In PRPF19 depleted cells, viral splicing might be affected, which ultimately could reduce virus production.

To check this possibility, I infected PRPF19 and NSi KD cells with PR8 at MOI 3, harvested at 18 hpi and extracted cellular RNA. Real time PCRs were carried out to

A

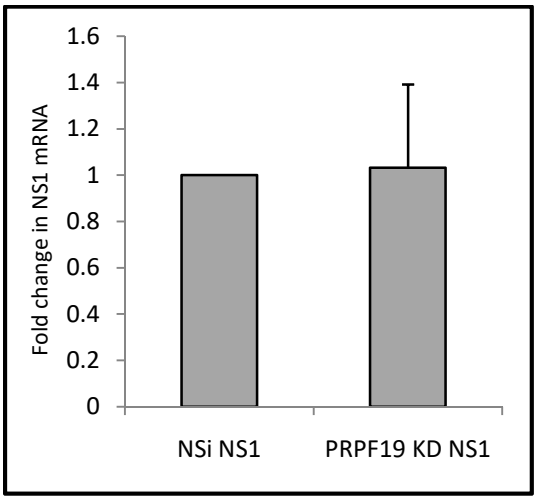
1.6
1.4
1.2
1
0.8
0.6
0.4
0.2
0
Fold change in NS1 mRNA
NSi NS1
PRPF19 KD NS1

B

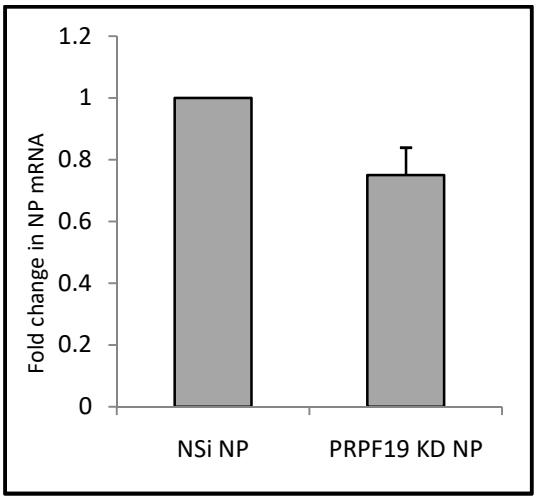
1.2
1
0.8
0.6
0.4
0.2
0
Fold change in NP mRNA
NSi NP
PRPF19 KD NP

C

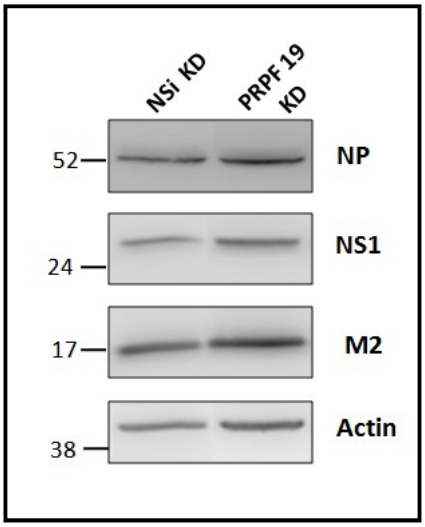
NSi KD
PRPF 19 KD
52
NP
24
NS1
17
M2
38
Actin

D

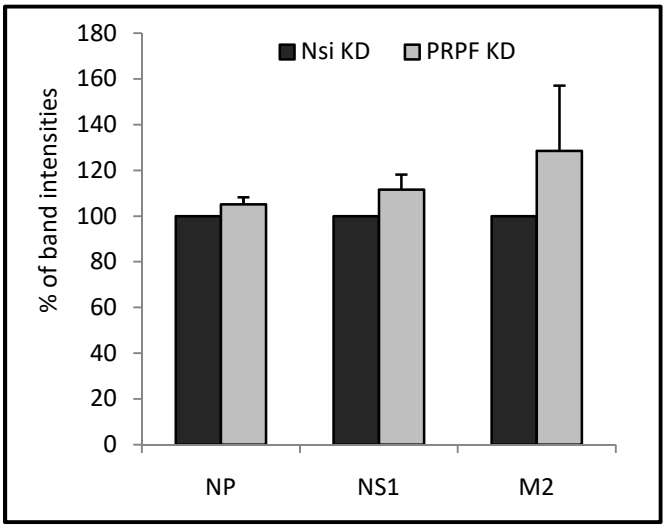
180
160
140
120
100
80
60
40
20
0
% of band intensities
Nsi KD
PRPF KD
NP
NS1
M2

Figure 34: IAV transcription and translation processes were not inhibited in PRPF19 depleted A549 cells.

A) NS1 mRNA levels in PR8-infected PRPF19 KD and NSi KD cell lysates were measured by real-time PCR. The mean from triplicate runs with error bars representing standard deviation. B) NP mRNA levels were measured in PR8 infected KD cell lysates. C) Western blot analysis indicating the production of different IAV proteins in PR8 infected PRPF19 KD and NSi cells. Whole cell lysates of 18 hours infected cells were electrophoresed on 4-12% SDS-PAGE, transferred to PVDV membranes, and membranes were probed for detecting NP, NS1, M2 and β-actin. D) Densitometry was done to measure infected bands from Western blot of NP, NS1 and M2 at 18 hpi in PRPF19 KD and NSi cells. Bands of different viral proteins were normalized to β-actin, n=2. Protein bands of NSi cells were considered as 100%. NSi is non-targeting siRNA.

measure viral NS1 and NP mRNAs. There was no significant difference in expressing viral NS1 mRNAs in PRPF19 KD cells compared to the NSi cells (Figure 34A). NP-mRNA expression was reduced to ~79% of the NSi (Figure 34B).

Whole cell lysates of both PR8-infected (MOI 3) NSi and PRPF19 KD cells were extracted at 18 hpi. Cell lysates were analyzed by Western blot analysis probing with Abs against IAV protein NS1, NP and M2 (Figure 34C). NS1 and M2 proteins are spliced products of 2 different gene segments, which were expressed higher in infected-PRPF19 KD cells than infected-NSi cells (Figure 34C and D). NP was also expressed in infected PRPF19 KD same as in infected-NSi cells (Figure 34C and D). Therefore, silencing of PRPF19 expression did not affect viral transcription, splicing or translation process, which also indicates that viral RNP entry into nucleus and mRNA export to the cytoplasm events are not PRPF19 dependent.

Although the viral proteins were synthesized very well in PRPF9 KD cells, infectious virus production was significantly reduced (Figure 33D). Supernatants of PR8 infected PRPF19 KD and NSi cells (MOI 0.05) were collected at 43 hpi, viruses were pelleted by ultracentrifugation and resuspended in small and equal volume of PBS. Virus titres of both regular and concentrated supernatants were identified by plaque assay (Figure 35A). In PRPF19 KD cells virus titres of both supernatant and concentrated supernatant were reduced to 20.8% and 21%, respectively compared to those of the NSi cells (Figure 35B), which confirmed that identical amount of PBS was added to viral pellet during purification. To measure proteins in particle released after virion budding, equal volume of purified viruses released from both PRPF19 KD and NSi cells were

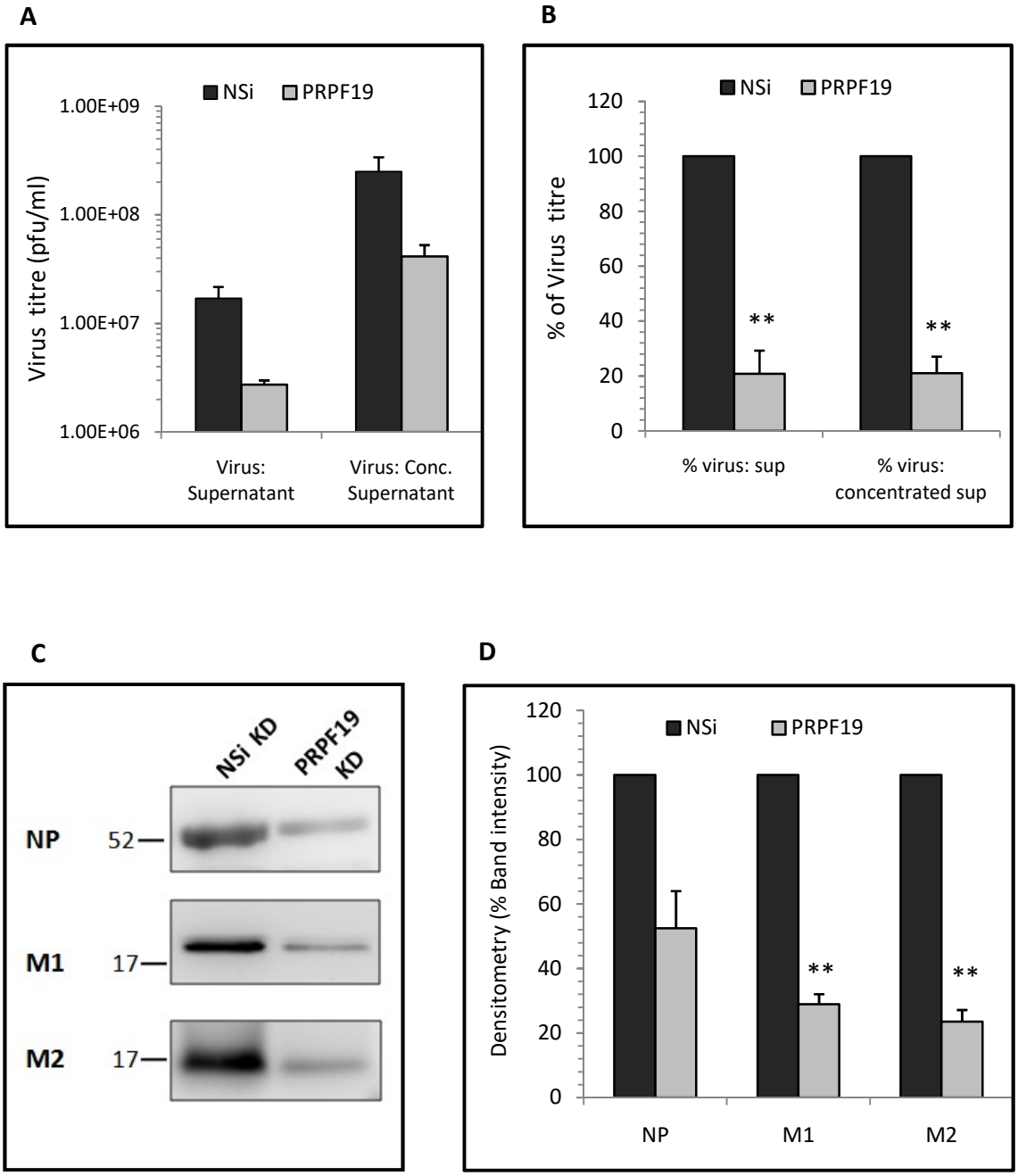
A
NSi
PRPF19
1.00E+09
1.00E+08
1.00E+07
1.00E+06
Virus titre (pfu/ml)
Virus: Supernatant
Virus: Conc. Supernatant
B
NSi
PRPF19
120
100
80
60
40
20
0
% of Virus titre
**
**
% virus: sup
% virus: concentrated sup
C
NSi KD
PRPF19 KD
NP
52
M1
17
M2
17
D
NSi
PRPF19
120
100
80
60
40
20
0
Densitometry (% Band intensity)
**
**
NP
M1
M2

Figure 35: IAV purification and detection of virion proteins obtained from PRPF19 KD infected supernatants.

A) PRPF19 KD and NSi cells were infected with PR8 at MOI 0.05. Supernatants were harvested at 43 hpi, concentrated by ultracentrifugation. Viral titres of regular and concentrated supernatants were determined by plaque assay and plotted into bar diagram as pfu/ml. B) Percentages of viral titres were plotted considering NSi titre as 100%, n=2, ** $p<0.005$. C) Equal volumes of purified viruses were resolved in 4-12% SDS-PAGE and transferred to PVDF membranes for Western blot analysis. Blots were probed with antibodies against NP, M1 and M2. D) Densitometry was done to measure the intensities (%) of NP, NS1 and M2 bands from purified viruses generated both from PRPF19 KD and NSi cells by Western blot analysis. Band intensities of NSi were considered as 100%. n=2. ** $p<0.005$. NSi is non-targeting siRNA.

analyzed by Western blot analysis probing with anti-NP, anti-M1 and anti-M2 Abs (Figure 35C). NP, M1 and M2 of virion particles in PRPF19 KD cell supernatant were reduced to 52.5%, 28.9% and 23.5%, respectively of the NSi (Figure 35C and D). Infectious virus production (pfu) was also reduced to ~20% in PRPF19 KD cells (Figure 33D). The average of NP, M1 and M2 proteins in particle expression in PRPF19 KD supernatant was ~35% of NSi. Therefore, I found that the average structural protein reduction was similar to the infectivity reduction in plaque assays in the supernatant of infected-PRPF19 KD cells (Figure 35 B and D)

3.11.3 Localization of IAV M1 and M2 PRPF19 knockdown cells

Although PRPF19 depletion significantly reduced infectious IAV production (Figures 33D), viral transcription and translation steps were not inhibited (Figure 34 A-D). Therefore, I wanted to determine the distributions of IAV M1 and M2 in infected-PRPF19 KD cells. To examine these, I infected PRPF19 KD and NSi cells with PR8 at MOI 3 and processed for imaging in superresolution Structured Illumination Microscopy (SIM) at 20 hpi. Mock infection was also included. 3D images of SIM indicated higher amount of M1 proteins distributed within the cytoplasmic region in PRPF19 KD cells compared to the NSi (Figure 31B and D). Similarly M2 protein concentration was higher in PRPF9 KD cells than that of in NSi cell (Figure 31F and H), which was also seen in Western blot results (Figure 34D). Therefore, it appeared that viral maturation process was hampered in infected PRPF19 KD cells.

Part 4. Discussion

4.1 Influenza NS1 and mAb as a tool for interactome study

Influenza virus is a significant infectious agent, which has the potential to cause pandemic outbreaks. Influenza viruses are intracellular parasites that utilize cellular machineries for their replication processes. NS1 is the only viral non-structural protein that is expressed in high abundance in Influenza infected cells [205]. NS1 is a multifunctional protein that plays important roles during IAV infection by suppressing antiviral responses such as interferon (IFN) induction [48]. NS1 does not incorporate within new virions; however, a high NS1 expression rate in infected cells indicates enormous possibilities of NS1-host interactions that can favour viral replication. mAbs can be an excellent tool to identify NS1 interacting partners in infected cells. In addition, NS1 can also be a good target for IAV detection and diagnosis during productive infections with the help of mAbs.

NS1 had been recognized to have 21 functional and 15 structural sequence features at the time of my mAb characterization [187, 188]. Two research groups generated mAbs targeting the highly pathogenic H5N1 NS1 protein, which were useful for viral detections and titrations [206, 207]. In addition Brown et al. generated some mAbs against A/WSN/1933 (H1N1) in 1983 to characterize antigenic variations of a wide range of Influenza viruses isolated from different origins [208]. However, most of the circulating IAVs that have caused the flu in human populations in the last decade are of either H1N1 of H3N2 subtypes. As mentioned earlier, there are various sequence features within NS1 from different Influenza viruses, and we believed that generating broadly cross reactive and highly NS1 specific mAbs might be useful tools to detect NS1

protein of a wide range of viral subtypes and its interacting partners. That is why broadly cross reactive mAbs were selected by immunizing mice with NS1 derived from HK1 (H3N2) and hybridomas were screened with NS1 derived from PR8 (H1N1). Therefore, these broadly cross reactive mAbs could be utilized to detect the host factors that are common to most of the circulating IAV strains including H1N1 and H3N2 subtypes.

4.2 Characterization of the NS1- mAbs

Extensive characterization of these mAbs was carried out and these mAbs demonstrated strong reactivity to denatured and native IAV-NS1 proteins derived from different stains including H1N1 and H3N2 types (Table 6). In immunoblot analysis, small variation of NS1 molecular masses was seen among some IAVs (Figure 10A and B), which reflects the sequence differences between these strains. Occasionally a much fainter band was observed around 42 kDa regions that might happen due to the representation of modified NS1 oligomers. However, an immunoprecipitated protein band (in addition to the IgG chains) near 26kDa region was consistently found in the IPs of PR8-infected cell lysates using mAb 3F5, and mass spectrometry identified this as PR8 NS1.

mAbs detected IAV NS1 earlier in infection by immunoblot analysis (5-6 hpi) than by immunofluorescence microscopy (8 hpi). Immunofluorescence microscopy usually focuses on specific cellular compartments to observe protein expression, but in immunoblot analysis proteins are extracted and concentrated from whole cell lysates in a small volume and analysed, which increases the sensitivity for protein detection. So, one possible explanation can be that NS1 is expressed earlier (~6 hpi), but I was only able to

focus the fluorescence signal at ~8 hpi. The epitope mapping of the 9 mAbs was performed by linear overlapping peptide analysis and these mAbs detected five different epitopes within PR8-NS1 protein. Similar reactivity was also seen when these mAbs were analysed against NS3 of D125G-mutated HK1 viruses. NS3 lacks 125-167 aa sequences, which is present in NS1 protein. For example, mAbs 3F5, 5F4 and 13D8 detected only NS1 but not NS3, which demonstrated that they identified epitopes residing in the 125-167 aa region of NS1 protein (Figure 15 A and B). Linear peptide epitope mapping more specifically detected their epitope (s) on ^{161}SPLPSLPGH^{169} (Table 6), which indicated the epitope mapping was very precise when two alternate strategies were utilized. More than 1800 non-redundant human IAV NS1 protein sequences were analyzed where three epitopes were present in > 95-97% of IAV NS1 sequences (section 3.4.3). A cocktail of 3 mAbs could recognize 100% of the IAV NS1 sequences at the time when the mAb characterizations were done. Using a mixture of 2-3 anti-NS1 mAbs can be used to detect different strains and types of IAV NS1 proteins. Thus these potential cross reactive mAbs could be utilized to find common host factors that interact with NS1 of different IAV strains including H1N1 and H3N2.

4.3 Efficiency of using mAb for detecting NS1 interacting host factors

My main goal was to detect host factors that interact with IAV NS1 during the natural infection and viral replication process. mAbs with strong binding ability can play that role in infected-cells. The anti-NS1 mAbs showed strong affinity in immunoprecipitating IAV-NS1 from infected cell lysates. The cell lysates (antigens) were pre-cleared by treating them with only the beads for 90 mins before adding to the beads-

mAb complex, which reduced the protein background in mass spectrometry analysis. In co-IP, washing the beads-mAb-antigen complexes with different buffers is a very crucial step, which removes unbound/non-specific proteins and antibodies. The ability of maintaining stable physiological interactions between NS1 and host proteins throughout the washing steps is a vital factor in detecting the host interacting partners in NS1 co-IP. In all co-IP experiments, multiple washing steps were carried out where non-specific protein binding or low-affinity protein-protein interactions might not be detected. Thus, I believe that the host proteins identified in co-IPs were strongly associated with IAV NS1. From the beginning of MS analysis, different parameters such as pre-clearing lysates, washing beads, MS run time had been optimized. In addition, the MS settings I used only detected high abundance proteins and sometimes missed the low abundance proteins in co-IP. Due to all of these optimizing steps and MS's performance, differences in the numbers of identified proteins in 3 different biological experiments were found in MS runs. Finally, 183 NS1-interacting host factors were identified in at least 2 biological experiments. Bioinformatics analyses have revealed that most of these factors are involved in different molecular functions, biological processes and pathways of host cells.

In the STRING analysis, many of these 183 NS1-interacting candidates interacted with each other (Figure 23), which may raise a new question whether the NS1 is directly interacting with all of these candidates or if secondary interactions are involved. All of these 183 host candidates are uniquely identified in PR8-infected co-IP with anti-NS1 mAb mixture (these were not identified in PR8-infected IP with isotype controls and mock-infected IP with anti-NS1 mAb mixture). It is very difficult to come to a conclusion

regarding the primary/secondary interactions in any global interactome study. However, I selected four representative host factors NUMA1, PRPF19, UTP6 and RPF1 for reciprocal co-IP and to check whether IAV NS1could be identified in the reciprocal co-IPs of those candidates. NS1 was detected in the co-IPs of NUMA1, PRPF19 and UTP6 (Figure 27). Although co-IP is the gold standard assay for protein-protein interactions with endogenous proteins, some other techniques have also been used to validate direct interaction between two protein candidates. These techniques include Fluorescence Resonance Energy Transfer (FRET) microscopy [209] and Biacore (a technique where optical biosensors are used) [210].

4.4 RNAi screening of NS1 interacting host factors

I used a custom Reverse Transfection Format (RTF) siRNA array to knock-down 107 host proteins that had been identified as NS1 interacting factors to evaluate their impact on IAV replication. These proteins are involved in different pathways, biological processes and molecular functions that I identified in the bioinformatics analysis. In the past some groups have used viral gene luciferase assays or immunostainings of the cells in 96 well formats to detect viral replications. I decided to measure viral titres to assess virus replication and infectious virus production directly from infected-KD cells. A549 cells produce high virus titre at 43 hpi when they are infected with low MOI; therefore I selected 43 hrs for harvesting viruses after viral infection at low MOI. The RTF siRNA array comes in 96 well plate format and one drawback of the RTF library is that it is very difficult to check the KD efficiency since each well of 96 well plate does not contain enough cells to check KD efficiency by Western. However, RTF siRNA array is very

beneficial and rapid method to screen gene candidates from a large number of genes. In my analysis 107 host proteins were screened where knockdown of 11 host proteins significantly reduced IAV replication to at most 30% compared to the control cells in three different independent RNAi experiments. After 48 hrs post KD, no significant reduction of A549 cell viability was observed post KD; however, infected-KD cells were less viable at 43 hpi (Figure 25 A and B). Influenza can cause virus-induced cell death during viral replication [211-213]. Cell viabilities of KD infected cells were less than the mock-infected wild A549 cells in my siRNA screening; therefore, the viral-induced cell death in infected cells could be the possible explanation of less cell viability after infection. On the other hand another point may come up where the viral titre in KD cells could be less compared to the N/T cells due to lower viability of the KD cells compared to the N/T after infection. To look into this issue I compared the cell viabilities of the infected-KD cells with the viral titre generated at 43 hpi. The ratios of viral titre and cell viability for all 11 KD A549 cells were calculated, which were reduced significantly in all KD cells except IL2 KD compared to the N/T (Figure 26). Thus, I believe that the viral titres in KD cells were reduced due to the KD cases, not because of lower cell viability compared to the N/T cells. Among these 11 KD gene candidates, HNRNPUL2, ILF2 and PRPF19 were previously identified as NS1 interacting proteins in VirHostNet 2.0 database; however, knocking down PRPF19 proteins was demonstrated to reduce Influenza virus production in a previous study [153]. NUMA1, RAI14, RBM28, RBM34, RPF1, SF3B3, SNRNP200, and UTP6 proteins were discovered first in my study, knocking down of which significantly reduced IAV replication. These RNAi screens were enriched in proteins involved in the aspects of host processes such as pre mRNA

processing, mRNA splicing, gene expression, nucleoside, nucleotide and nucleic acid metabolism.

RNA splicing is the editing step in eukaryotic cells where introns are removed and exons are joined together to form nascent pre-mRNA. In different cases this splicing generates unique proteins by shifting the exon sequences of the same mRNA and it is then called alternative splicing. Influenza viruses utilize the host's splicing system to produce NS1, NS2/NEP, M1 and M2 proteins by alternative splicing [61, 62]. Influenza NS1 interacts with spliceosomal subunits U2 and U6 during viral replication [199, 200]. Influenza virus inhibits cellular gene expression. NS1 interacts with some host factors; therefore, it blocks the host's pre-mRNA processing such as blocking polyadenylation and host mRNA export to the cytoplasm [127, 201]. These all lead to turning off host protein expression, so that viral transcripts get access to the cellular translation tools. I believe the novel NS1-interacting host factors that were identified in my screening; especially the factors which are required for viral replication (identified in RNAi screening) may have roles in controlling the viral/host mRNA maturation, splicing and gene expression to favour viral replication.

4.5 NUMA1

NUMA1 (also known as NuMA) contributes to maintaining the structural integrity of the cell. It also plays essential roles during the assembly and maintenance of the mitotic spindle in the cell cycle (reviewed in [158]). Both of these functions utilize microtubules (polymers of tubulin protein) [214]. Microtubules and dynein (a

microtubule motor protein) also play important roles in the exocytic pathway to transport newly synthesized proteins through the Golgi complex to the cell surface [215-217].

There is a strong connection between NUMA1 and microtubules. During mitosis, NUMA1 plays a vital role to join the microtubules to the spindle poles [158, 218]. The C-terminus of NUMA1 can directly bind with tubulin (a monomer of microtubules) [166]; however, previous studies also suggested that NUMA1 needed to associate with dynein to bind with microtubules [164, 165].

In my study, PR8 production (infectious viruses were detected by plaque assay) was significantly reduced in NUMA1 KD cells, which has not been previously reported. Then I tried to find the specific step/steps that was/were inhibited. No significant reduction of viral mRNA synthesis was found in NUMA1 deficient cells (Figure 29A) compared to the N/T control cells, which suggests that the IAV entry to the cell, import of incoming vRNPs to the nucleus and viral transcription are not NUMA1 dependent. In addition, NUMA1 deficient cells produced similar amounts of both structural and non-structural IAV proteins as N/T control cells, which indicate that viral mRNA transport to the cytoplasm and the translation process were unaffected in NUMA1 deficient cells (Figure 29B). I checked the IAV structural protein level in the supernatants of infected cells. The structural protein levels produced and released into the supernatant were significantly less in NUMA1 KD cells compared to the N/T cells (Figure 30C and D). In NUMA1 KD cells the amounts of structural protein released were comparable to viral titre, which were significantly lower compared to the N/T. This suggests no major changes in particle-to-PFU ratios in NUMA1 KD cells compared to the N/T cells. The decreased titres observed in NUMA1 KD A549 cells were due to altered maturation.

In viral maturation, newly synthesised vRNPs need to be exported from the nucleus into the cytoplasm, and transported to the cytoplasmic membrane for viral assembly and budding. IAV M1 plays a vital role in exporting vRNPs into the cytoplasm where M1 directly interacts with vRNPs [47, 71, 82]. Interactions among vRNPs, M1 and envelope proteins (HA, NA and M2) are required for viral assembly and budding where M1 protein acts as a linker between vRNPs and envelope (reviewed in [25, 82]). On the other hand, it is established in VirHostNet database that NS1 interacts with M1 [219], and I also found M1 in my NS1 inteactome studies during viral replication. In addition NS1 proteins were detected in the nucleus at early times of infection and later spread into the cytoplasm, as detected in my immunofluorescence microscopy images (Figure 13B).

Viral envelope proteins HA, NA and M2 utilize exocytic pathways to reach the assembly and budding site through the *trans* Golgi network [82, 220]. Viral M1 can bind to the cytoplasmic domains of HA and NA proteins [82, 220, 221]. After the export of vRNPs-M1 complexes into the cytoplasm, it was proposed that the vRNPs-M1 complexes are transported to the cell membrane for assembly by piggy-backing on the HA and NA cytoplasmic domains or via cytoskeleton elements [82, 83, 221-223].

In my super-resolution SIM images, an increase of IAV M1 protein was visible in the NUMA1-deficient cells that formed clusters in the cytoplasmic region, which is in close proximity to the nucleus of NUMA1 KD cells whereas no M1 clustering was observed in NSi (control) cells (Figure 31B and C). I also found the structural proteins NP (component of vRNP) level was higher in NUMA1 KD Western blot than in NSi (Figure 29C and D). Therefore, I believe that transport of M1 and M1 associated viral proteins to the assembly site was inhibited in NUMA1 deficient cells, which ultimately

reduced the infectious virus production in NUMA1 KD cells. On the other hand, an increase of IAV M2 proteins were also observed in NUMA1 KD immunofluorescence microscopy (Appendix B2) and SIM analysis compared to the NSi cells, and these were deposited near the NUMA1 KD cytoplasmic region (Figure 31F and G), which suggested that M2 was synthesised but could not assemble with other structural proteins and bud out of the cell incorporating with new virion particles. EM results also showed significant reduction of virus budding in NUMA KD cells compared to the NSi cells (Figure 32A and B).

Therefore, I propose a model depicting the role of NUMA1 in IAV maturation (Figure 36), in which the viral M1-RNPs complexes transport into the cytoplasm and M1 interacts with NS1. I first reported in my study that NS1 interacts with cellular NUMA1 protein during viral replication. I propose that NS1 works as a bridge between M1 and NUMA1 proteins. Thereafter, the strong connection between NUMA1 and microtubules (major component of exocytic pathway) facilitates the transport of viral M1-associated proteins (vRNPs) to the cytoplasm using exocytic pathway via trans-Golgi network for assembly and budding. I also propose that in the absence of NUMA1 protein, M1-vRNPs are not able to interact with the microtubule network; thereby, the transportation of these essential structural proteins to the assembly site (cytoplasmic membrane) is obstructed. In my study it was not confirmed whether HA and NA transports were inhibited or not and further studies are required to confirm this. In addition to the exocytic pathway, another previous study suggested that cytoskeletal microfilaments can interact with the M1 and NP vRNP, which facilitates M1-vRNP transport to the assembly [223]. This microfilament-mediated transport might contribute to the production of some

A.

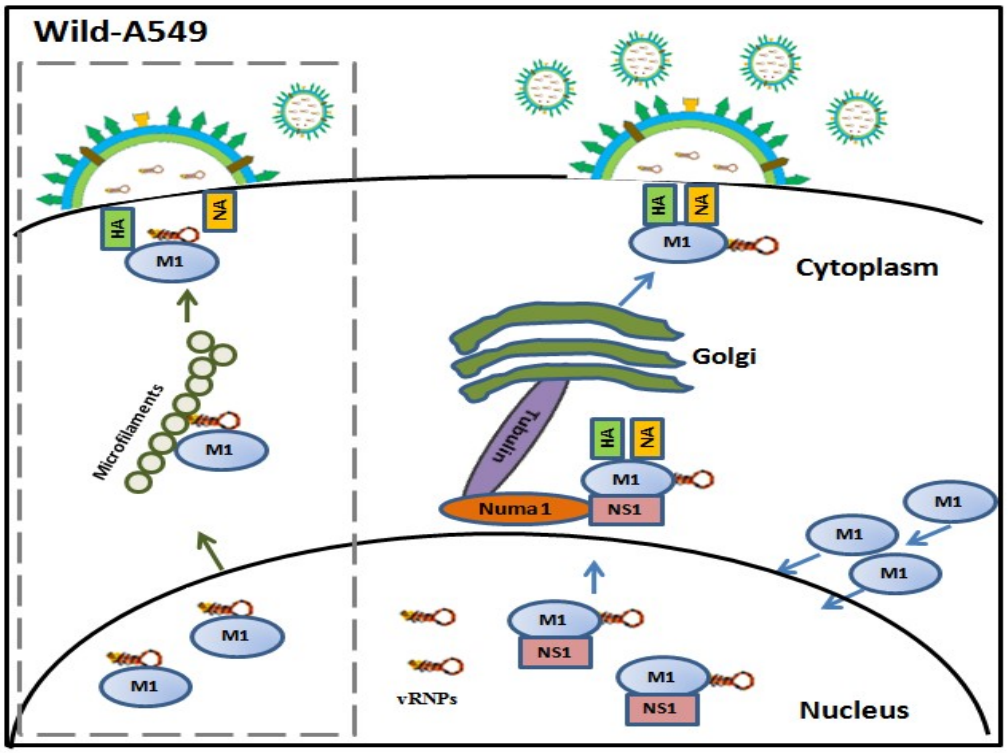
Wild-A549
HA
NA
M1
Cytoplasm
Golgi
Tubulin
Microfilaments
Numa1
NS1
vRNPs
Nucleus

B.

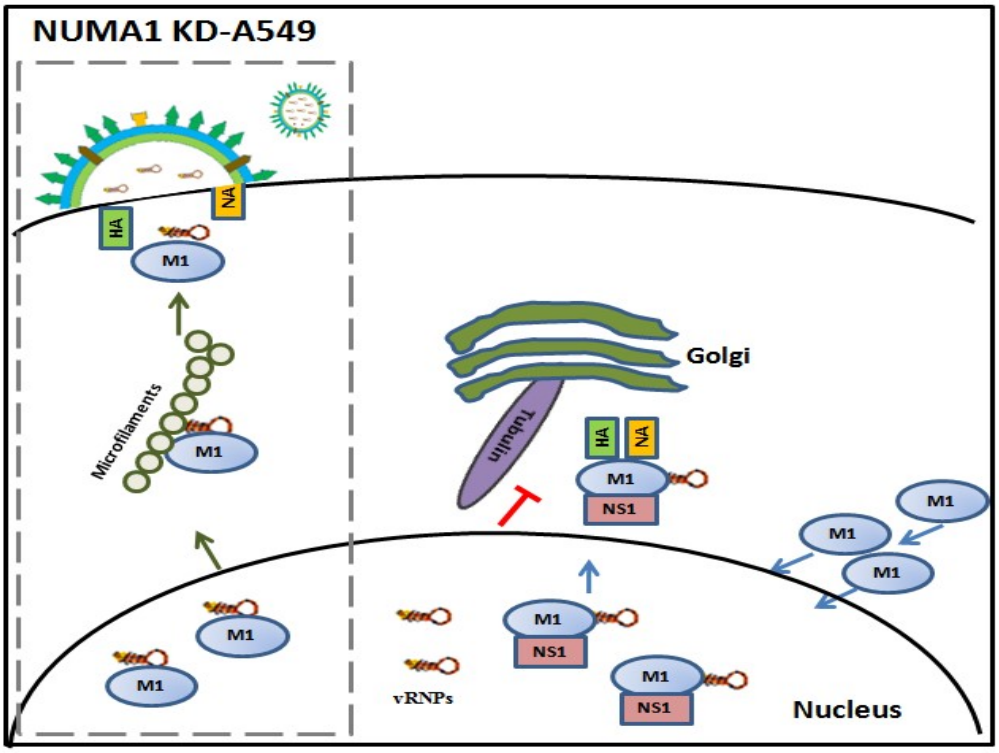
NUMA1 KD-A549
HA
NA
M1
Golgi
Tubulin
Microfilaments
NS1
vRNPs
Nucleus

Figure 36: Proposed model for the involvement of NUMA1 in promoting influenza A virus replication in this study.

A) In wild type A549 cells, Influenza M1 protein enters into the nucleus after translation and binds with newly synthesised vRNPs. M1 interacts with Influenza NS1 protein. M1-vRNPs associated proteins are exported from nucleus to the cytoplasm. M1 also binds to the cytoplasmic tails of HA and NA. During translocation of M1-associated proteins into the cytoplasm NS1 interacts with NUMA1, which strongly maintains connection with microtubule network (tubulin). Therefore, M1-associated viral proteins utilize the exocytic pathway for transportation to the cytoplasmic membrane for virion assembly and budding via trans-Golgi network. B) In NUMA1 KD cells, M1 protein binds with the viral RNPs, interacts with NS1 protein and is exported to the cytoplasmc region. Due to the absence of NUMA1 protein, NS1 of M1-associated protein complex cannot interact with NUMA, therefore the M1-associated proteins cannot utilize the microtubule-mediated exocytic pathway to reach the assembly site. The dashed lines illustrate the proposed mechanism in [223], through which M1 and vRNP transport through cytoskeleton elements.

viruses (2.6%-20% of the N/T) in my NUMA1 KD cells. My proposed model can illuminate the mechanism undertaken by NUMA1 protein to promote influenza virus replication by the exocytic pathway.

4.6 PRPF19

The pre-mRNA processing factor 19 (PRPF19), also known as PRF19 plays an important role in assembly and activating the spliceosome [169, 170]. Knocking down the PRPF19 gene significantly reduced infectious IAV production in my study. Influenza viruses utilize host cell splicing machinery to produce NS1 and NS2/NEP proteins from RNA segment 8, and M1 and M2 proteins from RNA segment 7 by alternative splicing [74, 75]. So, initially I assumed that the alternative splicing step might be affected; however, no significant reduction of viral transcription and translation including NS1 and M2 proteins were observed in my studies. In Influenza virus replication, production of new virions usually starts ~11 hpi and one infected cell can produce ~22 progeny viruses [224]. The NS1 and M2 proteins were expressed at a higher amount in PRPF19 KD cells than in NSi at 18 hpi (Figure 34C and D). M2 protein expression was higher in PRPF19 KD cell compared to the N/T cells (Appendix B2). For more precise localization of viral M1 and M2 proteins, SIM was carried out. In SIM, the intensity of M1 and M2 proteins were also higher in PRPF19 KD cell than in NSi cells (Figure 31B, D, F and H) at 20 hpi, which all suggested that the viral proteins were synthesised but could not incorporate into new virions. Therefore, I believe the viral entry, transcription and translation steps are not affected but the maturation of new virion during assembly/budding is hindered in

PRPF19-deficient A549 cells, which requires further experiments to find the specific mechanism of inhibition.

4.7 Conclusions

This is the first study where a panel of broadly cross reactive anti-NS1 mAbs were generated and utilized for global screening of NS1-interacting host factors in natural infection model, where infections were done with wild type IAV (not recombinant). 183 proteins were identified in my NS1 interactome studies among which 124 proteins were identified first in this study. These 124 proteins represent novel NS1-interacting targets that may be unique in human bronchial epithelial A549 cells. Some of the NS1-interactng host factors were identified as vital factors for IAV replication by RNAi screening. Studying the roles of these candidates during viral replication may guide us to uncover some mechanisms of the viral life cycle. Moreover, these factors may be experimentally proved as novel candidates for therapeutic development.

4.8 Future Directions

Although this thesis has demonstrated that our broadly cross reactive anti-NS1 efficiently identified the NS1-interacting host factors and 11 of these host factors were identified as crucial factors for IAV replication, there are still some things that remain unknown about these NS1 interacting proteins.

4.8.1 NS1 specific mAb

The novel panel of NS1-specific mAbs that were characterized in my study are broadly cross reactive among different strains of Influenza H1N1 and H3N2 subtypes.

These mAbs are able to detect five different epitopes of IAV-NS1, which are conserved among 95-97% strains of ~1800 non-redundant IAV NS1 sequences. So the application of this panel of mAbs can be useful for detecting NS1 proteins (as an Influenza virus marker) for diagnosis or characterization of infections. The mAbs can also be used to inhibit host interactions to assess the effect of blocking host factors that bind different sites of the NS1 protein. For example, these mAbs can be utilized to detect NUMA1 binding site in NS1. ELISA plate can be coated with NS1, treated alternatively with different mAbs that can block different NS1 epitopes; therefore, purified NUMA1 protein can be treated to check its binding capability with NS1, which can be detected by using biotinylated anti-NUMA1 Ab.

4.8.2 NS1 interacting host factors from the RNAi screening

The siRNA screening was very useful to me. It allowed me to identify a small group of proteins from a long list of NS1-interacting proteins, which would be interesting to pursue in future studies. Knocking down these 11 proteins significantly reduced infectious virus production. In terms of virus replication, NUMA1 and PFPF19 KD reduced infectious viral production to 2.6% and 16%, respectively, compared to the N/T cells in siRNA array, and I was able to validate their interaction with IAV NS1 protein by reciprocal IP. Thus, I selected these two candidates to investigate how these are linked to the IAV replication. More NS1-interacting host factors such as RBM28, SYNCRIP, SNRNP20 and SF3B3 were also discovered in my NS1 interactome and siRNA screening studies, knocking down of which significantly reduced infectious virus production to 8.9-25% compared to the N/T cells. These proteins are involved in different biological processes, molecular functions and pathways (indicated in Table 8) such as RNA

processing, mRNA metabolic process, RNA splicing, gene expression, helicase acivity, RNA binding, nucleotide binding and DNA binding. These factors can also be analyzed to identify the mechanisms/roles in influenza virus replication in future studies.

As another option, I would consider studying the group of NS1-interacting proteins such as DHX30, H2AFJ, FXR1, RSL1D1 and ELAVL1 as they increased infectious virus production after knocking down their genes, compared to the N/T cells. These NS1-interacting proteins may have some inhibitory effects on viral replication, which was probably reduced after knocking down their genes. Over-expression of these NS1-interacting proteins would be interesting to pursue, which would be useful for identifying antiviral activities. IAV replication can be monitored after over-expressing these proteins in A549 cells to investigate the roles of these factors in viral replication. On the other hand, knocking down of these genes in A549 cells can be used in cell culture models for high titre Influenza virus production.

All of my interactome and KD experiments were conducted in A549 cells. KD effects of these genes can be observed in more physiologically relevant primary cell lines, such as primary human bronchial epithelial cell (HBEC), which can provide us more relevant outcomes.

4.8.3 NUMA1 protein

I discovered that NUMA1 interacts with IAV NS1 protein and NUMA1 depleted cells significantly reduced IAV replication. Although virion production was reduced in NUMA1 deficient cells, viral protein production was not blocked. This suggests the viral maturation is inhibited in NUMA1 KD cells where transport of M1-vRNP complexes to

the assembly site was obstructed. Superresolution SIM analysis targeting the glycoproteins HA and NA can be done to confirm whether viral HA and NA transports to the assembly site in NUMA1 KD cells are affected or not. Viral maturation can be compared between the infected NUMA1 KD and N/T cells in SIM or confocal microscopy by monitoring the distribution of microtubule network and IAV M1 together. Additionally, the focus on NUMA1 activity can be further extended to other microorganisms and other viruses such as HIV and Hepatitis B virus replication.

4.8.4 PRPF19 protein

In my study of PRPF19 KD A549 cells, viral entry, transcription and translation processes are not inhibited. Although PRPF19 is an important factor in the cell's splicing machinery, expression of spliced proteins (NS1 and M2) indicated the viral splicing steps during IAV replication were not interrupted in PRPF19 KD cells. The viral maturation was inhibited in PRPF19 KD. There was no visible clustering of M1 and M2 proteins seen in SIM analysis, which indicated that the transport of M1 and its associated viral protein to the assembly site might not be affected. IAV NA, HA and M2 play important roles during virion budding. Therefore, observing the viral assembly and budding steps adjacent to the cytoplasmic membrane by immunogold labelling of NA and HA in transmission EM may reveal these maturation steps in PRPF19 KD cells.

APPENDIX A

Appendix A1: List of siRNA used in siRNA array in 96 well format

Appendix A1: List of siRNA used in siRNA array in 96 well format (plate 1)							
LP_8103_RTF (Plate 1), G-CUSTOM-147092							
Well	Pool Catalog Number	Duplex Catalog Number	Gene Symbol	GENE ID	Gene Accession	GI Number	Sequence
A02	M-003976-00	D-003976-01	IGF2BP3	10643	NM_006547	30795211	GAACGCACUAUUACAGUUA
A02	M-003976-00	D-003976-02	IGF2BP3	10643	NM_006547	30795211	UAGACAAACUGAAUGGAUU
A02	M-003976-00	D-003976-03	IGF2BP3	10643	NM_006547	30795211	GCAAAGGAUUCGGAAACUU
A02	M-003976-00	D-003976-04	IGF2BP3	10643	NM_006547	30795211	UCGAGGCGCUUUCAGGUAA
A03	M-009542-00	D-009542-01	PES1	23481	NM_014303	22091458	CAACGAAGGUGAUGGUGAU
A03	M-009542-00	D-009542-02	PES1	23481	NM_014303	22091458	GAAGGAAGGAGAUUACGUU
A03	M-009542-00	D-009542-03	PES1	23481	NM_014303	22091458	CCUUGAAGCUGGAGGAUAA
A03	M-009542-00	D-009542-04	PES1	23481	NM_014303	22091458	GAGCUUGGCUGACUUUAGG
A04	M-012128-00	D-012128-01	MPHOSPH10	10199	NM_005791	31317304	UGGCAAAGCUUCCUUCAUA
A04	M-012128-00	D-012128-02	MPHOSPH10	10199	NM_005791	31317304	GCAGAAGAACUAAGUAUUU
A04	M-012128-00	D-012128-03	MPHOSPH10	10199	NM_005791	31317304	GCAGUUAGUGAAACAAUUA
A04	M-012128-00	D-012128-04	MPHOSPH10	10199	NM_005791	31317304	GGGAUGAUGUAGUACGUAA
A05	M-019143-01	D-019143-01	NOP56	10528	NM_006392	32483373	GGACAUAUCUGCCAUUGAC
A05	M-019143-01	D-019143-02	NOP56	10528	NM_006392	32483373	GGAGAGAUACCACGAAAGA
A05	M-019143-01	D-019143-04	NOP56	10528	NM_006392	32483373	GAGCGACUGUCCUUCUAUG
A05	M-019143-01	D-019143-17	NOP56	10528	NM_006392	32483373	CCUAAUUGGGGAAGCGGUA
A06	M-006874-01	D-006874-01	DDX3X	1654	NM_001356	87196350	GCAAAUACUUGGUGUUAGA
A06	M-006874-01	D-006874-02	DDX3X	1654	NM_001356	87196350	ACAUUGAGCUUACUCGUUA
A06	M-006874-01	D-006874-04	DDX3X	1654	NM_001356	87196350	CUAUAUUCCUCCUCAUUUA
A06	M-006874-01	D-006874-17	DDX3X	1654	NM_001356	87196350	GGUAUUAGCACCAACGAGA
A07	M-011250-01	D-011250-01	DHX15	1665	NM_001358	68509925	AAACAGAAAUGCAGGAUAA
A07	M-011250-01	D-011250-02	DHX15	1665	NM_001358	68509925	CAGCAGCUAUCUCGAAUUA
A07	M-011250-01	D-011250-03	DHX15	1665	NM_001358	68509925	GAUGAGAUUUGCCCACAUA
A07	M-011250-01	D-011250-04	DHX15	1665	NM_001358	68509925	GAGAUCAGAUUUAAAGGUU
A08	M-014028-00	D-014028-01	RRP8	23378	NM_015324	34147331	GAAGAUGUAAGAACAAGUU
A08	M-014028-00	D-014028-02	RRP8	23378	NM_015324	34147331	CAAAUGAUCCACCAAAGCA
A08	M-014028-00	D-014028-03	RRP8	23378	NM_015324	34147331	GCAAAUAGAGUACUGAAGC
A08	M-014028-00	D-014028-04	RRP8	23378	NM_015324	34147331	CGAUUUCGCUACCUCAAUG
A09	M-011478-00	D-011478-01	SMARCA5	8467	NM_003601	21071057	GGAUUAAACUGGCUCAUUU
A09	M-011478-00	D-011478-02	SMARCA5	8467	NM_003601	21071057	GAGGAGAUGUAAUACCUUA
A09	M-011478-00	D-011478-03	SMARCA5	8467	NM_003601	21071057	GGAAUGGUAUACUCGGAUA
A09	M-011478-00	D-011478-04	SMARCA5	8467	NM_003601	21071057	GGGCAAAUAGAUUCGAGUA
A10	M-016218-00	D-016218-01	SYNCRIP	10492	NM_006372	23397426	GUAUGACGAUUACUACUAU
A10	M-016218-00	D-016218-02	SYNCRIP	10492	NM_006372	23397426	GCACAUAGUGAUUUAGAUG
A10	M-016218-00	D-016218-03	SYNCRIP	10492	NM_006372	23397426	GAGGUUAUGGCAAAGGUAA
A10	M-016218-00	D-016218-04	SYNCRIP	10492	NM_006372	23397426	GUAGAGGUGGUUAUGGAUA
A11	M-013639-00	D-013639-01	DKC1	1736	NM_001363	15011921	GGACAGGUUUCAUUAAUCU
A11	M-013639-00	D-013639-02	DKC1	1736	NM_001363	15011921	GCAGGAGUAUGUUGACUAC
A11	M-013639-00	D-013639-03	DKC1	1736	NM_001363	15011921	CUGCGACCAUGGUAUAGUA

Appendix A1: List of siRNA used in siRNA array in 96 well format (plate 1)							
Well	Pool Catalog Number	Duplex Catalog Number	Gene Symbol	GENE ID	Gene Accession	GI Number	Sequence
A11	M-013639-00	D-013639-04	DKC1	1736	NM_001363	15011921	GCGAGUUGUUUACCCUUUG
B01	M-011964-00	D-011964-01	H2AFY	9555	NM_004893	20336744	UGGAAUACCUGACAGCGGA
B01	M-011964-00	D-011964-02	H2AFY	9555	NM_004893	20336744	CCGAGUUGCUAGCGAAGAA
B01	M-011964-00	D-011964-03	H2AFY	9555	NM_004893	20336744	GUGAUCCACUGUAAUAGUC
B01	M-011964-00	D-011964-04	H2AFY	9555	NM_004893	20336744	CCAGUUACUUCGUGUCUAC
B02	M-014161-00	D-014161-01	SNRNP200	23020	NM_014014	40217846	UCAACAAGAUGAAGGGUUA
B02	M-014161-00	D-014161-02	SNRNP200	23020	NM_014014	40217846	AGAACAAUCUGGUCAAGUA
B02	M-014161-00	D-014161-03	SNRNP200	23020	NM_014014	40217846	GCAGAAAUCGUGCUAGGAA
B02	M-014161-00	D-014161-04	SNRNP200	23020	NM_014014	40217846	GCAGCUCAGUCGUUUCUAU
B03	M-017456-01	D-017456-01	SURF6	6838	NM_006753	157266286	GAAGAUCCGUGACGACGAA
B03	M-017456-01	D-017456-02	SURF6	6838	NM_006753	157266286	GGGCUGAUCUUCAAUAAGG
B03	M-017456-01	D-017456-03	SURF6	6838	NM_006753	157266286	CCACUGAGCCUGAGUCUGU
B03	M-017456-01	D-017456-04	SURF6	6838	NM_006753	157266286	GACAGCGACUGCAUGAGAA
B04	M-022489-01	D-022489-01	RSL1D1	26156	NM_015659	118498358	AGAUUGACCUUGCCUCAUA
B04	M-022489-01	D-022489-02	RSL1D1	26156	NM_015659	118498358	GGGAGACAUUUCUAUCAAA
B04	M-022489-01	D-022489-03	RSL1D1	26156	NM_015659	118498358	GACGCUCUCUUGACGCAUU
B04	M-022489-01	D-022489-04	RSL1D1	26156	NM_015659	118498358	UCCAGUAUCUGUAAACCUU
B05	M-019452-01	D-019452-01	PTBP3	9991	NM_005156	75991711	GAUCAUAUCAUUAGGUCUA
B05	M-019452-01	D-019452-02	PTBP3	9991	NM_005156	75991711	CCGUUACUAUGGUGAAUUA
B05	M-019452-01	D-019452-03	PTBP3	9991	NM_005156	75991711	GAUGGCGGAUGCAAAUCAA
B05	M-019452-01	D-019452-04	PTBP3	9991	NM_005156	75991711	UCUUAUAACAGUCGGUUUA
B06	M-005269-01	D-005269-01	HSPB1	3315	NM_001540	4996892	CCGAUGAGACUGCCGCCAA
B06	M-005269-01	D-005269-03	HSPB1	3315	NM_001540	4996892	GGCAGGACGAGCAUGGCUA
B06	M-005269-01	D-005269-04	HSPB1	3315	NM_001540	4996892	CCGGAGGAGUGGUCGCAGU
B06	M-005269-01	D-005269-05	HSPB1	3315	NM_001540	4996892	CAAGUUUCCUCCUCCCUGU
B07	M-017209-01	D-017209-01	H1F0	3005	NM_005318	85838503	CCAAGACUGUCAAAGCCAA
B07	M-017209-01	D-017209-17	H1F0	3005	NM_005318	85838503	UGUUACUUGUGCCGGGAAA
B07	M-017209-01	D-017209-18	H1F0	3005	NM_005318	85838503	AGAAGGUAGCCACGCCAAA
B07	M-017209-01	D-017209-19	H1F0	3005	NM_005318	85838503	UCGAUUUGGGAUUUGCUAA
B08	M-005168-01	D-005168-01	HSPA1A	3303	NM_005345	26787973	GAGAUCGACUCCCUGUUUG
B08	M-005168-01	D-005168-03	HSPA1A	3303	NM_005345	26787973	GAUCAACGACGGAGACAAG
B08	M-005168-01	D-005168-04	HSPA1A	3303	NM_005345	26787973	GCGCUGAACCCGCAGAACA
B08	M-005168-01	D-005168-05	HSPA1A	3303	NM_005345	26787973	GCUCCGACCUGUUCCGAAG
B09	M-012049-00	D-012049-01	HIST1H1B	3009	NM_005322	15718716	CCAAGGCAGUUAAGCCGAA
B09	M-012049-00	D-012049-02	HIST1H1B	3009	NM_005322	15718716	GGAGCGCAAUGGCCUUUCU
B09	M-012049-00	D-012049-03	HIST1H1B	3009	NM_005322	15718716	GCUAAGAAGAAGGCAACUA
B09	M-012049-00	D-012049-04	HIST1H1B	3009	NM_005322	15718716	GCUGCUAAGCGCAAAGCGA
B10	M-003774-01	D-003774-02	DDX5	1655	NM_004396	13514826	CACAAGAGGUGGAAACAUA
B10	M-003774-01	D-003774-03	DDX5	1655	NM_004396	13514826	GUGAUGAGCUUACCAGAAA
B10	M-003774-01	D-003774-04	DDX5	1655	NM_004396	13514826	GCAAAUGUCAUGGAUGUUA
B10	M-003774-01	D-003774-17	DDX5	1655	NM_004396	13514826	GGAUGUGUGUCAUGACGUA
B11	M-019764-00	D-019764-01	VDAC1	7416	NM_003374	4507878	CGACAUGGAUUUCGACAUU
B11	M-019764-00	D-019764-02	VDAC1	7416	NM_003374	4507878	GAAACCAAGUACAGAUGGA

Appendix A1: List of siRNA used in siRNA array in 96 well format (plate 1)							
Well	Pool Catalog Number	Duplex Catalog Number	Gene Symbol	GENE ID	Gene Accession	GI Number	Sequence
B11	M-019764-00	D-019764-03	VDAC1	7416	NM_003374	4507878	GACUGGAAUUUCAAGCAUA
B11	M-019764-00	D-019764-04	VDAC1	7416	NM_003374	4507878	GAAUACCGACAAUACACUA
B12	M-022399-00	D-022399-01	RBM34	23029	NM_015014	38016126	GAGUUGAUCUCGCAUCUGA
B12	M-022399-00	D-022399-02	RBM34	23029	NM_015014	38016126	GUUGGGAAUUUGCCUGUUA
B12	M-022399-00	D-022399-03	RBM34	23029	NM_015014	38016126	GGUCGCCAGUAGCUUAUUU
B12	M-022399-00	D-022399-04	RBM34	23029	NM_015014	38016126	GGAAUCUCCCUUAUAAAGU
C01	M-017382-01	D-017382-01	MATR3	9782	NM_018834	62750352	UAGAUGAACUGAGUCGUUA
C01	M-017382-01	D-017382-02	MATR3	9782	NM_018834	62750352	GACCAGGCCAGUAACAUUU
C01	M-017382-01	D-017382-03	MATR3	9782	NM_018834	62750352	ACCCAGUGCUUGAUUAUGA
C01	M-017382-01	D-017382-04	MATR3	9782	NM_018834	62750352	CCAGUGAGAGUUCAUUUAU
C02	M-020084-02	D-020084-01	NOP2	4839	NM_006170	76150622	GCAACGAUCACCUAAAUUA
C02	M-020084-02	D-020084-02	NOP2	4839	NM_006170	76150622	AGACAGAACUCGUCAGAUU
C02	M-020084-02	D-020084-03	NOP2	4839	NM_006170	76150622	GCAUACCCAUGAAAUUUAA
C02	M-020084-02	D-020084-05	NOP2	4839	NM_006170	76150622	AAGCGUUGCUGCCCAUUGA
C03	M-021976-01	D-021976-01	RBM25	58517	NM_021239	55741708	GAAAGGAGCUCAGAUCGUA
C03	M-021976-01	D-021976-02	RBM25	58517	NM_021239	55741708	GAAGCUACAUUAGUUGAUU
C03	M-021976-01	D-021976-03	RBM25	58517	NM_021239	55741708	GAUGGAACGUCGAAUUAGA
C03	M-021976-01	D-021976-04	RBM25	58517	NM_021239	55741708	CAGAAAAGGUUGCGUGAUA
C04	M-012011-01	D-012011-01	FXR1	8087	NM_001013438	61835163	CCAUACAGCUUACUUGAUA
C04	M-012011-01	D-012011-02	FXR1	8087	NM_001013438	61835163	GUAAACAUCUUAAGUGACA
C04	M-012011-01	D-012011-03	FXR1	8087	NM_001013438	61835163	CGUACGAAGUUGAUGCUUA
C04	M-012011-01	D-012011-04	FXR1	8087	NM_001013438	61835163	AAACGGAAUCUGAGCGUAA
C05	M-010599-02	D-010599-02	HSPA2	3306	NM_021979	147901657	GCACAGCGCGGUCAUAACG
C05	M-010599-02	D-010599-03	HSPA2	3306	NM_021979	147901657	CAUCGAAGAAGUGGACUAA
C05	M-010599-02	D-010599-04	HSPA2	3306	NM_021979	147901657	UCAACUGGCUCGACCGAAA
C05	M-010599-02	D-010599-05	HSPA2	3306	NM_021979	147901657	AAACUGAGGGGCAAGAUUA
C06	M-008630-01	D-008630-02	ADAR	103	NM_015841	70167031	CAUCAAAUGCCUCAAAUAA
C06	M-008630-01	D-008630-03	ADAR	103	NM_015841	70167031	UAAAUGCUGUGCUAAUUGA
C06	M-008630-01	D-008630-04	ADAR	103	NM_015841	70167031	GAAACCACCUGUUCAUUAC
C06	M-008630-01	D-008630-17	ADAR	103	NM_015841	70167031	ACUAAGGAGACAAGCGUCA
C07	M-010096-01	D-010096-01	EIF6	3692	NM_002212	31563381	GAGCUUCGUUCGAGAACAA
C07	M-010096-01	D-010096-02	EIF6	3692	NM_002212	31563381	GAUCGGAGGCUCAGAGAAC
C07	M-010096-01	D-010096-04	EIF6	3692	NM_002212	31563381	CGAGAACAACUGUGAGAUC
C07	M-010096-01	D-010096-05	EIF6	3692	NM_002212	31563381	CAAUUGAAGACCAGGAUGA
C08	M-005030-01	D-005030-01	PRKDC	5591	NM_006904	31340617	GCAAAGAGGUGGCAGUUAA
C08	M-005030-01	D-005030-03	PRKDC	5591	NM_006904	31340617	GAGCAUCACUUGCCUUUAA
C08	M-005030-01	D-005030-04	PRKDC	5591	NM_006904	31340617	GAUGAGAAGUCCUUAGGUA
C08	M-005030-01	D-005030-05	PRKDC	5591	NM_006904	31340617	GCAGGACCGUGCAAGGUUA
C09	M-020019-00	D-020019-01	KHDRBS1	10657	NM_006559	5730026	CAUAAGAACAUGAAACUGA
C09	M-020019-00	D-020019-02	KHDRBS1	10657	NM_006559	5730026	GCACCCAUAUGGACGUUAU
C09	M-020019-00	D-020019-03	KHDRBS1	10657	NM_006559	5730026	UAUGAUGGAUGAUAUCUGU
C09	M-020019-00	D-020019-04	KHDRBS1	10657	NM_006559	5730026	ACAAGGGAAUACAAUCAAA
C10	M-005151-00	D-005151-01	SRSF4	6429	NM_005626	34147660	GGCAAGACCUAAAGGAUUA

Appendix A1: List of siRNA used in siRNA array in 96 well format (plate 1)							
Well	Pool Catalog Number	Duplex Catalog Number	Gene Symbol	GENE ID	Gene Accession	GI Number	Sequence
C10	M-005151-00	D-005151-02	SRSF4	6429	NM_005626	34147660	GAAGUGGCCGAGAUAAAUA
C10	M-005151-00	D-005151-03	SRSF4	6429	NM_005626	34147660	GAAUCACGCUCCAGAUCAA
C10	M-005151-00	D-005151-04	SRSF4	6429	NM_005626	34147660	GCAAAGACCAAGCUGAAGA
C11	M-017431-01	D-017431-01	TBL3	10607	NM_006453	19913368	GGACAUCACUGCCUUUGAC
C11	M-017431-01	D-017431-02	TBL3	10607	NM_006453	19913368	GAUCAGAGCGUCCGUAUCU
C11	M-017431-01	D-017431-04	TBL3	10607	NM_006453	19913368	UCUGACAGCUGGCGACCAA
C11	M-017431-01	D-017431-17	TBL3	10607	NM_006453	19913368	ACUAUGCUGUGGAGCGCAA
C12	M-017599-00	D-017599-01	ILF2	3608	NM_004515	24234746	GAACAGGCAUCUAUCCUUU
C12	M-017599-00	D-017599-02	ILF2	3608	NM_004515	24234746	GAAACUGGCUUUGAAAUCA
C12	M-017599-00	D-017599-03	ILF2	3608	NM_004515	24234746	CAUGGUGGCUUUAGGAAGA
C12	M-017599-00	D-017599-04	ILF2	3608	NM_004515	24234746	GGACAUGGUCUGCUAUACA
D01	M-012394-01	D-012394-02	TARDBP	23435	NM_007375	42741653	GCUCAAGCAUGGAUUCUAA
D01	M-012394-01	D-012394-03	TARDBP	23435	NM_007375	42741653	CAAUAGCAAUAGACAGUUA
D01	M-012394-01	D-012394-04	TARDBP	23435	NM_007375	42741653	GCAAACUUCCUAAUUCUAA
D01	M-012394-01	D-012394-05	TARDBP	23435	NM_007375	42741653	GGCCUUCGGUUCUGGAAAU
D02	M-011842-01	D-011842-01	DDX10	1662	NM_004398	13514830	GAAUGGAAGUCUAUAAUGA
D02	M-011842-01	D-011842-02	DDX10	1662	NM_004398	13514830	GAGCCAAGCCGAUAAAGUA
D02	M-011842-01	D-011842-03	DDX10	1662	NM_004398	13514830	GAGGAUGCCAACACAUAUA
D02	M-011842-01	D-011842-17	DDX10	1662	NM_004398	13514830	CCUUUGAGGUUCUCCGAAA
D03	M-011528-01	D-011528-01	PABPC4	8761	NM_003819	6552335	GGGUGAAUCUCUACAUUAA
D03	M-011528-01	D-011528-03	PABPC4	8761	NM_003819	6552335	CCAAUGCCAUCUUAAAUCA
D03	M-011528-01	D-011528-04	PABPC4	8761	NM_003819	6552335	GGUAAGACCCUAAGUGUCA
D03	M-011528-01	D-011528-17	PABPC4	8761	NM_003819	6552335	GGAGAGAAUUAGUCGAUAU
D04	M-012550-02	D-012550-19	TCOF1	6949	NM_001008657	57164978	GCAGAGCAGCAGCGAGGAA
D04	M-012550-02	D-012550-21	TCOF1	6949	NM_001008657	57164978	GAGGAGGACUCAAGAAGCA
D04	M-012550-02	D-012550-22	TCOF1	6949	NM_001008657	57164978	GCAAAUACUACGUUGGUCU
D04	M-012550-02	D-012550-23	TCOF1	6949	NM_001008657	57164978	CCUCAGAGCUUGGUCGGAA
D05	M-026599-03	D-026599-01	SF3B2	10992	NM_006842	55749530	GAGAGAAAGUUCGGCCUAA
D05	M-026599-03	D-026599-03	SF3B2	10992	NM_006842	55749530	UGACAUCGACUACCAGAAA
D05	M-026599-03	D-026599-04	SF3B2	10992	NM_006842	55749530	GGACAAAGCCGCUCCACCU
D05	M-026599-03	D-026599-18	SF3B2	10992	NM_006842	55749530	AAGCGUAGGAACCGAAAGA
D06	M-004074-04	D-004074-01	PRPF4B	8899	NM_003913	89276755	GGAAAUAGGUCUAGUACUA
D06	M-004074-04	D-004074-06	PRPF4B	8899	NM_003913	89276755	GCGAGUAGCUGCUGAUGUU
D06	M-004074-04	D-004074-08	PRPF4B	8899	NM_003913	89276755	GUAGAAACCUCGUUAUUAA
D06	M-004074-04	D-004074-09	PRPF4B	8899	NM_003913	89276755	AGAAGUAGAUCUCCCAUUA
D07	M-019480-01	D-019480-01	TRA2A	29896	NM_013293	110227858	GAAGAAUUCGGGUGGAUUA
D07	M-019480-01	D-019480-02	TRA2A	29896	NM_013293	110227858	CGAGAUUCUUACUAUGAUA
D07	M-019480-01	D-019480-03	TRA2A	29896	NM_013293	110227858	CGUAGUCCAUCAAGGGUUU
D07	M-019480-01	D-019480-04	TRA2A	29896	NM_013293	110227858	UGGGCGAUCUCGAGGAUUU
D08	M-020392-00	D-020392-01	GNL2	29889	NM_013285	7019418	GAUCGAAUCCGGCCUCAUA
D08	M-020392-00	D-020392-02	GNL2	29889	NM_013285	7019418	AAACAAAGGUCUGGCAGUA
D08	M-020392-00	D-020392-03	GNL2	29889	NM_013285	7019418	CAACGUGGCUCCCAUUGCA
D08	M-020392-00	D-020392-04	GNL2	29889	NM_013285	7019418	GAACGGAGGCGAGCAGUAC

Appendix A1: List of siRNA used in siRNA array in 96 well format (plate 1)							
Well	Pool Catalog Number	Duplex Catalog Number	Gene Symbol	GENE ID	Gene Accession	GI Number	Sequence
D09	M-014065-01	D-014065-01	BOP1	23246	NM_015201	40353770	GGACGGAGCCCUUGAUGAC
D09	M-014065-01	D-014065-02	BOP1	23246	NM_015201	40353770	UCUCAGGCCUGGAAGAUUC
D09	M-014065-01	D-014065-04	BOP1	23246	NM_015201	40353770	GCUGCAGAGUGGCCAGUUU
D09	M-014065-01	D-014065-17	BOP1	23246	NM_015201	40353770	ACGGACAGGUGCAGCGAGU
D10	M-020373-00	D-020373-01	SAFB2	9667	NM_014649	7661935	CAAGAGAUGUGUUAAAGGA
D10	M-020373-00	D-020373-02	SAFB2	9667	NM_014649	7661935	CAAAGUAACUCCGGACAUU
D10	M-020373-00	D-020373-03	SAFB2	9667	NM_014649	7661935	GGACGGUCGUGAUGGAUAA
D10	M-020373-00	D-020373-04	SAFB2	9667	NM_014649	7661935	AAACUGAAGUGGCGAAUAG
D11	M-029652-01	D-029652-01	PDCD11	22984	NM_014976	70980548	GAACAAAGGUGCUAAACUA
D11	M-029652-01	D-029652-02	PDCD11	22984	NM_014976	70980548	GAACAAACCCGGAGACGAA
D11	M-029652-01	D-029652-03	PDCD11	22984	NM_014976	70980548	GGUGAAGGUUGUCGUAUUG
D11	M-029652-01	D-029652-04	PDCD11	22984	NM_014976	70980548	UCAAGUAUCUCCCAAUAAG
D12	M-020913-00	D-020913-01	BMS1	9790	NM_014753	41281482	GAAGAAAGCUCCUCACUCA
D12	M-020913-00	D-020913-02	BMS1	9790	NM_014753	41281482	CCAAACCUCCGAAAGCUUA
D12	M-020913-00	D-020913-03	BMS1	9790	NM_014753	41281482	UAUCAGAGAUUGCUUCGUG
D12	M-020913-00	D-020913-04	BMS1	9790	NM_014753	41281482	GAAGGGCAUUUCAGGAUCA
E01	M-014077-00	D-014077-01	RRS1	23212	NM_015169	46094056	UGACUAGGGCCACCAAUAA
E01	M-014077-00	D-014077-02	RRS1	23212	NM_015169	46094056	AAGAAUGGCUGAUUGAGGU
E01	M-014077-00	D-014077-03	RRS1	23212	NM_015169	46094056	GGGCAUCCGUCCCAAGAAG
E01	M-014077-00	D-014077-04	RRS1	23212	NM_015169	46094056	CUACCGGACACCAGAGUAA
E02	M-022651-01	D-022651-01	WDR43	23160	NM_015131	157743244	GUACAUGACCGGUUACUUA
E02	M-022651-01	D-022651-02	WDR43	23160	NM_015131	157743244	CCUCAUAUGUGUUUAGUAA
E02	M-022651-01	D-022651-03	WDR43	23160	NM_015131	157743244	CGAUGAACCUGUCUAUAUU
E02	M-022651-01	D-022651-04	WDR43	23160	NM_015131	157743244	ACGAAUAGCUUUCCAGUUC
E03	M-019927-00	D-019927-01	PWP2	5822	NM_005049	48762925	GAAGUUCGCUUACCGGUUU
E03	M-019927-00	D-019927-02	PWP2	5822	NM_005049	48762925	GGAAGAAGCGGGAGUUCAA
E03	M-019927-00	D-019927-03	PWP2	5822	NM_005049	48762925	GCAGUACGCACUAGCAGUU
E03	M-019927-00	D-019927-04	PWP2	5822	NM_005049	48762925	GGCAUGACCUCAAGACUGG
E04	M-020085-01	D-020085-01	SF3B3	23450	NM_012426	54112120	GGACAUAGGGUAAUUGUAU
E04	M-020085-01	D-020085-02	SF3B3	23450	NM_012426	54112120	GAUAUCCGCUGUCCAAUUC
E04	M-020085-01	D-020085-03	SF3B3	23450	NM_012426	54112120	UAGCUGAUCUGGCCAAUGA
E04	M-020085-01	D-020085-04	SF3B3	23450	NM_012426	54112120	GCCAAGGACCUGAUACUAA
E05	M-003773-04	D-003773-02	ELAVL1	1994	NM_001419	38201713	GCAAUUACCAGUUUCAAUG
E05	M-003773-04	D-003773-04	ELAVL1	1994	NM_001419	38201713	UCAAAGACGCCAACUUGUA
E05	M-003773-04	D-003773-05	ELAVL1	1994	NM_001419	38201713	CAAAGACGCCAACUUGUAC
E05	M-003773-04	D-003773-21	ELAVL1	1994	NM_001419	38201713	CGACUCAAUUGUCCCGAUA
E06	M-032789-01	D-032789-17	HNRNPUL2	221092	NM_001079559	118601080	CGGACAAAUCGCCGAAACA
E06	M-032789-01	D-032789-18	HNRNPUL2	221092	NM_001079559	118601080	GUAAAGAGACAGCGGGAUG
E06	M-032789-01	D-032789-19	HNRNPUL2	221092	NM_001079559	118601080	CGGGGUAAAUGGUGGCGAA
E06	M-032789-01	D-032789-20	HNRNPUL2	221092	NM_001079559	118601080	CAGAUUGCUUCCCGGACAA
E07	M-027238-01	D-027238-01	RPL7L1	285855	NM_198486	50053871	CGAAAGGAUUGACGGCGUG
E07	M-027238-01	D-027238-02	RPL7L1	285855	NM_198486	50053871	UGACAAGGUGCGUCUCAGA
E07	M-027238-01	D-027238-03	RPL7L1	285855	NM_198486	50053871	AUACAGUGAUUGAGGAGCA

Appendix A1: List of siRNA used in siRNA array in 96 well format (plate 1)							
Well	Pool Catalog Number	Duplex Catalog Number	Gene Symbol	GENE ID	Gene Accession	GI Number	Sequence
E07	M-027238-01	D-027238-04	RPL7L1	285855	NM_198486	50053871	GCGUAUAGUGGAACCUUAU
E09	M-017196-00	D-017196-01	DHX30	22907	NM_014966	20336289	GGGCCUAUCCCGCUCUUUA
E09	M-017196-00	D-017196-02	DHX30	22907	NM_014966	20336289	GACCAUAGAUGUUACCGAC
E09	M-017196-00	D-017196-03	DHX30	22907	NM_014966	20336289	GAACAACGAACCGCUUACA
E09	M-017196-00	D-017196-04	DHX30	22907	NM_014966	20336289	GCGUGGAGGUAGAAGGCUA
E10	M-017449-00	D-017449-01	ZC3HAV1	56829	NM_020119	33946332	GCACAUGGAUUCAGUAUGG
E10	M-017449-00	D-017449-02	ZC3HAV1	56829	NM_020119	33946332	GCAAGCACAUGCAGAAGAA
E10	M-017449-00	D-017449-03	ZC3HAV1	56829	NM_020119	33946332	GAACAAAGAGGAAUUAGCA
E10	M-017449-00	D-017449-04	ZC3HAV1	56829	NM_020119	33946332	CAAAUAUUCUCAUGAGGUU
E11	M-019232-00	D-019232-01	HIST2H2AB	317772	NM_175065	29171728	UCACAAGCCUGGCAAGAAC
E11	M-019232-00	D-019232-02	HIST2H2AB	317772	NM_175065	29171728	GCUGUCCUGUUGCCCAAGA
E11	M-019232-00	D-019232-03	HIST2H2AB	317772	NM_175065	29171728	CCGCGGAAAUUCUGGAGCU
E11	M-019232-00	D-019232-04	HIST2H2AB	317772	NM_175065	29171728	CCGUGAGGAAUGACGAAGA
E12	M-014795-00	D-014795-01	WDR75	84128	NM_032168	29789282	ACACAAGGGUUUAUUCUUA
E12	M-014795-00	D-014795-02	WDR75	84128	NM_032168	29789282	GAGAAGACAUUAUACAUCA
E12	M-014795-00	D-014795-03	WDR75	84128	NM_032168	29789282	GAACAGCCCACCUUGGUUA
E12	M-014795-00	D-014795-04	WDR75	84128	NM_032168	29789282	GAGCUACUAUUGAACAUAU
F01	M-013367-00	D-013367-01	FTSJ3	117246	NM_017647	17017990	GCCAAGGGAUGAUAUCUAU
F01	M-013367-00	D-013367-02	FTSJ3	117246	NM_017647	17017990	GACCGUUACUGAAUUGGUU
F01	M-013367-00	D-013367-03	FTSJ3	117246	NM_017647	17017990	GGCAAGAGCCGACGAGACA
F01	M-013367-00	D-013367-04	FTSJ3	117246	NM_017647	17017990	ACGUUUGGCUUGUGACUUU
F02	M-017004-01	D-017004-01	WDR36	134430	NM_139281	71164895	GAUGGUCGUUGGUUAAUAA
F02	M-017004-01	D-017004-02	WDR36	134430	NM_139281	71164895	GCAAGAGUUUCCACACCUA
F02	M-017004-01	D-017004-03	WDR36	134430	NM_139281	71164895	GCUCACAAGGGAUCUGUUA
F02	M-017004-01	D-017004-04	WDR36	134430	NM_139281	71164895	GGUAAGCUAUCUUGCUCAA
F03	M-017128-01	D-017128-01	DDX54	79039	NM_024072	51094100	GCACGAAAAUCCCGACAUA
F03	M-017128-01	D-017128-02	DDX54	79039	NM_024072	51094100	GAAUGCACCUCGGAUGUGG
F03	M-017128-01	D-017128-03	DDX54	79039	NM_024072	51094100	CGAAGCACCACGCCGAGUA
F03	M-017128-01	D-017128-04	DDX54	79039	NM_024072	51094100	CCACUCUCAUUGUGACUGA
F04	M-015372-02	D-015372-01	BRIX1	55299	NM_018321	55770899	GGACCAACUUUAUAUGAAA
F04	M-015372-02	D-015372-03	BRIX1	55299	NM_018321	55770899	GUAAGGAUAAGCUAUUUGU
F04	M-015372-02	D-015372-04	BRIX1	55299	NM_018321	55770899	GCAUCGGCGUGUCAUAAGA
F04	M-015372-02	D-015372-17	BRIX1	55299	NM_018321	55770899	CUUUAGUACACCACGGUAU
F05	M-014796-01	D-014796-01	UTP15	84135	NM_032175	50980308	CAAAGAAGCACCUAGAAUU
F05	M-014796-01	D-014796-03	UTP15	84135	NM_032175	50980308	GAGGACAAUUGCUAGUAUC
F05	M-014796-01	D-014796-04	UTP15	84135	NM_032175	50980308	GGAAUGACCAAUGGAAUAC
F05	M-014796-01	D-014796-17	UTP15	84135	NM_032175	50980308	GAAUAAUUAUGGCCGGAAA
F06	M-012167-00	D-012167-01	H1FX	8971	NM_006026	20336759	CCAAGAAGGUUCCGUGGUU
F06	M-012167-00	D-012167-02	H1FX	8971	NM_006026	20336759	GCUCGUCGCUGGCCAAGAU
F06	M-012167-00	D-012167-03	H1FX	8971	NM_006026	20336759	GGAAUGGCCAAGAAGGUGA
F06	M-012167-00	D-012167-04	H1FX	8971	NM_006026	20336759	GCGCCAACGGUUCCUUCAA
F07	M-008930-01	D-008930-01	TAF15	8148	NM_003487	21327699	GAACUUUGCUCGAAGGAAU
F07	M-008930-01	D-008930-03	TAF15	8148	NM_003487	21327699	GAUGAGCAGUCAAAUUAUG
F07	M-008930-01	D-008930-04	TAF15	8148	NM_003487	21327699	CAAAUAAGAAGACCGGAAA
F07	M-008930-01	D-008930-05	TAF15	8148	NM_003487	21327699	AUGAUGAGCAGUCAAAUUA

Appendix A1: List of siRNA used in siRNA array in 96 well format (plate 1)							
Well	Pool Catalog Number	Duplex Catalog Number	Gene Symbol	GENE ID	Gene Accession	GI Number	Sequence
F08	M-013450-01	D-013450-01	DDX17	10521	NM_001098505	148613857	CUACCAAUAUGAUAGGUUA
F08	M-013450-01	D-013450-03	DDX17	10521	NM_001098505	148613857	CGAUAGAGCUGGUUAUGCU
F08	M-013450-01	D-013450-04	DDX17	10521	NM_001098505	148613857	UAUCGGGAUCGUAGUGAAA
F08	M-013450-01	D-013450-17	DDX17	10521	NM_001098505	148613857	CAAGGAUGGUGGCCGGAGA
F09	M-011435-00	D-011435-01	HIST1H2AC	8334	NM_003512	21396481	ACGAGGAGCUCAACAAACU
F09	M-011435-00	D-011435-02	HIST1H2AC	8334	NM_003512	21396481	GUAAAGGCAACUACGCAGA
F09	M-011435-00	D-011435-03	HIST1H2AC	8334	NM_003512	21396481	CCGUAAAGGCAACUACGCA
F09	M-011435-00	D-011435-04	HIST1H2AC	8334	NM_003512	21396481	AGCUCGCGCCAAAGCGAAA
F11	M-015011-01	D-015011-02	CIRH1A	84916	NM_032830	14249535	GGUCAUGAGUCUCGGGCUA
F11	M-015011-01	D-015011-17	CIRH1A	84916	NM_032830	14249535	AAGCAGUGGGUGCGGACAA
F11	M-015011-01	D-015011-18	CIRH1A	84916	NM_032830	14249535	AAUUUAAGGUCCAUCGAGU
F11	M-015011-01	D-015011-19	CIRH1A	84916	NM_032830	14249535	CAGAUUGGCUGUUUCACGA
F12	M-015116-00	D-015116-01	IMP4	92856	NM_033416	15529981	GAACCGAGGUCGACAUGAA
F12	M-015116-00	D-015116-02	IMP4	92856	NM_033416	15529981	UCUCUGACAUCCUCCGAUA
F12	M-015116-00	D-015116-03	IMP4	92856	NM_033416	15529981	AAACCAGGACGACUACAUA
F12	M-015116-00	D-015116-04	IMP4	92856	NM_033416	15529981	GCAAUGUGGUCAUGCGGCA
G01	M-013635-00	D-013635-01	DDX27	55661	NM_017895	19743936	GCAGAUACACUCAAAGUAA
G01	M-013635-00	D-013635-02	DDX27	55661	NM_017895	19743936	GACCUCGGCUUAAUCGGAA
G01	M-013635-00	D-013635-03	DDX27	55661	NM_017895	19743936	GAGAUCAUCCGAAUGUGUU
G01	M-013635-00	D-013635-04	DDX27	55661	NM_017895	19743936	GAUCCGGCCUAAUCGUGAA
G02	D-001206-13	D-001210-01	siGENOME Non-targeting Control	0		0	UAGCGACUAAACACAUCAA
G02	D-001206-13	D-001210-02	siGENOME Non-targeting Control	0		0	UAAGGCUAUGAAGAGAUAC
G02	D-001206-13	D-001210-03	siGENOME Non-targeting Control	0		0	AUGUAUUGGCCUGUAUUAG
G02	D-001206-13	D-001210-04	siGENOME Non-targeting Control	0		0	AUGAACGUGAAUUGCUCAA
G03	M-029452-02	D-029452-01	FUBP3	8939	NM_003934	100816391	GUACAUCAAAGGACGGUAA
G03	M-029452-02	D-029452-02	FUBP3	8939	NM_003934	100816391	GUGGACCGCUGUCGAAAUG
G03	M-029452-02	D-029452-03	FUBP3	8939	NM_003934	100816391	UAAGUGUGGCCUCGUCAUA
G03	M-029452-02	D-029452-04	FUBP3	8939	NM_003934	100816391	UACUAGAGAUUAUCCGAGA
G04	M-019266-00	D-019266-01	ZFR	51663	NM_016107	38202203	GUAAUAAGCUGCAGUCAAC
G04	M-019266-00	D-019266-02	ZFR	51663	NM_016107	38202203	CACCACAGAUUCACUAUUG
G04	M-019266-00	D-019266-03	ZFR	51663	NM_016107	38202203	CAAAUGAGCCAACGUUUUA
G04	M-019266-00	D-019266-04	ZFR	51663	NM_016107	38202203	UCGGUUCCAUUGUAAAUUA
G05	M-020144-01	D-020144-01	RBM14	10432	NM_006328	50593004	UAGCCGAGCUCUCUGAUUA
G05	M-020144-01	D-020144-02	RBM14	10432	NM_006328	50593004	CCAGGCAGCUUCAUAUAAU
G05	M-020144-01	D-020144-03	RBM14	10432	NM_006328	50593004	GAGCUGCGCCGUCAUGAAA
G05	M-020144-01	D-020144-04	RBM14	10432	NM_006328	50593004	CUACGACGAUCCCUACAAA
G06	M-010854-00	D-010854-01	RBM15	64783	NM_022768	22095383	GGACAGAGGUGAUCGAGAU
G06	M-010854-00	D-010854-02	RBM15	64783	NM_022768	22095383	GAAGAUAGAAGCUGUGUAU
G06	M-010854-00	D-010854-03	RBM15	64783	NM_022768	22095383	GGACACCACCCUUACUAUA

Appendix A1: List of siRNA used in siRNA array in 96 well format (plate 1)							
Well	Pool Catalog Number	Duplex Catalog Number	Gene Symbol	GENE ID	Gene Accession	GI Number	Sequence
G06	M-010854-00	D-010854-04	RBM15	64783	NM_022768	22095383	GGUGAUAGUUGGGCAUAUA
G07	M-013483-01	D-013483-01	HNRNPAB	3182	NM_004499	55956920	GGAAGCAAGUGUGAGAUCA
G07	M-013483-01	D-013483-02	HNRNPAB	3182	NM_004499	55956920	GGUCGUUGACUGUACAAUA
G07	M-013483-01	D-013483-03	HNRNPAB	3182	NM_004499	55956920	GGUUUAUCCUGUUCAAAGA
G07	M-013483-01	D-013483-04	HNRNPAB	3182	NM_004499	55956920	GAUCCAAAGUUGAACAAAA
G08	M-019834-00	D-019834-01	EBNA1BP2	10969	NM_006824	5803110	GGAGAGCUAUGAUGAUGUA
G08	M-019834-00	D-019834-02	EBNA1BP2	10969	NM_006824	5803110	CAAGAGGCCUGGCAAGAAA
G08	M-019834-00	D-019834-03	EBNA1BP2	10969	NM_006824	5803110	CCAGAAAGCUGUUGAUCCA
G08	M-019834-00	D-019834-04	EBNA1BP2	10969	NM_006824	5803110	GAGAAAGCCCAUAUGAUGA
G09	M-020341-01	D-020341-01	MYBBP1A	10514	NM_001105538	157694493	UAGCAAAGGUCACCGAGAA
G09	M-020341-01	D-020341-02	MYBBP1A	10514	NM_001105538	157694493	UCGCAGACCUCCUGUUGAA
G09	M-020341-01	D-020341-03	MYBBP1A	10514	NM_001105538	157694493	CGACCGCUAUGGCCUAUUG
G09	M-020341-01	D-020341-04	MYBBP1A	10514	NM_001105538	157694493	CAACAGAAGCUCAGAGAGU
G10	M-006483-02	D-006483-01	H2AFJ	55766	NM_177925	145301619	GGAAGUGUCUGCGGCCAUA
G10	M-006483-02	D-006483-02	H2AFJ	55766	NM_177925	145301619	GAAGAUACCGUCGGAUCGA
G10	M-006483-02	D-006483-05	H2AFJ	55766	NM_177925	145301619	UAAACAAGCUGCUGGGCAA
G10	M-006483-02	D-006483-06	H2AFJ	55766	NM_177925	145301619	UGGAGUACCUUACGGCGGA
G11	D-001206-14	D-001210-02	siGENOME Non-targeting Control	0		0	UAAGGCUAUGAAGAGAUAC
G11	D-001206-14	D-001210-03	siGENOME Non-targeting Control	0		0	AUGUAUUGGCCUGUAUUAG
G11	D-001206-14	D-001210-04	siGENOME Non-targeting Control	0		0	AUGAACGUGAAUUGCUCAA
G11	D-001206-14	D-001210-05	siGENOME Non-targeting Control	0		0	UGGUUUACAUGUCGACUAA
G12	M-016395-01	D-016395-01	UTP14A	10813	NM_006649	21361347	GAAAUGCUCUGUAGAUUGA
G12	M-016395-01	D-016395-02	UTP14A	10813	NM_006649	21361347	GCAACUGAGUAGAGUCAAA
G12	M-016395-01	D-016395-03	UTP14A	10813	NM_006649	21361347	GGUGCUGUCUGAAUUGAGA
G12	M-016395-01	D-016395-17	UTP14A	10813	NM_006649	21361347	AGUUUGAGCAGCUGCGGAA
H02	D-001206-13	D-001210-01	siGENOME Non-targeting Control	0		0	UAGCGACUAAACACAUCAA
H02	D-001206-13	D-001210-02	siGENOME Non-targeting Control	0		0	UAAGGCUAUGAAGAGAUAC
H02	D-001206-13	D-001210-03	siGENOME Non-targeting Control	0		0	AUGUAUUGGCCUGUAUUAG
H02	D-001206-13	D-001210-04	siGENOME Non-targeting Control	0		0	AUGAACGUGAAUUGCUCAA
H03	M-016319-00	D-016319-01	GNL3	26354	NM_014366	37497106	GGACAUACAUGAAGAAUUG
H03	M-016319-00	D-016319-02	GNL3	26354	NM_014366	37497106	GUGGACAGGUGCCUCAUUA
H03	M-016319-00	D-016319-03	GNL3	26354	NM_014366	37497106	CCAGGAAACUGUUGAUGAA
H03	M-016319-00	D-016319-04	GNL3	26354	NM_014366	37497106	CAUCGUAUCUCCACUUAAU
H04	M-019588-01	D-019588-01	RBM4	5936	NM_002896	93277121	GAGCAGUGCGUACGCCUUA
H04	M-019588-01	D-019588-02	RBM4	5936	NM_002896	93277121	GCAGCUGCCUCCGUGUAUA

Appendix A1: List of siRNA used in siRNA array in 96 well format (plate 1)							
Well	Pool Catalog Number	Duplex Catalog Number	Gene Symbol	GENE ID	Gene Accession	GI Number	Sequence
H04	M-019588-01	D-019588-04	RBM4	5936	NM_002896	93277121	GUCCAAAGAGUGUCCGAUA
H04	M-019588-01	D-019588-13	RBM4	5936	NM_002896	93277121	GGGCUGAAAUUCCGAGCUG
H05	M-018620-00	D-018620-01	MAK16	84549	NM_032509	31543090	CGACACAAAUGUAAGCAGA
H05	M-018620-00	D-018620-02	MAK16	84549	NM_032509	31543090	CAAGAUCACCCAAUACCUA
H05	M-018620-00	D-018620-03	MAK16	84549	NM_032509	31543090	GCAAAUAGUCAGUAUGCCA
H05	M-018620-00	D-018620-04	MAK16	84549	NM_032509	31543090	GGGAUACACUAGGAAACAA
H06	M-016687-01	D-016687-01	NIFK	84365	NM_032390	37059742	GAAGAUGUCGAGUUUCAAA
H06	M-016687-01	D-016687-02	NIFK	84365	NM_032390	37059742	CCACCUACCUAACCUACUU
H06	M-016687-01	D-016687-04	NIFK	84365	NM_032390	37059742	CCAAUCCUGUCGCUUAAUC
H06	M-016687-01	D-016687-17	NIFK	84365	NM_032390	37059742	CGGUAUAAUCGGAAUCGGA
H07	M-012467-01	D-012467-01	GTPBP4	23560	NM_012341	55953086	GAUAGACACGUGUUUGAUA
H07	M-012467-01	D-012467-02	GTPBP4	23560	NM_012341	55953086	CGAAAGACUCCAACCGUUA
H07	M-012467-01	D-012467-03	GTPBP4	23560	NM_012341	55953086	UACCAAAUACAUCGCAUUA
H07	M-012467-01	D-012467-04	GTPBP4	23560	NM_012341	55953086	UGAUGAAUAUUCUCUACGA
H08	M-010397-01	D-010397-01	DDX24	57062	NM_020414	14251213	GAGAUGACAUGGUUUGUGA
H08	M-010397-01	D-010397-03	DDX24	57062	NM_020414	14251213	UCAGAAACCUGGAGCAGUU
H08	M-010397-01	D-010397-04	DDX24	57062	NM_020414	14251213	GAAUCAAAGUUGUGGGAAA
H08	M-010397-01	D-010397-17	DDX24	57062	NM_020414	14251213	GCGAAUCCGUUUAGCUCGA
H09	M-014402-00	D-014402-01	NAT10	55226	NM_024662	13399321	GGAAUAUGGUGGACUAUCA
H09	M-014402-00	D-014402-02	NAT10	55226	NM_024662	13399321	UAAGAAGUGUCUCGUCAUU
H09	M-014402-00	D-014402-03	NAT10	55226	NM_024662	13399321	CAACAUCACUCGGAUAGUC
H09	M-014402-00	D-014402-04	NAT10	55226	NM_024662	13399321	GGAAGGGUCGUUCGCAUUG
H10	M-017622-01	D-017622-01	XRN2	22803	NM_012255	51702528	GAACCGAACUUUACCAUUA
H10	M-017622-01	D-017622-02	XRN2	22803	NM_012255	51702528	GAAGUGGUAUUAUCCAUUU
H10	M-017622-01	D-017622-03	XRN2	22803	NM_012255	51702528	GAACAAAUUUGAUGUGGAU
H10	M-017622-01	D-017622-04	XRN2	22803	NM_012255	51702528	CUAAAUGCCUUCGCUAUUA
H11	D-001206-14	D-001210-02	siGENOME Non-targeting Control	0		0	UAAGGCUAUGAAGAGAUAC
H11	D-001206-14	D-001210-03	siGENOME Non-targeting Control	0		0	AUGUAUUGGCCUGUAUUAG
H11	D-001206-14	D-001210-04	siGENOME Non-targeting Control	0		0	AUGAACGUGAAUUGCUCAA
H11	D-001206-14	D-001210-05	siGENOME Non-targeting Control	0		0	UGGUUUACAUGUCGACUAA

Appendix A1: List of siRNA used in siRNA array in 96 well format (plate 2)							
LP_8103_RTF (Plate 2), G-CUSTOM-147092							
Well	Pool Catalog Number	Duplex Catalog Number	Gene Symbol	GENE ID	Gene Accession	GI Number	Sequence
A09	M-015939-02	D-015939-01	HEATR1	55127	NM_018072	73695474	UAAAGAAGCUUGAAAGUGU
A09	M-015939-02	D-015939-02	HEATR1	55127	NM_018072	73695474	GCUCAGAAGUCCUCAGAUA
A09	M-015939-02	D-015939-03	HEATR1	55127	NM_018072	73695474	CCGCUGACAUAUUAAUUAA
A09	M-015939-02	D-015939-04	HEATR1	55127	NM_018072	73695474	UGGGUUAAGUUGCUUGAUA
A10	M-017285-00	D-017285-01	NOL6	65083	NM_022917	39777587	GGACGGAGCCAUUCGGGAA
A10	M-017285-00	D-017285-02	NOL6	65083	NM_022917	39777587	GGGAUCAGUUUAUGUCUCA
A10	M-017285-00	D-017285-03	NOL6	65083	NM_022917	39777587	UGAGAAGUGUCUUGCAGUU
A10	M-017285-00	D-017285-04	NOL6	65083	NM_022917	39777587	CUUAAUCGCCUUCGGGAGA
A11	M-024715-00	D-024715-01	RPF2	84154	NM_032194	39930468	GAAGCGACCUGCAGAAAGG
A11	M-024715-00	D-024715-02	RPF2	84154	NM_032194	39930468	UAACAGAAGACCACGAGAA
A11	M-024715-00	D-024715-03	RPF2	84154	NM_032194	39930468	GGAUUCAUAUGCAGAAGCA
A11	M-024715-00	D-024715-04	RPF2	84154	NM_032194	39930468	CGAUGUAACAGAAGAUUAU
B09	M-031985-01	D-031985-01	SCAF1	58506	NM_021228	32698749	GGAAGGCCGUCCACAAGAU
B09	M-031985-01	D-031985-03	SCAF1	58506	NM_021228	32698749	AAAGAUGGCUCUCGGUGUC
B09	M-031985-01	D-031985-04	SCAF1	58506	NM_021228	32698749	GGCAGAGGCUUGUCGGGAA
B09	M-031985-01	D-031985-17	SCAF1	58506	NM_021228	32698749	UUGAAACUCUGGACGUAUU
B10	M-031267-01	D-031267-01	RPF1	80135	NM_025065	145275209	UCAACGGGAUUACAUAUUC
B10	M-031267-01	D-031267-02	RPF1	80135	NM_025065	145275209	GCGAUAAGGCUCCACCAAA
B10	M-031267-01	D-031267-03	RPF1	80135	NM_025065	145275209	CAAACAGCGGCGACACUUA
B10	M-031267-01	D-031267-04	RPF1	80135	NM_025065	145275209	CAGACCUGAUUGUUAUUAA
B11	M-013451-00	D-013451-01	DDX18	8886	NM_006773	38327633	GGGCAUGCCUUGCUCAUUU
B11	M-013451-00	D-013451-02	DDX18	8886	NM_006773	38327633	GAAAUACCACUAUGAGUUG
B11	M-013451-00	D-013451-03	DDX18	8886	NM_006773	38327633	GAAGUCGACUGGAUUGUUC
B11	M-013451-00	D-013451-04	DDX18	8886	NM_006773	38327633	GAUCUGAACGUCAACAGUA
C09	M-021145-00	D-021145-01	RBM28	55131	NM_018077	8922387	CGAGAAGGCUUGAUUCGUG
C09	M-021145-00	D-021145-02	RBM28	55131	NM_018077	8922387	UAAGGCAUGUCGAGGCUUU
C09	M-021145-00	D-021145-03	RBM28	55131	NM_018077	8922387	GGCCUGACCUUAUUUGUGG
C09	M-021145-00	D-021145-04	RBM28	55131	NM_018077	8922387	GCGAUAGUAUUGAUGAUGG
C10	M-014434-01	D-014434-01	SLTM	79811	NM_001013843	62244003	UAAGGAAGCUGAACGGAUU
C10	M-014434-01	D-014434-02	SLTM	79811	NM_001013843	62244003	CGAGAACGCAUUAGAAUAA
C10	M-014434-01	D-014434-03	SLTM	79811	NM_001013843	62244003	GAACGGGAACGCUUACAGA
C10	M-014434-01	D-014434-04	SLTM	79811	NM_001013843	62244003	GGAACGCAUUCGUAUUGAA
C11	M-010579-01	D-010579-01	UTP6	55813	NM_018428	49574528	GAAAGACGAUGUUCAACUU
C11	M-010579-01	D-010579-02	UTP6	55813	NM_018428	49574528	GAACUGAAUUGUUUAGAGA
C11	M-010579-01	D-010579-04	UTP6	55813	NM_018428	49574528	GAAAGAACCAUGACUGUAU
C11	M-010579-01	D-010579-17	UTP6	55813	NM_018428	49574528	GAUAAUUCAGGAACGCAUA
D09	M-013919-00	D-013919-01	RAI14	26064	NM_015577	13470085	GCUGAUAGCUUAUUGGAUA
D09	M-013919-00	D-013919-02	RAI14	26064	NM_015577	13470085	GGACACAGCGCCUUACAUC
D09	M-013919-00	D-013919-03	RAI14	26064	NM_015577	13470085	GGUCAUAUCAGUUUACAGA
D09	M-013919-00	D-013919-04	RAI14	26064	NM_015577	13470085	GCAGAACUGGUAUGCUUAA
D10	M-004668-02	D-004668-01	PRPF19	27339	NM_014502	34222313	CAGAAGAGCUCAGCAAAUA
D10	M-004668-02	D-004668-02	PRPF19	27339	NM_014502	34222313	GAUAACAACUUUGAGGUAA
D10	M-004668-02	D-004668-04	PRPF19	27339	NM_014502	34222313	GAUCUGCGCAAGCUUAAGA
D10	M-004668-02	D-004668-17	PRPF19	27339	NM_014502	34222313	CUAACGAAGUGCCGGAGCA
D11	M-012328-01	D-012328-01	WDR3	10885	NM_006784	5803220	GCAACUGGCUCCGCUGAUA
D11	M-012328-01	D-012328-03	WDR3	10885	NM_006784	5803220	CAAGGUGACAGUUACUUUA
D11	M-012328-01	D-012328-17	WDR3	10885	NM_006784	5803220	CUAUUGAGUUGUACCGAGA
D11	M-012328-01	D-012328-18	WDR3	10885	NM_006784	5803220	AAGCAUUGUUUCUACGAGA

Appendix A1: List of siRNA used in siRNA array in 96 well format (plate 2)							
Well	Pool Catalog Number	Duplex Catalog Number	Gene Symbol	GENE ID	Gene Accession	GI Number	Sequence
E09	M-017973-00	D-017973-01	NOP58	51602	NM_015934	34222329	GGAAUUAGUUGGAGCACGG
E09	M-017973-00	D-017973-02	NOP58	51602	NM_015934	34222329	GAUUGAAGUUUAGCGCUGA
E09	M-017973-00	D-017973-03	NOP58	51602	NM_015934	34222329	ACAACUACAUUAUGCGAUG
E09	M-017973-00	D-017973-04	NOP58	51602	NM_015934	34222329	CCUCAAAUCUAGACGGGAU
E10	M-016782-02	D-016782-01	RRP7A	27341	NM_015703	62751922	CUACGCAGCUAUUCCAAUC
E10	M-016782-02	D-016782-02	RRP7A	27341	NM_015703	62751922	CCAAAGGAGUCAAGGUCGA
E10	M-016782-02	D-016782-03	RRP7A	27341	NM_015703	62751922	ACACGUUCAUGGAGGCAUA
E10	M-016782-02	D-016782-18	RRP7A	27341	NM_015703	62751922	AGACGGAAGCGCAGCCGAA
E11	M-020991-01	D-020991-01	UTP18	51096	NM_016001	118344455	GGAAGUGCCUUAACAGAUU
E11	M-020991-01	D-020991-02	UTP18	51096	NM_016001	118344455	GCAAGGUUCUUUAUGUCUA
E11	M-020991-01	D-020991-03	UTP18	51096	NM_016001	118344455	GAACUGAUUGGAAGCAUGA
E11	M-020991-01	D-020991-04	UTP18	51096	NM_016001	118344455	GAACUUGGUUACAGGUGUU
F09	M-020513-01	D-020513-01	DNTTIP2	30836	NM_014597	54633314	UAUGAAAGCUCCAGAAAUG
F09	M-020513-01	D-020513-02	DNTTIP2	30836	NM_014597	54633314	GAAUGAAGAGGAUACUUUA
F09	M-020513-01	D-020513-03	DNTTIP2	30836	NM_014597	54633314	ACACUAGCCUUCAACAGUU
F09	M-020513-01	D-020513-04	DNTTIP2	30836	NM_014597	54633314	UUGGGUGGUUUGUAUAUUA
F10	M-020867-01	D-020867-01	HP1BP3	50809	NM_016287	125991232	CCACUGCUCUGAAGAAGUA
F10	M-020867-01	D-020867-02	HP1BP3	50809	NM_016287	125991232	CAAGUUAGGUGAGAAGGUA
F10	M-020867-01	D-020867-03	HP1BP3	50809	NM_016287	125991232	GUGGAAGCCUGAUGGAAUA
F10	M-020867-01	D-020867-04	HP1BP3	50809	NM_016287	125991232	GUCCAAACCUGCACCUAAA
G09	M-005272-01	D-005272-01	NUMA1	4926	NM_006185	71361681	GGGAACAGUUUGAAUAUAA
G09	M-005272-01	D-005272-02	NUMA1	4926	NM_006185	71361681	GCAAGAGGCUGAGAGGAAA
G09	M-005272-01	D-005272-03	NUMA1	4926	NM_006185	71361681	GCAGUAGCCUGAAGCAGAA
G09	M-005272-01	D-005272-04	NUMA1	4926	NM_006185	71361681	GAACCAGCCUCACCUAUCU
G10	M-007182-01	D-007182-01	TRIP12	9320	NM_004238	10863902	GAACUGACAUCUCUGAUUU
G10	M-007182-01	D-007182-02	TRIP12	9320	NM_004238	10863902	CCAAAGAUCUGCUUACAAA
G10	M-007182-01	D-007182-04	TRIP12	9320	NM_004238	10863902	CAAAUAAGCCACAUAGUAA
G10	M-007182-01	D-007182-18	TRIP12	9320	NM_004238	10863902	GAACACAGAUGGUGCGAUA
G11	D-001206-14	D-001210-02	siGENOME Non-targeting Control	0		0	UAAGGCUAUGAAGAGAUAC
G11	D-001206-14	D-001210-03	siGENOME Non-targeting Control	0		0	AUGUAUUGGCCUGUAUUAG
G11	D-001206-14	D-001210-04	siGENOME Non-targeting Control	0		0	AUGAACGUGAAUUGCUCAA
G11	D-001206-14	D-001210-05	siGENOME Non-targeting Control	0		0	UGGUUUACAUGUCGACUAA
H09	M-016695-01	D-016695-01	NOL11	25926	NM_015462	142378677	CGAAAACUCUGUUAUAAAG
H09	M-016695-01	D-016695-02	NOL11	25926	NM_015462	142378677	UCACGCUGUUUCUUAAGUA
H09	M-016695-01	D-016695-03	NOL11	25926	NM_015462	142378677	CAAGGAAGGUGCUGUUCGU
H09	M-016695-01	D-016695-04	NOL11	25926	NM_015462	142378677	UGGAGAGUAUGUUGUUGUA
H10	M-016096-01	D-016096-01	NOP16	51491	NM_016391	158518424	CUAAAUCGGUACGGCAGAA
H10	M-016096-01	D-016096-02	NOP16	51491	NM_016391	158518424	GUUACAGUGUCAACCGAAA
H10	M-016096-01	D-016096-03	NOP16	51491	NM_016391	158518424	CCCGUGAUGAGAAGAAUUA
H10	M-016096-01	D-016096-04	NOP16	51491	NM_016391	158518424	CCGGAAUGCUCGACGGAAG
H11	D-001206-14	D-001210-02	siGENOME Non-targeting Control	0		0	UAAGGCUAUGAAGAGAUAC

Appendix A1: List of siRNA used in siRNA array in 96 well format (plate 2)							
Well	Pool Catalog Number	Duplex Catalog Number	Gene Symbol	GENE ID	Gene Accession	GI Number	Sequence
H11	D-001206-14	D-001210-03	siGENOME Non-targeting Control	0		0	AUGUAUUGGCCUGUAUUAG
H11	D-001206-14	D-001210-04	siGENOME Non-targeting Control	0		0	AUGAACGUGAAUUGCUCAA
H11	D-001206-14	D-001210-05	siGENOME Non-targeting Control	0		0	UGGUUUACAUGUCGACUAA

Appendix A2: List of NS1 interacting host proteins identified in Biological replicate 1

Appendix A2: List of NS1 interacting host proteins identified in Biological replicate 1									
N	% Cov	%Cov (50)	%Cov (95)	Uniprot	Gene Symbol	Protein	Species	Peptides (95%)	Unused
4	35.7	33.3	32.6	Q12906	ILF3	Interleukin enhancer-binding factor 3	HUMAN	23	42.2
228	41.5	27.4	25.3	Q562R1	ACTBL2	Beta-actin-like protein 2	HUMAN	15	14.53
6	32.1	23.2	23.2	Q9NR30	DDX21	Nucleolar RNA helicase 2	HUMAN	14	27.57
10	29.8	26.9	25.6	O00567	NOP56	Nucleolar protein 56	HUMAN	13	23.87
22	26.1	18.3	18.3	O43390	HNRNPR	Heterogeneous nuclear ribonucleoprotein R	HUMAN	13	19.81
9	12.3	9.0	9.0	Q14690	PDCD11	Protein RRP5 homolog	HUMAN	13	24.61
20	22.9	20.1	20.1	P52272	HNRNPM	Heterogeneous nuclear ribonucleoprotein M	HUMAN	12	16.03
12	24.1	19.8	19.8	Q00839	HNRNPU	Heterogeneous nuclear ribonucleoprotein U	HUMAN	12	22.03
14	27.8	17.0	16.0	P46087	NOP2	Putative ribosomal RNA methyltransferase NOP2	HUMAN	11	19.36
23	37.5	37.5	31.5	P26599	PTBP1	Polypyrimidine tract-binding protein 1	HUMAN	10	14.9
20	12.8	9.1	8.4	Q07157	TJP1	Tight junction protein ZO-1	HUMAN	10	19.35
21	15.8	7.9	6.4	Q13813	SPTAN1	Spectrin alpha chain, brain	HUMAN	10	19.28
21	21.0	12.5	12.5	Q96KR1	ZFR	Zinc finger RNA-binding protein	HUMAN	10	15.16
43	21.2	13.0	13.0	O60716	CTNND1	Catenin delta-1	HUMAN	9	11.92
28	18.2	13.9	13.9	O76021	RSL1D1	Ribosomal L1 domain-containing protein 1	HUMAN	9	17.26
25	37.4	37.4	31.0	Q12905	ILF2	Interleukin enhancer-binding factor 2	HUMAN	9	18.29
18	29.7	24.0	20.3	Q9NVP1	DDX18	ATP-dependent RNA helicase DDX18	HUMAN	9	17.53
31	28.2	22.1	18.9	Q9Y2X3	NOP58	Nucleolar protein 58	HUMAN	9	12.35
51	20.7	20.7	17.5	O60506	SYNCRIP	Heterogeneous nuclear ribonucleoprotein Q	HUMAN	8	14.4
28	35.2	35.2	35.2	P22087	FBL	rRNA 2'-O-methyltransferase fibrillarin	HUMAN	8	13.23
37	10.2	10.2	10.2	Q9BUJ2	HNRNPUL1	Heterogeneous nuclear ribonucleoprotein U-like protein 1	HUMAN	7	13.72
32	43.0	35.8	28.0	Q9BYG3	MKI67IP	MKI67 FHA domain-interacting nucleolar phosphoprotein	HUMAN	7	12.02
30	8.3	6.8	6.1	Q9H583	HEATR1	HEAT repeat-containing protein 1	HUMAN	7	12.41
42	14.4	9.1	9.1	Q9P0K7	RAI14	Ankycorbin	HUMAN	7	11.95
22	16.7	10.2	9.1	Q9P2E9	RRBP1	Ribosome-binding protein 1	HUMAN	7	15.03
37	9.3	3.9	3.9	O75369-4	FLNB	Isoform Var-2 of Filamin-B	HUMAN	6	11.89
387	8.2	8.2	8.2	P05976	MYL1	Myosin light chain 1/3, skeletal muscle isoform	HUMAN	6	2.45
387	8.2	8.2	8.2	P08590	MYL3	Myosin light chain 3	HUMAN	6	2.45
74	16.4	10.5	10.5	P13647	KRT5	Keratin, type II cytoskeletal 5	HUMAN	6	11.6
57	20.3	20.3	16.3	P31943	HNRNPH1	Heterogeneous nuclear ribonucleoprotein H	HUMAN	6	7.82
45	18.4	18.4	18.4	P39023	RPL3	60S ribosomal protein L3	HUMAN	6	9.09
47	37.3	37.3	37.3	P67809	YBX1	Nuclease-sensitive element-binding protein 1	HUMAN	6	12
46	11.6	11.6	9.1	Q14151	SAFB2	Scaffold attachment factor B2	HUMAN	6	12.26
36	7.4	4.5	4.5	Q14980	NUMA1	Nuclear mitotic apparatus protein 1	HUMAN	6	11.12
403	19.2	16.3	12.6	Q58FF8	HSP90AB2P	Putative heat shock protein HSP 90-beta 2	HUMAN	6	8.86
119	12.4	7.0	3.9	Q7Z406-5	MYH14	Isoform 5 of Myosin-14	HUMAN	6	9.58

Appendix A2: List of NS1 interacting host proteins identified in Biological replicate 1									
N	% Cov	%Cov (50)	%Cov (95)	Uniprot	Gene Symbol	Protein	Species	Peptides (95%)	Unused
54	19.2	14.3	12.1	Q9Y3I0	C22orf28	UPF0027 protein C22orf28	HUMAN	6	9.47
47	16.3	9.8	8.7	O43143	DHX15	Putative pre-mRNA-splicing factor ATP-dependent RNA helicase DHX15	HUMAN	5	8.66
51	12.8	8.9	8.9	P19338	NCL	Nucleolin	HUMAN	5	8.15
61	21.5	21.5	21.5	Q15717	ELAVL1	ELAV-like protein 1	HUMAN	5	7.14
58	13.7	12.0	8.7	Q1KMD3	HNRNPUL2	Heterogeneous nuclear ribonucleoprotein U-like protein 2	HUMAN	5	8.38
57	10.2	9.1	9.1	Q7Z2W4	ZC3HAV1	Zinc finger CCCH-type antiviral protein 1	HUMAN	5	9.06
41	18.6	11.3	9.1	Q8IY81	FTSJ3	Putative rRNA methyltransferase 3	HUMAN	5	9.87
182	15.1	9.4	9.4	Q92841	DDX17	Probable ATP-dependent RNA helicase DDX17	HUMAN	5	7.47
39	10.4	9.4	6.0	Q9BQG0	MYBBP1A	Myb-binding protein 1A	HUMAN	5	10.67
43	16.7	9.3	9.3	Q9BZE4	GTPBP4	Nucleolar GTP-binding protein 1	HUMAN	5	9.64
58	14.0	9.4	7.8	Q9UHB6	LIMA1	LIM domain and actin-binding protein 1	HUMAN	5	9
90	10.4	8.3	8.3	O00571	DDX3X	ATP-dependent RNA helicase DDX3X	HUMAN	4	8
74	21.7	21.7	14.6	P16401	HIST1H1B	Histone H1.5	HUMAN	4	6.05
63	11.2	11.2	11.2	P35637	FUS	RNA-binding protein FUS	HUMAN	4	7.38
64	9.9	5.4	5.4	P43243	MATR3	Matrin-3	HUMAN	4	7.12
63	20.6	20.6	18.0	P51991	HNRNPA3	Heterogeneous nuclear ribonucleoprotein A3	HUMAN	4	8.06
142	8.7	4.1	3.3	P55265	ADAR	Double-stranded RNA-specific adenosine deaminase	HUMAN	4	2.86
122	14.1	14.1	14.1	P61158	ACTR3	Actin-related protein 3	HUMAN	4	4.47
65	17.7	17.7	14.7	P62424	RPL7A	60S ribosomal protein L7a	HUMAN	4	7.11
105	35.5	35.5	25.4	P62906	RPL10A	60S ribosomal protein L10a	HUMAN	4	5.23
94	22.6	22.6	22.6	Q13151	HNRNPA0	Heterogeneous nuclear ribonucleoprotein A0	HUMAN	4	5.07
288	16.2	9.9	5.9	Q13310	PABPC4	Polyadenylate-binding protein 4	HUMAN	4	7.81
55	10.6	10.6	10.6	Q14137	BOP1	Ribosome biogenesis protein BOP1	HUMAN	4	8
60	13.9	9.6	9.6	Q14684	RRP1B	Ribosomal RNA processing protein 1 homolog B	HUMAN	4	7.29
63	23.3	16.4	16.4	Q15050	RRS1	Ribosome biogenesis regulatory protein homolog	HUMAN	4	7.01
58	33.1	33.1	33.1	Q7Z7K6	CENPV	Centromere protein V	HUMAN	4	7.76
73	11.8	6.6	5.5	Q8IWA0	WDR75	WD repeat-containing protein 75	HUMAN	4	6.17
52	7.0	7.0	5.7	Q9GZR7	DDX24	ATP-dependent RNA helicase DDX24	HUMAN	4	8.15
48	10.0	8.4	6.0	Q9H0A0	NAT10	N-acetyltransferase 10	HUMAN	4	8.49
81	13.5	10.1	8.5	Q9NZI8	IGF2BP1	Insulin-like growth factor 2 mRNA-binding protein 1	HUMAN	4	5.7
95	31.3	31.3	31.3	Q9Y3E5	PTRH2	Peptidyl-tRNA hydrolase 2, mitochondrial	HUMAN	4	6
46	14.2	14.2	10.6	Q9Y5J1	UTP18	U3 small nucleolar RNA-associated protein 18 homolog	HUMAN	4	8.99
87	8.6	8.6	6.4	O00425	IGF2BP3	Insulin-like growth factor 2 mRNA-binding protein 3	HUMAN	3	6.03
64	8.2	8.2	6.6	O00541	PES1	Pescadillo homolog	HUMAN	3	6.72
88	7.0	7.0	7.0	O15213	WDR46	WD repeat-containing protein 46	HUMAN	3	6
87	9.3	9.3	9.3	O43818	RRP9	U3 small nucleolar RNA-interacting protein 2	HUMAN	3	6
96	23.1	19.5	11.1	O60832	DKC1	H/ACA ribonucleoprotein complex subunit 4	HUMAN	3	4.52
112	11.0	6.5	6.5	P02545	LMNA	Lamin-A/C	HUMAN	3	4.97

Appendix A2: List of NS1 interacting host proteins identified in Biological replicate 1									
N	% Cov	%Cov (50)	%Cov (95)	Uniprot	Gene Symbol	Protein	Species	Peptides (95%)	Unused
121	27.8	13.9	13.9	P05388	RPLP0	60S acidic ribosomal protein P0	HUMAN	3	4.47
91	17.8	6.4	6.4	P06396	GSN	Gelsolin	HUMAN	3	6
83	26.5	14.3	11.3	P06733	ENO1	Alpha-enolase	HUMAN	3	6.34
90	20.1	20.1	20.1	P06748	NPM1	Nucleophosmin	HUMAN	3	4.85
261	8.6	8.6	6.2	P08107	HSPA1A	Heat shock 70 kDa protein 1A/1B	HUMAN	3	6.23
89	6.5	4.0	4.0	P13639	EEF2	Elongation factor 2	HUMAN	3	6.01
113	12.2	7.9	7.9	P14618	PKM2	Pyruvate kinase isozymes M1/M2	HUMAN	3	4.83
261	6.2	6.2	6.2	P17066	HSPA6	Heat shock 70 kDa protein 6	HUMAN	3	6
92	15.3	5.2	5.2	P17844	DDX5	Probable ATP-dependent RNA helicase DDX5	HUMAN	3	5.88
66	23.8	14.2	11.6	P22626	HNRNPA2B1	Heterogeneous nuclear ribonucleoproteins A2/B1	HUMAN	3	6.66
118	21.0	17.3	17.3	P23396	RPS3	40S ribosomal protein S3	HUMAN	3	4.51
102	20.0	20.0	16.7	P27348	YWHAQ	14-3-3 protein theta	HUMAN	3	5.41
101	31.8	17.5	17.5	P47755	CAPZA2	F-actin-capping protein subunit alpha-2	HUMAN	3	5.94
120	23.4	12.3	8.2	P52597	HNRNPF	Heterogeneous nuclear ribonucleoprotein F	HUMAN	3	5.21
93	24.5	17.8	17.8	P52907	CAPZA1	F-actin-capping protein subunit alpha-1	HUMAN	3	6
56	11.3	8.8	6.3	P54652	HSPA2	Heat shock-related 70 kDa protein 2	HUMAN	3	5.8
92	46.4	39.2	39.2	P60903	S100A10	Protein S100-A10	HUMAN	3	6
98	29.8	29.8	29.8	P62263	RPS14	40S ribosomal protein S14	HUMAN	3	6
213	10.7	10.7	10.7	P62829	RPL23	60S ribosomal protein L23	HUMAN	3	2
70	18.8	15.6	11.1	Q02878	RPL6	60S ribosomal protein L6	HUMAN	3	6.41
136	26.1	26.1	20.2	Q07020	RPL18	60S ribosomal protein L18	HUMAN	3	4.03
93	14.0	10.2	7.0	Q07666	KHDRBS1	KH domain-containing, RNA-binding, signal transduction-associated protein 1	HUMAN	3	4.51
113	7.5	4.3	4.3	Q08170	SFRS4	Splicing factor, arginine/serine-rich 4	HUMAN	3	4
78	8.3	5.3	5.3	Q12788	TBL3	Transducin beta-like protein 3	HUMAN	3	6.01
99	5.4	4.5	3.6	Q12965	MYO1E	Myosin-Ie	HUMAN	3	5.76
113	9.3	6.1	6.1	Q13247	SFRS6	Splicing factor, arginine/serine-rich 6	HUMAN	3	4
81	4.0	3.4	3.4	Q13428	TCOF1	Treacle protein	HUMAN	3	6
98	4.7	2.8	2.8	Q14692	BMS1	Ribosome biogenesis protein BMS1 homolog	HUMAN	3	4.29
78	4.5	3.5	3.5	Q15393	SF3B3	Splicing factor 3B subunit 3	HUMAN	3	5.85
75	13.2	10.5	8.2	Q5BKZ1	ZNF326	Zinc finger protein 326	HUMAN	3	6
107	10.1	3.4	3.4	Q86V48	LUZP1	Leucine zipper protein 1	HUMAN	3	5.2
92	12.0	7.3	7.3	Q8TED0	UTP15	U3 small nucleolar RNA-associated protein 15 homolog	HUMAN	3	4.65
111	3.0	2.2	1.7	Q92616	GCN1L1	Translational activator GCN1	HUMAN	3	5.06
126	12.5	12.5	12.5	Q96HS1	PGAM5	Serine/threonine-protein phosphatase PGAM5, mitochondrial	HUMAN	3	4.34
100	8.9	8.9	6.5	Q96I24	FUBP3	Far upstream element-binding protein 3	HUMAN	3	4.21
113	4.1	4.1	4.1	Q96T37	RBM15	Putative RNA-binding protein 15	HUMAN	3	3.57
86	8.7	8.7	8.7	Q99729	HNRNPAB	Heterogeneous nuclear ribonucleoprotein A/B	HUMAN	3	3.2
74	20.9	16.0	13.4	Q9H7B2	RPF2	Ribosome production factor 2 homolog	HUMAN	3	6.15
103	11.7	6.8	6.8	Q9NVI7	ATAD3A	ATPase family AAA domain-containing protein 3A	HUMAN	3	5.38

Appendix A2: List of NS1 interacting host proteins identified in Biological replicate 1									
N	% Cov	%Cov (50)	%Cov (95)	Uniprot	Gene Symbol	Protein	Species	Peptides (95%)	Unused
79	9.9	4.4	4.4	Q9NWH9	SLTM	SAFB-like transcription modulator	HUMAN	3	5.82
85	12.5	12.5	12.5	Q9NWT1	PAK1IP1	p21-activated protein kinase-interacting protein 1	HUMAN	3	6
84	8.2	7.0	7.0	Q9NYH9	UTP6	U3 small nucleolar RNA-associated protein 6 homolog	HUMAN	3	6
71	14.7	14.7	10.5	Q9UKM9	RALY	RNA-binding protein Raly	HUMAN	3	6.36
82	7.1	5.3	3.2	Q9UM54	MYO6	Myosin-VI	HUMAN	3	6.46
80	10.5	6.4	6.4	Q9UNX4	WDR3	WD repeat-containing protein 3	HUMAN	3	6
86	7.3	2.9	2.9	Q9UQ35-2	SRRM2	Isoform 2 of Serine/arginine repetitive matrix protein 2	HUMAN	3	6.08
76	13.9	13.9	13.9	Q9Y224	C14orf166	UPF0568 protein C14orf166	HUMAN	3	6
128	30.0	15.0	10.7	O15144	ARPC2	Actin-related protein 2/3 complex subunit 2	HUMAN	2	4.22
136	6.7	2.9	2.9	O60264	SMARCA5	SWI/SNF-related matrix-associated actin-dependent regulator of chromatin subfamily A member 5	HUMAN	2	3.35
173	6.4	4.9	4.9	O75083	WDR1	WD repeat-containing protein 1	HUMAN	2	3.51
93	18.0	18.0	9.9	O75367	H2AFY	Core histone macro-H2A.1	HUMAN	2	5.1
168	13.3	7.8	7.8	O75477	ERLIN1	Erlin-1	HUMAN	2	2.89
154	40.5	40.5	40.5	O75531	BANF1	Barrier-to-autointegration factor	HUMAN	2	4
122	10.2	5.5	5.5	O75683	SURF6	Surfeit locus protein 6	HUMAN	2	3.1
142	11.5	7.5	7.5	O75955	FLOT1	Flotillin-1	HUMAN	2	4
168	9.1	8.6	8.6	O94905	ERLIN2	Erlin-2	HUMAN	2	3.68
128	3.3	3.3	3.3	O94906	PRPF6	Pre-mRNA-processing factor 6	HUMAN	2	3.64
164	5.5	1.4	1.4	O95425	SVIL	Supervillin	HUMAN	2	3.75
141	11.0	4.8	4.8	P00352	ALDH1A1	Retinal dehydrogenase 1	HUMAN	2	4
158	4.5	4.5	4.5	P02790	HPX	Hemopexin	HUMAN	2	3.23
145	15.6	10.7	10.7	P04083	ANXA1	Annexin A1	HUMAN	2	4
188	14.9	8.7	8.7	P04406	GAPDH	Glyceraldehyde-3-phosphate dehydrogenase	HUMAN	2	2.69
127	46.3	16.1	11.2	P04792	HSPB1	Heat shock protein beta-1	HUMAN	2	4.25
165	7.2	7.2	4.4	P04843	RPN1	Dolichyl-diphosphooligosaccharide--protein glycosyltransferase subunit 1	HUMAN	2	3.75
106	8.1	8.1	8.1	P06753	TPM3	Tropomyosin alpha-3 chain	HUMAN	2	3.04
106	8.1	8.1	8.1	P07951	TPM2	Tropomyosin beta chain	HUMAN	2	3.04
118	19.9	18.3	5.5	P08621	SNRNP70	U1 small nuclear ribonucleoprotein 70 kDa	HUMAN	2	3.25
106	8.1	8.1	8.1	P09493	TPM1	Tropomyosin alpha-1 chain	HUMAN	2	3.04
101	15.6	8.7	8.4	P0C7M2	HNRPA1L3	Putative heterogeneous nuclear ribonucleoprotein A1-like 3	HUMAN	2	4.5
185	13.3	4.4	4.4	P10809	HSPD1	60 kDa heat shock protein, mitochondrial	HUMAN	2	2.87
148	3.1	3.1	1.4	P11388	TOP2A	DNA topoisomerase 2-alpha	HUMAN	2	2.64
186	4.8	4.8	3.6	P14923	JUP	Junction plakoglobin	HUMAN	2	2.83
148	4.0	4.0	4.0	P17655	CAPN2	Calpain-2 catalytic subunit	HUMAN	2	4
150	24.0	17.0	10.6	P21796	VDAC1	Voltage-dependent anion-selective channel protein 1	HUMAN	2	2.46
120	5.7	5.7	4.2	P21980	TGM2	Protein-glutamine gamma-glutamyltransferase 2	HUMAN	2	4.48
177	23.5	23.5	23.5	P23528	CFL1	Cofilin-1	HUMAN	2	3.26
178	14.9	5.6	5.6	P26196	DDX6	Probable ATP-dependent RNA helicase DDX6	HUMAN	2	3.22

Appendix A2: List of NS1 interacting host proteins identified in Biological replicate 1									
N	% Cov	%Cov (50)	%Cov (95)	Uniprot	Gene Symbol	Protein	Species	Peptides (95%)	Unused
152	27.5	19.4	10.9	P26373	RPL13	60S ribosomal protein L13	HUMAN	2	3.46
167	6.3	2.8	2.8	P27816-6	MAP4	Isoform 6 of Microtubule-associated protein 4	HUMAN	2	3.7
125	4.8	3.3	2.3	P28290	SSFA2	Sperm-specific antigen 2	HUMAN	2	4.4
143	23.0	18.8	18.8	P30050	RPL12	60S ribosomal protein L12	HUMAN	2	4
191	21.4	8.7	8.7	P31942	HNRNPH3	Heterogeneous nuclear ribonucleoprotein H3	HUMAN	2	2.6
212	9.8	9.8	9.8	P31946	YWHAB	14-3-3 protein beta/alpha	HUMAN	2	2.77
174	5.8	3.4	3.4	P35221	CTNNA1	Catenin alpha-1	HUMAN	2	3.32
110	12.5	4.3	4.3	P42166	TMPO	Lamina-associated polypeptide 2, isoform alpha	HUMAN	2	4
110	11.2	6.6	6.6	P42167	TMPO	Lamina-associated polypeptide 2, isoforms beta/gamma	HUMAN	2	4
144	8.1	6.1	6.1	P48643	CCT5	T-complex protein 1 subunit epsilon	HUMAN	2	4
112	4.7	3.3	3.3	P49756	RBM25	RNA-binding protein 25	HUMAN	2	3.6
145	25.6	11.2	11.2	P50914	RPL14	60S ribosomal protein L14	HUMAN	2	3.59
183	7.5	7.5	5.3	P50990	CCT8	T-complex protein 1 subunit theta	HUMAN	2	3.02
114	9.5	7.1	7.1	P51114	FXR1	Fragile X mental retardation syndrome-related protein 1	HUMAN	2	4.01
137	7.0	2.7	2.7	P53396	ACLY	ATP-citrate synthase	HUMAN	2	4.02
131	7.1	5.8	5.8	P55795	HNRNPH2	Heterogeneous nuclear ribonucleoprotein H2	HUMAN	2	4
102	6.9	6.9	5.2	P56182	RRP1	Ribosomal RNA processing protein 1 homolog A	HUMAN	2	4.19
129	22.0	18.8	13.1	P56537	EIF6	Eukaryotic translation initiation factor 6	HUMAN	2	2.6
153	10.4	10.4	10.4	P59190	RAB15	Ras-related protein Rab-15	HUMAN	2	3.44
153	10.6	10.6	10.6	P61006	RAB8A	Ras-related protein Rab-8A	HUMAN	2	3.44
104	15.7	12.3	12.3	P61313	RPL15	60S ribosomal protein L15	HUMAN	2	4.03
118	23.5	23.5	23.5	P61353	RPL27	60S ribosomal protein L27	HUMAN	2	4
164	17.4	14.2	9.7	P61981	YWHAG	14-3-3 protein gamma	HUMAN	2	3
161	11.5	11.5	11.5	P62241	RPS8	40S ribosomal protein S8	HUMAN	2	4
114	19.9	14.7	14.7	P62750	RPL23A	60S ribosomal protein L23a	HUMAN	2	3.57
153	14.6	10.7	10.7	P62820	RAB1A	Ras-related protein Rab-1A	HUMAN	2	3.45
119	12.9	12.9	12.9	P62913	RPL11	60S ribosomal protein L11	HUMAN	2	3.16
106	12.5	9.3	9.3	P67936	TPM4	Tropomyosin alpha-4 chain	HUMAN	2	3.04
176	1.7	0.8	0.8	P78527	PRKDC	DNA-dependent protein kinase catalytic subunit	HUMAN	2	3.27
172	9.9	5.7	5.7	P83111	LACTB	Serine beta-lactamase-like protein LACTB, mitochondrial	HUMAN	2	3.56
140	13.3	13.3	13.3	P84098	RPL19	60S ribosomal protein L19	HUMAN	2	2.96
166	11.6	5.8	5.8	Q00325	SLC25A3	Phosphate carrier protein, mitochondrial	HUMAN	2	3.71
157	4.8	2.1	2.1	Q04637	EIF4G1	Eukaryotic translation initiation factor 4 gamma 1	HUMAN	2	3.28
230	13.0	13.0	9.8	Q04917	YWHAH	14-3-3 protein eta	HUMAN	2	3.17
128	10.9	6.4	6.4	Q05519	SFRS11	Splicing factor, arginine/serine-rich 11	HUMAN	2	4.02
179	24.6	15.1	10.5	Q06830	PRDX1	Peroxiredoxin-1	HUMAN	2	3.16
152	9.1	9.1	9.1	Q12792	TWF1	Twinfilin-1	HUMAN	2	4
166	3.9	2.8	2.2	Q13045	FLII	Protein flightless-1 homolog	HUMAN	2	2.86

Appendix A2: List of NS1 interacting host proteins identified in Biological replicate 1									
N	% Cov	%Cov (50)	%Cov (95)	Uniprot	Gene Symbol	Protein	Species	Peptides (95%)	Unused
151	7.2	7.2	7.2	Q13148	TARDBP	TAR DNA-binding protein 43	HUMAN	2	4
155	6.4	6.4	6.4	Q13283	G3BP1	Ras GTPase-activating protein-binding protein 1	HUMAN	2	4
123	9.5	6.6	6.6	Q13501	SQSTM1	Sequestosome-1	HUMAN	2	3.89
133	8.9	3.2	2.2	Q13523	PRPF4B	Serine/threonine-protein kinase PRP4 homolog	HUMAN	2	3.42
146	17.4	11.7	8.5	Q13595	TRA2A	Transformer-2 protein homolog alpha	HUMAN	2	2.04
209	11.1	4.9	4.9	Q14247	CTTN	Src substrate cortactin	HUMAN	2	2.05
147	3.8	3.8	3.8	Q14258	TRIM25	E3 ubiquitin/ISG15 ligase TRIM25	HUMAN	2	2.66
145	9.0	3.2	3.2	Q15269	PWP2	Periodic tryptophan protein 2 homolog	HUMAN	2	2.73
153	10.9	10.9	10.9	Q15286	RAB35	Ras-related protein Rab-35	HUMAN	2	3.44
131	4.5	3.2	3.2	Q15361	TTF1	Transcription termination factor 1	HUMAN	2	3.54
163	14.6	9.3	9.3	Q15365	PCBP1	Poly(rC)-binding protein 1	HUMAN	2	3.8
175	12.6	9.7	9.7	Q16629	SFRS7	Splicing factor, arginine/serine-rich 7	HUMAN	2	3.28
115	17.6	15.6	9.6	Q3ZCQ8	TIMM50	Mitochondrial import inner membrane translocase subunit TIM50	HUMAN	2	4.74
131	6.1	2.6	2.6	Q5JTH9	RRP12	RRP12-like protein	HUMAN	2	2.49
121	6.7	5.2	3.6	Q5SSJ5	HP1BP3	Heterochromatin protein 1-binding protein 3	HUMAN	2	3.12
173	7.6	3.1	3.1	Q5T9A4	ATAD3B	ATPase family AAA domain-containing protein 3B	HUMAN	2	2.59
115	30.4	22.6	22.6	Q6NVV1	R13AX	Putative 60S ribosomal protein L13a-like MGC87657	HUMAN	2	3.7
103	10.9	7.8	7.8	Q6RFH5	WDR74	WD repeat-containing protein 74	HUMAN	2	4.14
135	25.0	15.5	15.5	Q71UM5	RPS27L	40S ribosomal protein S27-like	HUMAN	2	2
189	7.6	2.9	2.9	Q7KZF4	SND1	Staphylococcal nuclease domain-containing protein 1	HUMAN	2	2.64
181	7.8	3.4	2.5	Q7L2E3	DHX30	Putative ATP-dependent RNA helicase DHX30	HUMAN	2	3.05
117	24.0	10.8	4.4	Q8IVT2	C19orf21	Uncharacterized protein C19orf21	HUMAN	2	4.55
121	22.4	8.5	8.5	Q8NHW5	RLA0L	60S acidic ribosomal protein P0-like	HUMAN	2	2.36
153	3.3	3.3	3.3	Q8TDD1	DDX54	ATP-dependent RNA helicase DDX54	HUMAN	2	4
130	29.2	11.6	8.5	Q8TDN6	BRIX1	Ribosome biogenesis protein BRX1 homolog	HUMAN	2	3.54
138	8.1	8.1	8.1	Q92804	TAF15	TATA-binding protein-associated factor 2N	HUMAN	2	3.06
153	14.9	10.9	10.9	Q92928	RAB1C	Putative Ras-related protein Rab-1C	HUMAN	2	3.45
153	10.6	10.6	10.6	Q92930	RAB8B	Ras-related protein Rab-8B	HUMAN	2	3.44
132	15.7	13.1	10.5	Q99848	EBNA1BP2	Probable rRNA-processing protein EBP2	HUMAN	2	3.5
150	20.0	20.0	20.0	Q9BSD7	C1orf57	Nucleoside-triphosphatase C1orf57	HUMAN	2	4
149	11.6	11.6	11.6	Q9BZG1	RAB34	Ras-related protein Rab-34	HUMAN	2	4
135	11.8	9.0	9.0	Q9GZL7	WDR12	Ribosome biogenesis protein WDR12	HUMAN	2	3.38
127	6.3	4.3	3.1	Q9H0D6	XRN2	5'-3' exoribonuclease 2	HUMAN	2	2.71
139	8.7	4.1	4.1	Q9H0H5	RACGAP1	Rac GTPase-activating protein 1	HUMAN	2	4.01
153	14.9	10.9	10.9	Q9H0U4	RAB1B	Ras-related protein Rab-1B	HUMAN	2	3.45
155	7.9	4.5	4.5	Q9H6R4	NOL6	Nucleolar protein 6	HUMAN	2	2.27
171	5.7	2.9	2.9	Q9H8V3	ECT2	Protein ECT2	HUMAN	2	2.65
100	4.6	3.3	3.3	Q9NW13	RBM28	RNA-binding protein 28	HUMAN	2	4.01

Appendix A2: List of NS1 interacting host proteins identified in Biological replicate 1									
N	% Cov	%Cov (50)	%Cov (95)	Uniprot	Gene Symbol	Protein	Species	Peptides (95%)	Unused
105	4.9	3.6	3.6	Q9NYF8	BCLAF1	Bcl-2-associated transcription factor 1	HUMAN	2	4
147	6.5	6.5	6.5	Q9NZ01	TECR	Trans-2,3-enoyl-CoA reductase	HUMAN	2	4
146	6.8	6.8	6.8	Q9P0L0	VAPA	Vesicle-associated membrane protein-associated protein A	HUMAN	2	4
139	15.9	13.1	13.1	Q9Y277	VDAC3	Voltage-dependent anion-selective channel protein 3	HUMAN	2	3.02
117	18.0	18.0	18.0	Q9Y3C1	NOP16	Nucleolar protein 16	HUMAN	2	4
150	24.8	20.9	20.9	Q9Y3U8	RPL36	60S ribosomal protein L36	HUMAN	2	3.54

Appendix A3: List of NS1 interacting host proteins identified in Biological replicate 2

Appendix A3: List of NS1 interacting host proteins identified in Biological replicate 2									
N	%Cov	%Cov(50)	%Cov(95)	Uniprot	Gene Symbol	Protein	Species	Peptides (95%)	Unused
15	54.3	44.1	42.4	P14866	HNRNPL	Heterogeneous nuclear ribonucleoprotein L	HUMAN	30	31.72
11	31.9	25.4	24.7	Q96KR1	ZFR	Zinc finger RNA-binding protein	HUMAN	20	35.58
10	42.3	31.3	27.8	Q12906	ILF3	Interleukin enhancer-binding factor 3	HUMAN	19	35.75
7	27.1	17.8	15.9	Q14690	PDCD11	Protein RRP5 homolog	HUMAN	19	37.82
17	36.7	29.9	29.9	Q8IY81	FTSJ3	Putative rRNA methyltransferase 3	HUMAN	16	30.25
27	35.9	32.8	30.1	O00567	NOP56	Nucleolar protein 56	HUMAN	15	22.4
18	29.0	24.4	23.5	P43243	MATR3	Matrin-3	HUMAN	15	29.4
19	12.1	9.6	8.3	Q9H583	HEATR1	HEAT repeat-containing protein 1	HUMAN	14	27.31
33	40.6	26.7	25.1	Q9NVP1	DDX18	ATP-dependent RNA helicase DDX18	HUMAN	14	20.77
31	26.1	22.8	21.5	O43390	HNRNPR	Heterogeneous nuclear ribonucleoprotein R	HUMAN	13	21.8
22	30.2	25.0	20.2	P46087	NOP2	Putative ribosomal RNA methyltransferase NOP2	HUMAN	12	25.03
49	35.1	32.4	30.0	Q9Y5J1	UTP18	U3 small nucleolar RNA-associated protein 18 homolog	HUMAN	12	17.71
44	45.2	43.3	37.3	Q15050	RRS1	Ribosome biogenesis regulatory protein homolog	HUMAN	11	18.42
34	15.3	10.8	10.2	Q9BQG0	MYBBP1A	Myb-binding protein 1A	HUMAN	11	20.55
51	40.5	37.9	33.0	Q9UKM9	RALY	RNA-binding protein Raly	HUMAN	11	17.52
41	10.2	7.4	6.4	O75643	SNRNP200	U5 small nuclear ribonucleoprotein 200 kDa helicase	HUMAN	10	19.16
77	31.9	20.9	19.5	P04259	KRT6B	Keratin, type II cytoskeletal 6B	HUMAN	10	19.16
53	26.8	17.4	14.8	Q8IWA0	WDR75	WD repeat-containing protein 75	HUMAN	10	17.11
45	27.0	21.0	21.0	Q969X6	CIRH1A	Cirhin	HUMAN	10	18.31
32	26.6	22.2	18.4	Q9UNX4	WDR3	WD repeat-containing protein 3	HUMAN	10	20.94
42	42.6	39.6	35.8	P26599	PTBP1	Polypyrimidine tract-binding protein 1	HUMAN	9	18.56
48	27.9	23.5	21.1	Q14137	BOP1	Ribosome biogenesis protein BOP1	HUMAN	9	17.8
50	17.1	13.7	11.5	Q14692	BMS1	Ribosome biogenesis protein BMS1 homolog	HUMAN	9	17.6
40	51.2	42.3	35.6	Q15717	ELAVL1	ELAV-like protein 1	HUMAN	9	19.31
18	18.9	10.5	9.6	Q7L2E3	DHX30	Putative ATP-dependent RNA helicase DHX30	HUMAN	9	17.57
43	34.9	23.0	20.0	Q9BZE4	GTPBP4	Nucleolar GTP-binding protein 1	HUMAN	9	18.5
59	23.1	17.2	15.7	Q9H8H0	NOL11	Nucleolar protein 11	HUMAN	9	15.16
70	25.1	17.4	12.9	O15226	NKRF	NF-kappa-B-repressing factor	HUMAN	8	12.94
54	19.9	18.7	15.6	Q12788	TBL3	Transducin beta-like protein 3	HUMAN	8	16.72
63	16.8	14.6	13.2	Q5QJE6	DNTTIP2	Deoxynucleotidyltransferase terminal-interacting protein 2	HUMAN	8	14.42
37	22.0	21.0	12.5	Q8NI36	WDR36	WD repeat-containing protein 36	HUMAN	8	19.87
67	37.1	30.1	24.1	Q8TED0	UTP15	U3 small nucleolar RNA-associated protein 15 homolog	HUMAN	8	13.57
90	35.3	19.0	19.0	P25705	ATP5A1	ATP synthase subunit alpha, mitochondrial	HUMAN	7	10.68
62	38.2	33.7	27.8	Q02878	RPL6	60S ribosomal protein L6	HUMAN	7	14.44
75	18.6	13.1	12.0	Q1KMD3	HNRNPUL2	Heterogeneous nuclear ribonucleoprotein U-like protein 2	HUMAN	7	12.28
85	32.4	28.1	24.8	Q99848	EBNA1BP2	Probable rRNA-processing protein EBP2	HUMAN	7	11.2
65	39.5	23.6	21.3	Q9GZL7	WDR12	Ribosome biogenesis protein WDR12	HUMAN	7	14.26
73	31.0	28.4	25.8	Q9H7B2	RPF2	Ribosome production factor 2 homolog	HUMAN	7	12.33
84	23.6	18.6	17.0	O00566	MPHOSPH10	U3 small nucleolar ribonucleoprotein protein MPP10	HUMAN	6	11.27
93	21.5	17.2	15.7	O15213	WDR46	WD repeat-containing protein 46	HUMAN	6	10.03
95	22.1	16.8	16.8	P16401	HIST1H1B	Histone H1.5	HUMAN	6	9.63
59	17.9	16.7	13.7	P48668	KRT6C	Keratin, type II cytoskeletal 6C	HUMAN	6	10.19

Appendix A3: List of NS1 interacting host proteins identified in Biological replicate 2									
N	%Cov	%Cov(50)	%Cov(95)	Uniprot	Gene Symbol	Protein	Species	Peptides (95%)	Unused
31	22.2	14.5	12.3	P52272	HNRNPM	Heterogeneous nuclear ribonucleoprotein M	HUMAN	6	11.55
96	37.1	31.4	31.4	P56537	EIF6	Eukaryotic translation initiation factor 6	HUMAN	6	9.54
346	22.2	10.6	7.5	Q13310	PABPC4	Polyadenylate-binding protein 4	HUMAN	6	6.46
82	14.6	10.0	10.0	Q15269	PWP2	Periodic tryptophan protein 2 homolog	HUMAN	6	11.3
89	25.5	15.4	13.7	Q5SSJ5	HP1BP3	Heterochromatin protein 1-binding protein 3	HUMAN	6	10.71
92	26.5	22.3	22.3	Q6RFH5	WDR74	WD repeat-containing protein 74	HUMAN	6	10.11
94	18.4	12.0	10.9	Q7Z2W4	ZC3HAV1	Zinc finger CCCH-type antiviral protein 1	HUMAN	6	9.94
79	15.0	10.9	10.9	Q8TDD1	DDX54	ATP-dependent RNA helicase DDX54	HUMAN	6	11.81
76	20.0	14.1	10.0	Q9H0D6	XRN2	5'-3' exoribonuclease 2	HUMAN	6	12.14
78	17.1	11.6	8.8	Q9NW13	RBM28	RNA-binding protein 28	HUMAN	6	12.02
97	7.0	5.2	2.9	P18583-5	SON	Isoform D of Protein SON	HUMAN	5	9.39
120	35.6	16.4	11.0	P38159	RBMX	Heterogeneous nuclear ribonucleoprotein G	HUMAN	5	7.4
86	42.2	32.3	28.3	Q8TDN6	BRIX1	Ribosome biogenesis protein BRX1 homolog	HUMAN	5	11.06
108	18.2	11.2	11.2	Q96PK6	RBM14	RNA-binding protein 14	HUMAN	5	8.46
91	18.2	9.8	8.6	Q9BUJ2	HNRNPUL1	Heterogeneous nuclear ribonucleoprotein U-like protein 1	HUMAN	5	10.45
123	34.5	21.2	21.2	Q9BYG3	MKI67IP	MKI67 FHA domain-interacting nucleolar phosphoprotein	HUMAN	5	7.21
114	11.0	9.1	7.0	Q9H6R4	NOL6	Nucleolar protein 6	HUMAN	5	7.92
35	16.3	10.7	10.7	Q9NR30	DDX21	Nucleolar RNA helicase 2	HUMAN	5	10.05
44	17.8	12.0	12.0	Q9NZI8	IGF2BP1	Insulin-like growth factor 2 mRNA-binding protein 1	HUMAN	5	7.41
107	24.1	21.0	20.6	Q9UMY1	NOL7	Nucleolar protein 7	HUMAN	5	8.47
100	16.2	13.8	10.9	O00541	PES1	Pescadillo homolog	HUMAN	4	9.09
126	16.4	10.1	10.1	O43818	RRP9	U3 small nucleolar RNA-interacting protein 2	HUMAN	4	7.01
110	34.2	23.8	15.4	P12236	SLC25A6	ADP/ATP translocase 3	HUMAN	4	8.2
158	35.9	28.6	21.8	P18124	RPL7	60S ribosomal protein L7	HUMAN	4	5.31
49	20.0	18.0	14.2	P31943	HNRNPH1	Heterogeneous nuclear ribonucleoprotein H	HUMAN	4	6.59
111	23.0	14.4	14.4	P42696	RBM34	RNA-binding protein 34	HUMAN	4	8
131	27.6	13.5	13.5	P46777	RPL5	60S ribosomal protein L5	HUMAN	4	6.66
48	10.2	5.6	5.6	P55265	ADAR	Double-stranded RNA-specific adenosine deaminase	HUMAN	4	7.54
125	14.0	8.8	7.4	Q14684	RRP1B	Ribosomal RNA processing protein 1 homolog B	HUMAN	4	7.06
103	9.3	5.4	2.9	Q14980	NUMA1	Nuclear mitotic apparatus protein 1	HUMAN	4	8.69
135	25.1	17.3	13.4	Q15061	WDR43	WD repeat-containing protein 43	HUMAN	4	6.52
113	13.5	11.8	11.8	Q1ED39	C16orf88	Protein C16orf88	HUMAN	4	8
102	49.2	49.2	30.0	Q8IUE6	HIST2H2AB	Histone H2A type 2-B	HUMAN	4	8.13
402	49.2	49.2	35.4	Q93077	HIST1H2AC	Histone H2A type 1-C	HUMAN	4	6.87
58	22.9	22.9	22.9	Q96C57	C12orf43	Uncharacterized protein C12orf43	HUMAN	4	5.9
99	19.3	9.2	6.8	Q96GQ7	DDX27	Probable ATP-dependent RNA helicase DDX27	HUMAN	4	9.11
101	31.0	22.8	14.6	Q9BVP2	GNL3	Guanine nucleotide-binding protein-like 3	HUMAN	4	9.03
138	28.3	22.0	19.7	Q9BXY0	MAK16	Protein MAK16 homolog	HUMAN	4	6.29
124	15.6	10.4	8.6	Q9GZR7	DDX24	ATP-dependent RNA helicase DDX24	HUMAN	4	7.07
121	30.1	24.4	21.8	Q9H9Y2	RPF1	Ribosome production factor 1	HUMAN	4	7.3
129	12.2	5.2	5.2	Q9NXF1	TEX10	Testis-expressed sequence 10 protein	HUMAN	4	6.75
122	16.3	10.8	10.8	Q9NY93	DDX56	Probable ATP-dependent RNA helicase DDX56	HUMAN	4	7.22
104	33.1	26.4	17.9	Q9UMS4	PRPF19	Pre-mRNA-processing factor 19	HUMAN	4	8.67
65	12.6	12.6	8.6	O00425	IGF2BP3	Insulin-like growth factor 2 mRNA-binding protein 3	HUMAN	3	5.03

Appendix A3: List of NS1 interacting host proteins identified in Biological replicate 2									
N	%Cov	%Cov(50)	%Cov(95)	Uniprot	Gene Symbol	Protein	Species	Peptides (95%)	Unused
140	21.2	10.1	8.6	O60832	DKC1	H/ACA ribonucleoprotein complex subunit 4	HUMAN	3	6.14
169	20.4	20.4	12.9	O75367	H2AFY	Core histone macro-H2A.1	HUMAN	3	4.84
185	20.6	16.0	11.9	P07305	H1F0	Histone H1.0	HUMAN	3	4.23
53	8.9	8.9	7.4	P19525	EIF2AK2	Interferon-induced, double-stranded RNA-activated protein kinase	HUMAN	3	6.6
160	24.4	15.0	12.5	P22626	HNRNPA2B1	Heterogeneous nuclear ribonucleoproteins A2/B1	HUMAN	3	5.21
130	21.9	16.5	12.2	P56182	RRP1	Ribosomal RNA processing protein 1 homolog A	HUMAN	3	6.66
69	11.5	9.5	9.5	P83111	LACTB	Serine beta-lactamase-like protein LACTB, mitochondrial	HUMAN	3	4.77
182	21.3	18.7	18.7	Q13151	HNRNPA0	Heterogeneous nuclear ribonucleoprotein A0	HUMAN	3	4.36
206	13.6	6.7	4.6	Q13435	SF3B2	Splicing factor 3B subunit 2	HUMAN	3	3.83
167	11.2	5.6	5.6	Q13823	GNL2	Nucleolar GTP-binding protein 2	HUMAN	3	4.88
147	10.3	6.0	6.0	Q15397	KIAA0020	Pumilio domain-containing protein KIAA0020	HUMAN	3	6
144	7.6	4.2	4.2	Q5JTH9	RRP12	RRP12-like protein	HUMAN	3	6.02
136	33.3	20.7	16.3	Q6DKI1	RPL7L1	60S ribosomal protein L7-like 1	HUMAN	3	6.44
142	28.5	17.2	14.8	Q96G21	IMP4	U3 small nucleolar ribonucleoprotein protein IMP4	HUMAN	3	6.11
127	19.6	16.1	9.8	Q96I24	FUBP3	Far upstream element-binding protein 3	HUMAN	3	6.85
145	15.6	9.7	5.8	Q9BVJ6	UTP14A	U3 small nucleolar RNA-associated protein 14 homolog A	HUMAN	3	6.01
85	20.3	13.8	13.8	Q9GZZ8	LACRT	Extracellular glycoprotein lacritin	HUMAN	3	3.77
134	11.5	5.3	4.4	Q9H0A0	NAT10	N-acetyltransferase 10	HUMAN	3	6.54
224	6.9	4.7	3.8	Q9NWH9	SLTM	SAFB-like transcription modulator	HUMAN	3	3.09
137	14.6	9.9	6.7	Q9NYH9	UTP6	U3 small nucleolar RNA-associated protein 6 homolog	HUMAN	3	6.4
271	16.9	10.2	10.2	Q9P0M6	H2AFY2	Core histone macro-H2A.2	HUMAN	3	4.65
133	44.4	36.5	26.4	Q9Y3C1	NOP16	Nucleolar protein 16	HUMAN	3	6.58
178	6.3	4.2	2.8	O00159	MYO1C	Myosin-Ic	HUMAN	2	4.43
222	11.4	7.7	7.7	O43159	RRP8	Ribosomal RNA-processing protein 8	HUMAN	2	3.32
203	12.1	10.0	8.5	O95758	ROD1	Regulator of differentiation 1	HUMAN	2	4.42
210	17.2	8.0	5.0	O95793	STAU1	Double-stranded RNA-binding protein Staufen homolog 1	HUMAN	2	3.7
229	12.7	12.7	12.7	P04792	HSPB1	Heat shock protein beta-1	HUMAN	2	2.77
68	4.8	1.6	1.0	P15924	DSP	Desmoplakin	HUMAN	2	4.37
95	20.9	20.9	20.9	P18136	KV313	Ig kappa chain V-III region HIC	HUMAN	2	3.17
183	9.8	5.4	4.1	Q13206	DDX10	Probable ATP-dependent RNA helicase DDX10	HUMAN	2	4.29
194	13.2	6.2	6.2	Q14103	HNRNPD	Heterogeneous nuclear ribonucleoprotein D0	HUMAN	2	4
199	2.2	2.2	2.2	Q14151	SAFB2	Scaffold attachment factor B2	HUMAN	2	2.64
155	2.4	2.4	2.4	Q14624	ITIH4	Inter-alpha-trypsin inhibitor heavy chain H4	HUMAN	2	2
180	4.7	2.3	1.4	Q14669	TRIP12	Probable E3 ubiquitin-protein ligase TRIP12	HUMAN	2	4.39
334	31.3	23.4	18.0	Q71UI9	H2AFV	Histone H2A.V	HUMAN	2	3.35
226	17.8	15.3	12.4	Q7Z7K6	CENPV	Centromere protein V	HUMAN	2	2.96
111	5.2	3.2	3.2	Q8IVF2	AHNAK2	Protein AHNAK2	HUMAN	2	2.01
223	9.3	2.6	2.6	Q8IXT5	RBM12B	RNA-binding protein 12B	HUMAN	2	3.11
98	6.3	5.2	5.2	Q8IYB3	SRRM1	Serine/arginine repetitive matrix protein 1	HUMAN	2	2.67
196	6.4	5.0	5.0	Q8WTT2	NOC3L	Nucleolar complex protein 3 homolog	HUMAN	2	4
181	21.6	17.4	12.7	Q92522	H1FX	Histone H1x	HUMAN	2	4.36
77	8.8	3.7	3.7	Q92841	DDX17	Probable ATP-dependent RNA helicase DDX17	HUMAN	2	4.03
99	21.7	21.7	21.7	Q9BTM1	H2AFJ	Histone H2A.J	HUMAN	2	2.8
186	24.7	18.7	16.5	Q9BWF3	RBM4	RNA-binding protein 4	HUMAN	2	4.22
193	4.8	2.1	2.1	Q9H7N4	SCAF1	Splicing factor, arginine/serine-rich 19	HUMAN	2	4

Appendix A3: List of NS1 interacting host proteins identified in Biological replicate 2									
N	%Cov	%Cov(50)	%Cov(95)	Uniprot	Gene Symbol	Protein	Species	Peptides (95%)	Unused
184	29.4	25.0	15.2	Q9NV31	IMP3	U3 small nucleolar ribonucleoprotein protein IMP3	HUMAN	2	4.28
217	7.9	7.9	5.6	Q9NWT1	PAK1IP1	p21-activated protein kinase-interacting protein 1	HUMAN	2	3.47
227	5.7	5.7	5.7	Q9NY61	AATF	Protein AATF	HUMAN	2	2.92
220	2.6	1.5	1.5	Q9UIG0	BAZ1B	Tyrosine-protein kinase BAZ1B	HUMAN	2	3.39
221	12.7	7.9	5.9	Q9UJS0	SLC25A13	Calcium-binding mitochondrial carrier protein Aralar2	HUMAN	2	3.35
209	31.7	31.7	26.1	Q9Y221	NIP7	60S ribosome subunit biogenesis protein NIP7 homolog	HUMAN	2	3.74
189	22.1	15.0	9.3	Q9Y3A4	RRP7A	Ribosomal RNA-processing protein 7 homolog A	HUMAN	2	4.13

Appendix A4: List of NS1 interacting host proteins identified in Biological replicate 3 technical replicate 1

Appendix A4: List of NS1 interacting host proteins identified in Biological replicate 3 technical replicate 1									
N	%Cov	%Cov (50)	%Cov (95)	Uniprot	Gene Symbol	Protein	Species	Peptides (95%)	Unused
4	80.4	52.9	50.0	P07910	HNRNPC	Heterogeneous nuclear ribonucleoproteins C1/C2	HUMAN	69	61.4
3	46.1	40.5	36.0	Q08211	DHX9	ATP-dependent RNA helicase A	HUMAN	59	83.15
2	47.2	43.5	39.2	Q7L2E3	DHX30	Putative ATP-dependent RNA helicase DHX30	HUMAN	53	87.85
5	55.6	48.7	43.2	Q12906	ILF3	Interleukin enhancer-binding factor 3	HUMAN	48	60.93
1	23.4	16.8	13.8	Q15149	PLEC1	Plectin-1	HUMAN	46	94.33
13	41.0	30.3	29.6	Q96KR1	ZFR	Zinc finger RNA-binding protein	HUMAN	34	42.02
22	55.0	38.4	35.3	P14866	HNRNPL	Heterogeneous nuclear ribonucleoprotein L	HUMAN	33	28.44
7	25.6	19.9	17.9	Q6P2Q9	PRPF8	Pre-mRNA-processing-splicing factor 8	HUMAN	29	54.59
12	45.7	33.5	30.6	O43143	DHX15	Putative pre-mRNA-splicing factor ATP-dependent RNA helicase DHX15	HUMAN	28	46.27
8	31.7	23.7	20.5	Q14690	PDCD11	Protein RRP5 homolog	HUMAN	27	56.56
12	44.1	42.8	42.8	O43390	HNRNPR	Heterogeneous nuclear ribonucleoprotein R	HUMAN	27	43.09
18	46.2	37.3	32.2	P52272	HNRNPM	Heterogeneous nuclear ribonucleoprotein M	HUMAN	26	37.44
14	54.7	48.8	42.4	O00567	NOP56	Nucleolar protein 56	HUMAN	24	43.65
14	41.0	41.0	41.0	P61978	HNRNPK	Heterogeneous nuclear ribonucleoprotein K	HUMAN	23	39.03
9	24.3	18.8	14.7	O75643	SNRNP200	U5 small nuclear ribonucleoprotein 200 kDa helicase	HUMAN	23	48.66
17	43.0	32.0	27.4	P43243	MATR3	Matrin-3	HUMAN	22	36.94
20	41.4	34.5	32.3	P46087	NOP2	Putative ribosomal RNA methyltransferase NOP2	HUMAN	22	37.05
15	27.1	20.6	18.1	P55265	ADAR	Double-stranded RNA-specific adenosine deaminase	HUMAN	20	37.77
17	42.0	30.8	29.2	O76021	RSL1D1	Ribosomal L1 domain-containing protein 1	HUMAN	20	37.44
26	49.3	46.4	33.3	Q9UKM9	RALY	RNA-binding protein Raly	HUMAN	20	26.01
25	32.7	24.4	19.0	Q1KMD3	HNRNPUL2	Heterogeneous nuclear ribonucleoprotein U-like protein 2	HUMAN	19	26.64
41	42.8	39.0	37.7	Q12905	ILF2	Interleukin enhancer-binding factor 2	HUMAN	18	26.79
29	32.8	29.2	26.2	Q92841	DDX17	Probable ATP-dependent RNA helicase DDX17	HUMAN	18	29.5
21	32.1	23.3	17.2	Q9P2E9	RRBP1	Ribosome-binding protein 1	HUMAN	18	36.88
31	41.6	35.7	32.9	Q9Y2X3	NOP58	Nucleolar protein 58	HUMAN	17	29.8
98	41.9	35.9	34.2	P52597	HNRNPF	Heterogeneous nuclear ribonucleoprotein F	HUMAN	16	18.27
47	54.6	46.3	43.6	Q15717	ELAVL1	ELAV-like protein 1	HUMAN	15	24.84
28	49.1	35.6	33.8	P38159	RBMX	Heterogeneous nuclear ribonucleoprotein G	HUMAN	15	25.26
43	44.0	32.9	25.8	P11940	PABPC1	Polyadenylate-binding protein 1	HUMAN	15	26.43
32	25.7	23.0	22.9	Q9H0D6	XRN2	5'-3' exoribonuclease 2	HUMAN	14	28.48
42	15.9	9.5	9.5	Q9H583	HEATR1	HEAT repeat-containing protein 1	HUMAN	14	26.58
40	39.6	32.6	22.6	Q9BZE4	GTPBP4	Nucleolar GTP-binding protein 1	HUMAN	14	26.81
29	36.5	23.9	23.5	Q9NR30	DDX21	Nucleolar RNA helicase 2	HUMAN	14	25.03
49	49.5	46.9	46.3	P26599	PTBP1	Polypyrimidine tract-binding protein 1	HUMAN	14	24.28
23	21.9	18.8	17.3	O75533	SF3B1	Splicing factor 3B subunit 1	HUMAN	14	27.91

Appendix A4: List of NS1 interacting host proteins identified in Biological replicate 3 technical replicate 1									
N	%Cov	%Cov (50)	%Cov (95)	Uniprot	Gene Symbol	Protein	Species	Peptides (95%)	Unused
24	25.8	21.9	19.4	Q15029	EFTUD2	116 kDa U5 small nuclear ribonucleoprotein component	HUMAN	13	26.7
62	29.3	22.4	21.3	Q92499	DDX1	ATP-dependent RNA helicase DDX1	HUMAN	13	21.38
44	38.3	26.9	25.0	Q5SSJ5	HP1BP3	Heterochromatin protein 1-binding protein 3	HUMAN	13	25.87
57	40.5	22.4	21.0	Q9NVP1	DDX18	ATP-dependent RNA helicase DDX18	HUMAN	12	22.19
19	39.0	31.7	24.3	Q9NZI8	IGF2BP1	Insulin-like growth factor 2 mRNA-binding protein 1	HUMAN	12	20.61
66	43.8	39.2	31.3	Q9Y3I0	C22orf28	UPF0027 protein C22orf28	HUMAN	12	20.52
45	29.8	25.5	21.1	Q8NI36	WDR36	WD repeat-containing protein 36	HUMAN	12	25.61
81	50.7	36.8	36.1	Q02878	RPL6	60S ribosomal protein L6	HUMAN	11	17.38
65	29.2	22.6	20.5	Q9GZR7	DDX24	ATP-dependent RNA helicase DDX24	HUMAN	11	20.93
61	36.9	27.1	27.1	Q96I24	FUBP3	Far upstream element-binding protein 3	HUMAN	11	21.46
70	30.0	24.4	18.3	O60506	SYNCRIP	Heterogeneous nuclear ribonucleoprotein Q	HUMAN	11	17.7
76	39.4	33.7	31.2	P22626	HNRNPA 2B1	Heterogeneous nuclear ribonucleoproteins A2/B1	HUMAN	11	18.47
273	35.4	35.4	35.4	Q8IUE6	HIST2H2 AB	Histone H2A type 2-B	HUMAN	11	10.21
54	39.9	28.0	23.2	O15226	NKRF	NF-kappa-B-repressing factor	HUMAN	11	22.84
72	41.9	27.4	20.6	Q14684	RRP1B	Ribosomal RNA processing protein 1 homolog B	HUMAN	11	18.98
68	23.3	15.1	14.2	Q9NWH9	SLTM	SAFB-like transcription modulator	HUMAN	11	20.01
71	35.1	31.1	26.6	P07437	TUBB	Tubulin beta chain	HUMAN	11	19.06
196	37.4	25.4	24.1	P55795	HNRNPH 2	Heterogeneous nuclear ribonucleoprotein H2	HUMAN	10	12.4
102	16.6	14.1	13.1	Q9BUJ2	HNRNPU L1	Heterogeneous nuclear ribonucleoprotein U-like protein 1	HUMAN	10	13.58
82	24.8	24.8	24.8	P16401	HIST1H1 B	Histone H1.5	HUMAN	10	17.07
46	24.2	22.4	20.2	Q9UMS4	PRPF19	Pre-mRNA-processing factor 19	HUMAN	10	16.95
64	13.7	8.3	6.9	Q14669	TRIP12	Probable E3 ubiquitin-protein ligase TRIP12	HUMAN	10	21.08
63	37.9	26.2	19.4	Q8IY81	FTSJ3	Putative rRNA methyltransferase 3	HUMAN	10	21.22
77	23.6	18.4	15.7	Q9NW13	RBM28	RNA-binding protein 28	HUMAN	10	18.29
36	29.1	17.0	15.3	Q14151	SAFB2	Scaffold attachment factor B2	HUMAN	10	20.4
95	29.3	21.9	19.1	Q9Y5J1	UTP18	U3 small nucleolar RNA-associated protein 18 homolog	HUMAN	10	15.09
73	36.7	35.5	25.3	P39023	RPL3	60S ribosomal protein L3	HUMAN	9	18.72
117	29.0	17.4	12.7	O00571	DDX3X	ATP-dependent RNA helicase DDX3X	HUMAN	9	14.93
45	38.7	27.3	27.3	P38919	EIF4A3	Eukaryotic initiation factor 4A-III	HUMAN	9	17.1
37	25.9	24.2	20.0	O00425	IGF2BP3	Insulin-like growth factor 2 mRNA-binding protein 3	HUMAN	9	17.24
79	19.3	9.1	7.2	Q14980	NUMA1	Nuclear mitotic apparatus protein 1	HUMAN	9	17.94
43	27.1	18.3	16.2	Q13435	SF3B2	Splicing factor 3B subunit 2	HUMAN	9	17.43
417	32.4	28.3	20.5	P68371	TUBB2C	Tubulin beta-2C chain	HUMAN	9	14.86
74	22.8	17.7	11.7	Q9UNX4	WDR3	WD repeat-containing protein 3	HUMAN	9	18.64
86	30.7	24.3	20.5	O15213	WDR46	WD repeat-containing protein 46	HUMAN	9	16.71
92	32.3	32.3	25.9	P62424	RPL7A	60S ribosomal protein L7a	HUMAN	8	15.34
20	42.9	34.7	23.3	P51991	HNRNPA 3	Heterogeneous nuclear ribonucleoprotein A3	HUMAN	8	17.75
90	55.2	49.9	35.1	Q8TDN6	BRIX1	Ribosome biogenesis protein BRX1 homolog	HUMAN	8	15.72

Appendix A4: List of NS1 interacting host proteins identified in Biological replicate 3 technical replicate 1									
N	%Cov	%Cov (50)	%Cov (95)	Uniprot	Gene Symbol	Protein	Species	Peptides (95%)	Unused
101	31.7	31.4	25.8	Q9H7B2	RPF2	Ribosome production factor 2 homolog	HUMAN	8	13.61
91	12.9	10.4	8.4	Q13523	PRPF4B	Serine/threonine-protein kinase PRP4 homolog	HUMAN	8	15.43
54	36.2	20.5	18.7	Q13573	SNW1	SNW domain-containing protein 1	HUMAN	8	14.6
89	29.4	18.5	15.7	P23246	SFPQ	Splicing factor, proline- and glutamine-rich	HUMAN	8	16.73
103	47.5	34.4	34.4	Q9Y224	C14orf166	UPF0568 protein C14orf166	HUMAN	8	13.56
93	25.8	18.5	14.3	O75152	ZC3H11A	Zinc finger CCCH domain-containing protein 11A	HUMAN	8	15.3
84	21.5	15.4	12.5	Q7Z2W4	ZC3HAV1	Zinc finger CCCH-type antiviral protein 1	HUMAN	8	16.91
73	21.2	19.8	14.7	Q9NUL3	STAU2	Double-stranded RNA-binding protein Staufen homolog 2	HUMAN	7	11.44
193	14.6	13.0	12.7	P54652	HSPA2	Heat shock-related 70 kDa protein 2	HUMAN	7	13.36
76	31.2	21.8	19.9	P09651	HNRNPA 1	Heterogeneous nuclear ribonucleoprotein A1	HUMAN	7	11.03
114	17.4	14.6	12.1	Q9H8H0	NOL11	Nucleolar protein 11	HUMAN	7	12.65
109	14.4	10.2	9.2	Q9H6R4	NOL6	Nucleolar protein 6	HUMAN	7	13.17
112	34.9	18.0	12.1	P19338	NCL	Nucleolin	HUMAN	7	12.97
119	22.6	14.3	12.4	O00541	PES1	Pescadillo homolog	HUMAN	7	12.5
320	30.0	22.2	13.7	Q13310	PABPC4	Polyadenylate-binding protein 4	HUMAN	7	14.6
116	45.4	29.1	25.8	Q99848	EBNA1BP 2	Probable rRNA-processing protein EBP2	HUMAN	7	12.59
31	8.0	7.7	7.7	Q92900	UPF1	Regulator of nonsense transcripts 1	HUMAN	7	14
94	14.7	7.4	4.5	Q7Z6E9	RBBP6	Retinoblastoma-binding protein 6	HUMAN	7	15.15
85	21.5	12.4	6.9	Q14692	BMS1	Ribosome biogenesis protein BMS1 homolog	HUMAN	7	16.75
97	26.8	16.1	16.1	Q14137	BOP1	Ribosome biogenesis protein BOP1	HUMAN	7	14.19
151	34.5	23.6	18.1	Q15050	RRS1	Ribosome biogenesis regulatory protein homolog	HUMAN	7	9.17
108	30.3	20.5	14.2	Q96PK6	RBM14	RNA-binding protein 14	HUMAN	7	13.26
139	19.4	12.7	8.1	Q15424	SAFB	Scaffold attachment factor B1	HUMAN	7	15.68
64	13.2	9.9	8.4	Q15393	SF3B3	Splicing factor 3B subunit 3	HUMAN	7	13.05
60	48.4	37.6	34.4	Q13242	SFRS9	Splicing factor, arginine/serine-rich 9	HUMAN	7	13.74
111	12.7	10.4	8.2	P42285	SKIV2L2	Superkiller viralicidic activity 2-like 2	HUMAN	7	13.01
88	29.5	26.4	24.6	Q71U36	TUBA1A	Tubulin alpha-1A chain	HUMAN	7	13.96
417	22.3	22.3	16.2	P04350	TUBB4	Tubulin beta-4 chain	HUMAN	7	9.53
110	21.8	14.7	13.6	Q9NYH9	UTP6	U3 small nucleolar RNA-associated protein 6 homolog	HUMAN	7	13.09
137	55.9	49.3	41.2	P61353	RPL27	60S ribosomal protein L27	HUMAN	6	10.64
81	15.1	7.5	7.5	Q9UKV3	ACIN1	Apoptotic chromatin condensation inducer in the nucleus	HUMAN	6	10.06
106	29.9	21.6	16.0	Q969X6	CIRH1A	Cirhin	HUMAN	6	13.36
65	25.0	18.2	16.3	P19525	EIF2AK2	Interferon-induced, double-stranded RNA-activated protein kinase	HUMAN	6	12.89
113	27.8	22.0	19.2	P42167	TMPO	Lamina-associated polypeptide 2, isoforms beta/gamma	HUMAN	6	12.74
124	25.9	25.9	25.9	Q9BYG3	MKI67IP	MKI67 FHA domain-interacting nucleolar phosphoprotein	HUMAN	6	11.84
128	14.9	11.5	8.8	Q15269	PWP2	Periodic tryptophan protein 2 homolog	HUMAN	6	11.52
104	41.0	28.4	18.3	Q1ED39	C16orf88	Protein C16orf88	HUMAN	6	13.53
120	25.0	13.5	11.8	Q96T37	RBM15	Putative RNA-binding protein 15	HUMAN	6	12.18

Appendix A4: List of NS1 interacting host proteins identified in Biological replicate 3 technical replicate 1									
N	%Cov	%Cov (50)	%Cov (95)	Uniprot	Gene Symbol	Protein	Species	Peptides (95%)	Unused
148	27.8	23.2	21.7	P56182	RRP1	Ribosomal RNA processing protein 1 homolog A	HUMAN	6	9.28
75	35.9	35.9	29.4	Q07955	SFRS1	Splicing factor, arginine/serine-rich 1	HUMAN	6	11.78
91	45.7	35.4	31.1	P84103	SFRS3	Splicing factor, arginine/serine-rich 3	HUMAN	6	10.62
115	13.1	7.4	5.3	Q13428	TCOF1	Treacle protein	HUMAN	6	12.4
357	26.1	23.0	21.2	P68366	TUBA4A	Tubulin alpha-4A chain	HUMAN	6	12.25
126	35.7	21.7	16.9	P08621	SNRNP70	U1 small nuclear ribonucleoprotein 70 kDa	HUMAN	6	11.58
123	16.7	10.5	10.5	Q9BVJ6	UTP14A	U3 small nucleolar RNA-associated protein 14 homolog A	HUMAN	6	11.86
184	35.5	22.2	17.0	Q8TED0	UTP15	U3 small nucleolar RNA-associated protein 15 homolog	HUMAN	6	6.6
159	23.3	21.6	16.0	Q15061	WDR43	WD repeat-containing protein 43	HUMAN	6	8.33
155	32.1	32.1	20.7	P62829	RPL23	60S ribosomal protein L23	HUMAN	5	8.8
146	42.7	34.4	34.4	P32969	RPL9	60S ribosomal protein L9	HUMAN	5	9.43
152	33.1	24.5	21.8	O75367	H2AFY	Core histone macro-H2A.1	HUMAN	5	9.07
138	25.8	16.7	10.3	Q5QJE6	DNTTIP2	Deoxynucleotidyltransferase terminal-interacting protein 2	HUMAN	5	10.49
140	19.6	11.5	8.0	P11387	TOP1	DNA topoisomerase 1	HUMAN	5	10.23
176	18.2	18.0	15.7	O15446	CD3EAP	DNA-directed RNA polymerase I subunit RPA34	HUMAN	5	7.2
85	26.7	15.1	11.6	O95793	STAU1	Double-stranded RNA-binding protein Staufen homolog 1	HUMAN	5	9.86
134	27.8	18.5	14.6	O60832	DKC1	H/ACA ribonucleoprotein complex subunit 4	HUMAN	5	10.8
230	20.6	13.9	10.3	P08107	HSPA1A	Heat shock 70 kDa protein 1A/1B	HUMAN	5	10.38
230	10.3	10.3	10.3	P34931	HSPA1L	Heat shock 70 kDa protein 1-like	HUMAN	5	10
88	31.8	26.9	24.3	Q13151	HNRNPA0	Heterogeneous nuclear ribonucleoprotein A0	HUMAN	5	9.15
188	20.6	20.6	16.5	P07305	H1F0	Histone H1.0	HUMAN	5	6.25
259	31.3	31.3	31.3	Q71UI9	H2AFV	Histone H2A.V	HUMAN	5	6.96
259	31.3	31.3	31.3	P0C0S5	H2AFZ	Histone H2A.Z	HUMAN	5	6.96
59	16.5	15.8	11.7	Q07666	KHDRBS1	KH domain-containing, RNA-binding, signal transduction-associated protein 1	HUMAN	5	7.85
71	11.7	8.7	4.7	Q9BQG0	MYBBP1A	Myb-binding protein 1A	HUMAN	5	11.75
131	13.8	13.8	13.8	Q9NW64	RBM22	Pre-mRNA-splicing factor RBM22	HUMAN	5	4.86
105	11.0	6.5	5.7	Q9HCS7	XAB2	Pre-mRNA-splicing factor SYF1	HUMAN	5	6.77
136	16.8	11.7	8.7	Q96GQ7	DDX27	Probable ATP-dependent RNA helicase DDX27	HUMAN	5	10.71
147	23.3	22.3	22.3	Q9BXY0	MAK16	Protein MAK16 homolog	HUMAN	5	9.39
180	14.7	13.0	13.0	O95758	ROD1	Regulator of differentiation 1	HUMAN	5	8.43
158	20.1	7.4	7.4	Q96SI9	STRBP	Spermatid perinuclear RNA-binding protein	HUMAN	5	9.69
141	21.5	9.7	7.5	Q12788	TBL3	Transducin beta-like protein 3	HUMAN	5	10.19
90	36.2	21.6	18.1	Q13595	TRA2A	Transformer-2 protein homolog alpha	HUMAN	5	8.55
157	19.7	8.5	7.3	O15042	SR140	U2-associated protein SR140	HUMAN	5	8.53
133	21.9	16.2	9.9	O43818	RRP9	U3 small nucleolar RNA-interacting protein 2	HUMAN	5	11.04
121	26.6	15.5	8.3	Q8IWA0	WDR75	WD repeat-containing protein 75	HUMAN	5	12.14
95	24.5	13.3	9.8	Q6PJT7	ZC3H14	Zinc finger CCCH domain-containing protein 14	HUMAN	5	7.92
158	20.3	16.0	10.6	Q5BKZ1	ZNF326	Zinc finger protein 326	HUMAN	5	8.37

Appendix A4: List of NS1 interacting host proteins identified in Biological replicate 3 technical replicate 1									
N	%Cov	%Cov (50)	%Cov (95)	Uniprot	Gene Symbol	Protein	Species	Peptides (95%)	Unused
225	28.6	28.6	28.6	P62847	RPS24	40S ribosomal protein S24	HUMAN	4	4.81
166	39.7	25.0	19.6	P18621	RPL17	60S ribosomal protein L17	HUMAN	4	7.73
173	31.5	18.3	15.6	P62917	RPL8	60S ribosomal protein L8	HUMAN	4	7.32
202	38.3	23.9	23.9	Q9Y221	NIP7	60S ribosome subunit biogenesis protein NIP7 homolog	HUMAN	4	5.8
171	13.0	5.4	5.4	Q03701	CEBPZ	CCAAT/enhancer-binding protein zeta	HUMAN	4	7.44
255	32.6	18.8	13.1	P56537	EIF6	Eukaryotic translation initiation factor 6	HUMAN	4	4.01
153	22.4	15.9	11.3	Q9BVP2	GNL3	Guanine nucleotide-binding protein-like 3	HUMAN	4	8.98
189	14.5	5.1	5.1	O43795	MYO1B	Myosin-Ib	HUMAN	4	6.23
175	16.1	9.5	5.3	Q9H0A0	NAT10	N-acetyltransferase 10	HUMAN	4	7.26
216	37.5	18.8	18.8	P55769	NHP2L1	NHP2-like protein 1	HUMAN	4	5.14
160	11.1	7.5	7.5	Q13206	DDX10	Probable ATP-dependent RNA helicase DDX10	HUMAN	4	8.05
142	8.8	3.2	2.4	P18583	SON	Protein SON	HUMAN	4	8.16
103	12.7	7.7	5.6	Q8IX01	SFRS14	Putative splicing factor, arginine/serine-rich 14	HUMAN	4	6.86
161	20.2	13.8	13.8	O43159	RRP8	Ribosomal RNA-processing protein 8	HUMAN	4	8.02
164	39.8	21.2	19.0	Q9BWF3	RBM4	RNA-binding protein 4	HUMAN	4	7.82
212	8.1	3.8	3.2	Q5JTH9	RRP12	RRP12-like protein	HUMAN	4	5.4
100	25.6	19.4	14.2	Q96HS1	PGAM5	Serine/threonine-protein phosphatase PGAM5, mitochondrial	HUMAN	4	7.22
191	15.9	15.9	15.6	P62140	PPP1CB	Serine/threonine-protein phosphatase PP1-beta catalytic subunit	HUMAN	4	6.21
174	13.4	2.8	2.8	Q8NI27	THOC2	THO complex subunit 2	HUMAN	4	7.28
417	10.6	10.6	8.8	Q3ZCM7	TUBB8	Tubulin beta-8 chain	HUMAN	4	5.87
275	18.8	10.4	10.4	O00566	MPHOSPH10	U3 small nucleolar ribonucleoprotein protein MPP10	HUMAN	4	3.88
93	33.9	28.0	28.0	Q96DI7	SNRNP40	U5 small nuclear ribonucleoprotein 40 kDa protein	HUMAN	4	8.03
163	16.6	16.6	8.5	Q14103	HNRNPD	Heterogeneous nuclear ribonucleoprotein D0	HUMAN	3	5.38
224	32.2	24.5	19.2	P62241	RPS8	40S ribosomal protein S8	HUMAN	3	4.82
221	34.3	18.1	18.1	P61313	RPL15	60S ribosomal protein L15	HUMAN	3	4.97
289	17.4	10.4	10.4	P62888	RPL30	60S ribosomal protein L30	HUMAN	3	3.44
208	31.0	15.2	15.2	P46777	RPL5	60S ribosomal protein L5	HUMAN	3	5.48
185	38.7	25.4	17.7	P18124	RPL7	60S ribosomal protein L7	HUMAN	3	6.6
219	31.7	14.2	14.2	Q6DKI1	RPL7L1	60S ribosomal protein L7-like 1	HUMAN	3	5.02
63	8.3	8.3	8.3	P23526	AHCY	Adenosylhomocysteinase	HUMAN	3	6
222	13.3	13.3	13.3	Q04828	AKR1C1	Aldo-keto reductase family 1 member C1	HUMAN	3	4.92
186	15.5	11.0	7.7	O00148	DDX39	ATP-dependent RNA helicase DDX39	HUMAN	3	6.51
475	16.6	6.6	3.7	Q9BQ39	DDX50	ATP-dependent RNA helicase DDX50	HUMAN	3	4.55
104	17.6	12.0	7.5	Q99459	CDC5L	Cell division cycle 5-like protein	HUMAN	3	6.83
201	25.8	20.0	17.1	Q7Z7K6	CENPV	Centromere protein V	HUMAN	3	5.84
89	3.4	3.4	3.4	Q9NZB2	FAM120A	Constitutive coactivator of PPAR-gamma-like protein 1	HUMAN	3	4.59
220	23.8	9.4	9.4	Q9NV06	DCAF13	DDB1- and CUL4-associated factor 13	HUMAN	3	5.01
282	4.8	1.5	0.8	P78527	PRKDC	DNA-dependent protein kinase catalytic subunit	HUMAN	3	3.73

Appendix A4: List of NS1 interacting host proteins identified in Biological replicate 3 technical replicate 1									
N	%Cov	%Cov (50)	%Cov (95)	Uniprot	Gene Symbol	Protein	Species	Peptides (95%)	Unused
260	14.3	10.6	10.6	P60842	EIF4A1	Eukaryotic initiation factor 4A-I	HUMAN	3	6
311	8.9	7.6	6.3	P51114	FXR1	Fragile X mental retardation syndrome-related protein 1	HUMAN	3	2.9
121	16.3	12.0	8.7	Q99729	HNRNPAB	Heterogeneous nuclear ribonucleoprotein A/B	HUMAN	3	3.05
114	8.3	5.5	5.5	O14979	HNRPDL	Heterogeneous nuclear ribonucleoprotein D-like	HUMAN	3	6.05
217	18.5	12.4	12.4	P31942	HNRNPH3	Heterogeneous nuclear ribonucleoprotein H3	HUMAN	3	5.07
248	35.3	23.5	23.5	O00422	SAP18	Histone deacetylase complex subunit SAP18	HUMAN	3	4.18
251	25.0	19.9	14.7	P68431	HIST1H3A	Histone H3.1	HUMAN	3	4.12
251	27.2	19.9	14.7	Q16695	HIST3H3	Histone H3.1t	HUMAN	3	4.12
251	25.0	19.9	14.7	Q71DI3	HIST2H3A	Histone H3.2	HUMAN	3	4.12
251	25.0	19.9	14.7	P84243	H3F3A	Histone H3.3	HUMAN	3	4.12
319	12.5	8.6	6.0	Q4G0J3	LARP7	La-related protein 7	HUMAN	3	2.53
204	12.7	6.1	5.2	O00159	MYO1C	Myosin-Ic	HUMAN	3	5.67
287	12.0	7.9	5.2	Q14978	NOLC1	Nucleolar and coiled-body phosphoprotein 1	HUMAN	3	3.53
307	16.0	6.0	6.0	Q9BSC4	NOL10	Nucleolar protein 10	HUMAN	3	2.76
281	28.7	28.7	22.5	Q9Y3C1	NOP16	Nucleolar protein 16	HUMAN	3	3.74
198	20.6	16.7	16.7	Q9UMY1	NOL7	Nucleolar protein 7	HUMAN	3	6
74	7.4	6.0	6.0	O75127	PTCD1	Pentatricopeptide repeat-containing protein 1	HUMAN	3	4.82
60	13.4	7.7	7.7	P51659	HSD17B4	Peroxisomal multifunctional enzyme type 2	HUMAN	3	6.06
190	19.6	13.2	10.8	Q9H0S4	DDX47	Probable ATP-dependent RNA helicase DDX47	HUMAN	3	6.21
228	39.3	22.9	22.9	P07737	PFN1	Profilin-1	HUMAN	3	4.65
218	5.6	2.4	1.8	Q8WYP5	AHCTF1	Protein ELYS	HUMAN	3	5.02
242	18.9	14.0	9.9	Q9GZL7	WDR12	Ribosome biogenesis protein WDR12	HUMAN	3	4.27
223	24.6	10.2	10.2	Q9GZR2	REXO4	RNA exonuclease 4	HUMAN	3	4.84
151	9.3	7.2	7.2	P35637	FUS	RNA-binding protein FUS	HUMAN	3	4
116	8.6	6.1	6.1	Q15459	SF3A1	Splicing factor 3A subunit 1	HUMAN	3	6.04
141	20.2	8.0	6.2	Q12874	SF3A3	Splicing factor 3A subunit 3	HUMAN	3	4.27
200	6.6	2.3	2.3	Q9H7N4	SCAF1	Splicing factor, arginine/serine-rich 19	HUMAN	3	5.92
209	23.0	12.2	9.6	Q13247	SFRS6	Splicing factor, arginine/serine-rich 6	HUMAN	3	5.48
124	23.1	23.1	16.4	Q16629	SFRS7	Splicing factor, arginine/serine-rich 7	HUMAN	3	5.57
206	20.5	10.1	8.5	Q9NQ55	PPAN	Suppressor of SWI4 1 homolog	HUMAN	3	5.59
194	9.2	4.8	3.9	O60264	SMARCA5	SWI/SNF-related matrix-associated actin-dependent regulator of chromatin subfamily A member 5	HUMAN	3	6.1
199	14.7	12.6	12.6	Q13148	TARDBP	TAR DNA-binding protein 43	HUMAN	3	5.96
227	4.5	4.5	4.5	Q9NXF1	TEX10	Testis-expressed sequence 10 protein	HUMAN	3	4.79
211	22.0	14.4	14.4	Q86W42	THOC6	THO complex subunit 6 homolog	HUMAN	3	5.43
123	15.3	14.9	14.9	P09661	SNRPA1	U2 small nuclear ribonucleoprotein A'	HUMAN	3	5.4
203	14.1	6.1	4.4	Q9P275	USP36	Ubiquitin carboxyl-terminal hydrolase 36	HUMAN	3	5.75
197	30.4	15.5	15.5	Q9Y277	VDAC3	Voltage-dependent anion-selective channel protein 3	HUMAN	3	6.01
107	6.3	3.9	2.0	P49750	YLPM1	YLP motif-containing protein 1	HUMAN	3	6.7

Appendix A4: List of NS1 interacting host proteins identified in Biological replicate 3 technical replicate 1									
N	%Cov	%Cov (50)	%Cov (95)	Uniprot	Gene Symbol	Protein	Species	Peptides (95%)	Unused
207	6.6	5.6	5.6	Q96MU7	YTHDC1	YTH domain-containing protein 1	HUMAN	3	5.57
236	6.4	3.3	2.6	Q14966	ZNF638	Zinc finger protein 638	HUMAN	3	4.39
97	17.6	11.1	6.5	P51398	DAP3	28S ribosomal protein S29, mitochondrial	HUMAN	2	3.49
100	8.1	8.1	6.1	P82933	MRPS9	28S ribosomal protein S9, mitochondrial	HUMAN	2	3.14
85	20.6	11.5	11.5	Q9P015	MRPL15	39S ribosomal protein L15, mitochondrial	HUMAN	2	4
168	26.9	18.5	18.5	P62244	RPS15A	40S ribosomal protein S15a	HUMAN	2	2.83
105	7.9	7.9	7.9	P15880	RPS2	40S ribosomal protein S2	HUMAN	2	2.79
90	12.6	12.6	12.6	P60866	RPS20	40S ribosomal protein S20	HUMAN	2	4
271	15.4	15.4	15.4	P62266	RPS23	40S ribosomal protein S23	HUMAN	2	4
104	33.9	20.9	20.9	P62854	RPS26	40S ribosomal protein S26	HUMAN	2	2.88
173	11.1	11.1	11.1	P23396	RPS3	40S ribosomal protein S3	HUMAN	2	2.55
317	24.3	11.4	11.4	P62701	RPS4X	40S ribosomal protein S4, X isoform	HUMAN	2	2.57
302	21.5	11.2	11.2	P27635	RPL10	60S ribosomal protein L10	HUMAN	2	2.93
265	29.2	25.3	12.9	P62913	RPL11	60S ribosomal protein L11	HUMAN	2	4
272	14.6	14.6	14.6	P30050	RPL12	60S ribosomal protein L12	HUMAN	2	4
258	14.9	11.2	11.2	P50914	RPL14	60S ribosomal protein L14	HUMAN	2	4.01
237	21.8	21.8	14.1	P62750	RPL23A	60S ribosomal protein L23a	HUMAN	2	4.39
378	13.4	8.3	8.3	P83731	RPL24	60S ribosomal protein L24	HUMAN	2	2
276	17.6	16.2	16.2	P46776	RPL27A	60S ribosomal protein L27a	HUMAN	2	3.85
294	20.7	20.7	15.7	P47914	RPL29	60S ribosomal protein L29	HUMAN	2	3.28
239	27.6	20.9	12.4	Q9Y3U8	RPL36	60S ribosomal protein L36	HUMAN	2	4.38
267	6.6	4.8	4.8	Q9NRG9	AAAS	Aladin	HUMAN	2	4
222	12.7	9.6	9.6	P52895	AKR1C2	Aldo-keto reductase family 1 member C2	HUMAN	2	2.78
222	10.8	6.5	6.5	P42330	AKR1C3	Aldo-keto reductase family 1 member C3	HUMAN	2	2.72
222	6.5	6.5	6.5	P17516	AKR1C4	Aldo-keto reductase family 1 member C4	HUMAN	2	2.72
437	11.0	4.4	4.4	Q16352	INA	Alpha-internexin	HUMAN	2	2.27
293	7.4	5.7	5.7	Q96CW1	AP2M1	AP-2 complex subunit mu	HUMAN	2	3.3
279	16.2	4.0	3.0	Q8TDD1	DDX54	ATP-dependent RNA helicase DDX54	HUMAN	2	3.78
264	16.1	7.7	7.7	Q9NX58	LYAR	Cell growth-regulating nucleolar protein	HUMAN	2	4
135	7.1	3.4	2.0	Q10570	CPSF1	Cleavage and polyadenylation specificity factor subunit 1	HUMAN	2	4.56
244	9.9	8.2	5.0	P38432	COIL	Coilin	HUMAN	2	4.27
172	4.6	2.6	2.6	Q9BZJ0	CRNKL1	Crooked neck-like protein 1	HUMAN	2	2.62
299	27.0	27.0	27.0	P63167	DYNLL1	Dynein light chain 1, cytoplasmic	HUMAN	2	2.99
130	9.8	4.0	4.0	Q14258	TRIM25	E3 ubiquitin/ISG15 ligase TRIM25	HUMAN	2	2.62
167	5.6	5.6	5.6	Q05639	EEF1A2	Elongation factor 1-alpha 2	HUMAN	2	2.94
296	11.8	8.7	8.7	P50402	EMD	Emerin	HUMAN	2	3.21
260	7.1	7.1	7.1	Q14240	EIF4A2	Eukaryotic initiation factor 4A-II	HUMAN	2	4
310	11.0	3.7	2.5	Q01780	EXOSC10	Exosome component 10	HUMAN	2	2.71
117	13.3	6.3	5.1	Q06787	FMR1	Fragile X mental retardation 1 protein	HUMAN	2	3.55

Appendix A4: List of NS1 interacting host proteins identified in Biological replicate 3 technical replicate 1									
N	%Cov	%Cov (50)	%Cov (95)	Uniprot	Gene Symbol	Protein	Species	Peptides (95%)	Unused
321	18.0	5.9	4.8	P51116	FXR2	Fragile X mental retardation syndrome-related protein 2	HUMAN	2	2.55
295	11.9	7.0	4.3	Q5T3I0	GPATCH4	G patch domain-containing protein 4	HUMAN	2	3.27
176	4.2	4.2	4.2	Q9NZM5	GLTSCR2	Glioma tumor suppressor candidate region gene 2 protein	HUMAN	2	2.45
107	17.3	5.6	5.6	Q12849	GRSF1	G-rich sequence factor 1	HUMAN	2	2.64
92	12.7	12.7	12.7	P04792	HSPB1	Heat shock protein beta-1	HUMAN	2	4
292	7.5	7.5	7.5	Q92522	H1FX	Histone H1x	HUMAN	2	3.34
79	35.4	35.4	21.5	P0C0S8	HIST1H2AG	Histone H2A type 1	HUMAN	2	4.4
79	32.1	26.7	21.4	Q96QV6	HIST1H2AA	Histone H2A type 1-A	HUMAN	2	4.27
79	32.3	26.9	21.5	P04908	HIST1H2AB	Histone H2A type 1-B/E	HUMAN	2	4.27
79	32.3	26.9	21.5	Q93077	HIST1H2AC	Histone H2A type 1-C	HUMAN	2	4.27
79	35.4	35.4	21.5	P20671	HIST1H2AD	Histone H2A type 1-D	HUMAN	2	4.4
79	35.9	35.9	21.9	Q96KK5	HIST1H2AH	Histone H2A type 1-H	HUMAN	2	4.4
79	35.9	35.9	21.9	Q99878	HIST1H2AJ	Histone H2A type 1-J	HUMAN	2	4.4
79	35.4	35.4	21.5	Q6FI13	HIST2H2AA3	Histone H2A type 2-A	HUMAN	2	4.4
79	35.7	35.7	21.7	Q16777	HIST2H2AC	Histone H2A type 2-C	HUMAN	2	4.4
79	32.3	26.9	21.5	Q7L7L0	HIST3H2A	Histone H2A type 3	HUMAN	2	4.27
79	35.7	35.7	21.7	Q9BTM1	H2AFJ	Histone H2A.J	HUMAN	2	4.4
79	29.4	24.5	19.6	P16104	H2AFX	Histone H2A.x	HUMAN	2	4.27
269	4.5	4.5	4.5	Q9Y6M1	IGF2BP2	Insulin-like growth factor 2 mRNA-binding protein 2	HUMAN	2	2.53
263	20.4	8.5	8.5	Q9H9L3	ISG20L2	Interferon-stimulated 20 kDa exonuclease-like 2	HUMAN	2	4
154	19.1	9.3	7.5	P55081	MFAP1	Microfibrillar-associated protein 1	HUMAN	2	3.9
315	22.4	10.3	10.3	Q9BU76	MMTAG2	Multiple myeloma tumor-associated protein 2	HUMAN	2	2.61
120	8.9	4.7	4.7	Q15233	NONO	Non-POU domain-containing octamer-binding protein	HUMAN	2	3.47
298	8.6	5.7	3.9	Q09161	NCBP1	Nuclear cap-binding protein subunit 1	HUMAN	2	3.05
127	6.2	3.6	3.6	Q7Z417	NUFIP2	Nuclear fragile X mental retardation-interacting protein 2	HUMAN	2	2.96
240	12.9	6.9	4.5	Q9UBU9	NXF1	Nuclear RNA export factor 1	HUMAN	2	4.36
318	8.8	4.0	4.0	Q13823	GNL2	Nucleolar GTP-binding protein 2	HUMAN	2	2.57
304	19.1	9.9	7.7	Q9NWT1	PAK1IP1	p21-activated protein kinase-interacting protein 1	HUMAN	2	2.92
313	4.6	3.7	3.7	Q13427	PPIG	Peptidyl-prolyl cis-trans isomerase G	HUMAN	2	2.65
273	13.4	3.9	3.9	Q9H307	PNN	Pinin	HUMAN	2	3.92
257	19.4	10.7	10.7	Q15365	PCBP1	Poly(rC)-binding protein 1	HUMAN	2	4.01
125	10.1	5.4	4.1	Q9H361	PABPC3	Polyadenylate-binding protein 3	HUMAN	2	4.24
270	20.8	20.8	20.8	Q9Y3B4	SF3B14	Pre-mRNA branch site protein p14	HUMAN	2	4
314	9.9	4.3	2.5	O75400	PRPF40A	Pre-mRNA-processing factor 40 homolog A	HUMAN	2	2.62
150	11.6	11.6	11.6	O75934	BCAS2	Pre-mRNA-splicing factor SPF27	HUMAN	2	4
101	6.7	3.9	3.9	Q9NUL7	DDX28	Probable ATP-dependent RNA helicase DDX28	HUMAN	2	3.08
284	10.7	4.5	3.5	Q9H8H2	DDX31	Probable ATP-dependent RNA helicase DDX31	HUMAN	2	3.66
96	6.4	6.4	6.4	Q99873	PRMT1	Protein arginine N-methyltransferase 1	HUMAN	2	3.64

Appendix A4: List of NS1 interacting host proteins identified in Biological replicate 3 technical replicate 1									
N	%Cov	%Cov (50)	%Cov (95)	Uniprot	Gene Symbol	Protein	Species	Peptides (95%)	Unused
249	7.7	7.5	5.2	Q8NCA5	FAM98A	Protein FAM98A	HUMAN	2	4.16
108	8.8	8.8	8.8	Q96PU8	QKI	Protein quaking	HUMAN	2	2.6
87	13.1	6.7	6.7	Q14568	HSP90AA2	Putative heat shock protein HSP 90-alpha A2	HUMAN	2	4.01
283	12.8	6.4	6.4	Q9Y383	LUC7L2	Putative RNA-binding protein Luc7-like 2	HUMAN	2	3.68
417	7.6	7.6	5.8	Q99867	TUBB4Q	Putative tubulin beta-4q chain	HUMAN	2	3.6
286	26.6	10.9	10.9	Q9H9Y2	RPF1	Ribosome production factor 1	HUMAN	2	3.59
235	32.6	21.4	7.7	P42696	RBM34	RNA-binding protein 34	HUMAN	2	4.45
106	4.9	4.9	4.9	Q14498	RBM39	RNA-binding protein 39	HUMAN	2	2.68
134	11.1	5.0	5.0	Q9BQ04	RBM4B	RNA-binding protein 4B	HUMAN	2	2.27
346	36.8	25.9	25.9	Q9Y5S9	RBM8A	RNA-binding protein 8A	HUMAN	2	2.02
89	10.2	10.2	10.2	Q15287	RNPS1	RNA-binding protein with serine-rich domain 1	HUMAN	2	4
247	14.5	9.6	6.6	Q9Y265	RUVBL1	RuvB-like 1	HUMAN	2	4.25
138	15.2	11.8	9.3	Q13501	SQSTM1	Sequestosome-1	HUMAN	2	4.37
110	8.2	4.2	4.2	P83111	LACTB	Serine beta-lactamase-like protein LACTB, mitochondrial	HUMAN	2	2.4
144	7.4	4.9	3.4	Q8IYB3	SRRM1	Serine/arginine repetitive matrix protein 1	HUMAN	2	4.12
291	4.4	3.1	3.1	P78362	SRPK2	Serine/threonine-protein kinase SRPK2	HUMAN	2	3.35
288	22.8	7.7	7.7	Q9NQZ2	UTP3	Something about silencing protein 10	HUMAN	2	3.5
186	14.0	8.4	5.1	Q13838	BAT1	Spliceosome RNA helicase BAT1	HUMAN	2	4.44
266	6.9	4.7	4.7	Q15637	SF1	Splicing factor 1	HUMAN	2	4
328	24.7	16.5	13.1	Q96G21	IMP4	U3 small nucleolar ribonucleoprotein protein IMP4	HUMAN	2	2.35
308	5.8	4.0	4.0	Q6NZY4	ZCCHC8	Zinc finger CCHC domain-containing protein 8	HUMAN	2	2.76
238	17.6	8.5	6.0	Q96ME7	ZNF512	Zinc finger protein 512	HUMAN	2	4.39

Appendix A5: List of NS1 interacting host proteins identified in Biological replicate 3 technical replicate 2

Appendix A5: List of NS1 interacting host proteins identified in Biological replicate 3 technical replicate 2									
N	%Cov	%Cov (50)	%Cov (95)	Uniprot	Gene Symbol	Protein	Species	Peptides (95%)	Unused
5	80.7	69.9	69.9	P07910	HNRNPC	Heterogeneous nuclear ribonucleoproteins C1/C2	HUMAN	75	69.29
3	41.1	37.1	34.2	Q08211	DHX9	ATP-dependent RNA helicase A	HUMAN	61	84.03
2	52.5	50.1	46.0	Q7L2E3	DHX30	Putative ATP-dependent RNA helicase DHX30	HUMAN	59	100.67
4	62.9	58.2	56.8	Q12906	ILF3	Interleukin enhancer-binding factor 3	HUMAN	53	74.73
2	20.9	16.9	13.4	Q15149	PLEC1	Plectin-1	HUMAN	45	95.27
7	58.7	45.8	45.8	P51991	HNRNPA3	Heterogeneous nuclear ribonucleoprotein A3	HUMAN	37	58.02
30	57.9	46.9	45.5	P14866	HNRNPL	Heterogeneous nuclear ribonucleoprotein L	HUMAN	36	32.15
10	36.4	28.4	26.8	Q96KR1	ZFR	Zinc finger RNA-binding protein	HUMAN	33	48.56
10	25.5	21.8	20.5	Q14690	PDCD11	Protein RRP5 homolog	HUMAN	28	54.56
17	41.1	41.1	35.1	O43390	HNRNPR	Heterogeneous nuclear ribonucleoprotein R	HUMAN	27	37.93
16	55.1	46.4	46.4	Q12905	ILF2	Interleukin enhancer-binding factor 2	HUMAN	27	40.47
15	52.0	52.0	47.6	O00567	NOP56	Nucleolar protein 56	HUMAN	27	44.13
29	43.1	36.2	36.2	P52272	HNRNPM	Heterogeneous nuclear ribonucleoprotein M	HUMAN	26	32.3
14	35.2	30.8	29.8	P43243	MATR3	Matrin-3	HUMAN	25	40.98
12	21.1	18.1	15.8	Q6P2Q9	PRPF8	Pre-mRNA-processing-splicing factor 8	HUMAN	25	47.3
19	41.0	41.0	38.4	P61978	HNRNPK	Heterogeneous nuclear ribonucleoprotein K	HUMAN	24	36.79
19	38.9	35.6	31.3	P46087	NOP2	Putative ribosomal RNA methyltransferase NOP2	HUMAN	23	40.73
25	51.0	46.4	35.9	Q9UKM9	RALY	RNA-binding protein Raly	HUMAN	23	28.69
9	35.9	35.9	33.0	P11940	PABPC1	Polyadenylate-binding protein 1	HUMAN	22	36.17
15	40.6	34.7	27.9	O43143	DHX15	Putative pre-mRNA-splicing factor ATP-dependent RNA helicase DHX15	HUMAN	22	40.65
20	24.9	20.7	18.3	P55265	ADAR	Double-stranded RNA-specific adenosine deaminase	HUMAN	20	35.31
44	30.9	25.8	24.9	Q1KMD3	HNRNPUL2	Heterogeneous nuclear ribonucleoprotein U-like protein 2	HUMAN	20	24.43
18	15.7	14.4	11.7	O75643	SNRNP200	U5 small nuclear ribonucleoprotein 200 kDa helicase	HUMAN	20	37.55
31	39.7	35.2	35.2	Q9Y2X3	NOP58	Nucleolar protein 58	HUMAN	19	31.99
21	22.5	18.6	18.0	Q9P2E9	RRBP1	Ribosome-binding protein 1	HUMAN	19	38.71
26	38.4	29.2	27.5	O76021	RSL1D1	Ribosomal L1 domain-containing protein 1	HUMAN	17	34.24
28	25.5	25.5	24.1	Q8NI36	WDR36	WD repeat-containing protein 36	HUMAN	17	33.36
47	44.8	44.5	44.5	Q15717	ELAVL1	ELAV-like protein 1	HUMAN	16	23.5
23	31.2	29.9	28.5	Q9NR30	DDX21	Nucleolar RNA helicase 2	HUMAN	16	30.43
36	31.4	28.2	22.8	Q92841	DDX17	Probable ATP-dependent RNA helicase DDX17	HUMAN	16	28.76
26	50.7	50.7	46.9	P07355	ANXA2	Annexin A2	HUMAN	15	28.52
39	29.5	27.8	25.9	Q5SSJ5	HP1BP3	Heterochromatin protein 1-binding protein 3	HUMAN	15	27.64
32	36.8	36.0	33.4	P22626	HNRNPA2B1	Heterogeneous nuclear ribonucleoproteins A2/B1	HUMAN	15	23.97
15	37.4	34.7	31.7	Q9NZI8	IGF2BP1	Insulin-like growth factor 2 mRNA-binding protein 1	HUMAN	15	25.59

Appendix A5: List of NS1 interacting host proteins identified in Biological replicate 3 technical replicate 2									
N	%Cov	%Cov (50)	%Cov (95)	Uniprot	Gene Symbol	Protein	Species	Peptides (95%)	Unused
48	37.3	37.3	37.3	P26599	PTBP1	Polypyrimidine tract-binding protein 1	HUMAN	15	23.42
28	25.9	23.4	20.5	Q15029	EFTUD2	116 kDa U5 small nuclear ribonucleoprotein component	HUMAN	14	27.08
98	41.9	40.0	36.4	P52597	HNRNPF	Heterogeneous nuclear ribonucleoprotein F	HUMAN	14	19.02
40	14.6	11.7	11.7	Q9BQG0	MYBBP1A	Myb-binding protein 1A	HUMAN	14	27.46
41	33.0	30.9	21.4	Q9BZE4	GTPBP4	Nucleolar GTP-binding protein 1	HUMAN	14	25.87
43	31.6	31.6	25.5	P36578	RPL4	60S ribosomal protein L4	HUMAN	13	25.06
57	44.8	44.8	34.7	Q02878	RPL6	60S ribosomal protein L6	HUMAN	13	21.66
64	31.6	25.4	24.0	Q9NVP1	DDX18	ATP-dependent RNA helicase DDX18	HUMAN	13	20.23
56	21.1	19.9	14.9	Q8IWA0	WDR75	WD repeat-containing protein 75	HUMAN	13	21.8
50	24.3	20.1	17.5	Q9H0D6	XRN2	5'-3' exoribonuclease 2	HUMAN	12	23.17
102	22.1	19.2	19.2	O00571	DDX3X	ATP-dependent RNA helicase DDX3X	HUMAN	12	18.22
34	44.0	36.3	36.3	P38159	RBMX	Heterogeneous nuclear ribonucleoprotein G	HUMAN	12	21.86
54	38.0	29.6	22.8	O15226	NKRF	NF-kappa-B-repressing factor	HUMAN	12	22.1
49	14.8	8.7	8.7	Q14980	NUMA1	Nuclear mitotic apparatus protein 1	HUMAN	12	23.27
61	32.7	26.9	20.8	Q14684	RRP1B	Ribosomal RNA processing protein 1 homolog B	HUMAN	12	20.86
31	27.1	23.0	21.0	Q14151	SAFB2	Scaffold attachment factor B2	HUMAN	12	22.78
70	40.6	36.5	36.1	P62424	RPL7A	60S ribosomal protein L7a	HUMAN	11	18.93
74	27.7	25.4	23.6	Q92499	DDX1	ATP-dependent RNA helicase DDX1	HUMAN	11	18.15
69	22.9	22.9	20.3	Q969X6	CIRH1A	Cirhin	HUMAN	11	19.31
60	30.1	30.1	26.9	Q96I24	FUBP3	Far upstream element-binding protein 3	HUMAN	11	20.94
135	35.4	35.4	30.0	Q8IUE6	HIST2H2AB	Histone H2A type 2-B	HUMAN	11	12.76
63	35.7	33.6	31.9	Q15233	NONO	Non-POU domain-containing octamer-binding protein	HUMAN	11	20.46
33	17.4	16.5	12.4	O75533	SF3B1	Splicing factor 3B subunit 1	HUMAN	11	22.26
48	30.5	23.6	22.3	O60506	SYNCRIP	Heterogeneous nuclear ribonucleoprotein Q	HUMAN	10	19.41
213	27.2	18.6	17.1	Q13310	PABPC4	Polyadenylate-binding protein 4	HUMAN	10	15.16
43	25.6	23.8	23.8	Q9UMS4	PRPF19	Pre-mRNA-processing factor 19	HUMAN	10	18.41
83	49.9	47.9	43.9	Q8TDN6	BRIX1	Ribosome biogenesis protein BRX1 homolog	HUMAN	10	16.79
72	20.0	13.7	12.0	Q9NWH9	SLTM	SAFB-like transcription modulator	HUMAN	10	18.56
90	34.8	34.8	34.8	P84103	SFRS3	Splicing factor, arginine/serine-rich 3	HUMAN	10	12
82	40.8	31.3	23.4	P07437	TUBB	Tubulin beta chain	HUMAN	10	16.85
59	46.9	39.2	33.3	Q9Y3I0	C22orf28	UPF0027 protein C22orf28	HUMAN	10	21.07
129	86.7	83.9	75.3	P04280	PRB1	Basic salivary proline-rich protein 1	HUMAN	9	11.67
75	10.6	8.4	6.5	Q9H583	HEATR1	HEAT repeat-containing protein 1	HUMAN	9	18.09
324	21.3	17.2	15.0	P54652	HSPA2	Heat shock-related 70 kDa protein 2	HUMAN	9	17.7
76	19.7	14.9	14.9	Q9BUJ2	HNRNPUL1	Heterogeneous nuclear ribonucleoprotein U-like protein 1	HUMAN	9	17.97
71	31.5	22.1	18.3	P19338	NCL	Nucleolin	HUMAN	9	18.66
95	22.8	19.7	18.5	Q14137	BOP1	Ribosome biogenesis protein BOP1	HUMAN	9	15.1
78	37.3	30.7	26.3	Q15050	RRS1	Ribosome biogenesis regulatory protein homolog	HUMAN	9	17.81

Appendix A5: List of NS1 interacting host proteins identified in Biological replicate 3 technical replicate 2									
N	%Cov	%Cov (50)	%Cov (95)	Uniprot	Gene Symbol	Protein	Species	Peptides (95%)	Unused
80	31.2	26.8	22.0	Q96PK6	RBM14	RNA-binding protein 14	HUMAN	9	17.49
45	29.7	27.2	23.1	Q13573	SNW1	SNW domain-containing protein 1	HUMAN	9	17.77
73	20.4	16.8	15.2	Q12788	TBL3	Transducin beta-like protein 3	HUMAN	9	18.46
79	30.1	28.0	26.1	Q8TED0	UTP15	U3 small nucleolar RNA-associated protein 15 homolog	HUMAN	9	17.59
96	51.2	43.8	38.5	Q9Y224	C14orf166	UPF0568 protein C14orf166	HUMAN	9	14.89
81	26.4	22.8	21.6	O15213	WDR46	WD repeat-containing protein 46	HUMAN	9	17.11
92	32.5	26.6	26.6	P39023	RPL3	60S ribosomal protein L3	HUMAN	8	15.38
93	17.4	16.2	16.2	Q9GZR7	DDX24	ATP-dependent RNA helicase DDX24	HUMAN	8	15.19
50	22.2	17.3	16.3	Q99459	CDC5L	Cell division cycle 5-like protein	HUMAN	8	15.78
105	34.7	32.5	27.1	O75367	H2AFY	Core histone macro-H2A.1	HUMAN	8	14
49	27.0	18.9	18.9	O95793	STAU1	Double-stranded RNA-binding protein Staufen homolog 1	HUMAN	8	16.03
108	23.9	23.9	23.9	P16401	HIST1H1B	Histone H1.5	HUMAN	8	14
39	18.0	18.0	16.6	O00425	IGF2BP3	Insulin-like growth factor 2 mRNA-binding protein 3	HUMAN	8	15.92
114	17.3	11.0	9.9	Q9H6R4	NOL6	Nucleolar protein 6	HUMAN	8	13.42
87	28.8	25.3	25.3	Q1ED39	C16orf88	Protein C16orf88	HUMAN	8	16.01
89	19.2	14.0	13.0	Q96T37	RBM15	Putative RNA-binding protein 15	HUMAN	8	15.66
88	21.5	16.5	11.7	Q8IY81	FTSJ3	Putative rRNA methyltransferase 3	HUMAN	8	15.88
107	26.1	23.2	20.6	Q9H7B2	RPF2	Ribosome production factor 2 homolog	HUMAN	8	14
100	21.1	12.3	12.3	Q9NW13	RBM28	RNA-binding protein 28	HUMAN	8	14.38
130	16.2	14.5	12.3	Q15424	SAFB	Scaffold attachment factor B1	HUMAN	8	13.83
52	15.9	13.2	13.2	Q13435	SF3B2	Splicing factor 3B subunit 2	HUMAN	8	15.05
334	27.9	19.1	17.3	P68371	TUBB2C	Tubulin beta-2C chain	HUMAN	8	12.42
90	20.0	18.6	16.7	Q9UNX4	WDR3	WD repeat-containing protein 3	HUMAN	8	15.57
56	26.5	26.5	24.8	P38919	EIF4A3	Eukaryotic initiation factor 4A-III	HUMAN	7	14.17
101	29.5	27.5	24.0	P42167	TMPO	Lamina-associated polypeptide 2, isoforms beta/gamma	HUMAN	7	14.26
113	16.0	10.7	9.9	Q9H0A0	NAT10	N-acetyltransferase 10	HUMAN	7	13.43
80	16.0	12.4	12.4	P17844	DDX5	Probable ATP-dependent RNA helicase DDX5	HUMAN	7	11.15
123	7.3	4.1	4.1	Q14669	TRIP12	Probable E3 ubiquitin-protein ligase TRIP12	HUMAN	7	12.7
117	32.4	24.5	24.5	Q99848	EBNA1BP2	Probable rRNA-processing protein EBP2	HUMAN	7	13.09
94	10.5	8.2	8.2	Q15393	SF3B3	Splicing factor 3B subunit 3	HUMAN	7	9.58
60	36.3	36.3	33.5	Q07955	SFRS1	Splicing factor, arginine/serine-rich 1	HUMAN	7	13.29
104	17.3	15.6	14.3	P23246	SFPQ	Splicing factor, proline- and glutamine-rich	HUMAN	7	14.16
116	9.2	6.9	6.9	Q13428	TCOF1	Treacle protein	HUMAN	7	13.24
110	26.8	19.7	19.7	P08621	SNRNP70	U1 small nuclear ribonucleoprotein 70 kDa	HUMAN	7	13.86
70	10.3	8.1	6.9	O15042	SR140	U2-associated protein SR140	HUMAN	7	12.16
122	17.6	15.7	15.7	Q9NYH9	UTP6	U3 small nucleolar RNA-associated protein 6 homolog	HUMAN	7	12.81
128	25.0	16.0	16.0	Q15061	WDR43	WD repeat-containing protein 43	HUMAN	7	12
106	18.4	15.1	13.7	O75152	ZC3H11A	Zinc finger CCCH domain-containing protein 11A	HUMAN	7	14

Appendix A5: List of NS1 interacting host proteins identified in Biological replicate 3 technical replicate 2									
N	%Cov	%Cov (50)	%Cov (95)	Uniprot	Gene Symbol	Protein	Species	Peptides (95%)	Unused
137	27.1	23.2	17.9	Q5BKZ1	ZNF326	Zinc finger protein 326	HUMAN	7	10.49
181	39.8	29.3	29.3	P62847	RPS24	40S ribosomal protein S24	HUMAN	6	7.55
131	30.2	26.2	26.2	P18124	RPL7	60S ribosomal protein L7	HUMAN	6	11.46
82	9.5	7.7	6.9	Q9UKV3	ACIN1	Apoptotic chromatin condensation inducer in the nucleus	HUMAN	6	10.76
67	21.1	15.6	13.9	Q9NUL3	STAU2	Double-stranded RNA-binding protein Staufen homolog 2	HUMAN	6	12.52
69	16.0	16.0	11.8	P19525	EIF2AK2	Interferon-induced, double-stranded RNA-activated protein kinase	HUMAN	6	12.21
115	22.4	14.1	14.1	P08729	KRT7	Keratin, type II cytoskeletal 7	HUMAN	6	10.73
101	15.7	15.7	13.4	P42166	TMPO	Lamina-associated polypeptide 2, isoform alpha	HUMAN	6	12.22
119	22.2	18.6	13.2	Q9H8H0	NOL11	Nucleolar protein 11	HUMAN	6	12.92
133	12.1	10.3	10.3	Q15269	PWP2	Periodic tryptophan protein 2 homolog	HUMAN	6	11.13
64	25.0	23.7	20.4	O60508	CDC40	Pre-mRNA-processing factor 17	HUMAN	6	12.69
144	30.7	27.3	27.3	Q13501	SQSTM1	Sequestosome-1	HUMAN	6	10
185	14.4	9.7	8.3	Q96SI9	STRBP	Spermatid perinuclear RNA-binding protein	HUMAN	6	8.89
72	38.5	32.1	29.0	Q13242	SFRS9	Splicing factor, arginine/serine-rich 9	HUMAN	6	12.34
108	32.6	21.6	21.6	Q13595	TRA2A	Transformer-2 protein homolog alpha	HUMAN	6	9.86
334	18.0	15.3	15.3	Q13509	TUBB3	Tubulin beta-3 chain	HUMAN	6	10.75
334	19.1	13.1	13.1	P04350	TUBB4	Tubulin beta-4 chain	HUMAN	6	7.86
132	12.7	11.0	9.8	Q7Z2W4	ZC3HAV1	Zinc finger CCCH-type antiviral protein 1	HUMAN	6	11.3
51	13.1	13.1	13.1	P82933	MRPS9	28S ribosomal protein S9, mitochondrial	HUMAN	5	8.49
147	45.2	39.7	39.7	P62249	RPS16	40S ribosomal protein S16	HUMAN	5	9.75
156	49.3	49.3	48.5	P61353	RPL27	60S ribosomal protein L27	HUMAN	5	8.68
155	21.8	18.7	18.7	P62917	RPL8	60S ribosomal protein L8	HUMAN	5	8.71
151	10.3	8.4	8.4	P11387	TOP1	DNA topoisomerase 1	HUMAN	5	9.13
227	22.9	22.9	22.9	P56537	EIF6	Eukaryotic translation initiation factor 6	HUMAN	5	5.14
136	13.3	10.6	10.6	P08107	HSPA1A	Heat shock 70 kDa protein 1A/1B	HUMAN	5	9.08
136	10.6	10.6	10.6	P34931	HSPA1L	Heat shock 70 kDa protein 1-like	HUMAN	5	9.08
102	26.9	26.9	26.9	Q13151	HNRNPA0	Heterogeneous nuclear ribonucleoprotein A0	HUMAN	5	8.94
461	16.5	10.6	7.1	P02538	KRT6A	Keratin, type II cytoskeletal 6A	HUMAN	5	8.84
461	16.5	10.6	7.1	P48668	KRT6C	Keratin, type II cytoskeletal 6C	HUMAN	5	8.84
92	9.8	9.8	9.8	P02545	LMNA	Lamin-A/C	HUMAN	5	9.82
182	23.9	17.7	17.7	Q9BYG3	MKI67IP	MKI67 FHA domain-interacting nucleolar phosphoprotein	HUMAN	5	7.51
171	37.5	18.8	18.8	P55769	NHP2L1	NHP2-like protein 1	HUMAN	5	8
149	16.3	11.2	8.5	O00541	PES1	Pescadillo homolog	HUMAN	5	9.42
138	10.5	9.4	7.7	Q96GQ7	DDX27	Probable ATP-dependent RNA helicase DDX27	HUMAN	5	10.45
34	27.4	23.6	23.6	A6NMY6	ANXA2P2	Putative annexin A2-like protein	HUMAN	5	9.59
46	6.8	5.8	5.8	Q92900	UPF1	Regulator of nonsense transcripts 1	HUMAN	5	8.7
141	10.5	7.7	5.7	Q14692	BMS1	Ribosome biogenesis protein BMS1 homolog	HUMAN	5	10.34
150	11.6	9.8	9.8	P49756	RBM25	RNA-binding protein 25	HUMAN	5	9.28

Appendix A5: List of NS1 interacting host proteins identified in Biological replicate 3 technical replicate 2									
N	%Cov	%Cov (50)	%Cov (95)	Uniprot	Gene Symbol	Protein	Species	Peptides (95%)	Unused
142	10.0	8.4	5.2	Q13523	PRPF4B	Serine/threonine-protein kinase PRP4 homolog	HUMAN	5	10.27
100	30.8	27.7	24.6	Q96HS1	PGAM5	Serine/threonine-protein phosphatase PGAM5, mitochondrial	HUMAN	5	8.01
99	20.0	19.6	19.6	P09661	SNRPA1	U2 small nuclear ribonucleoprotein A'	HUMAN	5	8.08
143	13.5	12.3	12.3	O00566	MPHOSPH10	U3 small nucleolar ribonucleoprotein protein MPP10	HUMAN	5	10.01
154	11.9	8.2	8.2	Q9BVJ6	UTP14A	U3 small nucleolar RNA-associated protein 14 homolog A	HUMAN	5	8.75
136	21.0	15.3	11.9	Q9Y5J1	UTP18	U3 small nucleolar RNA-associated protein 18 homolog	HUMAN	5	10.54
95	11.4	10.3	10.3	Q6PJT7	ZC3H14	Zinc finger CCCH domain-containing protein 14	HUMAN	5	9.52
183	25.1	25.1	21.4	P23396	RPS3	40S ribosomal protein S3	HUMAN	4	7.39
172	32.2	24.0	24.0	P62241	RPS8	40S ribosomal protein S8	HUMAN	4	8
184	33.7	30.9	30.9	P62913	RPL11	60S ribosomal protein L11	HUMAN	4	7.32
159	28.9	25.1	19.9	P26373	RPL13	60S ribosomal protein L13	HUMAN	4	8.4
173	24.5	19.6	19.6	P18621	RPL17	60S ribosomal protein L17	HUMAN	4	8
288	25.2	25.2	18.3	P62888	RPL30	60S ribosomal protein L30	HUMAN	4	3.21
162	24.4	20.7	16.3	Q6DKI1	RPL7L1	60S ribosomal protein L7-like 1	HUMAN	4	8.34
194	21.7	16.4	16.4	P52895	AKR1C2	Aldo-keto reductase family 1 member C2	HUMAN	4	6.06
106	10.5	5.2	3.8	Q10570	CPSF1	Cleavage and polyadenylation specificity factor subunit 1	HUMAN	4	7.77
50	7.4	6.0	6.0	Q9NZB2	FAM120A	Constitutive coactivator of PPAR-gamma-like protein 1	HUMAN	4	8
152	11.4	11.2	7.8	Q5QJE6	DNTTIP2	Deoxynucleotidyltransferase terminal-interacting protein 2	HUMAN	4	8.82
174	13.7	13.3	13.3	O15446	CD3EAP	DNA-directed RNA polymerase I subunit RPA34	HUMAN	4	8
44	12.1	12.1	10.4	Q05639	EEF1A2	Elongation factor 1-alpha 2	HUMAN	4	8.5
55	14.6	12.7	12.7	Q12849	GRSF1	G-rich sequence factor 1	HUMAN	4	8
160	20.9	13.3	11.7	Q9BVP2	GNL3	Guanine nucleotide-binding protein-like 3	HUMAN	4	8.39
111	16.6	16.6	13.5	Q14103	HNRNPD	Heterogeneous nuclear ribonucleoprotein D0	HUMAN	4	7.08
149	35.2	31.3	31.3	Q71UI9	H2AFV	Histone H2A.V	HUMAN	4	6.22
149	35.2	31.3	31.3	P0C0S5	H2AFZ	Histone H2A.Z	HUMAN	4	6.22
461	7.6	7.3	5.4	O95678	KRT75	Keratin, type II cytoskeletal 75	HUMAN	4	6.65
60	10.4	8.8	8.6	Q07666	KHDRBS1	KH domain-containing, RNA-binding, signal transduction-associated protein 1	HUMAN	4	6.39
189	9.8	5.9	5.9	O43795	MYO1B	Myosin-Ib	HUMAN	4	6.44
179	7.6	6.8	5.9	O00159	MYO1C	Myosin-Ic	HUMAN	4	7.7
167	26.4	26.4	22.5	Q9Y3C1	NOP16	Nucleolar protein 16	HUMAN	4	8.07
125	8.8	8.8	8.8	Q9NW64	RBM22	Pre-mRNA-splicing factor RBM22	HUMAN	4	6
170	20.0	17.7	17.7	Q9BXY0	MAK16	Protein MAK16 homolog	HUMAN	4	8.01
226	14.7	14.7	11.6	O95758	ROD1	Regulator of differentiation 1	HUMAN	4	6.59
161	17.8	17.8	15.2	P56182	RRP1	Ribosomal RNA processing protein 1 homolog A	HUMAN	4	8.38
225	16.9	13.7	13.7	Q9Y2P8	RCL1	RNA 3'-terminal phosphate cyclase-like protein	HUMAN	4	5.31
180	5.9	5.9	5.9	Q8IYB3	SRRM1	Serine/arginine repetitive matrix protein 1	HUMAN	4	7.68
112	11.2	11.2	11.2	Q12874	SF3A3	Splicing factor 3A subunit 3	HUMAN	4	6.78
176	9.5	7.3	5.7	P42285	SKIV2L2	Superkiller viralicidic activity 2-like 2	HUMAN	4	7.74

Appendix A5: List of NS1 interacting host proteins identified in Biological replicate 3 technical replicate 2									
N	%Cov	%Cov (50)	%Cov (95)	Uniprot	Gene Symbol	Protein	Species	Peptides (95%)	Unused
168	23.1	19.1	14.4	P68363	TUBA1B	Tubulin alpha-1B chain	HUMAN	4	8.04
168	23.2	19.1	14.5	Q9BQE3	TUBA1C	Tubulin alpha-1C chain	HUMAN	4	8.04
185	24.1	21.3	21.3	Q96G21	IMP4	U3 small nucleolar ribonucleoprotein protein IMP4	HUMAN	4	7.13
165	13.7	9.3	7.8	O43818	RRP9	U3 small nucleolar RNA-interacting protein 2	HUMAN	4	8.16
230	16.6	8.6	4.0	Q9P275	USP36	Ubiquitin carboxyl-terminal hydrolase 36	HUMAN	4	5.04
114	8.8	7.8	6.9	Q96MU7	YTHDC1	YTH domain-containing protein 1	HUMAN	4	6.63
84	12.1	10.3	10.3	P51398	DAP3	28S ribosomal protein S29, mitochondrial	HUMAN	3	4.72
60	24.0	20.3	14.2	Q9P015	MRPL15	39S ribosomal protein L15, mitochondrial	HUMAN	3	6.69
294	14.9	14.9	11.2	P50914	RPL14	60S ribosomal protein L14	HUMAN	3	3.06
195	31.9	18.1	18.1	P61313	RPL15	60S ribosomal protein L15	HUMAN	3	6.04
204	35.0	27.5	27.5	P46778	RPL21	60S ribosomal protein L21	HUMAN	3	6
257	18.6	12.9	12.9	P62829	RPL23	60S ribosomal protein L23	HUMAN	3	4.02
232	20.9	20.9	20.9	Q9Y3U8	RPL36	60S ribosomal protein L36	HUMAN	3	4.94
210	22.4	22.4	22.4	P32969	RPL9	60S ribosomal protein L9	HUMAN	3	6
200	6.2	3.2	3.2	O15523	DDX3Y	ATP-dependent RNA helicase DDX3Y	HUMAN	3	4.02
467	9.5	5.2	5.2	Q9BQ39	DDX50	ATP-dependent RNA helicase DDX50	HUMAN	3	5.01
254	30.0	30.0	30.0	P10163	PRB4	Basic salivary proline-rich protein 4	HUMAN	3	4.06
221	20.0	20.0	17.1	Q7Z7K6	CENPV	Centromere protein V	HUMAN	3	5.67
214	5.3	4.4	4.4	Q01780	EXOSC10	Exosome component 10	HUMAN	3	5.89
107	5.4	5.4	5.4	Q06787	FMR1	Fragile X mental retardation 1 protein	HUMAN	3	3.54
219	22.4	9.0	9.0	Q5T3I0	GPATCH4	G patch domain-containing protein 4	HUMAN	3	5.69
193	18.1	12.6	11.1	O60832	DKC1	H/ACA ribonucleoprotein complex subunit 4	HUMAN	3	6.18
132	9.6	9.6	9.6	Q99729	HNRNPAB	Heterogeneous nuclear ribonucleoprotein A/B	HUMAN	3	2.57
143	26.6	14.0	11.3	P09651	HNRNPA1	Heterogeneous nuclear ribonucleoprotein A1	HUMAN	3	4.87
174	6.4	6.4	6.4	O14979	HNRPDL	Heterogeneous nuclear ribonucleoprotein D-like	HUMAN	3	4.71
253	16.0	16.0	11.9	P07305	H1F0	Histone H1.0	HUMAN	3	4.09
69	11.7	11.7	11.7	P16403	HIST1H1C	Histone H1.2	HUMAN	3	6
69	15.4	11.3	11.3	P16402	HIST1H1D	Histone H1.3	HUMAN	3	6
69	11.4	11.4	11.4	P10412	HIST1H1E	Histone H1.4	HUMAN	3	6
116	19.5	17.4	10.2	P05783	KRT18	Keratin, type I cytoskeletal 18	HUMAN	3	6.46
184	8.2	8.2	8.2	P55081	MFAP1	Microfibrillar-associated protein 1	HUMAN	3	2.57
241	20.1	15.6	15.6	Q9BU76	MMTAG2	Multiple myeloma tumor-associated protein 2	HUMAN	3	4.44
224	10.0	6.8	5.6	Q09161	NCBP1	Nuclear cap-binding protein subunit 1	HUMAN	3	5.38
220	10.6	7.0	7.0	Q9BSC4	NOL10	Nucleolar protein 10	HUMAN	3	5.69
216	15.2	14.8	14.8	Q9UMY1	NOL7	Nucleolar protein 7	HUMAN	3	5.82
215	12.0	12.0	12.0	Q9NWT1	PAK1IP1	p21-activated protein kinase-interacting protein 1	HUMAN	3	5.89
74	6.0	6.0	6.0	O75127	PTCD1	Pentatricopeptide repeat-containing protein 1	HUMAN	3	5.82
178	6.7	5.5	4.7	Q9HCS7	XAB2	Pre-mRNA-splicing factor SYF1	HUMAN	3	2.91

Appendix A5: List of NS1 interacting host proteins identified in Biological replicate 3 technical replicate 2									
N	%Cov	%Cov (50)	%Cov (95)	Uniprot	Gene Symbol	Protein	Species	Peptides (95%)	Unused
222	8.2	7.1	5.1	Q13206	DDX10	Probable ATP-dependent RNA helicase DDX10	HUMAN	3	5.44
200	14.5	9.2	9.2	Q9H0S4	DDX47	Probable ATP-dependent RNA helicase DDX47	HUMAN	3	6
236	11.2	11.2	5.2	Q8NCA5	FAM98A	Protein FAM98A	HUMAN	3	4.81
120	5.5	3.1	2.2	P18583	SON	Protein SON	HUMAN	3	6.11
172	8.1	2.8	2.8	Q8IX01	SFRS14	Putative splicing factor, arginine/serine-rich 14	HUMAN	3	3.5
234	6.9	3.0	3.0	Q7Z6E9	RBBP6	Retinoblastoma-binding protein 6	HUMAN	3	4.9
249	13.9	13.9	13.9	Q9Y3A4	RRP7A	Ribosomal RNA-processing protein 7 homolog A	HUMAN	3	4.17
212	10.8	10.8	10.8	O43159	RRP8	Ribosomal RNA-processing protein 8	HUMAN	3	6
202	10.6	8.0	8.0	Q9H9Y2	RPF1	Ribosome production factor 1	HUMAN	3	6
190	22.1	13.0	10.2	P42696	RBM34	RNA-binding protein 34	HUMAN	3	6.33
81	6.8	6.8	6.8	Q14498	RBM39	RNA-binding protein 39	HUMAN	3	5.24
233	16.5	10.2	10.2	Q9BWF3	RBM4	RNA-binding protein 4	HUMAN	3	4.92
155	30.5	25.9	25.9	Q9Y5S9	RBM8A	RNA-binding protein 8A	HUMAN	3	4
223	10.8	7.6	7.6	P35637	FUS	RNA-binding protein FUS	HUMAN	3	5.4
123	12.8	10.2	10.2	Q15287	RNPS1	RNA-binding protein with serine-rich domain 1	HUMAN	3	6.02
192	22.7	13.6	10.5	O75683	SURF6	Surfeit locus protein 6	HUMAN	3	6.24
217	5.6	3.9	3.9	O60264	SMARCA5	SWI/SNF-related matrix-associated actin-dependent regulator of chromatin subfamily A member 5	HUMAN	3	5.79
150	10.3	7.8	5.4	Q92804	TAF15	TATA-binding protein-associated factor 2N	HUMAN	3	4
201	5.6	4.7	4.7	Q9NXF1	TEX10	Testis-expressed sequence 10 protein	HUMAN	3	6
203	17.9	13.5	13.5	Q86W42	THOC6	THO complex subunit 6 homolog	HUMAN	3	6
168	20.0	16.0	11.3	Q71U36	TUBA1A	Tubulin alpha-1A chain	HUMAN	3	6.03
139	25.5	14.0	14.0	Q96DI7	SNRNP40	U5 small nuclear ribonucleoprotein 40 kDa protein	HUMAN	3	4.13
87	20.7	16.1	10.7	Q9Y2R9	MRPS7	28S ribosomal protein S7, mitochondrial	HUMAN	2	4.45
98	19.7	11.6	11.6	P52815	MRPL12	39S ribosomal protein L12, mitochondrial	HUMAN	2	4
188	31.8	31.1	23.8	P62263	RPS14	40S ribosomal protein S14	HUMAN	2	2.26
312	24.6	17.7	17.7	P62244	RPS15A	40S ribosomal protein S15a	HUMAN	2	2.44
310	15.4	15.4	15.4	P62266	RPS23	40S ribosomal protein S23	HUMAN	2	2.53
187	20.9	20.9	20.9	P62854	RPS26	40S ribosomal protein S26	HUMAN	2	2.45
306	31.0	31.0	31.0	P42677	RPS27	40S ribosomal protein S27	HUMAN	2	2.68
265	19.8	13.7	13.7	P62701	RPS4X	40S ribosomal protein S4, X isoform	HUMAN	2	4
302	24.2	14.6	14.6	P30050	RPL12	60S ribosomal protein L12	HUMAN	2	2.79
285	14.3	10.3	10.3	P40429	RPL13A	60S ribosomal protein L13a	HUMAN	2	3.59
151	17.6	16.2	16.2	P46776	RPL27A	60S ribosomal protein L27a	HUMAN	2	4
313	24.8	18.4	18.4	P62899	RPL31	60S ribosomal protein L31	HUMAN	2	2.42
303	17.9	17.9	7.7	P49207	RPL34	60S ribosomal protein L34	HUMAN	2	2.74
286	8.4	8.4	8.4	P05141	SLC25A5	ADP/ATP translocase 2	HUMAN	2	3.44
268	4.0	2.8	2.8	Q9P0K7	RAI14	Ankycorbin	HUMAN	2	4
298	5.6	5.6	5.6	O00148	DDX39	ATP-dependent RNA helicase DDX39	HUMAN	2	2.94

Appendix A5: List of NS1 interacting host proteins identified in Biological replicate 3 technical replicate 2									
N	%Cov	%Cov (50)	%Cov (95)	Uniprot	Gene Symbol	Protein	Species	Peptides (95%)	Unused
296	10.6	4.9	3.3	Q8TDD1	DDX54	ATP-dependent RNA helicase DDX54	HUMAN	2	3
176	4.7	3.6	3.6	Q8IWX8	CHERP	Calcium homeostasis endoplasmic reticulum protein	HUMAN	2	3.24
297	10.5	6.3	6.3	P45973	CBX5	Chromobox protein homolog 5	HUMAN	2	3
94	1.8	1.8	1.8	P53675	CLTCL1	Clathrin heavy chain 2	HUMAN	2	4
173	7.6	5.7	5.7	Q8N684	CPSF7	Cleavage and polyadenylation specificity factor subunit 7	HUMAN	2	3.49
266	9.2	4.9	4.9	P38432	COIL	Coilin	HUMAN	2	4
144	7.2	3.4	3.4	Q9BZJ0	CRNKL1	Crooked neck-like protein 1	HUMAN	2	4.03
280	5.7	5.7	5.7	Q14258	TRIM25	E3 ubiquitin/ISG15 ligase TRIM25	HUMAN	2	4
428	9.4	7.4	7.4	P60842	EIF4A1	Eukaryotic initiation factor 4A-I	HUMAN	2	3.47
117	4.7	4.7	3.4	P51114	FXR1	Fragile X mental retardation syndrome-related protein 1	HUMAN	2	2.68
127	4.5	4.5	3.3	P51116	FXR2	Fragile X mental retardation syndrome-related protein 2	HUMAN	2	2.68
186	6.3	6.3	6.3	Q9NZM5	GLTSCR2	Glioma tumor suppressor candidate region gene 2 protein	HUMAN	2	2.51
342	27.6	14.3	14.3	Q9NY12	GAR1	H/ACA ribonucleoprotein complex subunit 1	HUMAN	2	2.01
276	16.1	12.7	12.7	P04792	HSPB1	Heat shock protein beta-1	HUMAN	2	4
142	14.5	14.5	8.4	P31942	HNRNPH3	Heterogeneous nuclear ribonucleoprotein H3	HUMAN	2	4.08
179	29.4	17.6	17.6	O00422	SAP18	Histone deacetylase complex subunit SAP18	HUMAN	2	2.87
69	7.0	7.0	7.0	Q02539	HIST1H1A	Histone H1.1	HUMAN	2	4
69	7.2	7.2	7.2	P22492	HIST1H1T	Histone H1t	HUMAN	2	4
301	10.8	10.3	10.3	Q92522	H1FX	Histone H1x	HUMAN	2	2.82
118	17.5	17.5	17.5	P62805	HIST1H4A	Histone H4	HUMAN	2	2.88
137	4.5	4.5	4.5	Q9Y6M1	IGF2BP2	Insulin-like growth factor 2 mRNA-binding protein 2	HUMAN	2	4
93	8.5	4.4	4.4	P08779	KRT16	Keratin, type I cytoskeletal 16	HUMAN	2	2.97
279	4.5	4.5	4.5	Q4G0J3	LARP7	La-related protein 7	HUMAN	2	4
304	3.9	2.8	2.8	P49790	NUP153	Nuclear pore complex protein Nup153	HUMAN	2	2.73
283	5.0	3.7	3.7	Q14978	NOLC1	Nucleolar and coiled-body phosphoprotein 1	HUMAN	2	3.74
284	5.3	4.4	3.1	Q9Y3T9	NOC2L	Nucleolar complex protein 2 homolog	HUMAN	2	3.68
287	4.1	4.1	4.1	Q13823	GNL2	Nucleolar GTP-binding protein 2	HUMAN	2	3.41
309	4.0	4.0	4.0	Q13427	PPIG	Peptidyl-prolyl cis-trans isomerase G	HUMAN	2	2.55
114	3.3	3.3	3.3	P51659	HSD17B4	Peroxisomal multifunctional enzyme type 2	HUMAN	2	3.28
147	7.8	3.9	3.9	Q9H307	PNN	Pinin	HUMAN	2	4.02
116	5.5	4.2	4.2	Q8TCS8	PNPT1	Polyribonucleotide nucleotidyltransferase 1, mitochondrial	HUMAN	2	3.12
158	20.8	20.8	20.8	Q9Y3B4	SF3B14	Pre-mRNA branch site protein p14	HUMAN	2	4
159	9.7	9.7	9.7	Q9ULR0	ISY1	Pre-mRNA-splicing factor ISY1 homolog	HUMAN	2	4
160	11.6	11.6	11.6	O75934	BCAS2	Pre-mRNA-splicing factor SPF27	HUMAN	2	4
250	8.2	6.8	4.5	Q9Y2R4	DDX52	Probable ATP-dependent RNA helicase DDX52	HUMAN	2	4.16
240	11.2	11.2	6.4	Q9NY93	DDX56	Probable ATP-dependent RNA helicase DDX56	HUMAN	2	4.45
291	3.9	2.3	2.3	O96028	WHSC1	Probable histone-lysine N-methyltransferase NSD2	HUMAN	2	3.14
263	2.6	1.5	1.5	Q8WYP5	AHCTF1	Protein ELYS	HUMAN	2	4

Appendix A5: List of NS1 interacting host proteins identified in Biological replicate 3 technical replicate 2									
N	%Cov	%Cov (50)	%Cov (95)	Uniprot	Gene Symbol	Protein	Species	Peptides (95%)	Unused
112	27.8	27.8	27.8	P60903	S100A10	Protein S100-A10	HUMAN	2	2.49
64	8.7	6.1	6.1	Q14568	HSP90AA2	Putative heat shock protein HSP 90-alpha A2	HUMAN	2	3.89
64	5.5	5.5	5.5	Q58FF8	HSP90AB2P	Putative heat shock protein HSP 90-beta 2	HUMAN	2	3.89
133	11.1	6.9	5.0	Q58FF7	HSP90AB3P	Putative heat shock protein HSP 90-beta-3	HUMAN	2	4.07
246	14.2	11.8	7.6	Q9GZL7	WDR12	Ribosome biogenesis protein WDR12	HUMAN	2	4.26
233	12.3	5.8	5.8	Q9BQ04	RBM4B	RNA-binding protein 4B	HUMAN	2	2.79
281	9.4	7.1	2.2	Q5JTH9	RRP12	RRP12-like protein	HUMAN	2	3.86
308	12.8	8.5	8.5	Q9Y3B9	RRP15	RRP15-like protein	HUMAN	2	2.57
316	5.1	3.1	3.1	P78362	SRPK2	Serine/threonine-protein kinase SRPK2	HUMAN	2	2.29
271	10.6	7.6	7.6	P62136	PPP1CA	Serine/threonine-protein phosphatase PP1-alpha catalytic subunit	HUMAN	2	4
271	12.5	7.6	7.6	P62140	PPP1CB	Serine/threonine-protein phosphatase PP1-beta catalytic subunit	HUMAN	2	4
271	7.7	7.7	7.7	P36873	PPP1CC	Serine/threonine-protein phosphatase PP1-gamma catalytic subunit	HUMAN	2	4
298	9.1	5.6	5.6	Q13838	BAT1	Spliceosome RNA helicase BAT1	HUMAN	2	2.94
137	8.7	6.8	5.4	Q15459	SF3A1	Splicing factor 3A subunit 1	HUMAN	2	4.27
251	23.7	16.2	12.9	Q01081	U2AF1	Splicing factor U2AF 35 kDa subunit	HUMAN	2	4.09
170	7.1	4.3	4.3	Q08170	SFRS4	Splicing factor, arginine/serine-rich 4	HUMAN	2	3.59
170	6.1	6.1	6.1	Q13247	SFRS6	Splicing factor, arginine/serine-rich 6	HUMAN	2	3.59
262	64.5	54.8	54.8	P02808	STATH	Statherin	HUMAN	2	4
248	16.5	11.6	6.1	Q9NQ55	PPAN	Suppressor of SWI4 1 homolog	HUMAN	2	4.22
175	5.1	5.1	5.1	Q13148	TARDBP	TAR DNA-binding protein 43	HUMAN	2	3.26
104	9.0	9.0	9.0	P62995	TRA2B	Transformer-2 protein homolog beta	HUMAN	2	4
355	23.7	11.7	11.7	P21796	VDAC1	Voltage-dependent anion-selective channel protein 1	HUMAN	2	4.01
140	15.5	15.5	8.5	Q9Y277	VDAC3	Voltage-dependent anion-selective channel protein 3	HUMAN	2	4.12
270	5.9	4.5	4.5	Q6NZY4	ZCCHC8	Zinc finger CCHC domain-containing protein 8	HUMAN	2	4

Appendix A6: Molecular functions of NS1-interacting host factors mapped with PANTHER database in DAVID

Molecular functionsof NS1-interacting host factors mapped with PANTHER database in DAVID				
Term (molecular function)	Count	%	P Value	Uniprot IDs of the proteins
Histone	8	4.40	5.55E-07	Q9BTM1, Q71UI9, O75367, P16401, Q93077, P07305, Q8IUE6, Q92522
Helicase	14	7.69	2.45E-08	Q9NR30, O75643, Q8TDD1, Q7L2E3, O00571, P17844, O60264, Q92841, Q9NY93, O43143, Q9GZR7, Q9NVP1, Q13206, Q96GQ7
mRNA splicing factor	13	7.14	2.75E-10	Q13595, O75643, Q13247, Q9UMS4, Q92804, P26599, O95758, Q08170, P35637, Q16629, Q8NI36, Q15393, P08621
RNA helicase	13	7.14	4.67E-11	Q9NR30, O75643, Q8TDD1, O00571, Q7L2E3, P17844, Q92841, Q9NY93, O43143, Q9GZR7, Q9NVP1, Q13206, Q96GQ7
mRNA processing factor	17	9.34	6.87E-13	Q13595, O75643, Q13247, Q8IYB3, Q9UMS4, Q92804, P26599, O95758, Q08170, P35637, Q9UKM9, Q16629, Q8NI36, O43390, Q15393, P08621, O60506
Other RNA-binding protein	21	11.54	4.01E-15	Q9NWH9, O95793, Q07666, Q13310, Q9H6R4, P49756, Q9UMS4, Q96I24, Q14151, Q96KR1, Q9NZI8, O00541, Q96PK6, Q9BWF3, Q1KMD3, Q96T37, Q9NW13, P51114, P43243, O00425, Q9BUJ2, P19338
Ribosomal protein	31	17.03	8.78E-21	P18124, P52597, P46777, P62750, P61353, P31943, P30050, P31942, Q14137, P62424, O43390, Q9Y3A4, P62241, P62829, Q15050, P61313, Q6DKI1, P23396, P62263, O60506, Q8TDN6, P62913, Q9BVJ6, O00541, P55795, Q02878, P50914, O76021, Q9Y3U8, P26373, P39023
Ribonucleoprotein	21	11.54	6.08E-22	Q13151, P52272, Q9H9Y2, P51991, P22626, Q9Y2X3, P14866, Q9BYG3, Q9H583, O00567, O00566, Q99729, Q96PK6, Q15717, P42696, Q9BWF3, P26599, O95758, Q9UKM9, Q96G21, Q14103, P38159
Nucleic acid binding	118	64.84	1.47E-58	Q12905, P52597, P62750, O00571, Q15717, Q96PK6, Q14137, Q16629, Q96T37, O43390, P61313, Q9BUJ2, P62263, P23396, O60506, Q7Z2W4, Q13151, O75367, Q9H9Y2, P22626, Q9H6R4, Q8IYB3, Q8TDD1, O15226, P17844, O00567, O00566, Q92522, Q99729, P55795, P46087, Q9UKM9, P16401, Q02878, P51114, Q13206, Q13148, P56537, P39023, P38159, Q13595, Q9NWH9, Q92804, P30050, O95758, Q9BQG0, P62241, Q6DKI1, P51991, Q8IY81, P55265, Q7L2E3, Q14151, O60264, O00541, O75683, Q9NY93, Q08170, Q1KMD3, Q9GZR7, P50914, Q9NYH9, Q9Y3U8, P26373, Q71UI9, Q9H0D6, P61353, Q9H583, P31943, P31942, Q9BWF3, P62424, Q9Y3A4, P07305, Q8NI36, P62829, Q13310, P49756, Q9Y2X3, Q13247, Q9BYG3, P62913, Q9BVJ6, P42696, P26599, P35637, O43143, Q9NVP1, Q15393, Q9NW13, P19338, P18124, Q07666, P46777, P14866, Q93077, Q9UMS4, Q96KR1, Q8IUE6, Q14690, Q92841, O60832, Q9BTM1, Q15050, O00425, Q9NR30, O95793, Q8TDN6, P52272, O75643, Q96I24, Q9NZI8, Q9H7B2, Q96G21, P08621, O76021, Q14103, P43243, Q96GQ7

Appendix A7: Biological processes of NS1-interacting host factors mapped with PANTHER database in DAVID

Biological processes of NS1-interacting host factors mapped with PANTHER database in DAVID				
Term (Biological process)	Count	%	PValue	Uniprot IDs of the proteins
Protein complex assembly	4	2.20	3.26E-02	Q9BXY0, P08107, P54652, O00541
Chromatin packaging and remodeling	9	4.95	7.77E-04	Q9BTM1, Q71UI9, O75367, P16401, Q93077, P07305, Q14151, Q8IUE6, Q92522
Translational regulation	7	3.85	1.43E-04	P18124, O95793, Q9BVP2, P19525, Q96I24, Q6DKI1, P56537
Protein biosynthesis	24	13.19	1.48E-10	P18124, P46777, P62750, P19525, P62913, P61353, Q9BZE4, P30050, P55795, Q14137, P62424, Q02878, P62241, P62829, P50914, O76021, P61313, P23396, Q6DKI1, P62263, Q9Y3U8, P26373, P56537, P39023
rRNA metabolism	15	8.24	1.01E-14	Q8TDN6, Q9H9Y2, Q9Y2X3, Q8IY81, Q9H583, O00541, O00567, O00566, Q14690, O60832, P46087, Q14137, Q96G21, Q9Y3A4, P19338
Nucleoside, nucleotide and nucleic acid metabolism	90	49.45	2.56E-23	P52597, Q71UI9, Q9H0D6, Q9BVP2, O00571, Q9H583, P31943, Q13823, P31942, Q96PK6, Q15717, Q9BWF3, Q14137, Q16629, O43390, P07305, Q8NI36, Q9Y3A4, O60506, Q7Z2W4, Q13151, O75367, Q13310, Q9H9Y2, P22626, Q9Y2X3, P49756, Q13247, Q8TDD1, O15226, P17844, Q9BVJ6, O00567, Q9H7N4, O00566, Q92522, Q99729, P55795, P46087, P26599, Q9UKM9, O43143, P16401, Q9NVP1, Q15393, P51114, Q9NW13, Q13148, Q13206, P19338, P38159, Q13595, Q9NWH9, P14866, Q93077, Q9UMS4, Q14692, Q8IUE6, Q14690, Q92841, P78527, O60832, Q9BTM1, Q9UNX4, O95758, Q9BQG0, Q15050, Q99848, Q9NR30, O95793, Q8TDN6, P52272, O75643, P51991, Q8IY81, P55265, Q7L2E3, Q14151, Q96I24, O00541, O60264, Q9NY93, Q9H7B2, Q08170, Q96G21, Q9GZR7, P08621, Q15269, Q14103, Q9NYH9, Q96GQ7
mRNA splicing	32	17.58	4.10E-28	Q9NWH9, P52597, Q13595, P14866, Q9UMS4, P31943, P31942, Q96PK6, Q9BWF3, O95758, Q16629, Q8NI36, O43390, O60506, Q13151, P22626, P51991, O75643, Q13247, Q7L2E3, Q96I24, Q9H7N4, Q99729, P55795, P26599, Q08170, O43143, Q9UKM9, P08621, Q15393, Q14103, Q13148, P38159
Pre-mRNA processing	36	19.78	1.27E-28	Q9NWH9, P52597, Q13595, P14866, Q9UMS4, P31943, P31942, Q15717, Q96PK6, Q9BWF3, O95758, Q16629, Q8NI36, O43390, O60506, Q13151, P52272, Q13310, P22626, P51991, O75643, P49756, Q13247, Q7L2E3, Q96I24, Q9H7N4, Q99729, P55795, P26599, Q08170, O43143, Q9UKM9, P08621, Q15393, Q14103, Q13148, P38159

Appendix A8: Pathways involved with the NS1-interacting host factors mapped in DAVID

Pathways involved with the NS1-interacting host factors mapped in DAVID					
Category	Term (Pathway)	Count	%	PValue	Uniprot IDs of the proteins
KEGG	Ribosome	17	9.34	3.86E-17	P18124, P46777, P62750, P62913, P61353, P30050, P55795, P62424, Q02878, P62241, P62829, P50914, P61313, P23396, Q9Y3U8, P26373, P39023
KEGG	Spliceosome	18	9.89	7.96E-16	Q13595, P52272, P51991, O75643, P49756, Q13247, Q9UMS4, P54652, P17844, Q13435, P08107, Q08170, O43143, Q16629, Q15393, P08621, Q15365, P38159
KEGG_	Systemic lupus erythematosus	5	2.75	1.57E-02	Q9BTM1, Q71UI9, O75367, Q93077, Q8IUE6
REACTOME	Processing of Capped Intron-Containing Pre-mRNA	23	12.64	1.36E-20	Q13151, P52597, P52272, P51991, P22626, O75643, Q8IYB3, P14866, Q13247, P31943, Q13435, P55795, P26599, Q08170, P35637, Q16629, O43390, Q15393, P08621, Q14103, Q9BUJ2, Q15365, P38159
REACTOME	Metabolism of proteins	20	10.99	7.19E-11	P18124, Q9H0D6, P46777, P62750, P62913, P61353, O00567, P30050, P55795, P62424, Q02878, P62241, P62829, P50914, P61313, P23396, P62263, Q9Y3U8, P26373, P39023
REACTOME	3' -UTR-mediated translational regulation	18	9.89	5.83E-14	P18124, P46777, P62750, P62913, P61353, P30050, P55795, P62424, Q02878, P62241, P62829, P50914, P61313, P23396, P62263, Q9Y3U8, P26373, P39023
REACTOME	Influenza Infection	37	20.33	2.41E-38	P18124, P52597, P46777, P62750, P14866, P61353, P31943, P30050, P62424, Q16629, O43390, P62829, P62241, P61313, P62263, Q9BUJ2, P23396, Q13151, P52272, P22626, P51991, Q8IYB3, Q13247, P19525, P62913, P55795, P26599, P35637, Q02878, P50914, P08621, Q14103, Q15365, Q9Y3U8, P26373, P39023, P38159
REACTOME	Gene Expression	40	21.98	2.16E-29	P18124, P52597, P46777, P62750, P14866, P61353, P31943, P30050, P62424, Q16629, O43390, P62829, P62241, P61313, Q9BUJ2, P62263, P23396, Q13151, P52272, O75643, P22626, P51991, Q8IYB3, Q13247, P62913, Q13435, P55795, P26599, Q08170, P35637, Q02878, P50914, P08621, Q15393, Q14103, Q15365, Q9Y3U8, P26373, P39023, P38159

Appendix A9: Molecular functions of NS1-interacting host factors mapped with Gene Ontology (GO) in DAVID

Molecular functionsof NS1-interacting host factors mapped with Gene Ontology (GO) in DAVID				
Term (molecular function)	Count	%	PValue	Uniprot IDs of the proteins
Adenyl ribonucleotide binding	24	13.19	5.04E-02	Q12905, Q9NR30, Q9H0A0, O75643, Q8TDD1, P19525, P54652, Q7L2E3, O00571, P17844, O60264, Q14692, Q92841, P78527, Q13523, Q9NY93, Q58FF8, P08107, O43143, Q9NVP1, Q9GZR7, O00159, Q13206, Q96GQ7
ATP binding	24	13.19	4.44E-02	Q12905, Q9NR30, Q9H0A0, O75643, Q8TDD1, P19525, P54652, Q7L2E3, O00571, P17844, O60264, Q14692, Q92841, P78527, Q13523, Q9NY93, Q58FF8, P08107, O43143, Q9NVP1, Q9GZR7, O00159, Q13206, Q96GQ7
Translation regulator activity	3	1.65	3.88E-02	Q9NZI8, O00425, P62263
Telomeric DNA binding	3	1.65	1.11E-02	P22626, Q14103, P19338
DNA binding	39	21.43	4.45E-03	Q12906, Q12905, P18124, Q71UI9, Q07666, Q9UMS4, Q93077, O00571, Q96KR1, Q8IUE6, Q92804, P78527, Q9BTM1, P07305, P42166, Q9BQG0, Q14258, P23396, P42167, P18583, O75367, Q5BKZ1, P22626, Q8IYB3, P55265, Q96I24, Q14151, O15226, O60264, Q92522, Q99729, O75683, P35637, P16401, Q02878, Q14103, Q13148, P19338, Q5SSJ5, Q15365
rRNA binding	4	2.20	3.65E-03	Q9H9Y2, P46777, P62750, P62913
Poly-pyrimidine tract binding	3	1.65	3.10E-03	P26599, Q13310, P31943
single-stranded RNA binding	4	2.20	2.97E-03	P26599, Q13310, P31943, O60506
RNA splicing factor activity, transesterification mechanism	4	2.20	2.10E-03	Q08170, Q8IYB3, Q15393, O00566
mRNA 5'-UTR binding	3	1.65	6.83E-04	Q9NZI8, O00425, P62263
ATPase activity	14	7.69	6.51E-05	Q9NR30, O75643, Q8TDD1, Q7L2E3, O00571, P17844, O60264, Q92841, Q9NY93, O43143, Q9GZR7, Q9NVP1, Q13206, Q96GQ7
ATPase activity, coupled	13	7.14	3.78E-05	Q9NR30, O75643, Q8TDD1, O00571, Q7L2E3, P17844, Q92841, Q9NY93, O43143, Q9GZR7, Q9NVP1, Q13206, Q96GQ7
ATP-dependent RNA helicase activity	6	3.30	2.40E-06	Q9NY93, Q9NR30, Q8TDD1, Q9NVP1, Q9GZR7, O00571
double-stranded RNA binding	7	3.85	1.23E-06	Q12906, Q12905, P18583, O95793, P19525, P55265, O15226
Structural molecule activity	24	13.19	2.79E-07	P18124, P46777, P62750, P48668, P62913, P61353, P30050, P02545, P55795, P62424, Q02878, P62241, P62829, P50914, O76021, P43243, P61313, P23396, Q6DKI1, Q14980, P62263, Q9Y3U8, P26373, P39023
RNA-dependent ATPase activity	7	3.85	9.14E-08	Q9NY93, Q9NR30, Q8TDD1, Q9NVP1, Q9GZR7, O00571, Q92841
Helicase activity	14	7.69	3.39E-09	Q9NR30, O75643, Q8TDD1, Q7L2E3, O00571, P17844, O60264, Q92841, Q9NY93, O43143, Q9GZR7, Q9NVP1, Q13206, Q96GQ7
mRNA binding	11	6.04	1.94E-09	Q15717, P18124, Q13310, P49756, Q14103, Q9NZI8, O00425, P23396, P62263, O60506, Q99729
ATP-dependent helicase activity	13	7.14	5.65E-10	Q9NR30, O75643, Q8TDD1, O00571, Q7L2E3, P17844, Q92841, Q9NY93, O43143, Q9GZR7, Q9NVP1, Q13206, Q96GQ7

Molecular functionsof NS1-interacting host factors mapped with Gene Ontology (GO) in DAVID				
Term (molecular function)	Count	%	PValue	Uniprot IDs of the proteins
Purine NTP-dependent helicase activity	13	7.14	5.65E-10	Q9NR30, O75643, Q8TDD1, O00571, Q7L2E3, P17844, Q92841, Q9NY93, O43143, Q9GZR7, Q9NVP1, Q13206, Q96GQ7
RNA helicase activity	10	5.49	1.27E-11	Q9NY93, Q9NR30, O43143, Q8TDD1, Q9NVP1, Q9GZR7, O00571, P17844, Q13206, Q92841
Structural constituent of ribosome	20	10.99	1.70E-14	P18124, P46777, P62750, P62913, P61353, P30050, P55795, P62424, Q02878, P62241, P62829, P50914, O76021, P61313, P23396, Q6DKI1, P62263, Q9Y3U8, P26373, P39023
Nucleotide binding	68	37.36	4.18E-17	Q12905, P52597, Q9H0A0, Q9BVP2, P62750, O00571, P31943, Q13823, Q9BZE4, P31942, Q96PK6, Q15717, Q13523, Q9BWF3, Q16629, O43390, Q96T37, O60506, Q13151, Q13310, P22626, Q13247, Q8TDD1, P49756, Q9BYG3, P17844, Q99729, P55795, P42696, P26599, P35637, O43143, Q9UKM9, Q9NVP1, O00159, Q13148, Q13206, Q9NW13, P19338, Q9Y277, P38159, Q13595, Q9NWH9, P14866, Q14692, Q92804, Q92841, P78527, Q58FF8, P08107, O95758, O00425, Q9NR30, P52272, O75643, P51991, P19525, P54652, Q7L2E3, Q14151, Q9NZI8, O60264, Q9NY93, Q08170, Q9GZR7, P08621, Q14103, P43243, Q96GQ7
RNA binding	90	49.45	2.37E-77	Q12906, Q12905, P52597, P62750, O00571, P31943, P31942, Q96PK6, Q15717, Q9BWF3, Q9Y221, P62424, Q16629, O43390, Q9Y3A4, Q96T37, P61313, P23396, Q9BUJ2, P62263, O60506, Q7Z2W4, Q13151, P18583, Q13310, Q9H9Y2, Q9H6R4, P22626, Q9Y2X3, P49756, Q8IYB3, Q13247, Q8TDD1, Q9BYG3, P62913, P17844, O15226, O00567, Q9H7N4, Q99729, P55795, P46087, P42696, P26599, Q9UKM9, P35637, Q02878, Q9NVP1, P51114, Q9NW13, Q13148, Q13206, P19338, Q15365, P38159, P39023, P18124, Q13595, Q9NWH9, P46777, Q07666, P14866, Q96KR1, Q92804, Q14690, Q92841, P30050, O60832, O95758, O00425, Q9NR30, O95793, P52272, P51991, P19525, P55265, Q7L2E3, Q14151, Q96I24, Q9NZI8, O43818, O75683, Q9NY93, Q08170, Q9GZR7, P50914, P08621, O76021, Q14103, P43243, P26373

Appendix A10: Biological processes of NS1-interacting host factors mapped with GO in DAVID

Biological processes of NS1-interacting host factors mapped with GO in DAVID				
Term (Biological process)	Count	%	PValue	Uniprot IDs of the proteins
Response to unfolded protein	4	2.20	4.20E-02	P08107, P19525, P54652, P04792
RNA catabolic process	4	2.20	3.37E-02	P08107, Q9H0D6, Q13310, Q14103
Maturation of 5.8S rRNA	2	1.10	2.16E-02	Q9GZL7, O00541
Maturation of 5.8S rRNA from tricistronic rRNA transcript (SSU-rRNA, 5.8S rRNA, LSU-rRNA)	2	1.10	2.16E-02	Q9GZL7, O00541
Posttranscriptional regulation of gene expression	8	4.40	8.24E-03	Q15717, Q14103, Q9NZI8, O00425, P04792, Q9BZE4, P78527, O60506
Chromatin organization	12	6.59	2.79E-03	O75367, Q71UI9, Q7Z7K6, Q93077, O60264, Q8IUE6, Q92522, Q96PK6, Q9BTM1, Q9BWF3, P16401, P07305, Q5SSJ5
Regulation of RNA stability	4	2.20	2.15E-03	Q15717, Q14103, Q9NZI8, O60506
Regulation of mRNA stability	4	2.20	1.66E-03	Q15717, Q14103, Q9NZI8, O60506
Ribonucleoprotein complex assembly	6	3.30	9.10E-04	Q9Y221, O75643, Q13247, Q14692, P62263, P56537
Chromosome organization	15	8.24	8.18E-04	O75367, Q71UI9, Q7Z7K6, Q93077, O60264, Q8IUE6, Q92522, P78527, Q96PK6, O60832, Q9BTM1, Q9BWF3, P16401, P07305, Q15050, Q5SSJ5
mRNA stabilization	4	2.20	5.20E-04	Q15717, Q14103, Q9NZI8, O60506
Maturation of LSU-rRNA from tricistronic rRNA transcript (SSU-rRNA, 5.8S rRNA, LSU-rRNA)	3	1.65	3.49E-04	Q14137, Q9GZL7, O00541
maturation of LSU-rRNA	3	1.65	3.49E-04	Q14137, Q9GZL7, O00541
Macromolecular complex assembly	19	10.44	3.17E-04	O75367, Q71UI9, O75643, Q13247, Q7Z7K6, Q93077, Q9BYG3, O60264, Q14692, Q8IUE6, Q92522, Q9BTM1, Q9Y221, P16401, P07305, Q15393, P62263, Q5SSJ5, P56537
Macromolecular complex subunit organization	20	10.99	2.47E-04	O75367, Q71UI9, Q9H0D6, O75643, Q13247, Q7Z7K6, Q93077, Q9BYG3, O60264, Q14692, Q8IUE6, Q92522, Q9BTM1, Q9Y221, P16401, P07305, Q15393, P62263, Q5SSJ5, P56537
Ribosome assembly	4	2.20	1.43E-04	Q9Y221, Q14692, P62263, P56537
Chromatin assembly or disassembly	11	6.04	1.19E-06	Q9BTM1, Q71UI9, O75367, Q7Z7K6, P16401, Q93077, P07305, O60264, Q8IUE6, Q5SSJ5, Q92522
Nucleosome organization	10	5.49	7.32E-07	Q9BTM1, Q71UI9, O75367, P16401, Q93077, P07305, O60264, Q8IUE6, Q5SSJ5, Q92522
DNA packaging	11	6.04	5.58E-07	Q9BTM1, Q71UI9, O75367, Q7Z7K6, P16401, Q93077, P07305, O60264, Q8IUE6, Q5SSJ5, Q92522
Cellular macromolecular complex assembly	17	9.34	3.60E-07	O75367, Q71UI9, O75643, Q7Z7K6, Q13247, Q93077, O60264, Q14692, Q8IUE6, Q92522, Q9BTM1, Q9Y221, P16401, P07305, P62263, Q5SSJ5, P56537
Ribosomal large subunit biogenesis	6	3.30	3.41E-08	P18124, P46777, P62913, P50914, Q9GZL7, O00541

Biological processes of NS1-interacting host factors mapped with GO in DAVID				
Term (Biological process)	Count	%	PValue	Uniprot IDs of the proteins
Cellular macromolecular complex subunit organization	18	9.89	3.31E-07	O75367, Q71UI9, Q9H0D6, O75643, Q13247, Q7Z7K6, Q93077, O60264, Q14692, Q8IUE6, Q92522, Q9BTM1, Q9Y221, P16401, P07305, P62263, Q5SSJ5, P56537
Nucleosome assembly	10	5.49	3.04E-07	Q9BTM1, Q71UI9, O75367, P16401, Q93077, P07305, O60264, Q8IUE6, Q5SSJ5, Q92522
Protein-DNA complex assembly	11	6.04	5.12E-08	Q9BTM1, Q71UI9, O75367, Q7Z7K6, P16401, Q93077, P07305, O60264, Q8IUE6, Q5SSJ5, Q92522
Chromatin assembly	11	6.04	3.30E-08	Q9BTM1, Q71UI9, O75367, Q7Z7K6, P16401, Q93077, P07305, O60264, Q8IUE6, Q5SSJ5, Q92522
Translation	25	13.74	1.39E-13	P18124, P62750, P46777, P61353, P30050, P62424, P62241, P62829, P61313, O00425, P23396, P62263, Q6DKI1, Q13310, P19525, P62913, P55795, Q9P2E9, Q02878, P50914, O76021, Q9Y3U8, P56537, P26373, P39023
Translational elongation	18	9.89	5.61E-16	P18124, P46777, P62750, P62913, P61353, P30050, P55795, P62424, Q02878, P62241, P62829, P50914, P61313, P23396, P62263, Q9Y3U8, P26373, P39023
RNA splicing, via transesterification reactions	26	14.29	9.78E-23	P52597, Q13595, P14866, P31943, P31942, Q16629, O43390, Q9BUJ2, Q13151, P52272, P51991, P22626, O75643, P49756, Q8IYB3, Q13247, Q13435, P55795, P26599, Q08170, P35637, Q15393, P08621, Q14103, Q15365, P38159
RNA splicing, via transesterification reactions with bulged adenosine as nucleophile	26	14.29	9.78E-23	P52597, Q13595, P14866, P31943, P31942, Q16629, O43390, Q9BUJ2, Q13151, P52272, P51991, P22626, O75643, P49756, Q8IYB3, Q13247, Q13435, P55795, P26599, Q08170, P35637, Q15393, P08621, Q14103, Q15365, P38159
Nuclear mRNA splicing, via spliceosome	26	14.29	9.78E-23	P52597, Q13595, P14866, P31943, P31942, Q16629, O43390, Q9BUJ2, Q13151, P52272, P51991, P22626, O75643, P49756, Q8IYB3, Q13247, Q13435, P55795, P26599, Q08170, P35637, Q15393, P08621, Q14103, Q15365, P38159
ncRNA metabolic process	31	17.03	3.33E-24	P18124, P46777, Q9H583, Q14690, O60832, Q9UNX4, Q14137, O43159, Q12788, Q8NI36, Q9GZL7, P62263, P56182, Q9H9Y2, Q9Y2X3, Q8IY81, Q9BYG3, P62913, Q9BVJ6, O00541, O00567, O00566, Q9Y5J1, O43818, P46087, Q9NY93, Q14684, Q96G21, P50914, Q8TED0, Q9NYH9
ncRNA processing	30	16.48	1.29E-25	P18124, P46777, Q9H583, Q14690, O60832, Q9UNX4, Q14137, O43159, Q12788, Q8NI36, Q9GZL7, P62263, P56182, Q9H9Y2, Q9Y2X3, Q8IY81, P62913, Q9BVJ6, O00541, O00567, O00566, Q9Y5J1, O43818, P46087, Q9NY93, Q14684, Q96G21, P50914, Q8TED0, Q9NYH9
RNA stabilization	4	2.20	5.20E-04	Q15717, Q14103, Q9NZI8, O60506

Biological processes of NS1-interacting host factors mapped with GO in DAVID				
Term (Biological process)	Count	%	PValue	Uniprot IDs of the proteins
RNA splicing	37	20.33	1.35E-28	P52597, Q13595, P14866, Q9UMS4, P31943, P31942, Q96PK6, Q13523, Q9BWF3, Q16629, O43390, Q9BUJ2, O60506, Q13151, P52272, P22626, P51991, O75643, P49756, Q8IYB3, Q13247, P17844, O00566, Q9H7N4, Q13435, P55795, P26599, Q08170, O43143, Q9UKM9, P35637, P08621, Q15393, Q14103, Q13148, Q9NW13, Q15365, P38159
mRNA processing	40	21.98	2.66E-30	Q13595, P52597, Q9H0D6, Q07666, P14866, Q9UMS4, P31943, P31942, Q96PK6, Q13523, Q9BWF3, O95758, Q16629, O43390, Q9BUJ2, O60506, Q13151, P52272, O75643, P22626, P51991, P49756, Q8IYB3, Q13247, P55265, P17844, Q9H7N4, Q13435, P55795, P26599, Q08170, O43143, Q9UKM9, P35637, P08621, Q15393, Q14103, Q13148, Q9NW13, Q15365, P38159
mRNA metabolic process	43	23.63	1.81E-31	Q13595, P52597, Q9H0D6, Q07666, P14866, Q9UMS4, P31943, P31942, Q96PK6, Q15717, Q13523, Q9BWF3, P08107, O95758, Q16629, O43390, Q9BUJ2, O60506, Q13151, P52272, O75643, P22626, P51991, P49756, Q8IYB3, Q13247, P55265, P17844, Q9NZI8, Q9H7N4, Q13435, P55795, P26599, Q08170, O43143, Q9UKM9, P35637, P08621, Q15393, Q14103, Q13148, Q9NW13, Q15365, P38159
rRNA metabolic process	31	17.03	2.01E-36	P18124, P46777, Q9H583, Q14690, O60832, Q9UNX4, Q14137, O43159, Q12788, Q8NI36, Q9GZL7, P62263, P56182, Q9H9Y2, Q9Y2X3, Q8IY81, Q9BYG3, P62913, Q9BVJ6, O00541, O00567, O00566, Q9Y5J1, O43818, P46087, Q9NY93, Q14684, Q96G21, P50914, Q8TED0, Q9NYH9
Ribonucleoprotein complex biogenesis	42	23.08	1.38E-43	P18124, P46777, Q9H583, Q13823, Q14692, Q9BZE4, Q14690, O60832, Q9UNX4, Q9Y221, Q14137, O43159, Q12788, P62424, Q8NI36, Q15050, Q9GZL7, P62263, Q99848, P56182, Q8TDN6, Q9H9Y2, O75643, Q9Y2X3, Q13247, Q8IY81, P62913, Q9BVJ6, O00541, O00567, O00566, Q9Y5J1, O43818, O75683, Q9NY93, P46087, Q14684, Q96G21, P50914, Q8TED0, Q9NYH9, P56537
ribosome biogenesis	40	21.98	6.59E-48	P18124, P46777, Q9H583, Q13823, Q14692, Q9BZE4, Q14690, O60832, Q9UNX4, Q9Y221, Q14137, O43159, Q12788, P62424, Q8NI36, Q15050, Q9GZL7, P62263, Q99848, P56182, Q8TDN6, Q9H9Y2, Q9Y2X3, Q8IY81, P62913, Q9BVJ6, O00541, O00567, O00566, Q9Y5J1, O43818, O75683, Q9NY93, P46087, Q14684, Q96G21, P50914, Q8TED0, Q9NYH9, P56537

Biological processes of NS1-interacting host factors mapped with GO in DAVID				
Term (Biological process)	Count	%	PValue	Uniprot IDs of the proteins
RNA processing	74	40.66	1.27E-62	P52597, Q9H0D6, Q9H583, P31943, P31942, Q96PK6, Q13523, Q9BWF3, Q14137, Q16629, O43390, Q8NI36, P62263, Q9BUJ2, O60506, Q13151, Q13310, Q9H9Y2, P22626, Q9Y2X3, Q13247, Q8TDD1, Q8IYB3, P49756, P62913, P17844, Q9BVJ6, O00567, O00566, Q9H7N4, Q9Y5J1, P55795, P46087, P26599, Q14684, P35637, O43143, Q9UKM9, Q15393, Q9NW13, Q8TED0, Q13148, Q15365, P38159, P18124, Q13595, P46777, Q07666, P14866, Q9UMS4, Q14690, Q92841, O60832, Q9UNX4, O95758, O43159, Q12788, Q9GZL7, P56182, P52272, O75643, P51991, Q8IY81, P55265, O00541, O43818, Q13435, Q9NY93, Q08170, Q96G21, P50914, P08621, O76021, Q14103, Q9NYH9
rRNA processing	30	16.48	2.42E-35	P18124, P46777, Q9H583, Q14690, O60832, Q9UNX4, Q14137, O43159, Q12788, Q8NI36, Q9GZL7, P62263, P56182, Q9H9Y2, Q9Y2X3, Q8IY81, P62913, Q9BVJ6, O00541, O00567, O00566, Q9Y5J1, O43818, P46087, Q9NY93, Q14684, Q96G21, P50914, Q8TED0, Q9NYH9

Appendix B1: Epitope mapping of anti-NS1 mAbs

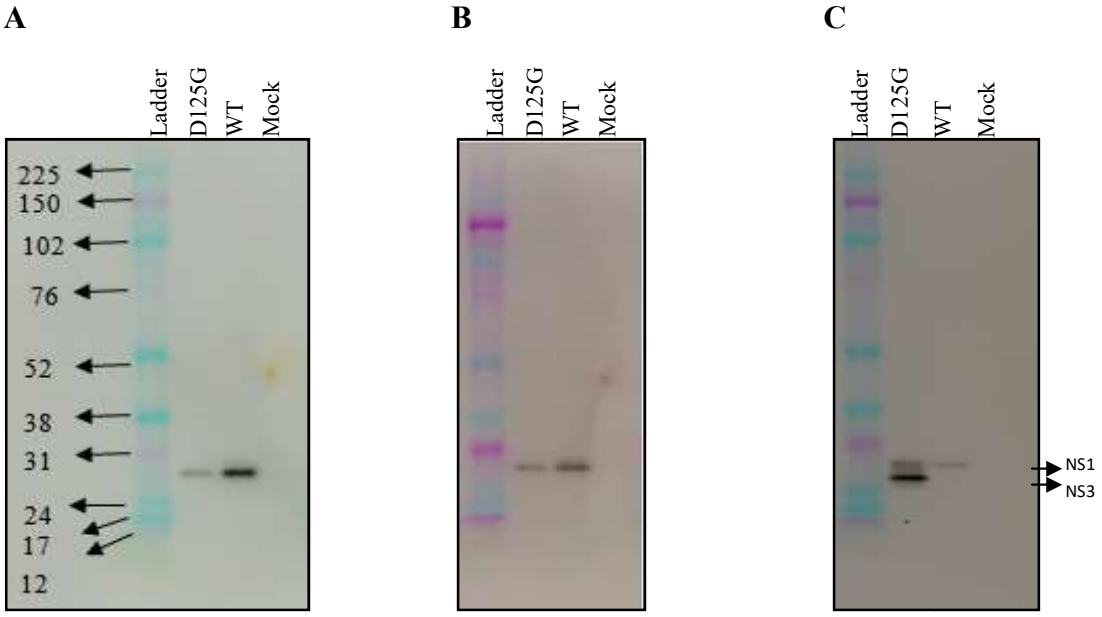

Appendix B1: Epitope mapping of anti-NS1 mAbs. A549 cells were infected with bothwild-type HK1 and D125G mutant HK1. Cell lysates were resolved in SDS-PAGE, transferred to PVDF membrane and the reactivities of anti-NS1 mAb 3F5 (A), 13D8 (B), and 5D6 (C) checked against wild-type HK1 NS1 and D125G mutant NS1 variant, NS3 that lacks NS1 aa 125-167. The molecular weight markers are indicated on the left side of the membranes.

Appendix B2: Immunofluorescence microscopy of M2 in NUMA1 and PRPF19 knockdown cells

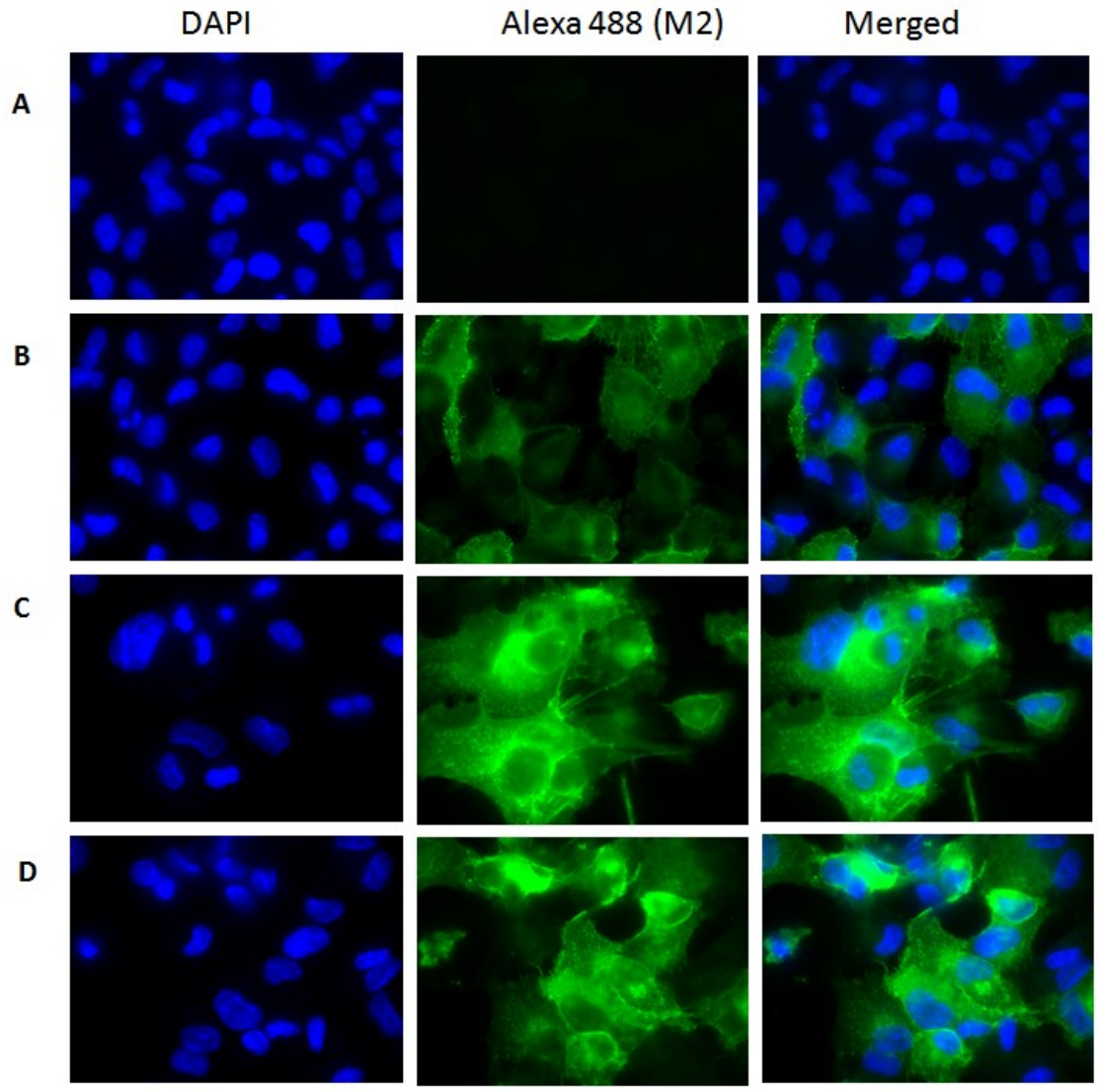

Appendix B2: Immunofluorescence microscopy of M2 in NUMA1 and PRPF19 knockdown cells. Mock infected NSi (A), PR8-infected NSi (B), PR8-infected NUMA1 KD (C) and PR8- PRPF19 KD (D) A549 cells were fixed, stained for IAV M2 protein and analyzed in immunofluorescence microscopy. M2 proteins were detected with Alexa Fluor 488 anti-M2 (green).

Appendix B3: Lists of publications

Published manuscripts:

1. **Rahim MN**, Selman M, Sauder PJ, Forbes NE, Stecho W, Xu W, Lebar M, Brown EG, Coombs KM. Generation and characterization of a new panel of broadly-reactive monoclonal anti-NS1 antibodies for detection of Influenza A virus. *Journal of General Virology*. 2013. 94(3): 592-604. PMID: 23223621

   My contribution: Objective 1 of my thesis was published in this manuscript. This manuscript is directly linked to my thesis. One of my immunofluorescence images was selected as cover image in the 2013. 94(3) issue.)

2. Tran AT, **Rahim MN**, Ranadheera C, Kroeker A, Cortens JP, Opanubi KJ, Wilkins JA, Coombs KM. Knockdown of specific host factors protects against influenza virus-induced cell death. *Cell Death Dis.* 2013 Aug 15;4:e769. PMID: 23949218.
   My contribution: I designed and performed some Western blots and I also had contributions on writing and editing the manuscript.

3. Yeganeh B, Rezaei Moghadam A, Tran AT, **Rahim MN**, Ande SR, Hashemi M, Coombs KM, Ghavami S. Asthma and Influenza Virus Infection: Focusing on Cell Death and Stress Pathways in Influenza Virus Replication. 2013. *Ir. J Allergy Asthma Immunol.* 12(1):1-17. PMID: 23454774

   My contribution: In this review paper my contribution was to write the section "Influenza virus replication process".

Manuscripts on progress:

1. **Rahim MN** and Coombs KM. Identification of NS1 interacting host factors during influenza A virus natural infection and NS1-NUMA1 interaction play crucial role in viral maturation.
   - We are planning to submit in *PLOS Pathogens*. This manuscript contains the contents of the Objective 2 and part of Objective 3 of my thesis. This manuscript is directly linked to my thesis.

2. **Rahim MN** and Coombs KM. Influenza A virus NS1 protein interacts with host pre-mRNA Processing Factor 19 to support viral replication.
   - This manuscript contains the contents of the Objective 3 of my thesis. We are planning to submit as a short communication/report. This manuscript is directly linked to my thesis.

References

1. Wahlgren, J., *Influenza A viruses: an ecology review.* Infect Ecol Epidemiol, 2011. **1**.
2. Capua I, M.F., *A colour atlas and text on avian influenza.* 2001: Bologna: Papi editore.
3. Smith W, A.C., Laidlaw PP., *A virus obtained from influenza patients.* Lancet, 1933. **222**(5732): p. 66–68.
4. Schild, G.C., et al., *Antigenic analysis of influenza A virus surface antigens: considerations for the nomenclature of influenza virus. Brief review.* Arch Virol, 1980. **63**(3-4): p. 171-84.
5. Tong, S., et al., *New world bats harbor diverse influenza A viruses.* PLoS Pathog, 2013. **9**(10): p. e1003657.
6. Wu, Y., et al., *Bat-derived influenza-like viruses H17N10 and H18N11.* Trends Microbiol, 2014. **22**(4): p. 183-91.
7. Biere, B., B. Bauer, and B. Schweiger, *Differentiation of influenza B virus lineages Yamagata and Victoria by real-time PCR.* J Clin Microbiol, 2010. **48**(4): p. 1425-7.
8. Taubenberger, J.K. and J.C. Kash, *Influenza virus evolution, host adaptation, and pandemic formation.* Cell Host Microbe, 2010. **7**(6): p. 440-51.
9. Webster, R.G., et al., *Evolution and ecology of influenza A viruses.* Microbiol Rev, 1992. **56**(1): p. 152-79.
10. Wikramaratna, P.S. and S. Gupta, *Influenza outbreaks.* Cell Microbiol, 2009. **11**(7): p. 1016-24.
11. Smith, N.M., et al., *Prevention and Control of Influenza: recommendations of the Advisory Committee on Immunization Practices (ACIP).* MMWR Recomm Rep, 2006. **55**(Rr-10): p. 1-42.
12. Gamblin, S.J. and J.J. Skehel, *Influenza hemagglutinin and neuraminidase membrane glycoproteins.* J Biol Chem, 2010. **285**(37): p. 28403-9.
13. Johnson, N.P. and J. Mueller, *Updating the accounts: global mortality of the 1918-1920 "Spanish" influenza pandemic.* Bull Hist Med, 2002. **76**(1): p. 105-15.
14. Morens, D.M., J.K. Taubenberger, and A.S. Fauci, *Predominant role of bacterial pneumonia as a cause of death in pandemic influenza: implications for pandemic influenza preparedness.* J Infect Dis, 2008. **198**(7): p. 962-70.
15. Taubenberger, J.K., et al., *Characterization of the 1918 influenza virus polymerase genes.* Nature, 2005. **437**(7060): p. 889-93.
16. Rogers, D.E., D.B. Louria, and E.D. Kilbourne, *The syndrome of fatal influenza virus pneumonia.* Trans Assoc Am Physicians, 1958. **71**: p. 260-73.
17. Scholtissek, C., et al., *On the origin of the human influenza virus subtypes H2N2 and H3N2.* Virology, 1978. **87**(1): p. 13-20.
18. Kawaoka, Y., S. Krauss, and R.G. Webster, *Avian-to-human transmission of the PB1 gene of influenza A viruses in the 1957 and 1968 pandemics.* J Virol, 1989. **63**(11): p. 4603-8.
19. Dawood, F.S., et al., *Emergence of a novel swine-origin influenza A (H1N1) virus in humans.* N Engl J Med, 2009. **360**(25): p. 2605-15.

20. Garten, R.J., et al., *Antigenic and genetic characteristics of swine-origin 2009 A(H1N1) influenza viruses circulating in humans.* Science, 2009. **325**(5937): p. 197-201.
21. Perez-Padilla, R., et al., *Pneumonia and respiratory failure from swine-origin influenza A (H1N1) in Mexico.* N Engl J Med, 2009. **361**(7): p. 680-9.
22. Pada, S. and P.A. Tambyah, *Overview/reflections on the 2009 H1N1 pandemic.* Microbes Infect, 2011. **13**(5): p. 470-8.
23. Palese, P.S., ML., *Orthomyxoviridae: The Viruses and their Replication. Fields Virology*. Orthomyxoviridae: The Viruses and their Replication., ed. D. Knipe and P. Howley. 2007: Philadelphia: Lippincott Williams & Wilkins.
24. Richardson, J.C. and R.K. Akkina, *NS2 protein of influenza virus is found in purified virus and phosphorylated in infected cells.* Arch Virol, 1991. **116**(1-4): p. 69-80.
25. Bouvier, N.M. and P. Palese, *The biology of influenza viruses.* Vaccine, 2008. **26 Suppl 4**: p. D49-53.
26. Stanekova, Z. and E. Vareckova, *Conserved epitopes of influenza A virus inducing protective immunity and their prospects for universal vaccine development.* Virol J, 2010. **7**: p. 351.
27. Zheng, B., et al., *D225G mutation in hemagglutinin of pandemic influenza H1N1 (2009) virus enhances virulence in mice.* Exp Biol Med (Maywood), 2010. **235**(8): p. 981-8.
28. Tumpey, T.M., et al., *A two-amino acid change in the hemagglutinin of the 1918 influenza virus abolishes transmission.* Science, 2007. **315**(5812): p. 655-9.
29. Stegmann, T., *Membrane fusion mechanisms: the influenza hemagglutinin paradigm and its implications for intracellular fusion.* Traffic, 2000. **1**(8): p. 598-604.
30. Schmitt, A.P. and R.A. Lamb, *Influenza virus assembly and budding at the viral budozone.* Adv Virus Res, 2005. **64**: p. 383-416.
31. Cros, J.F. and P. Palese, *Trafficking of viral genomic RNA into and out of the nucleus: influenza, Thogoto and Borna disease viruses.* Virus Res, 2003. **95**(1-2): p. 3-12.
32. Rossman, J.S. and R.A. Lamb, *Autophagy, apoptosis, and the influenza virus M2 protein.* Cell Host Microbe, 2009. **6**(4): p. 299-300.
33. Chen, B.J., et al., *The influenza virus M2 protein cytoplasmic tail interacts with the M1 protein and influences virus assembly at the site of virus budding.* J Virol, 2008. **82**(20): p. 10059-70.
34. Watanabe, T., et al., *Viral RNA polymerase complex promotes optimal growth of 1918 virus in the lower respiratory tract of ferrets.* Proc Natl Acad Sci U S A, 2009. **106**(2): p. 588-92.
35. Guilligay, D., et al., *The structural basis for cap binding by influenza virus polymerase subunit PB2.* Nat Struct Mol Biol, 2008. **15**(5): p. 500-6.
36. Yuan, P., et al., *Crystal structure of an avian influenza polymerase PA(N) reveals an endonuclease active site.* Nature, 2009. **458**(7240): p. 909-13.
37. Dias, A., et al., *The cap-snatching endonuclease of influenza virus polymerase resides in the PA subunit.* Nature, 2009. **458**(7240): p. 914-8.

38. Chu, C., et al., *Functional analysis of conserved motifs in influenza virus PB1 protein.* PLoS One, 2012. **7**(5): p. e36113.
39. Gonzalez, S. and J. Ortin, *Distinct regions of influenza virus PB1 polymerase subunit recognize vRNA and cRNA templates.* Embo j, 1999. **18**(13): p. 3767-75.
40. Noda, T. and Y. Kawaoka, *Structure of influenza virus ribonucleoprotein complexes and their packaging into virions.* Rev Med Virol, 2010. **20**(6): p. 380-91.
41. Wise, H.M., et al., *A complicated message: Identification of a novel PB1-related protein translated from influenza A virus segment 2 mRNA.* J Virol, 2009. **83**(16): p. 8021-31.
42. Chen, W., et al., *A novel influenza A virus mitochondrial protein that induces cell death.* Nat Med, 2001. **7**(12): p. 1306-12.
43. Zamarin, D., et al., *Influenza virus PB1-F2 protein induces cell death through mitochondrial ANT3 and VDAC1.* PLoS Pathog, 2005. **1**(1): p. e4.
44. Conenello, G.M., et al., *A single mutation in the PB1-F2 of H5N1 (HK/97) and 1918 influenza A viruses contributes to increased virulence.* PLoS Pathog, 2007. **3**(10): p. 1414-21.
45. O'Neill, R.E., et al., *Nuclear import of influenza virus RNA can be mediated by viral nucleoprotein and transport factors required for protein import.* J Biol Chem, 1995. **270**(39): p. 22701-4.
46. Paterson, D. and E. Fodor, *Emerging roles for the influenza A virus nuclear export protein (NEP).* PLoS Pathog, 2012. **8**(12): p. e1003019.
47. Boulo, S., et al., *Nuclear traffic of influenza virus proteins and ribonucleoprotein complexes.* Virus Res, 2007. **124**(1-2): p. 12-21.
48. Hale, B.G., et al., *The multifunctional NS1 protein of influenza A viruses.* J Gen Virol, 2008. **89**(Pt 10): p. 2359-76.
49. Hatada, E. and R. Fukuda, *Binding of influenza A virus NS1 protein to dsRNA in vitro.* J Gen Virol, 1992. **73 (Pt 12)**: p. 3325-9.
50. Krug, R.M., *Functions of the influenza A virus NS1 protein in antiviral defense.* Curr Opin Virol, 2015. **12**: p. 1-6.
51. Wang, X., et al., *Functional replacement of the carboxy-terminal two-thirds of the influenza A virus NS1 protein with short heterologous dimerization domains.* J Virol, 2002. **76**(24): p. 12951-62.
52. Li, Y., Y. Yamakita, and R.M. Krug, *Regulation of a nuclear export signal by an adjacent inhibitory sequence: the effector domain of the influenza virus NS1 protein.* Proc Natl Acad Sci U S A, 1998. **95**(9): p. 4864-9.
53. Garcia-Sastre, A., et al., *Influenza A virus lacking the NS1 gene replicates in interferon-deficient systems.* Virology, 1998. **252**(2): p. 324-30.
54. Hai, R., et al., *Influenza B virus NS1-truncated mutants: live-attenuated vaccine approach.* J Virol, 2008. **82**(21): p. 10580-90.
55. Solorzano, A., et al., *Mutations in the NS1 protein of swine influenza virus impair anti-interferon activity and confer attenuation in pigs.* J Virol, 2005. **79**(12): p. 7535-43.
56. Steel, J., et al., *Live attenuated influenza viruses containing NS1 truncations as vaccine candidates against H5N1 highly pathogenic avian influenza.* J Virol, 2009. **83**(4): p. 1742-53.

57. Ludwig, S., et al., *Phylogenetic relationship of the nonstructural (NS) genes of influenza A viruses.* Virology, 1991. **183**(2): p. 566-77.
58. Treanor, J.J., et al., *The B allele of the NS gene of avian influenza viruses, but not the A allele, attenuates a human influenza A virus for squirrel monkeys.* Virology, 1989. **171**(1): p. 1-9.
59. Forbes, N.E., et al., *Multifunctional adaptive NS1 mutations are selected upon human influenza virus evolution in the mouse.* PLoS One, 2012. **7**(2): p. e31839.
60. Selman, M., et al., *Adaptive mutation in influenza A virus non-structural gene is linked to host switching and induces a novel protein by alternative splicing.* Emerg Microbes Infect, 2012. **1**(11): p. e42.
61. Lamb, R.A. and P.W. Choppin, *Identification of a second protein (M2) encoded by RNA segment 7 of influenza virus.* Virology, 1981. **112**(2): p. 729-37.
62. Lamb, R.A., et al., *Mapping of the two overlapping genes for polypeptides NS1 and NS2 on RNA segment 8 of influenza virus genome.* Proc Natl Acad Sci U S A, 1980. **77**(4): p. 1857-61.
63. Briedis, D.J. and R.A. Lamb, *Influenza B virus genome: sequences and structural organization of RNA segment 8 and the mRNAs coding for the NS1 and NS2 proteins.* J Virol, 1982. **42**(1): p. 186-93.
64. Steinhauer, D.A. and J.J. Holland, *Rapid evolution of RNA viruses.* Annu Rev Microbiol, 1987. **41**: p. 409-33.
65. Chen, R. and E.C. Holmes, *Avian influenza virus exhibits rapid evolutionary dynamics.* Mol Biol Evol, 2006. **23**(12): p. 2336-41.
66. Carrat, F. and A. Flahault, *Influenza vaccine: the challenge of antigenic drift.* Vaccine, 2007. **25**(39-40): p. 6852-62.
67. Tscherne, D.M. and A. Garcia-Sastre, *Virulence determinants of pandemic influenza viruses.* J Clin Invest, 2011. **121**(1): p. 6-13.
68. Klenk, H.D., W. Garten, and M. Matrosovich, *Molecular mechanisms of interspecies transmission and pathogenicity of influenza viruses: Lessons from the 2009 pandemic.* Bioessays, 2011. **33**(3): p. 180-8.
69. Ahmed, R., M.B. Oldstone, and P. Palese, *Protective immunity and susceptibility to infectious diseases: lessons from the 1918 influenza pandemic.* Nat Immunol, 2007. **8**(11): p. 1188-93.
70. Matrosovich, M.N., et al., *Human and avian influenza viruses target different cell types in cultures of human airway epithelium.* Proc Natl Acad Sci U S A, 2004. **101**(13): p. 4620-4.
71. Samji, T., *Influenza A: understanding the viral life cycle.* Yale J Biol Med, 2009. **82**(4): p. 153-9.
72. Skehel, J.J. and D.C. Wiley, *Receptor binding and membrane fusion in virus entry: the influenza hemagglutinin.* Annu Rev Biochem, 2000. **69**: p. 531-69.
73. Sieczkarski, S.B. and G.R. Whittaker, *Viral entry.* Curr Top Microbiol Immunol, 2005. **285**: p. 1-23.
74. Mikulasova, A., E. Vareckova, and E. Fodor, *Transcription and replication of the influenza a virus genome.* Acta Virol, 2000. **44**(5): p. 273-82.
75. Engelhardt, O.G. and E. Fodor, *Functional association between viral and cellular transcription during influenza virus infection.* Rev Med Virol, 2006. **16**(5): p. 329-45.

76. Bancroft, C.T. and T.G. Parslow, *Evidence for segment-nonspecific packaging of the influenza a virus genome.* J Virol, 2002. **76**(14): p. 7133-9.
77. Enami, M., et al., *An influenza virus containing nine different RNA segments.* Virology, 1991. **185**(1): p. 291-8.
78. Fujii, Y., et al., *Selective incorporation of influenza virus RNA segments into virions.* Proc Natl Acad Sci U S A, 2003. **100**(4): p. 2002-7.
79. Muramoto, Y., et al., *Hierarchy among viral RNA (vRNA) segments in their role in vRNA incorporation into influenza A virions.* J Virol, 2006. **80**(5): p. 2318-25.
80. Liang, Y., Y. Hong, and T.G. Parslow, *cis-Acting packaging signals in the influenza virus PB1, PB2, and PA genomic RNA segments.* J Virol, 2005. **79**(16): p. 10348-55.
81. Fujii, K., et al., *Importance of both the coding and the segment-specific noncoding regions of the influenza A virus NS segment for its efficient incorporation into virions.* J Virol, 2005. **79**(6): p. 3766-74.
82. Nayak, D.P., E.K. Hui, and S. Barman, *Assembly and budding of influenza virus.* Virus Res, 2004. **106**(2): p. 147-65.
83. Rossman, J.S. and R.A. Lamb, *Influenza virus assembly and budding.* Virology, 2011. **411**(2): p. 229-36.
84. Das, K., et al., *Structures of influenza A proteins and insights into antiviral drug targets.* Nat Struct Mol Biol, 2010. **17**(5): p. 530-8.
85. CDC, A.A.f.I., *http://www.cdc.gov/flu/professionals/antivirals/antiviral-agents-flu.htm*. CDC 2014.
86. Pinto, L.H. and R.A. Lamb, *Controlling influenza virus replication by inhibiting its proton channel.* Mol Biosyst, 2007. **3**(1): p. 18-23.
87. Hayden, F.G. and A.J. Hay, *Emergence and transmission of influenza A viruses resistant to amantadine and rimantadine.* Curr Top Microbiol Immunol, 1992. **176**: p. 119-30.
88. De Clercq, E. and J. Neyts, *Avian influenza A (H5N1) infection: targets and strategies for chemotherapeutic intervention.* Trends Pharmacol Sci, 2007. **28**(6): p. 280-5.
89. Muthuri, S.G., et al., *Impact of neuraminidase inhibitor treatment on outcomes of public health importance during the 2009-2010 influenza A(H1N1) pandemic: a systematic review and meta-analysis in hospitalized patients.* J Infect Dis, 2013. **207**(4): p. 553-63.
90. Reece, P.A., *Neuraminidase inhibitor resistance in influenza viruses.* J Med Virol, 2007. **79**(10): p. 1577-86.
91. Lackenby, A., C.I. Thompson, and J. Democratis, *The potential impact of neuraminidase inhibitor resistant influenza.* Curr Opin Infect Dis, 2008. **21**(6): p. 626-38.
92. Iwasaki, A. and P.S. Pillai, *Innate immunity to influenza virus infection.* Nat Rev Immunol, 2014. **14**(5): p. 315-28.
93. Manicassamy, B., et al., *Analysis of in vivo dynamics of influenza virus infection in mice using a GFP reporter virus.* Proc Natl Acad Sci U S A, 2010. **107**(25): p. 11531-6.
94. Kreijtz, J.H., R.A. Fouchier, and G.F. Rimmelzwaan, *Immune responses to influenza virus infection.* Virus Res, 2011. **162**(1-2): p. 19-30.

95. Alexopoulou, L., et al., *Recognition of double-stranded RNA and activation of NF-kappaB by Toll-like receptor 3.* Nature, 2001. **413**(6857): p. 732-8.
96. Schulz, O., et al., *Toll-like receptor 3 promotes cross-priming to virus-infected cells.* Nature, 2005. **433**(7028): p. 887-92.
97. Pichlmair, A., et al., *RIG-I-mediated antiviral responses to single-stranded RNA bearing 5'-phosphates.* Science, 2006. **314**(5801): p. 997-1001.
98. Rehwinkel, J., et al., *RIG-I detects viral genomic RNA during negative-strand RNA virus infection.* Cell, 2010. **140**(3): p. 397-408.
99. Jiang, F., et al., *Structural basis of RNA recognition and activation by innate immune receptor RIG-I.* Nature, 2011. **479**(7373): p. 423-7.
100. Kowalinski, E., et al., *Structural basis for the activation of innate immune pattern-recognition receptor RIG-I by viral RNA.* Cell, 2011. **147**(2): p. 423-35.
101. Ichinohe, T., I.K. Pang, and A. Iwasaki, *Influenza virus activates inflammasomes via its intracellular M2 ion channel.* Nat Immunol, 2010. **11**(5): p. 404-10.
102. Martinon, F., A. Mayor, and J. Tschopp, *The inflammasomes: guardians of the body.* Annu Rev Immunol, 2009. **27**: p. 229-65.
103. Thomas, P.G., et al., *The intracellular sensor NLRP3 mediates key innate and healing responses to influenza A virus via the regulation of caspase-1.* Immunity, 2009. **30**(4): p. 566-75.
104. McAuley, J.L., et al., *Activation of the NLRP3 inflammasome by IAV virulence protein PB1-F2 contributes to severe pathophysiology and disease.* PLoS Pathog, 2013. **9**(5): p. e1003392.
105. Kim, H.M., et al., *Alveolar macrophages are indispensable for controlling influenza viruses in lungs of pigs.* J Virol, 2008. **82**(9): p. 4265-74.
106. Jayasekera, J.P., et al., *Enhanced antiviral antibody secretion and attenuated immunopathology during influenza virus infection in nitric oxide synthase-2-deficient mice.* J Gen Virol, 2006. **87**(Pt 11): p. 3361-71.
107. Peper, R.L. and H. Van Campen, *Tumor necrosis factor as a mediator of inflammation in influenza A viral pneumonia.* Microb Pathog, 1995. **19**(3): p. 175-83.
108. Wijburg, O.L., et al., *Alveolar macrophages regulate the induction of primary cytotoxic T-lymphocyte responses during influenza virus infection.* J Virol, 1997. **71**(12): p. 9450-7.
109. Arnon, T.I., et al., *Recognition of viral hemagglutinins by NKp44 but not by NKp30.* Eur J Immunol, 2001. **31**(9): p. 2680-9.
110. Mandelboim, O., et al., *Recognition of haemagglutinins on virus-infected cells by NKp46 activates lysis by human NK cells.* Nature, 2001. **409**(6823): p. 1055-60.
111. Staeheli, P., et al., *Mx protein: constitutive expression in 3T3 cells transformed with cloned Mx cDNA confers selective resistance to influenza virus.* Cell, 1986. **44**(1): p. 147-58.
112. Turan, K., et al., *Nuclear MxA proteins form a complex with influenza virus NP and inhibit the transcription of the engineered influenza virus genome.* Nucleic Acids Res, 2004. **32**(2): p. 643-52.
113. Perreira, J.M., et al., *IFITMs Restrict the Replication of Multiple Pathogenic Viruses.* Journal of Molecular Biology, 2013. **425**(24): p. 4937-4955.

114. Brass, A.L., et al., *The IFITM proteins mediate cellular resistance to influenza A H1N1 virus, West Nile virus, and dengue virus.* Cell, 2009. **139**(7): p. 1243-54.
115. Sadler, A.J. and B.R. Williams, *Interferon-inducible antiviral effectors.* Nat Rev Immunol, 2008. **8**(7): p. 559-68.
116. Balachandran, S., et al., *Essential role for the dsRNA-dependent protein kinase PKR in innate immunity to viral infection.* Immunity, 2000. **13**(1): p. 129-41.
117. Dauber, B., et al., *Influenza B virus ribonucleoprotein is a potent activator of the antiviral kinase PKR.* PLoS Pathog, 2009. **5**(6): p. e1000473.
118. van de Sandt, C.E., J.H. Kreijtz, and G.F. Rimmelzwaan, *Evasion of influenza A viruses from innate and adaptive immune responses.* Viruses, 2012. **4**(9): p. 1438-76.
119. Hale, B.G., R.A. Albrecht, and A. Garcia-Sastre, *Innate immune evasion strategies of influenza viruses.* Future Microbiol, 2010. **5**(1): p. 23-41.
120. Quinlivan, M., et al., *Attenuation of equine influenza viruses through truncations of the NS1 protein.* J Virol, 2005. **79**(13): p. 8431-9.
121. Donelan, N.R., C.F. Basler, and A. Garcia-Sastre, *A recombinant influenza A virus expressing an RNA-binding-defective NS1 protein induces high levels of beta interferon and is attenuated in mice.* J Virol, 2003. **77**(24): p. 13257-66.
122. Talon, J., et al., *Activation of interferon regulatory factor 3 is inhibited by the influenza A virus NS1 protein.* J Virol, 2000. **74**(17): p. 7989-96.
123. Wang, X., et al., *Influenza A virus NS1 protein prevents activation of NF-kappaB and induction of alpha/beta interferon.* J Virol, 2000. **74**(24): p. 11566-73.
124. Gack, M.U., et al., *Roles of RIG-I N-terminal tandem CARD and splice variant in TRIM25-mediated antiviral signal transduction.* Proc Natl Acad Sci U S A, 2008. **105**(43): p. 16743-8.
125. Opitz, B., et al., *IFNbeta induction by influenza A virus is mediated by RIG-I which is regulated by the viral NS1 protein.* Cell Microbiol, 2007. **9**(4): p. 930-8.
126. Guo, Z., et al., *NS1 protein of influenza A virus inhibits the function of intracytoplasmic pathogen sensor, RIG-I.* Am J Respir Cell Mol Biol, 2007. **36**(3): p. 263-9.
127. Nemeroff, M.E., et al., *Influenza virus NS1 protein interacts with the cellular 30 kDa subunit of CPSF and inhibits 3'end formation of cellular pre-mRNAs.* Mol Cell, 1998. **1**(7): p. 991-1000.
128. Lee, T.G., et al., *Purification and partial characterization of a cellular inhibitor of the interferon-induced protein kinase of Mr 68,000 from influenza virus-infected cells.* Proc Natl Acad Sci U S A, 1990. **87**(16): p. 6208-12.
129. Guan, Z., et al., *Interaction of Hsp40 with influenza virus M2 protein: implications for PKR signaling pathway.* Protein Cell, 2010. **1**(10): p. 944-55.
130. Silverman, R.H., *Viral encounters with 2',5'-oligoadenylate synthetase and RNase L during the interferon antiviral response.* J Virol, 2007. **81**(23): p. 12720-9.
131. Min, J.Y. and R.M. Krug, *The primary function of RNA binding by the influenza A virus NS1 protein in infected cells: Inhibiting the 2'-5' oligo (A) synthetase/RNase L pathway.* Proc Natl Acad Sci U S A, 2006. **103**(18): p. 7100-5.
132. Varga, Z.T., et al., *The influenza virus protein PB1-F2 inhibits the induction of type I interferon at the level of the MAVS adaptor protein.* PLoS Pathog, 2011. **7**(6): p. e1002067.

133. Iwai, A., et al., *Influenza A virus polymerase inhibits type I interferon induction by binding to interferon beta promoter stimulator 1.* J Biol Chem, 2010. **285**(42): p. 32064-74.
134. Coombs, K.M., et al., *Quantitative proteomic analyses of influenza virus-infected cultured human lung cells.* J Virol, 2010. **84**(20): p. 10888-906.
135. Kroeker, A.L., et al., *Influenza A infection of primary human airway epithelial cells up-regulates proteins related to purine metabolism and ubiquitin-related signaling.* J Proteome Res, 2013. **12**(7): p. 3139-51.
136. Kroeker, A.L., et al., *Response of primary human airway epithelial cells to influenza infection: a quantitative proteomic study.* J Proteome Res, 2012. **11**(8): p. 4132-46.
137. Vester, D., et al., *Quantitative analysis of cellular proteome alterations in human influenza A virus-infected mammalian cell lines.* Proteomics, 2009. **9**(12): p. 3316-27.
138. Karlas, A., et al., *Genome-wide RNAi screen identifies human host factors crucial for influenza virus replication.* Nature, 2010. **463**(7282): p. 818-22.
139. Konig, R., et al., *Human host factors required for influenza virus replication.* Nature, 2010. **463**(7282): p. 813-7.
140. Watanabe, T., et al., *Influenza virus-host interactome screen as a platform for antiviral drug development.* Cell Host Microbe, 2014. **16**(6): p. 795-805.
141. Liu, Y.C., et al., *Cytoplasmic viral RNA-dependent RNA polymerase disrupts the intracellular splicing machinery by entering the nucleus and interfering with Prp8.* PLoS Pathog, 2014. **10**(6): p. e1004199.
142. Jorba, N., et al., *Analysis of the interaction of influenza virus polymerase complex with human cell factors.* Proteomics, 2008. **8**(10): p. 2077-88.
143. Engelhardt, O.G., M. Smith, and E. Fodor, *Association of the influenza A virus RNA-dependent RNA polymerase with cellular RNA polymerase II.* J Virol, 2005. **79**(9): p. 5812-8.
144. Deng, T., et al., *Role of ran binding protein 5 in nuclear import and assembly of the influenza virus RNA polymerase complex.* J Virol, 2006. **80**(24): p. 11911-9.
145. Tafforeau, L., et al., *Generation and comprehensive analysis of an influenza virus polymerase cellular interaction network.* J Virol, 2011. **85**(24): p. 13010-8.
146. Huarte, M., et al., *PA Subunit from Influenza Virus Polymerase Complex Interacts with a Cellular Protein with Homology to a Family of Transcriptional Activators.* Journal of Virology, 2001. **75**(18): p. 8597-8604.
147. Guirimand, T., S. Delmotte, and V. Navratil, *VirHostNet 2.0: surfing on the web of virus/host molecular interactions data.* Nucleic Acids Res, 2015. **43**(Database issue): p. D583-7.
148. Mok, B.W., et al., *The NS1 protein of influenza A virus interacts with cellular processing bodies and stress granules through RNA-associated protein 55 (RAP55) during virus infection.* J Virol, 2012. **86**(23): p. 12695-707.
149. Wang, Y., J. Zhou, and Y. Du, *hnRNP A2/B1 interacts with influenza A viral protein NS1 and inhibits virus replication potentially through suppressing NS1 RNA/protein levels and NS1 mRNA nuclear export.* Virology, 2014. **449**: p. 53-61.

150. Lin, L., et al., *Identification of RNA helicase A as a cellular factor that interacts with influenza A virus NS1 protein and its role in the virus life cycle.* J Virol, 2012. **86**(4): p. 1942-54.
151. Chen, G., et al., *Cellular DDX21 RNA helicase inhibits influenza A virus replication but is counteracted by the viral NS1 protein.* Cell Host Microbe, 2014. **15**(4): p. 484-93.
152. Tawaratsumida, K., et al., *Quantitative proteomic analysis of the influenza A virus nonstructural proteins NS1 and NS2 during natural cell infection identifies PACT as an NS1 target protein and antiviral host factor.* J Virol, 2014. **88**(16): p. 9038-48.
153. Kuo, R.L., et al., *Interactome Analysis of the NS1 Protein Encoded by Influenza A H1N1 Virus Reveals a Positive Regulatory Role of Host Protein PRP19 in Viral Replication.* J Proteome Res, 2016. **15**(5): p. 1639-48.
154. Thulasi Raman, S.N. and Y. Zhou, *Networks of Host Factors that Interact with NS1 Protein of Influenza A Virus.* Front Microbiol, 2016. **7**: p. 654.
155. de Chassey, B., et al., *The interactomes of influenza virus NS1 and NS2 proteins identify new host factors and provide insights for ADAR1 playing a supportive role in virus replication.* PLoS Pathog, 2013. **9**(7): p. e1003440.
156. Falcon, A.M., et al., *Interaction of influenza virus NS1 protein and the human homologue of Staufen in vivo and in vitro.* Nucleic Acids Res, 1999. **27**(11): p. 2241-7.
157. Lydersen, B.K. and D.E. Pettijohn, *Human-specific nuclear protein that associates with the polar region of the mitotic apparatus: distribution in a human/hamster hybrid cell.* Cell, 1980. **22**(2 Pt 2): p. 489-99.
158. Radulescu, A.E. and D.W. Cleveland, *NuMA after 30 years: the matrix revisited.* Trends Cell Biol, 2010. **20**(4): p. 214-22.
159. Kallajoki, M., K. Weber, and M. Osborn, *A 210 kDa nuclear matrix protein is a functional part of the mitotic spindle; a microinjection study using SPN monoclonal antibodies.* Embo j, 1991. **10**(11): p. 3351-62.
160. Zeng, C., D. He, and B.R. Brinkley, *Localization of NuMA protein isoforms in the nuclear matrix of mammalian cells.* Cell Motil Cytoskeleton, 1994. **29**(2): p. 167-76.
161. Fant, X., A. Merdes, and L. Haren, *Cell and molecular biology of spindle poles and NuMA.* Int Rev Cytol, 2004. **238**: p. 1-57.
162. Sun, Q.Y. and H. Schatten, *Role of NuMA in vertebrate cells: review of an intriguing multifunctional protein.* Front Biosci, 2006. **11**: p. 1137-46.
163. Cleveland, D.W., *NuMA: a protein involved in nuclear structure, spindle assembly, and nuclear re-formation.* Trends Cell Biol, 1995. **5**(2): p. 60-4.
164. Merdes, A., et al., *A complex of NuMA and cytoplasmic dynein is essential for mitotic spindle assembly.* Cell, 1996. **87**(3): p. 447-58.
165. Merdes, A., et al., *Formation of spindle poles by dynein/dynactin-dependent transport of NuMA.* J Cell Biol, 2000. **149**(4): p. 851-62.
166. Haren, L. and A. Merdes, *Direct binding of NuMA to tubulin is mediated by a novel sequence motif in the tail domain that bundles and stabilizes microtubules.* J Cell Sci, 2002. **115**(Pt 9): p. 1815-24.

167. Taimen, P., et al., *NuMA and nuclear lamins are cleaved during viral infection--inhibition of caspase activity prevents cleavage and rescues HeLa cells from measles virus-induced but not from rhinovirus 1B-induced cell death.* Virology, 2004. **320**(1): p. 85-98.
168. Yamauchi, Y., et al., *Herpes simplex virus induces extensive modification and dynamic relocalisation of the nuclear mitotic apparatus (NuMA) protein in interphase cells.* J Cell Sci, 2008. **121**(Pt 12): p. 2087-96.
169. Jurica, M.S. and M.J. Moore, *Pre-mRNA splicing: awash in a sea of proteins.* Mol Cell, 2003. **12**(1): p. 5-14.
170. Yin, J., J.M. Zhu, and X.Z. Shen, *New insights into pre-mRNA processing factor 19: A multi-faceted protein in humans.* Biol Cell, 2012. **104**(12): p. 695-705.
171. Cheng, S.C., et al., *PRP19: a novel spliceosomal component.* Mol Cell Biol, 1993. **13**(3): p. 1876-82.
172. Grote, M., et al., *Molecular architecture of the human Prp19/CDC5L complex.* Mol Cell Biol, 2010. **30**(9): p. 2105-19.
173. Vander Kooi, C.W., et al., *The Prp19 U-box crystal structure suggests a common dimeric architecture for a class of oligomeric E3 ubiquitin ligases.* Biochemistry, 2006. **45**(1): p. 121-30.
174. Tarn, W.Y., K.R. Lee, and S.C. Cheng, *Yeast precursor mRNA processing protein PRP19 associates with the spliceosome concomitant with or just after dissociation of U4 small nuclear RNA.* Proc Natl Acad Sci U S A, 1993. **90**(22): p. 10821-5.
175. Tarn, W.Y., K.R. Lee, and S.C. Cheng, *The yeast PRP19 protein is not tightly associated with small nuclear RNAs, but appears to associate with the spliceosome after binding of U2 to the pre-mRNA and prior to formation of the functional spliceosome.* Mol Cell Biol, 1993. **13**(3): p. 1883-91.
176. Chan, S.P., et al., *The Prp19p-associated complex in spliceosome activation.* Science, 2003. **302**(5643): p. 279-82.
177. Yin, J., et al., *DNA damage induces down-regulation of Prp19 via impairing Prp19 stability in hepatocellular carcinoma cells.* PLoS One, 2014. **9**(2): p. e89976.
178. Dellago, H., et al., *ATM-dependent phosphorylation of SNEVhPrp19/hPso4 is involved in extending cellular life span and suppression of apoptosis.* Aging (Albany NY), 2012. **4**(4): p. 290-304.
179. Mahajan, K.N. and B.S. Mitchell, *Role of human Pso4 in mammalian DNA repair and association with terminal deoxynucleotidyl transferase.* Proc Natl Acad Sci U S A, 2003. **100**(19): p. 10746-51.
180. Beck, B.D., et al., *Human Pso4 is a metnase (SETMAR)-binding partner that regulates metnase function in DNA repair.* J Biol Chem, 2008. **283**(14): p. 9023-30.
181. Zhang, N., et al., *The Pso4 mRNA splicing and DNA repair complex interacts with WRN for processing of DNA interstrand cross-links.* J Biol Chem, 2005. **280**(49): p. 40559-67.
182. Lu, X. and R.J. Legerski, *The Prp19/Pso4 core complex undergoes ubiquitylation and structural alterations in response to DNA damage.* Biochem Biophys Res Commun, 2007. **354**(4): p. 968-74.

183. Harlow, E.L., D, *Antibodies: a Laboratory Manual*. 1988, Cold Spring Harbor, NY: Cold Spring Harbor Laboratory. .
184. Slootstra, J.W., et al., *Structural aspects of antibody-antigen interaction revealed through small random peptide libraries.* Mol Divers, 1996. **1**(2): p. 87-96.
185. Righolt, C.H., et al., *Differences in nuclear DNA organization between lymphocytes, Hodgkin and Reed-Sternberg cells revealed by structured illumination microscopy.* J Cell Biochem, 2014. **115**(8): p. 1441-8.
186. Rahim, M.N., et al., *Generation and characterization of a new panel of broadly reactive anti-NS1 mAbs for detection of influenza A virus.* J Gen Virol, 2013. **94**(Pt 3): p. 593-605.
187. Squires, R.B., et al., *Influenza research database: an integrated bioinformatics resource for influenza research and surveillance.* Influenza Other Respir Viruses, 2012. **6**(6): p. 404-16.
188. Noronha, J.M., et al., *Influenza virus sequence feature variant type analysis: evidence of a role for NS1 in influenza virus host range restriction.* J Virol, 2012. **86**(10): p. 5857-66.
189. Bornholdt, Z.A. and B.V. Prasad, *X-ray structure of NS1 from a highly pathogenic H5N1 influenza virus.* Nature, 2008. **456**(7224): p. 985-8.
190. Bao, Y., et al., *The influenza virus resource at the National Center for Biotechnology Information.* J Virol, 2008. **82**(2): p. 596-601.
191. Huang da, W., B.T. Sherman, and R.A. Lempicki, *Systematic and integrative analysis of large gene lists using DAVID bioinformatics resources.* Nat Protoc, 2009. **4**(1): p. 44-57.
192. Park, Y.W. and M.G. Katze, *Translational control by influenza virus. Identification of cis-acting sequences and trans-acting factors which may regulate selective viral mRNA translation.* J Biol Chem, 1995. **270**(47): p. 28433-9.
193. Garfinkel, M.S. and M.G. Katze, *Translational control by influenza virus. Selective translation is mediated by sequences within the viral mRNA 5′-untranslated region.* J Biol Chem, 1993. **268**(30): p. 22223-6.
194. de la Luna, S., et al., *Influenza virus NS1 protein enhances the rate of translation initiation of viral mRNAs.* J Virol, 1995. **69**(4): p. 2427-33.
195. Aragon, T., et al., *Eukaryotic translation initiation factor 4GI is a cellular target for NS1 protein, a translational activator of influenza virus.* Mol Cell Biol, 2000. **20**(17): p. 6259-68.
196. Marc, D., *Influenza virus non-structural protein NS1: interferon antagonism and beyond.* J Gen Virol, 2014. **95**(Pt 12): p. 2594-611.
197. Robb, N.C., et al., *The influenza A virus NS1 protein interacts with the nucleoprotein of viral ribonucleoprotein complexes.* J Virol, 2011. **85**(10): p. 5228-31.
198. Dubois, J., O. Terrier, and M. Rosa-Calatrava, *Influenza viruses and mRNA splicing: doing more with less.* MBio, 2014. **5**(3): p. e00070-14.
199. Qiu, Y., M. Nemeroff, and R.M. Krug, *The influenza virus NS1 protein binds to a specific region in human U6 snRNA and inhibits U6-U2 and U6-U4 snRNA interactions during splicing.* Rna, 1995. **1**(3): p. 304-16.

200. Wang, W. and R.M. Krug, *U6atac snRNA, the highly divergent counterpart of U6 snRNA, is the specific target that mediates inhibition of AT-AC splicing by the influenza virus NS1 protein.* Rna, 1998. **4**(1): p. 55-64.
201. Satterly, N., et al., *Influenza virus targets the mRNA export machinery and the nuclear pore complex.* Proc Natl Acad Sci U S A, 2007. **104**(6): p. 1853-8.
202. Shtyrya, Y.A., L.V. Mochalova, and N.V. Bovin, *Influenza virus neuraminidase: structure and function.* Acta Naturae, 2009. **1**(2): p. 26-32.
203. P.M., C., *NA enzyme and antigen.* The influenza viruses. 1989., New York: Plenum Publishing Corporation. 175–218.
204. Compans, R.W., J. Content, and P.H. Duesberg, *Structure of the ribonucleoprotein of influenza virus.* J Virol, 1972. **10**(4): p. 795-800.
205. Krug, R.M. and P.R. Etkind, *Cytoplasmic and nuclear virus-specific proteins in influenza virus-infected MDCK cells.* Virology, 1973. **56**(1): p. 334-48.
206. Tan, Z., et al., *A new panel of NS1 antibodies for easy detection and titration of influenza A virus.* J Med Virol, 2010. **82**(3): p. 467-75.
207. Rai, M., et al., *Production and characterization of monoclonal antibodies against NS1 protein of H5N1 avian influenza virus.* Hybridoma (Larchmt), 2010. **29**(2): p. 183-6.
208. Brown, L.E., V.S. Hinshaw, and R.G. Webster, *Antigenic variation in the influenza A virus nonstructural protein, NS1.* Virology, 1983. **130**(1): p. 134-43.
209. Wouters, F.S. and P.I. Bastiaens, *Imaging protein-protein interactions by fluorescence resonance energy transfer (FRET) microscopy.* Curr Protoc Cell Biol, 2001. **Chapter 17**: p. Unit 17.1.
210. Leonard, P., S. Hearty, and R. O'Kennedy, *Measuring protein-protein interactions using Biacore.* Methods Mol Biol, 2011. **681**: p. 403-18.
211. Brydon, E.W., S.J. Morris, and C. Sweet, *Role of apoptosis and cytokines in influenza virus morbidity.* FEMS Microbiol Rev, 2005. **29**(4): p. 837-50.
212. Hinshaw, V.S., et al., *Apoptosis: a mechanism of cell killing by influenza A and B viruses.* J Virol, 1994. **68**(6): p. 3667-73.
213. Takizawa, T., et al., *Induction of programmed cell death (apoptosis) by influenza virus infection in tissue culture cells.* J Gen Virol, 1993. **74 (Pt 11)**: p. 2347-55.
214. Avila, J., *Microtubule functions.* Life Sci, 1992. **50**(5): p. 327-34.
215. Bonifacino, J.S. and J. Lippincott-Schwartz, *Coat proteins: shaping membrane transport.* Nat Rev Mol Cell Biol, 2003. **4**(5): p. 409-14.
216. Lafont F, S.K., Seminars in Cell & Developmental Biology

1996. **7**(3): p. 343-355.
217. Polishchuk, R.S., A.A. Mironov, and A. Luini, *Exocytic Pathway*, in *Encyclopedic Reference of Genomics and Proteomics in Molecular Medicine*. 2006, Springer Berlin Heidelberg: Berlin, Heidelberg. p. 536-540.
218. Seldin, L., A. Muroyama, and T. Lechler, *NuMA-microtubule interactions are critical for spindle orientation and the morphogenesis of diverse epidermal structures.* Elife, 2016. **5**.
219. Shapira, S.D., et al., *A physical and regulatory map of host-influenza interactions reveals pathways in H1N1 infection.* Cell, 2009. **139**(7): p. 1255-67.
220. Calder, L.J., et al., *Structural organization of a filamentous influenza A virus.* Proc Natl Acad Sci U S A, 2010. **107**(23): p. 10685-90.

221. Ali, A., et al., *Influenza virus assembly: effect of influenza virus glycoproteins on the membrane association of M1 protein.* J Virol, 2000. **74**(18): p. 8709-19.
222. Nayak, D.P., et al., *Influenza virus morphogenesis and budding.* Virus Res, 2009. **143**(2): p. 147-61.
223. Avalos, R.T., Z. Yu, and D.P. Nayak, *Association of influenza virus NP and M1 proteins with cellular cytoskeletal elements in influenza virus-infected cells.* J Virol, 1997. **71**(4): p. 2947-58.
224. Baccam, P., et al., *Kinetics of influenza A virus infection in humans.* J Virol, 2006. **80**(15): p. 7590-9.